BioMed Research International

Cochlear Implant and Its Related Science

Guest Editors: Chung-Feng Hwang, Yang Chen, Hung-Ching Lin, Prepageran Narayanan, Seung-Ha Oh, and Eric Truy

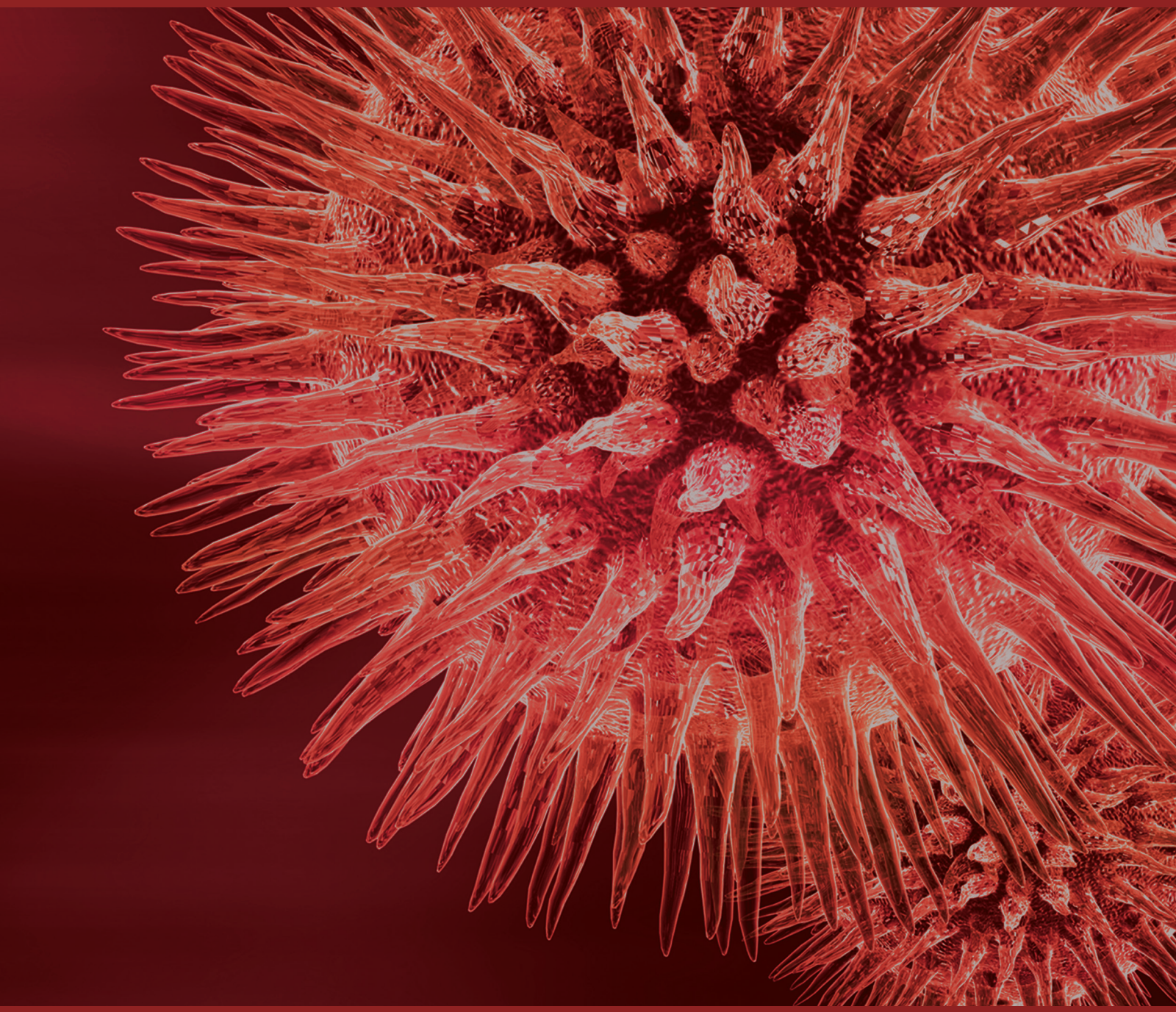

Cochlear Implant and Its Related Science

BioMed Research International

Cochlear Implant and Its Related Science

Guest Editors: Chung-Feng Hwang, Yang Chen, Hung-Ching Lin, Prepageran Narayanan, Seung-Ha Oh, and Eric Truy

Contents

Hindawi Publishing Corporation
BioMed Research International
Volume 2015, Article ID 683967, 2 pages
http://dx.doi.org/10.1155/2015/683967

Editorial

Cochlear Implant and Its Related Science

Chung-Feng Hwang,[1] Yang Chen,[2] Hung-Ching Lin,[3] Prepageran Narayanan,[4] Seung-Ha Oh,[5] and Eric Truy[6]

[1]*Department of Otolaryngology, Kaohsiung Chang Gung Memorial Hospital and Chang Gung University College of Medicine, Kaohsiung 83301, Taiwan*
[2]*Department of Speech-Language Pathology, Duquesne University, Pittsburgh, PA 15282, USA*
[3]*Department of Audiology and Speech Language Pathology, Mackay Medical College, Taipei 10449, Taiwan*
[4]*Department of Otorhinolaryngology, Head and Neck Surgery, University of Malaya, 506030 Kuala Lumpur, Malaysia*
[5]*Department of Otolaryngology, Seoul National University College of Medicine, Seoul 110-744, Republic of Korea*
[6]*ENT Departments, Hôpital Femme-Mère-Enfant and Edouard Herriot University Hospitals, Claude Bernard University, 69003 Lyon, France*

Correspondence should be addressed to Seung-Ha Oh; shaoh@snu.ac.kr

Received 19 April 2015; Accepted 19 April 2015

The prevalence of hearing loss (presbycusis) is 35–50% in those aged 65 years or older; consequently, hearing assistant devices become more and more important [1]. Cochlear implantation (CI) is believed to be one of the most important technologic achievements to have occurred in the 20th century for the treatment of profound hearing loss, continually improved since its approval by the International Consensus Conference in 1995 [2]. Recent advances in biology and medicine have introduced new concepts in the study of CI and its related science. Many changes have taken place including improvements in hardware technique, expansion of candidacy, and clinical outcome. The cornucopia of all novel technologies and approaches serves as important blessings for hearing-impaired people. This special issue is to exhibit the diversity and advances in recent progress that contributes to the different subspecialties of CI and its related science.

It has motivated intense investigation on developing stem cell therapy as a new therapeutic strategy, for example, through the transplantation of stem cells into the inner ear for hearing restoration [3]. H.-C. Chen et al. investigated the long-term effect of hypoxia on stemness and the bioenergetic status of cochlear stem/progenitor cells cultured at different low oxygen tensions.

Recent advances in hearing preservation studies have introduced new concepts and technologies to be applied in CI [4, 5]. To develop skills sufficient for hearing preservation CI surgery, surgeons need to perform several electrode insertion trials in ex vivo temporal bones, thereby consuming relatively expensive electrode carriers. J.-P. Kobler et al. design low-cost dummy electrodes that are cheap alternatives for surgical training and for in vitro, ex vivo, and in vivo research purposes. P. T. Bhatti et al. also present an effective method for tailoring the flexibility of a commercial thin-film polymer electrode array for intracochlear electrical stimulation.

The benefits of residual hearing preservation in cochlear implant recipients have promoted the development of atraumatic surgeries. The surgeons prefer round window approach to preserve low frequency hearing [6]. The incidence and severity of intracochlear trauma were not influenced by electrode array insertion through the anterosuperior or anteroinferior quadrant of the round window membrane.

A bone-anchored hearing aid (BAHA) or bone-anchored hearing device is a type of hearing aid based on bone conduction [7, 8]. They are more expensive than conventional hearing aids, and their placement involves invasive surgery which carries a risk of complications [8]. The use of a wide fixture implant and the nonskin thinning surgical technique indicates that the combination is a safe procedure with good stability and no abutment losses in M. Hultcrantz's research.

The diagnostic value of high resolution computed tomography (HRCT) and magnetic resonance imaging (MRI) before CI is very high [9]. M. Busi et al. suggest that CI is a safe and effective procedure even for patients with brain and inner ear abnormalities at neuroimaging investigations with HRCT and MRI. Nonetheless, common cavity and stenosis of the internal auditory canal (less than 2 mm) are negative prognostic factors even if brain lesions are absent.

Limiting the assessment of CI performance strictly to speech perception improvement does not properly evaluate the characteristics of the prosthesis-neural interface. Electrophysiological testing should provide a more accurate proxy of the interaction between the electrodes of the CI and the auditory neurons. F. Venail et al. modeled the activation of auditory neurons in CI recipients. Distribution of Neural Responses Telemetry residues could provide a proxy of auditory neurons functioning in implanted cochleas.

The outcome of CI varies over a wide range among pediatric patients [10]. M. Park et al. assess the correlation between performance intelligence and postoperative CI outcome. Performance intelligence, especially social cognition, was strongly related to the postoperative CI outcome. Therefore, auditory rehabilitation, including social rehabilitation, should maximize the postoperative CI outcomes.

According to H.-S. Hsieh et al., implanted children tend to write stories that are shorter, worse organized, and without a plot, while formulating morphosyntactically correct sentences. Special attention is required on their auditory and language performances, which could be the underlying causes of the written language problems.

In this special issue, we collected both basic and clinical original research articles stimulating the continuing efforts to understand the cochlear implant technology, the development of strategies to treat deafness, and the evaluation of outcomes. It is our wish to increase interest in CI and its related science research with this special issue and further accelerate the development of novel therapies for hearing impairment.

Acknowledgments

Finally, as guest editors, we thank all authors, the editors, and anonymous reviewers who have contributed to the special issue.

Chung-Feng Hwang
Yang Chen
Hung-Ching Lin
Prepageran Narayanan
Seung-Ha Oh
Eric Truy

References

[1] K. Parham, B. J. McKinnon, D. Eibling, and G. A. Gates, "Challenges and opportunities in presbycusis," *Otolaryngology—Head and Neck Surgery*, vol. 144, no. 4, pp. 491–495, 2011.

[2] K. Jaekel, B. Richter, and R. Laszig, "The history of cochlear implantation: from Volta to multichannel-intracochlear stimulation," *Laryngo-Rhino-Otologie*, vol. 81, no. 9, pp. 649–658, 2002.

[3] K. Nishimura, T. Nakagawa, K. Ono et al., "Transplantation of mouse induced pluripotent stem cells into the cochlea," *NeuroReport*, vol. 20, no. 14, pp. 1250–1254, 2009.

[4] W. Gstoettner, J. Kiefer, W.-D. Baumgartner, S. Pok, S. Peters, and O. Adunka, "Hearing preservation in cochlear implantation for electric acoustic stimulation," *Acta Oto-Laryngologica*, vol. 124, no. 4, pp. 348–352, 2004.

[5] P. C. Miranda, A. L. Sampaio, R. A. Lopes, A. Ramos Venosa, and C. A. Oliveira, "Hearing preservation in cochlear implant surgery," *International Journal of Otolaryngology*, vol. 2014, Article ID 468515, 6 pages, 2014.

[6] H. Skarzynski, A. Lorens, A. Piotrowska, and I. Anderson, "Preservation of low frequency hearing in partial deafness cochlear implantation (PDCI) using the round window surgical approach," *Acta Oto-Laryngologica*, vol. 127, no. 1, pp. 41–48, 2007.

[7] R. M. Janssen, P. Hong, and N. K. Chadha, "Bilateral bone-anchored hearing aids for bilateral permanent conductive hearing loss: a systematic review," *Otolaryngology—Head and Neck Surgery*, vol. 147, no. 3, pp. 412–422, 2012.

[8] R. Banga, R. Lawrence, A. Reid, and A.-L. McDermott, "Bone-anchored hearing aids versus conventional hearing aids," *Advances in Oto-Rhino-Laryngology*, vol. 71, pp. 132–139, 2011.

[9] R. Bettman, E. Beek, A. Van Olphen, F. Zonneveld, and E. Huizing, "MRI versus CT in assessment of cochlear patency in cochlear implant candidates," *Acta Oto-Laryngologica*, vol. 124, no. 5, pp. 577–581, 2004.

[10] C.-F. Hwang, H.-C. Chen, C.-H. Yang, J.-P. Peng, and C.-H. Weng, "Comparison of Mandarin tone and speech perception between advanced combination encoder and continuous interleaved sampling speech-processing strategies in children," *American Journal of Otolaryngology—Head and Neck Medicine and Surgery*, vol. 33, no. 3, pp. 338–344, 2012.

Hindawi Publishing Corporation
BioMed Research International
Volume 2015, Article ID 394687, 10 pages
http://dx.doi.org/10.1155/2015/394687

Research Article

Modeling of Auditory Neuron Response Thresholds with Cochlear Implants

Frederic Venail,[1,2] Thibault Mura,[3,4] Mohamed Akkari,[1] Caroline Mathiolon,[1] Sophie Menjot de Champfleur,[5] Jean Pierre Piron,[1] Marielle Sicard,[1] Françoise Sterkers-Artieres,[6] Michel Mondain,[1,2] and Alain Uziel[1,2]

[1]*ENT Department and University Montpellier 1, University Hospital Gui de Chauliac, 34295 Montpellier, France*
[2]*Audiology Department I-PAudioM, INSERM U1051 Unit, Institute for Neurosciences of Montpellier, 34081 Montpellier, France*
[3]*Department of Medical Information and Biostatistics, University Hospital of Montpellier, Montpellier, France*
[4]*U 1061, CIC 1001, INSERM, 34295 Montpellier, France*
[5]*Neuroradiology Department, University Hospital Gui de Chauliac, 34295 Montpellier, France*
[6]*Audiophonology and Speech Disorders Department, Institute Saint Pierre, 34250 Palavas, France*

Correspondence should be addressed to Frederic Venail; frederic.venail@inserm.fr

Received 14 November 2014; Accepted 21 January 2015

Academic Editor: Chung-Feng Hwang

The quality of the prosthetic-neural interface is a critical point for cochlear implant efficiency. It depends not only on technical and anatomical factors such as electrode position into the cochlea (depth and scalar placement), electrode impedance, and distance between the electrode and the stimulated auditory neurons, but also on the number of functional auditory neurons. The efficiency of electrical stimulation can be assessed by the measurement of e-CAP in cochlear implant users. In the present study, we modeled the activation of auditory neurons in cochlear implant recipients (nucleus device). The electrical response, measured using auto-NRT (neural responses telemetry) algorithm, has been analyzed using multivariate regression with cubic splines in order to take into account the variations of insertion depth of electrodes amongst subjects as well as the other technical and anatomical factors listed above. NRT thresholds depend on the electrode squared impedance ($\beta = -0.11 \pm 0.02$, $P < 0.01$), the scalar placement of the electrodes ($\beta = -8.50 \pm 1.97$, $P < 0.01$), and the depth of insertion calculated as the characteristic frequency of auditory neurons (CNF). Distribution of NRT residues according to CNF could provide a proxy of auditory neurons functioning in implanted cochleas.

1. Introduction

Cochlear implants (CIs) allow the restoration of auditory perception through the direct electrical stimulation of the primary auditory neurons, located within the spiral ganglion of the cochlea. Typically, the outcome of CIs is assessed by evaluating the improvement in speech perception after implantation. However, speech perception is a high level function depending not only on CI functioning, but also on additional factors such as educational and speech therapy support after implantation, as well as the duration and cause of hearing loss, age, and educational level prior to it [1–3]. Thus, limiting the assessment of CI performance strictly to speech perception improvement does not properly evaluate the characteristics of the prosthesis-neural interface.

To study such an interface, electrophysiological testing should provide a more accurate proxy of the interaction between the electrodes of the CI and the auditory neurons. Among the different methods of measurements, electrically evoked compound action potentials (e-CAP) recorded within the CI may reflect this interaction. Indeed, the electrical current required to elicit an e-CAP may be directly correlated to neuronal density and excitability [4].

The use of e-CAP threshold recordings for CI fitting raised the interest of clinicians in the past 2 decades [5–7]. While correlations between psychophysical percepts and e-CAP thresholds with cochlear implant remain controversial, most authors agree that the "shape" of e-CAP thresholds represents a function of electrode position and follows

the same distribution than psychophysical thresholds and comfort levels (T- and C-levels, [5, 6]).

Therefore, measuring e-CAP thresholds may provide a more accurate evaluation of residual auditory neuron population than speech perception testing. However, while literature is sparse regarding the impact of additional cues on e-CAPs, it is reasonable to assume that unknown factors could influence e-CAP thresholds. Indeed, if we refer to general principles of other electrically stimulating devices, electrode impedance and the distance between the electrode and the neurons should affect e-CAP thresholds. Other cochlear specific factors like the size of the cochlea, the depth of insertion, scalar placement of the electrodes, and obviously the number of residual functional auditory neurons, eventually associated with age and the duration of profound hearing loss, may also influence e-CAP thresholds [8–13].

In the present study, we propose a statistical model to describe the interactions between the cochlear neural response elicited by electrical pulses and biophysical, clinical, as well as cochlear specific factors in cochlear implanted subjects.

2. Methods

2.1. Population Study. This study, conducted under IRB approval, included data from 536 active electrodes in 31 subjects implanted between 2006 and 2012 (14 males, 17 females, mean age 32.3 yrs ± 10.5, min 17 yrs, max 63 yrs). Hearing loss etiology was progressive sensorineural deafness in 11 cases, genetic deafness in 8 cases, autoimmune disease in 4 cases, ototoxic medication in 4 cases, otosclerosis in 3 cases, and viral meningitis in 1 case.

The age and duration of profound hearing loss were respectively 40.26 ± 23.20 yrs (min 0, max 80 yrs) and 5.30 ± 5.32 (min 1 yr, max 30 yrs). Mean age at cochlear implantation was 45.56 ± 23.35 (min 4 yrs, max 84 yrs).

The CIs used were Nucleus (Cochlear) devices: CI24 RE CA with contour advanced (perimodiolar curved electrode array, PMA) in 27 patients (462 electrodes, 86.2%); CI24 RE ST with straight electrode array (SA) in 2 patients (31 electrodes, 5.8%); and CI422 with slim straight electrode array (SSA) in the remaining 2 patients (43 electrodes, 8%).

Full insertion of the electrode array through a round window approach was performed in all cases. Patients requiring cochlear reimplantation were excluded in order to avoid any additional factors that could potentially alter the CAP threshold.

2.2. Electrophysiological Recordings. All recordings were performed at least 6 months following implantation to ensure the stabilization of impedance levels. Electrophysiological recordings were performed on each active electrode at the time of referral.

Impedance of the recording electrodes and CAP (neural response telemetry NRT) thresholds were recorded with Custom Sound 4.0 software (Cochlear). All subjects were stimulated using the advanced combinational encoder (ACE) strategy at stimulation rates ranging between 900 and 1200 Hz. The impedances (kOhms) were recorded in MP1+2 and NRT thresholds (current level, C.L.) determined by the auto-NRT function on each active electrode [14]. Biphasic pulses were used at 80 pps rate with pulse duration of 25 μs per phase and with an interpulse gap of 8 μs. The stimulation started at relatively low intensity (100 C.L.) to avoid overstimulation in awake subjects. The thresholds were confirmed by the Auto-NRT algorithm using an optimization loop with ascending and descending series of stimulation to refine the threshold assessments.

2.3. Imaging Study. Cone beam computed tomography was performed for every subject to evaluate the position of the electrode array in the cochlea (Newton 5G, 125 ∗ 125 ∗ 125 μm voxel size for reconstructions). Axial and midmodiolar reconstructions were performed to evaluate the size of the cochlea, the angle of electrode array insertion, the distance between each electrode and the modiolus and the scalar placement of the electrodes. On the axial reconstruction, the large diameter of the cochlea was calculated to estimate the length of the cochlea as described by Escudé et al. [15] (Figure 1(a)). The depth of insertion was estimated using the angle of insertion from the round window to the most apical electrode (Figure 1(b)). The distance between each electrode and the modiolus was calculated as the shortest distance (perpendicular) between the center of the electrode and the inner wall of the cochlea (Figures 1(c) and 1(d)). Midmodiolar reconstructions enabled the localization of the scalar position for each electrode, that is, within the scala tympani (ST) or the scala vestibuli (SV) (Figures 2(a) and 2(b)).

The theoretical characteristic frequency of the neurons stimulated by each electrode contact was calculated using the Greenwood function modified by Stakhovskaya et al. [16], with the following parameters: cochlear duct length (CDL), insertion depth, electrode array length, and distance between electrode contacts for every electrode array subtype.

The CDL was calculated as described by Escudé et al. [15] by applying the following formula $\mathrm{CDL} = 2.62A * \ln(1 + \theta/235) = 4.3259A$; with A equal to the length in mm of the large diameter of the cochlea (Figure 1(a)) and θ equal to the angle of a cochlea coiled on 2.75 turns (990°).

The relative position of each electrode was calculated as follows:

$$X_{e1} = \frac{\left(2.62A * \log\left(1 + \theta_{e1}/235\right)\right)}{\mathrm{CDL}},$$
$$X_{en} = \frac{\left[\left(2.62A * \log\left(1 + \theta_{e1}/235\right)\right) - Y_n\right]}{\mathrm{CDL}} \quad (1)$$

X_{e1} = relative position of electrode 1 according to CDL, X_{en} = relative position of electrode n according to CDL, θ_{e1} = angle of insertion of electrode 1, Y_n = distance between electrode 1 and electrode n (in mm, according to manufacturer's data).

Then the cochlear place-frequency map for n was calculated according to Greenwood's function [17] for each electrode as follows:

$$\mathrm{CF}_{\mathrm{neur}(n)} = 165.4 * \left(10^{2.1Z_{en}} - 0.88\right), \quad (2)$$

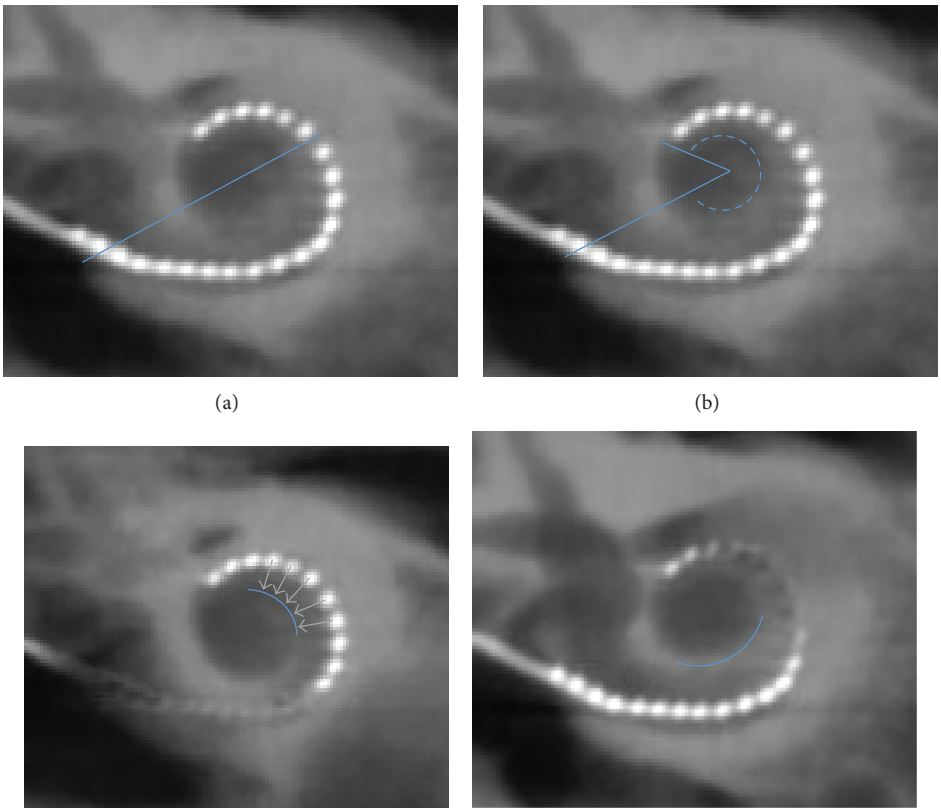

(a) (b) (c) (d)

Figure 1: Calculation of the depth of insertion and distance between electrodes and the inner wall of the cochlea. (a) On an axial reconstruction, the large diameter of the cochlea was calculated to estimate the length of the cochlea as described by Escudé et al. (b) On an axial reconstruction, the angle of electrode array insertion was defined as that between the tangeant lines touching the most apical and the most basal electrodes. (c) On the same reconstruction, the distance between each electrode and the inner wall of the cochlea (outlined in blue) was calculated as the shortest orthogonal distance. (d) This calculation was repeated on several reconstructions to evaluate the whole electrode array.

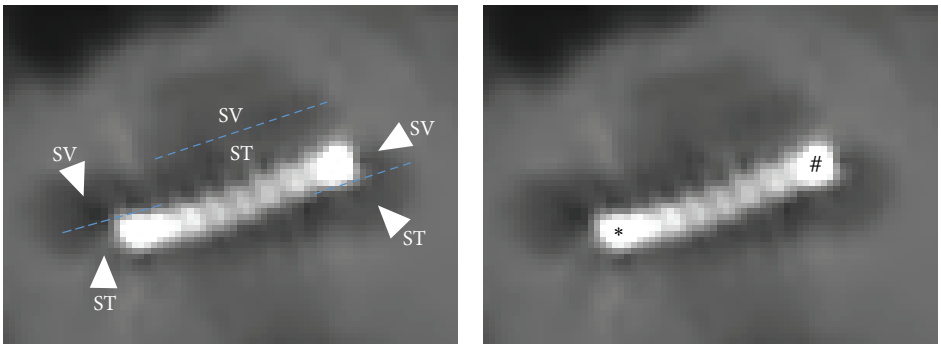

(a) (b)

Figure 2: Midmodiolar reconstruction of cochlea implanted with contour advanced electrode array. (a) Several reconstructions were performed around the midmodiolar axis to evaluate the position of each electrode. After segmentation, each turn of the cochlea was separated into scala tympani (ST) or scala vestibuli (SV) compartments. (b) On this reconstruction we can see a scala vestibuli mislocation of the electrode array. Indeed the basal electrode (*) is clearly located in the SV at the level of the first turn of the cochlea, whereas the apical one (#) is localized in the SV of the first turn of the cochlea.

with $CF_{neur(n)}$ = characteristic neuron frequency at the position of the electrode n, Z_{en} = relative position of the neurons connected to the hair cells at the position X_{en}.

Z_{en} was calculated using Stakhovskaya's formula [16].

$$Z_{en} = \frac{100}{\left[1 + (23/x_{en} - x_{en}/0.0099 + 0.76)^2\right]}. \quad (3)$$

2.4. Statistical Analysis. The characteristics of patients included in the present study are described with proportions for categorical variables and with mean and Standard Deviation (SD) values for continuous variables. When several measurements were made for a same subject, the mean of the average value for each subject was computed along with a within-subject SD (as described by Bland and Altman [18]) and between subject SD (on the average value of each subject). Interactions between NRT thresholds and neuron frequency per electrode were described graphically with mean and standard error of the mean (SEM).

Interactions between NRT threshold and demographical, clinical, and technical (of the CI) parameters were analyzed using a univariate linear mixed model to account for correlation between the repeated measurements of each subject (measurements of 22 different electrodes in the same subject, causing within-subject SD). For quantitative parameters, different types of relations were tested: linear, quadratic, cubic and polynomial. The type of association that maximized the Bayesian Index Criteria (BIC) was chosen to analyze the NRT threshold as a function of auditory neuron characteristic frequency. In order to model the complexity of the relation between NRT threshold and the characteristic neural frequency, we used a piecewise polynomial regression mixed model with cubic basis with two knots at 5000 and 10000 Hz using SAS PROC MIXED [19]. To analyze independent relations between NRT threshold and these parameters we used a multivariate linear mixed model, which included all the parameters. All the mixed models included a subject-specific random intercept. Significance of fixed effects was tested using the Wald Test. The relation between NRT threshold and the characteristic neural frequency is represented graphically with 95% confidence intervals. All statistical analyses were performed at the conventional two-tailed α level of 0.05 using the SAS statistical software (SAS Enterprise Guide 4.1, SAS Institute, Cary, N.C.).

3. Results

3.1. Analysis of Inter and Intra-Individual Variations of NRT Thresholds. In our population study, the mean impedance value was 8.71 kOhms (within subject SD 1.60, between subject SD 2.05, min 2.86, max 19.07 kOhms). Raw data from NRT thresholds spanned from 105 to 244 current levels (C.L., mean 169.68, within subject SD 13.66, between subject SD 18.60). The analysis of NRT thresholds electrode by electrode could not be summarized in a linear, quadratic, cubic, logarithmic or exponential relationship as shown in Figure 3.

We then evaluated the inter-individual variations of electrode arrays' insertion depth to determine if they could affect NRT thresholds. The average length of cochleae was 35.05 ± 4.68 mm (mean ± Standard Deviation consistently used throughout the text, min 26.38, max 43.42 mm). The mean depth of insertion of the electrode array was 343 ± 24 degrees (min 275, max 360°). According to the type of electrode array, mean insertion was 346 ± 22° with the PMA, 312 ± 46° with the SA, and 335 ± 35° with the SSA. All patients implanted with either an SA (CI24 ST) or an SSA (CI422) displayed the entire electrode array within the scala tympani, whereas 35.48% of patients with a PMA (CI24 CA) displayed a translocation of the electrode array within the scala vestibuli (Figure 2).

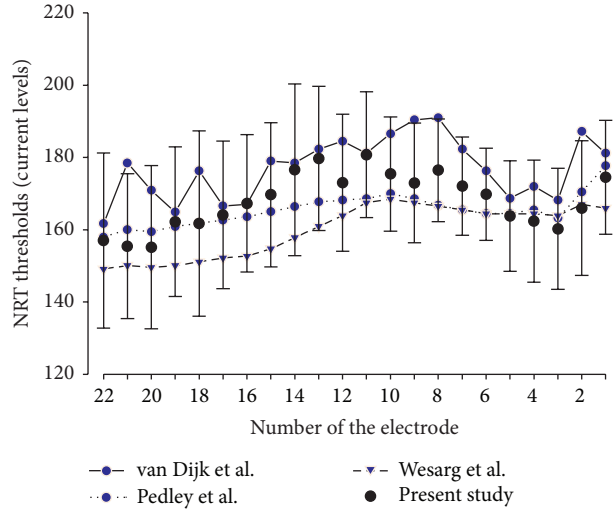

Figure 3: Mean NRT thresholds (±Standard Deviation) as a function of electrode number. Large interindividual variations of NRT threshold levels may be observed on the same electrode. No linear relationship is observed between NRT and electrode number as previously published.

Considering that the observed inter-individual variations in depth of insertion may account for variations in NRT threshold, we plotted the NRT thresholds as a function of depth of insertion, calculated as the characteristic frequency of auditory neurons in the spiral ganglion (Figure 4). We transformed the variable depth of insertion (%) into characteristic frequency of auditory neurons (Hz) in order to use this variable for the modeling of the NRT thresholds using different types of regression models. Additionally, utilizing the report of characteristic frequency of auditory neurons instead of percentage of insertion depth allowed the use of a semi-logarithmic scale, which is more relevant for clinical application than relative depth of insertion.

As shown in Figure 4, the position of the electrode array within the cochlea may vary across subjects with a mean auditory neuron frequency ranging from a third to a full octave for the same electrode. Plotting NRT thresholds against characteristic neuron frequency for each electrode (Figure 5(a)) revealed the large variability of both NRT threshold and frequency for the same electrode, arguing against the use of electrode number as an independent variable. We therefore decided to use characteristic neuron frequency instead of

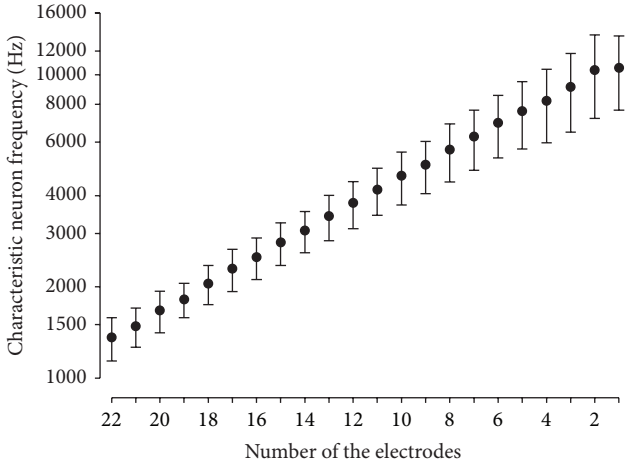

Figure 4: Mean characteristic auditory neuron frequency (±Standard Deviation) as a function of electrode number. Mean auditory frequency follows a linear relationship with electrode number, with a frequency increasing along with the number of the electrode. However, standard deviation bars show that the same frequency may be stimulated by up to 5 adjacent electrodes depending on the subject, thus arguing against the use of the electrode number to accurately evaluate insertion depth.

electrode number in this study to provide a more accurate idea of electrode positioning within the cochlea (Figure 5(b)).

3.2. Statistical Analyses and Modeling of NRT Thresholds. First, a univariate linear mixed model was used to measure the effect of numerical variables (age at test, age of profound deafness, duration of profound deafness, age at implantation, impedance, distance electrode-lamina spiralis) and categorical variables (electrode position: ST/SV, type of electrode array: Slim Straight/Perimodiolar/Straight etiology of hearing loss: Progressive SNHL/Viral/Genetic/Autoimmune/Ototoxic/Otosclerosis) on NRT thresholds.

Univariate analysis showed a significant association of NRT thresholds with squared distance ($P = 0.02$) and a substantial although not significant association with squared impedance ($P = 0.09$). A significant ($P = 0.04$) negative association was found in subjects with ototoxic exposure. No association was found with age at evaluation, implantation or profound deafness, duration of the profound deafness, scalar position, and the type of electrode array (Table 1).

In order to model the complex relation between NRT threshold and the characteristic neural frequency, we used a piecewise polynomial regression mixed model with cubic basis with two knots at 5000 and 10000 Hz. Results of univariate regression are shown in Figure 6(a). After a steep increase of NRT between 500 and 3000 Hz, NRT thresholds dropped in the 4000–5000 Hz region before displaying a dome-like shape curve with a peak around 10000 Hz.

Using the same model, a multivariate analysis was performed to take into account the combined effects of numerical (including characteristic neural frequency) and categorical variables altogether. The multivariate model showed that

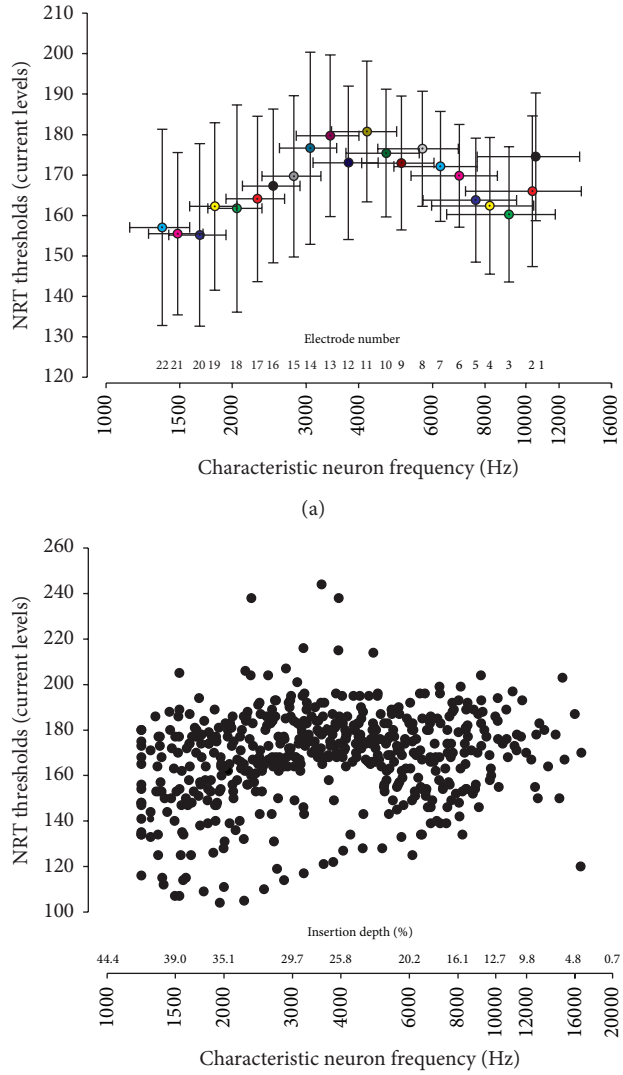

Figure 5: Mean NRT thresholds (±Standard Deviation) and mean characteristic auditory neuron frequency (±Standard Deviation) as a function of electrode number. Displaying NRT thresholds as a function of auditory neuron frequency for each electrode (a) clearly reveals the large variation of both NRT and frequency for the same electrode. Thus, a precise assessment requires the consideration of each electrode individually as a single point of coordinates (frequency, NRT), rather than the use of the electrode number (b).

NRT thresholds were negatively correlated (NRT threshold decreasing with an increasing variable value) with the scalar placement in the scala tympani ($P < 0.01$), and with the impedance of the electrodes ($P < 0.01$). This reveals that scala tympani placement of the electrode array led to a mean decrease of 8.50 ± 1.97 C.L. in NRT thresholds by comparison with scala vestibuli placement (Table 1). Every 1 kOhm elevation of electrode impedance resulted in a mean NRT threshold decrease of 0.11 ± 0.02 C.L. (Table 1).

Table 1: Parameter estimates of the linear mixed model evaluating the relation between neural response thresholds and demographical, clinical, and technical factors.

Fixed effect	Univariate analysis		Multivariate analysis	
	Crude β-estimate* (SE)	P value†	Adjusted β-estimate* (SE)	P value†
Age at test	0.13 (0.13)	0.31	0.29 (0.19)	0.11
Age of profound deafness	0.06 (0.12)	0.58	‡	—
Duration of profound deafness	−0.54 (0.48)	0.26	−0.17 (0.64)	0.78
Age at implantation	0.03 (0.11)	0.77	‡	—
Impedance ∗ impedance	**−0.03 (0.01)**	**0.09**	**−0.11 (0.02)**	**<0.01**
Distance ∗ distance	3.43 (1.44)	0.02	2.20 (1.46)	0.13
Neuron frequency	**Figure 6(a)**	**<0.01**	**Figure 6(b)**	**<0.01**
Position				
Scala vestibuli	**ref**		**ref**	
Scala tympani	**−0.21 (1.99)**	**0.91**	**−8.50 (1.97)**	**<0.01**
Electrode array				
Slim Straight	ref		ref	
Perimodiolar	−5.11 (12.95)	0.69	−5.94 (16.26)	0.71
Straight	1.02 (17.72)	17.72	13.43 (22.07)	0.54
Etiology of hearing loss				
Progressive SNHL	ref		ref	
Viral	0.53 (17.61)	0.97	2.55 (21.24)	0.90
Genetic	−5.36 (6.24)	0.39	−3.44 (7.22)	0.63
Autoimmune	−8.22 (9.74)	0.40	−10.50 (11.94)	0.37
Ototoxic	−19.34 (9.79)	0.04	−24.33 (13.24)	0.06
Otosclerosis	−2.23 (11.00)	0.83	−4.09 (13.45)	0.76

SE: standard error.

*β-estimate: mean increase in NRT threshold according to the increase of one unit of the considered quantitative explanatory variable. For qualitative explanatory variables, the β-estimate is the mean difference in NRT compared to the reference category (ref).

†β-estimates were compared to the value 0; a corresponding P value <0.05 indicates a significant association between NRT and the explanatory variable.

‡"Age of profound deafness" and "Age at implantation" were not entered into the multivariate model because of their high colinearity with "Age at test."

In this multivariate analysis, no significant effect was found for the etiology of the hearing loss, the type of electrode array, the age at evaluation, implantation or profound deafness, or the duration of profound deafness. Although a close to significance, multivariate analysis did not support the significant difference found either for the ototoxic exposure ($P = 0.06$) in univariate analysis, or for the distance between each electrode and the inner wall of the cochlea ($P = 0.13$) (Table 1).

The relation between NRT thresholds and characteristic neuron frequency after adjustment on significant variables (squared impedance and scalar position) is represented in Figure 6(b). In addition to a similar "double bump" aspect of the univariate regression curve described above, a trend to an elevated threshold along with the characteristic neuron frequency was observed.

4. Discussion

Previous studies have failed in their attempts to correlate speech perception thresholds with most of the electrophysiological measurements performed with a CI [20, 21]. Indeed, speech perception not only relies on the efficacy of the electrical stimulation, but also involves central auditory pathways in addition to brain language areas and networks [1–3]. However, it is reasonable to assume that more specific psychoacoustical perceptions, like enhanced loudness growth or pitch perception [11, 12, 22] are directly linked to the activation of the residual auditory neurons by the electrical stimulation delivered by the electrode array. Indeed Cohen [12] and Kirby et al. [23] clearly showed that loudness growth function was proportional to e-CAP growth function, meaning that a stimulation with an increased current level causes an enhanced activation of auditory neurons, either directly by a recruitment of more neurons in the same region of the spiral ganglion, or indirectly by the spread of excitation of the electrical stimulation. However, e-CAP amplitude does not directly predict loudness, since it depends on additional factors discussed hereafter.

The relation between the electrodes and the neurons depends not only on the electrode array itself, but also on its insertion into the cochlea. Some authors recommend the use of perimodiolar arrays instead of straight arrays to favor a reduced NRT threshold. However, previous studies showed that perimodiolar placement of electrodes has no effect on NRT thresholds [24, 25], an observation consistent with our study.

On the other hand, perimodiolar arrays were associated with increased scala vestibuli mislocation in the present study and in several others [26, 27]. This type of mislocation does

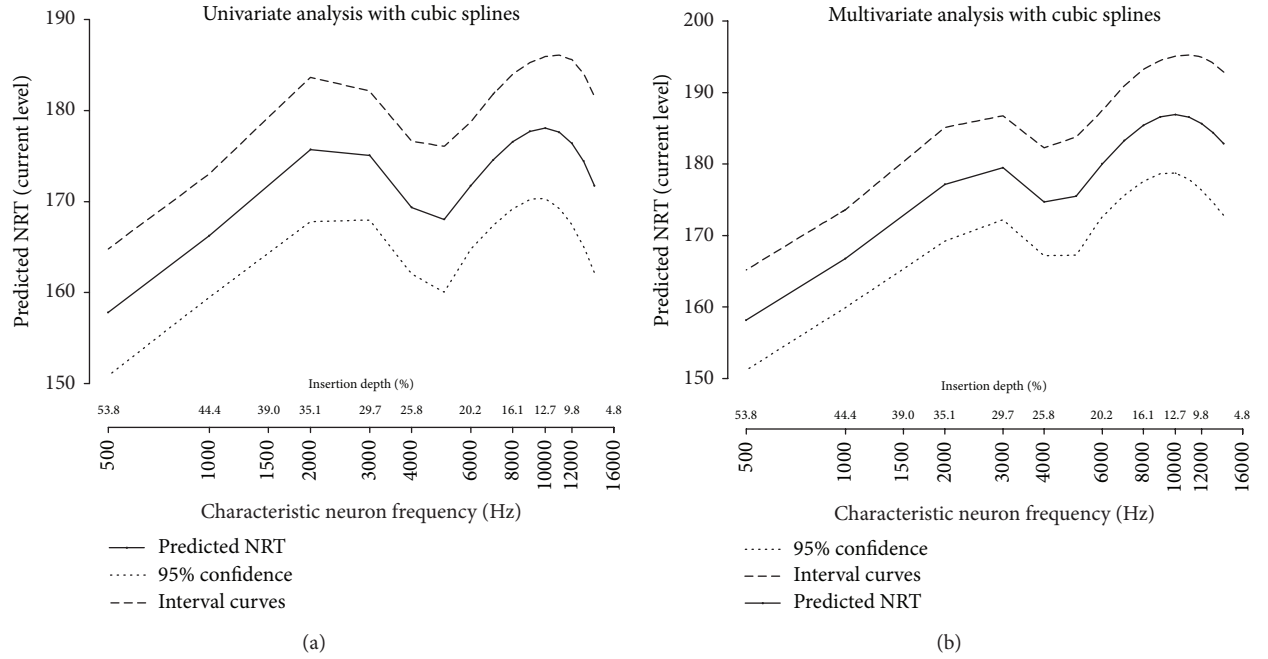

Figure 6: Modeling of NRT threshold as a function of characteristic auditory neuron frequency ((a): univariate regression, (b): multivariate regression including other variables). As can be seen, the prediction of NRT threshold level (black line) with 95% confidence interval (dashed lines), either univariate (a) or adjusted (b) for impedance and scalar placement (variables significantly associated with NRT threshold) shows an aspect of "double bump" curve with a trend to thresholds elevation along with the increase of characteristic frequency of auditory neurons.

jeopardize the preservation of residual hearing and yet the use of perimodiolar arrays remains appealing in cases where no residual hearing needs to be preserved. Thus, it is also important to determine whether the scalar placement (scala tympani or vestibuli) alone impacts NRT thresholds. In the present study, we found a negative effect of scala vestibuli positioning of the electrodes on NRT thresholds. Therefore, in addition to favoring cochlear structure preservation, scala tympani insertion appears to be an important factor to reduce NRT thresholds. Furthermore, we suggest that preservation of such cochlear structure is also beneficial for speech perception performances with CI [2].

In this present study, the insertions of electrode arrays (perimodiolar and straight) were performed using a round window approach. However, the perimodiolar contour advanced arrays were initially designed to be inserted through a cochleostomy. The insertion of perimodiolar arrays through the round window is responsible of a deeper insertion and of a shortest distance between the basal electrodes and the modiolus [28], but may result in even more damages of cochlear structures [29, 30]. Thus the surgical approach, in addition to the electrode array subtype, has to be taken into consideration for NRT thresholds variability.

Increase in electrode impedance has been suggested to reflect the degree of cochlear fibrosis [31]. Indeed, changes in impedance in the postoperative period, followed by stabilization between 3 and 12 months postoperatively support this fact [32]. Fibrotic scars can reduce the performance of CIs by raising the threshold stimulation levels and energy consumption of the implant. Surprisingly, we found that electrodes with higher impedance had a moderate but significant reduction of NRT thresholds (average reduction of 0.11 C.L. per kOhm), regardless of the type of array or depth of insertion. Thus, it is conceivable that the fibrotic tissues surrounding the electrode array may contribute to focus the electrical current to the nearest wall of the cochlea and that the excitation does not spread into the spaces filled with perilymph. This reduction of NRT threshold could also be explained by a measurement artifact. Indeed, high impedance electrodes require more voltage to deliver the same current intensity. In this NRT recording paradigm, one cannot eliminate the effect of voltage in addition to current on either the generation of e-CAP measurements or on the recording by the automatic threshold detection algorithm. Similar variations of algorithm detection sensitivity have already been noticed by van Dijk et al. [14] and Wesarg et al. [33] when changing the pulse rate (80 versus 250 pps) and by consequences the charges per second.

Interestingly, we found a non-, but nearly, significant effect of the distance between the electrodes and the medial wall of the cochlea (where the spiral ganglion neurons are located) on NRT thresholds. The lack of statistical significance could reflect a limitation of our study, such as a lack of sensitivity of the CT cone beam reconstruction measurements to accurately evaluate this distance. In accordance with the role of electrode modiolus-distance, Holden et al. [2] found that a reduced distance between the electrodes and the modiolus, evaluated with cone beam imaging, could

increase speech perception. Additional histological studies on implanted temporal bone specimens need to be conducted to further address this point.

Unlike speech perception results [1, 3], age at implantation, duration, and age of profound hearing loss had no significant effect on NRT thresholds. This observation supports the fact that these variables may act directly on the central auditory pathways and language areas with little or no effect on the peripheral auditory system.

In the present study, we found no impact of hearing loss etiology on NRT thresholds, despite a nearly significant effect of ototoxic exposure (drugs). This is consistent with the fact that aminoglycosides affect preferentially hair cells and stria vascularis and have minimal effects on auditory neuron survival (reviewed in [34]). Other deafness etiologies like otosclerosis, age-related hearing loss, genetic mutation, or noise may affect hair cells, the stria vascularis and neurons. Consequently, a more specific phenotyping would be necessary to identify specific cases in which auditory neurons are less damaged.

Only few studies have reported that speech perception outcomes may be related to etiology of hearing loss (reviewed in [3]). More particularly, some etiologies that affect cochlear anatomy, such as meningitis causing fibrosis, lead to poorer scores than Menière's disease, in which loss of neurons occurs later on [35]. This observation fits with our model, in which we studied separately the impact of etiology and the number of residual neurons through NRT thresholds. Our findings suggest that differences in speech perception outcome may be more connected to residual neurons than to the etiology of the loss of hearing itself.

In this study, we showed that NRT thresholds depend on the electrode depth of insertion into the cochlea.

While some studies report that NRT thresholds follow a base-apex gradient [36, 37], with basal electrodes near to the high frequency neurons displaying higher thresholds than apical electrodes placed closer to low-medium frequency neurons, others found no linear distribution of NRT thresholds [6, 14, 33, 38, 39] (see examples in Figure 3).

These differences could be explained by the number of electrodes used, instead of characteristic neuron frequency, resulting in an inaccurate localization of the electrode in the cochlea, in addition to a large variation of electrode positioning amongst subjects. As we have demonstrated, the depth of insertion of the electrode array, as well as the size of the cochlea, may vary between subjects and thus, estimation of the electrode depth of insertion using electrode number is insufficiently accurate.

In the present study, we noticed a "double bump" aspect of the relation between NRT thresholds and insertion depth, in addition to a moderate decrease of thresholds from the base to the apex of the cochlea. This report is to date, the first one using a multivariate analysis to describe separately the contribution of electrode insertion depth in addition to other factors on NRT thresholds values.

Assuming that the predicted NRT thresholds, calculated as a residual value of multivariate analysis, reflect indirectly the excitability level of the remaining auditory nerve fibers, one should expect that those values are a proxy of the functional auditory neuron population in the spiral ganglion neuron of implanted patients [4]. However, it is unclear why the obtained curve displays a "double bump" aspect with an elevation of thresholds at 10000 Hz (12.7% or 126° of cochlear length) and 3000 Hz (29.7% or 294° of cochlear length). Using perimodiolar arrays, Marx et al. [27] showed that a traumatism causing vestibular translocation of the electrode array may occur around 90–270° of insertion in 30% of cases. Thus, elevation of NRT thresholds may be caused by the traumatism of insertion, but does not explain the "double bump" ascending aspect of the curve, with a drop of NRT threshold at 4000 Hz.

Interestingly, the hearing sensitivity curve (ISO 226-2003 norm) of normal hearing individuals also displays a "double bump" ascending aspect of the curve by 500 Hz, with an increased sensitivity at 4000 Hz. Even if the hearing sensitivity of normal hearing individuals cannot be compared to the hearing sensitivity of implanted patients, it can be proposed that the increased sensitivity observed around 4000 Hz in normal hearing people relies, at least partially, on an increased capacity to recruit auditory neurons at this frequency, a hypothesis supported by our data in cochlear implant recipients.

Therefore, comparing the NRT threshold profiles of patients using our modeling might help in detecting subjects with abnormal neuron activation, and identify instances of auditory neuropathies or severe auditory neuron loss. This neuronal loss, in addition to personal or environmental factors (such as the duration of hearing loss, age of deafness, educational level, and speech therapy suppor) independent of cochlear implant characteristics, might explain cases of poor speech perception outcomes. Nevertheless, further histological studies will be needed to confirm this hypothesis.

5. Conclusion

With CIs, NRT thresholds vary according to the scalar placement of electrodes and their impedance. Scala tympani insertion is required not only to preserve residual hearing and cochlear structures, but also to improve the sensitivity of cochlear neurons.

Perimodiolar arrays did not display any advantage over straight arrays with regards to NRT thresholds and are associated with more frequent misplacement into the scala vestibuli. NRT thresholds, adjusted for scalar placement and impedance, may reflect auditory neuron sensitivity across the cochlea.

Ultimately, analyses of NRT thresholds might provide further information on the number of residual auditory neurons in each part of the cochlea and enable the evaluation of prosthetic-neural interface quality and consequential efficacy.

Conflict of Interests

The authors declare that there is not conflict of interests.

References

[1] P. Blamey, F. Artieres, D. Başkent et al., "actors affecting auditory performance of postlinguistically deaf adults using

cochlear implants: an update with 2251 patient," *Audiology & Neurotology*, vol. 18, no. 1, pp. 36–47, 2013.

[2] L. K. Holden, C. C. Finley, J. B. Firszt et al., "Factors affecting open-set word recognition in adults with cochlear implants," *Ear and Hearing*, vol. 34, no. 3, pp. 342–360, 2013.

[3] D. S. Lazard, C. Vincent, F. Venail et al., "Pre-, per- and postoperative factors affecting performance of postlinguistically deaf adults using cochlear implants: a new conceptual model over time," *PLoS ONE*, vol. 7, no. 11, Article ID e48739, 2012.

[4] W. Lai and N. Dillier, "Neural adaptation and the ECAP response threshold: a Pilot Study," *Cochlear Implants International*, vol. 10, supplement 1, pp. 63–67, 2009.

[5] R. Kaplan-Neeman, Y. Henkin, Z. Yakir et al., "NRT-based versus behavioral-based map: a comparison of parameters and speech perception in young children," *Journal of Basic and Clinical Physiology and Pharmacology*, vol. 15, no. 1-2, pp. 57–69, 2004.

[6] K. Pedley, C. Psarros, K. Gardner-Berry et al., "Evaluation of NRT and behavioral measures for MAPping elderly cochlear implant users," *International Journal of Audiology*, vol. 46, no. 5, pp. 254–262, 2007.

[7] L. G. Potts, M. W. Skinner, B. D. Gotter, M. J. Strube, and C. A. Brenner, "Relation between neural response telemetry thresholds, T- and C-levels, and loudness judgments in 12 adult nucleus 24 cochlear implant recipients," *Ear and Hearing*, vol. 28, no. 4, pp. 495–511, 2007.

[8] A. Botros and C. Psarros, "Neural response telemetry reconsidered: II. The influence of neural population on the ecap recovery function and refractoriness," *Ear and Hearing*, vol. 31, no. 3, pp. 380–391, 2010.

[9] S. Brill, J. Müller, R. Hagen et al., "Site of cochlear stimulation and its effect on electrically evoked compound action potentials using the MED-EL standard electrode array," *BioMedical Engineering Online*, vol. 8, article 40, 2009.

[10] K. M. S. Clay and C. J. Brown, "Adaptation of the electrically evoked compound action potential (ECAP) recorded from nucleus CI24 cochlear implant users," *Ear and Hearing*, vol. 28, no. 6, pp. 850–861, 2007.

[11] L. T. Cohen, "Practical model description of peripheral neural excitation in cochlear implant recipients: 3. ECAP during bursts and loudness as function of burst duration," *Hearing Research*, vol. 247, no. 2, pp. 112–121, 2009.

[12] L. T. Cohen, "Practical model description of peripheral neural excitation in cochlear implant recipients: 1. Growth of loudness and ECAP amplitude with current," *Hearing Research*, vol. 247, no. 2, pp. 87–99, 2009.

[13] M. K. Cosetti, W. H. Shapiro, J. E. Green et al., "Intraoperative neural response telemetry as a predictor of performance," *Otology & Neurotology*, vol. 31, no. 7, pp. 1095–1099, 2010.

[14] B. van Dijk, A. M. Botros, R.-D. Battmer et al., "Clinical results of AutoNRT, a completely automatic ECAP recording system for cochlear implants," *Ear and Hearing*, vol. 28, no. 4, pp. 558–570, 2007.

[15] B. Escudé, C. James, O. Deguine, N. Cochard, E. Eter, and B. Fraysse, "The size of the cochlea and predictions of insertion depth angles for cochlear implant electrodes," *Audiology and Neurotology*, vol. 11, supplement 1, pp. 27–33, 2006.

[16] O. Stakhovskaya, D. Sridhar, B. H. Bonham, and P. A. Leake, "Frequency map for the human cochlear spiral ganglion: implications for cochlear implants," *Journal of the Association for Research in Otolaryngology*, vol. 8, no. 2, pp. 220–233, 2007.

[17] D. D. Greenwood, "A cochlear frequency-position function for several species—29 years later," *Journal of the Acoustical Society of America*, vol. 87, no. 6, pp. 2592–2605, 1990.

[18] J. M. Bland and D. G. Altman, "Measurement error," *British Medical Journal*, vol. 313, no. 7059, p. 744, 1996.

[19] A. Edan, "Smoothing with SAS PROC MIXED," in *Proceedings of the 28th SAS User Group International*, p. 268, Washington, DC, USA, 2003.

[20] K. Seyle and C. J. Brown, "Speech perception using maps based on neural response telemetry measures," *Ear and Hearing*, vol. 23, no. 1, supplement, pp. 72S–79S, 2002.

[21] S. Vlahović, B. Šindija, I. Aras, M. Glunčić, and R. Trotić, "Differences between electrically evoked compound action potential (ECAP) and behavioral measures in children with cochlear implants operated in the school age vs. operated in the first years of life," *International Journal of Pediatric Otorhinolaryngology*, vol. 76, no. 5, pp. 731–739, 2012.

[22] M. L. Hughes and P. J. Abbas, "The relation between electrophysiologic channel interaction and electrode pitch ranking in cochlear implant recipients," *The Journal of the Acoustical Society of America*, vol. 119, no. 3, pp. 1527–1537, 2006.

[23] B. Kirby, C. Brown, P. Abbas, C. Etler, and S. O'Brien, "Relationships between electrically evoked potentials and loudness growth in bilateral cochlear implant users," *Ear and Hearing*, vol. 33, no. 3, pp. 389–398, 2012.

[24] S. van Weert, R. J. Stokroos, M. M. J. G. Rikers, and P. van Dijk, "Effect of peri-modiolar cochlear implant positioning on auditory nerve responses: a neural response telemetry study," *Acta Oto-Laryngologica*, vol. 125, no. 7, pp. 725–731, 2005.

[25] X. Xi, F. Ji, D. Han, M. Hong, and A. Chen, "Electrode interaction in cochlear implant recipients: comparison of straight and contour electrode arrays," *ORL*, vol. 71, no. 4, pp. 228–237, 2009.

[26] A. Aschendorff, J. Kromeier, T. Klenzner, and R. Laszig, "Quality control after insertion of the nucleus contour and contour advance electrode in adults," *Ear and Hearing*, vol. 28, no. 2, supplement, pp. 75S–79S, 2007.

[27] M. Marx, F. Risi, B. Escudé et al., "Reliability of cone beam computed tomography in scalar localization of the electrode array: a radio histological study," *European Archives of Oto-Rhino-Laryngology*, vol. 271, no. 4, pp. 673–679, 2014.

[28] O. F. Adunka, H. C. Pillsbury, and J. Kiefer, "Combining perimodiolar electrode placement and atraumatic insertion properties in cochlear implantation—Fact or fantasy?" *Acta Oto-Laryngologica*, vol. 126, no. 5, pp. 475–482, 2006.

[29] R. J. Briggs, M. Tykocinski, E. Saunders et al., "Surgical implications of perimodiolar cochlear implant electrode design: avoiding intracochlear damage and scala vestibuli insertion," *Cochlear Implants International*, vol. 2, no. 2, pp. 135–149, 2001.

[30] M. A. Souter, R. J. S. Briggs, C. G. Wright, and P. S. Roland, "Round window insertion of precurved perimodiolar electrode arrays: how successful is it?" *Otology & Neurotology*, vol. 32, no. 1, pp. 58–63, 2011.

[31] G. M. Clark, S. A. Shute, R. K. Shepherd, and T. D. Carter, "Cochlear implantation: osteoneogenesis, electrode-tissue impedance, and residual hearing," *The Annals of Otology, Rhinology & Laryngology. Supplement*, vol. 166, pp. 40–42, 1995.

[32] H. Jia, F. Venail, J.-P. Piron et al., "Effect of surgical technique on electrode impedance after cochlear implantation," *Annals of Otology, Rhinology and Laryngology*, vol. 120, no. 8, pp. 529–534, 2011.

[33] T. Wesarg, R.-D. Battmer, L. C. Garrido et al., "Effect of changing pulse rate on profile parameters of perceptual thresholds and loudness comfort levels and relation to ECAP thresholds in recipients of the Nucleus CI24RE device," *International Journal of Audiology*, vol. 49, no. 10, pp. 775–787, 2010.

[34] J. Schacht, A. E. Talaska, and L. P. Rybak, "Cisplatin and aminoglycoside antibiotics: hearing loss and its prevention," *Anatomical Record*, vol. 295, no. 11, pp. 1837–1850, 2012.

[35] U. Khetarpal and H. F. Schuknecht, "Temporal bone findings in a case of bilateral Meniere's disease treated by parenteral streptomycin and endolymphatic shunt," *Laryngoscope*, vol. 100, no. 4, pp. 407–414, 1990.

[36] A. Hagr, "Intra-operative neural response telemetry and acoustic reflex assessment using an advance-in-stylet technique and modiolus-hugging: a prospective cohort study," *Sultan Qaboos University Medical Journal*, vol. 11, no. 3, pp. 369–376, 2011.

[37] Y. Tian, W. Li, Z. Wang, N. Yang, L. Hui, and X. Jiang, "Site of cochlear stimulation and its effect on electrically evoked compound action potentials using the Nucleus24 cochlear implants," *Lin Chung Er Bi Yan Hou Tou Jing Wai Ke Za Zhi*, vol. 26, no. 22, pp. 1014–1019, 2012.

[38] A. Botros and C. Psarros, "Neural response telemetry reconsidered: I. The relevance of ecap threshold profiles and scaled profiles to cochlear implant fitting," *Ear and Hearing*, vol. 31, no. 3, pp. 367–379, 2010.

[39] L. Spivak, C. Auerbach, A. Vambutas, S. Geshkovich, L. Wexler, and B. Popecki, "Electrical compound action potentials recorded with automated neural response telemetry: threshold changes as a function of time and electrode position," *Ear and Hearing*, vol. 32, no. 1, pp. 104–113, 2011.

Hindawi Publishing Corporation
BioMed Research International
Volume 2015, Article ID 313274, 7 pages
http://dx.doi.org/10.1155/2015/313274

Research Article

The Relation between Nonverbal IQ and Postoperative CI Outcomes in Cochlear Implant Users: Preliminary Result

Mina Park,[1] Jae-Jin Song,[2] Seo Jin Oh,[3] Min-Sup Shin,[4] Jun Ho Lee,[1,5] and Seung Ha Oh[1,5]

[1]*Department of Otorhinolaryngology-Head and Neck Surgery, Seoul National University College of Medicine, Seoul National University Hospital, Seoul, Republic of Korea*
[2]*Department of Otorhinolaryngology-Head and Neck Surgery, Seoul National University Bundang Hospital, Seongnam, Republic of Korea*
[3]*Department of Psychiatry, Seoul National University Hospital, Seoul, Republic of Korea*
[4]*Department of Child Adolescent Psychiatry, Seoul National University College of Medicine, Seoul, Republic of Korea*
[5]*Sensory Organ Research Institute, Seoul National University Medical Research Center, Seoul, Republic of Korea*

Correspondence should be addressed to Seung Ha Oh; shaoh@snu.ac.kr

Received 27 November 2014; Accepted 5 January 2015

Academic Editor: Johan H. M. Frijns

Objectives. This study assessed the correlation between performance intelligence and the postoperative cochlear implant (CI) outcome in Korean-speaking children. In addition, the relationship between the performance intelligence subscales and the post-CI speech outcome was evaluated. *Materials and Methods*. Thirteen pediatric CI users (five males, eight females; median age at implantation 6.2 (range 1.3–14.2) years; median age at intelligence test 9.3 (range 5–16) years) who were tested using the Korean Educational Development Institute-Wechsler Intelligence Scale for children were studied. The correlations between the intelligence scores and 1-2 years postoperative Categories of Auditory Performance (CAP) scores and between subscales of performance and 1-2 years postoperative CAP scores were analyzed. *Results*. There was no correlation between the categories of verbal intelligence quotient (IQ) and performance IQ for "mentally retarded" and "average," respectively (Spearman's rho = 0.42, $P = 0.15$). There was a strong correlation between performance IQ and the postoperative CAP scale (Spearman's rho = 0.8977, $P = 0.0008$). "Picture arrangement" and "picture completion," reflecting social cognition, were strongly correlated with the postoperative CAP scales. *Conclusion*. Performance intelligence, especially social cognition, was strongly related to the postoperative CI outcome of cochlear implant users. Therefore, auditory rehabilitation, including social rehabilitation, should maximize the postoperative CI outcomes.

1. Introduction

Cochlear implant (CI) is a standard treatment option for children with profound hearing loss. However, the outcome of CI varies over a wide range among pediatric patients. Some prelingually deafened children show outstanding behavioral performance, such as the rapid acquisition of spoken language and the production of intelligible speech after years of CI-assisted rehabilitative effort, while other children develop awareness of environmental or speech sounds but never catch up with normal age-appropriate auditory language [1].

Therefore, it is relevant, both scientifically and clinically, to unravel the factors underlying the wide variability in CI outcome. Researchers have repeatedly suggested that demographic factors—such as age at the onset of severe-to-profound hearing loss, the duration of the severe-to-profound hearing loss, age at CI, and absence or presence of linguistic experience—are factors underlying the CI outcome variability [2–4]. Others have argued that the preoperative resting-state or task-driven cortical activity is a crucial indicator of an accurate individual prognosis [5–8].

In addition to these factors, recent studies have emphasized the role of the cognitive function of the subjects on the CI outcome [9]. Cognitive function tests consist of verbal and performance (nonverbal) tests. Since the feasibility of verbal testing is limited in deaf children, a performance test

that presents tasks visually is important when evaluating the cognitive function of deaf subjects [10, 11]. Concerning the relationship between cognitive function and CI outcome, a study of Mandarin-speaking children using CI reported that the verbal intelligence quotient (IQ) might not represent the true intelligence of CI users [7]. However, there is little information on the correlation between the performance IQ subscales and postoperative CI outcome.

Therefore, we assessed the correlation between the performance IQ and postoperative CI outcome in prelingually deafened pediatric CI users. We also determined the performance IQ subscales that are most relevant to the CI outcome in Korean-speaking CI users using the Korean Educational Development Institute-Wechsler Intelligence Scale for Children (KEDI-WISC) [12].

2. Materials and Methods

2.1. Subjects. Of the children who underwent CI at the Department of Otorhinolaryngology-Head and Neck Surgery, Seoul National University Children's Hospital, 18 prelingually deafened children who were subjected to the KEDI-WISC to evaluate their verbal and performance IQs between 16 April 2009 and 5 August 2013 were initially included in this study. Children who had severe inner ear anomalies, cochlear nerve aplasia/hypoplasia, or severe bony cochlear nerve canal narrowing on temporal bone computed tomography (CT) or internal auditory canal magnetic resonance imaging (MRI) were excluded. Of the 18 initially included children, 5 with full-scale IQs classified as "severe mental retardation (full-scale IQ < 40)" were excluded because their verbal and performance IQ scores were unreliable. This study was approved by the Institutional Review Board of Seoul National University Hospital (number 1409-088-609).

The 13 children ultimately included comprised five males and eight females. Their median ages at CI and the KEDI-WISC test were 6.2 (range 1.3–14.2) and 9.3 (range 5–16) years, respectively. All of the children had profound sensorineural hearing loss (>90 dB HL on pure-tone audiometry or auditory brainstem response) in both ears. Depending on the age and compliance of the subject, the auditory brain stem response or auditory steady-state response were evaluated, or play audiometry or visual reinforcement audiometry was performed. The demographic characteristics of the included children are summarized in Table 1.

Table 1: Demographic characteristics of the included patients.

Male/female	5 : 8
Side of implantation, R/L	9 : 4
Age at implantation (median)	1.3 years to 14.2 years (6.2 years)
Age at intelligence test (median)	5 years to 16 years (9.3 years)
Bilateral profound sensorineural hearing loss	13 (100%)
Etiology of deafness	
Unknown (no inner ear anomaly)	11 (84.6%)
Inner ear anomaly (Mondini malformation, EVAS)	2 (15.4%)
Linguistic, pre-/postlingual	13 : 0

2.2. Korean Educational Development Institute-Wechsler Intelligence Scale for Children. We administered the KEDI-WISC to assess the intellectual function of the 13 children. The KEDI-WISC, a modified version of the Wechsler Intelligence Scale for children, is an intelligence test for Korean-speaking children between the ages of 5 and 15 years [13, 14]. This test consists of two subsets: verbal IQ and performance IQ [13, 14]. Both the verbal and performance IQ parts of the test were administered to all study participants using a standardized procedure by two pediatric clinical neuropsychologists, each with more than 10 years of clinical experience. The instructions were given to all children in a loud voice, and most children were able to understand the task through their hearing aids or CI. The examiner demonstrated each task to ensure that the children understood the instructions.

The verbal IQ test evaluates "information," "similarities," "arithmetic," "vocabulary," and "comprehension," while the performance IQ test evaluates "picture completion," "picture arrangement," "block design," "object assembly," and "coding" (Table 2). Of the performance IQ subscales, "picture completion" and "picture arrangement" represent social cognition [15, 16], while "block design," "object assembly," and "coding" represent visual motor coordination [16, 17]. The total verbal and performance scores are obtained and can then be converted into the verbal and performance IQs by comparison with normative data for the general population of the same age. The full-scale IQ can be obtained by combining the verbal and performance IQs.

Using the verbal and performance IQ, intelligence is divided into seven categories: mentally retarded (IQ ≤ 69), borderline (70–79), low average (80–89), average (90–109), high average (110–119), superior (120–129), and very superior (≥130). Of note, an IQ ≤ 40 is categorized as "severely mentally retarded." An IQ of 80 separates the intelligence categories into borderline and low average (Table 3).

2.3. Post-CI Outcome. The post-CI outcome was measured using the postoperative Categories of Auditory Performance (CAP) scale 1-2 (median, 1) years postoperatively. The CAP scores indicate the following: CAP 0 (no awareness of environmental sounds), 1 (awareness of environmental sounds), 2 (response to speech sounds), 3 (identification of environmental sounds), 4 (discrimination of some speech sounds without lip-reading), 5 (understanding of common phrases without lip-reading), 6 (understanding of conversation without lip-reading), and 7 (use of a telephone with a known listener) [19].

2.4. Analysis of Possible Related Factors. To compare the scores of the five performance IQ subscales, the Kruskal-Wallis test was performed. The Mann-Whitney U-test was used to compare pairs of subscales. Spearman's rank correlation test was performed to examine the correlations between the verbal and performance IQs, between the performance

Table 2: The subsets of Korean Educational Development Institute-Wechsler.

Verbal IQ	
Information	A consecutive of orally presented questions that tap the child's general knowledge.
Similarities	A consecutive of orally presented of questions that ask how two words are alike or similar.
Arithmetic	A consecutive of arithmetic questions which the child solves mentally and gives answers.
Vocabulary	A consecutive of requirements that the child is asked to define a provided word.
Comprehension	A consecutive of questions about social situations or common concepts.
Performance IQ	
Picture completion	A series of pictures with a missing part, and the child is asked to identify the missing part by pointing and/or naming.
Picture arrangement	A series of pictures presented in an incorrect order, and the child is asked to place in the correct order to tell a story that makes sense.
Block design	A series of printed geometric pattern, and the child is asked to duplicate using red-and-white blocks.
Object assembly	A series of fragments of common objects, each presented in a standardized shape, and the child is asked to assemble to form a meaningful whole.
Coding	A series of simple shapes, each paired with a code. The child asked to draw the shape in its corresponding code.

Table 3: The diagnostic categories of intelligence quotient.

Category	Scaled score	IQ
Very superior	≥13	≥130
Superior	12	120–129
High average	11	110–119
Average	10	90–109
	9	
Low average	8	80–89
Borderline	7	70–79
Mental retardation	6	55–69: mild
	5	40–55: moderate
	<4	<40: severe

Adopted form [18].

IQ and postoperative CAP scores, and between each performance subscale and the postoperative CAP scores. Statistical significance was set at $P < 0.05$. All analyses were performed using the Statistical Package for the Social Sciences (SPSS) 21.0 (SPSS, Chicago, IL).

3. Results

3.1. Verbal, Performance, and Full-Scale IQ. The mean full-scale IQ of the 13 subjects was 74.5 ± 19.0 (range 47–113), falling in the category "borderline." When the full-scale IQ was subdivided into verbal and performance IQs, the mean verbal and performance IQs were 65.2 ± 21.2 (range 48–111) and 91.9 ± 17.5 (range 55–118), respectively. The categories of verbal and performance IQ were in the "mentally retarded" and "average" categories, respectively.

3.2. Subset Scores of the Performance IQ Test. The mean scores for the five subsets of the performance IQ test are shown in Figure 1. There was a significant difference among the scaled scores for the five performance IQ subscales

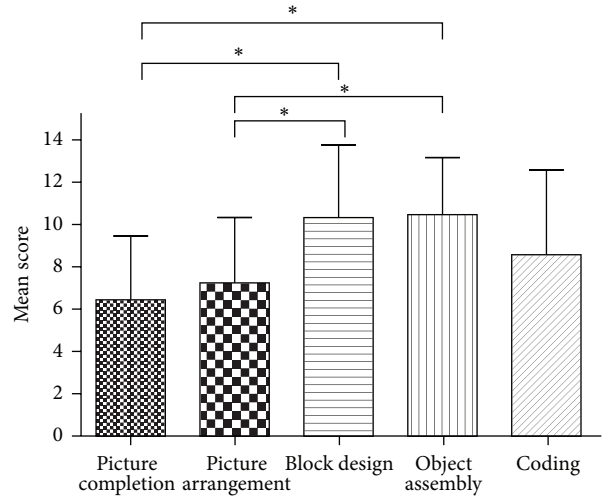

Figure 1: The mean (±SD) subscale scores for the performance IQ.

($P = 0.010$, Kruskal-Wallis test). *Post hoc* individual Mann-Whitney U-tests revealed significant differences between "picture completion" and "block design" ($P = 0.009$), "picture completion" and "object assembly" ($P = 0.002$), "picture arrangement" and "block design" ($P = 0.043$), and "picture arrangement" and "object assembly" ($P = 0.018$). That is, the scores of the "picture completion" and "picture arrangement" subscales, reflecting social cognition, were significantly lower than those of "block design" and "object assembly," reflecting visual motor coordination.

3.3. Correlation between Verbal and Performance IQs. Figure 2 shows the verbal and performance IQ data for each subject. The performance IQ was higher than the verbal IQ in all children, with a single exception (Figure 2(a)). There was no significant correlation between the verbal

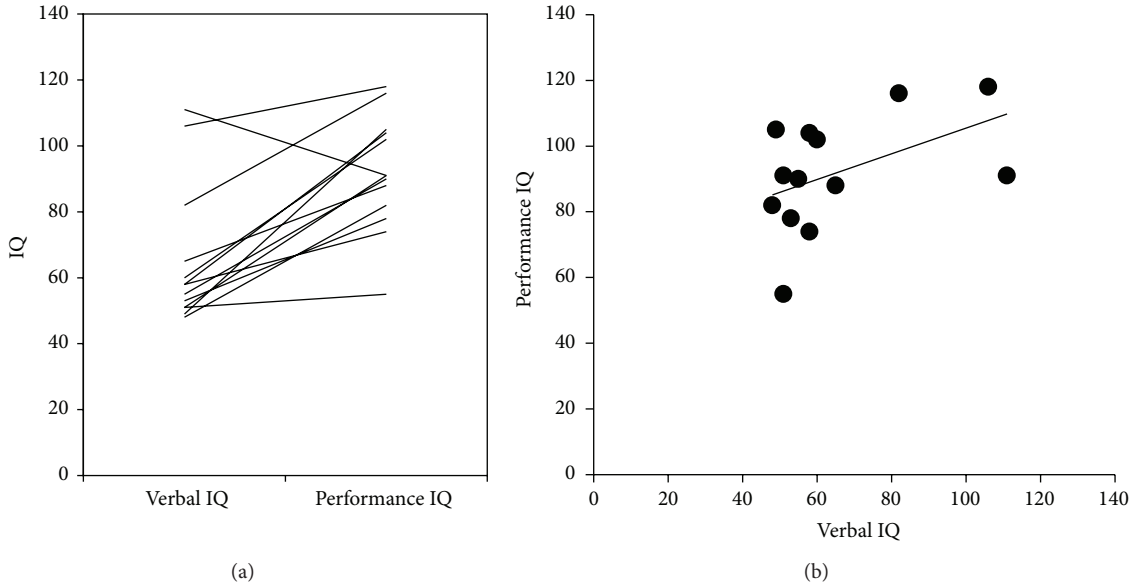

Figure 2: The raw data (a) and correlation (b) between the verbal and performance IQs. There was no correlation between the verbal and performance IQs (Spearman's rho = 0.4207, $P = 0.1523$).

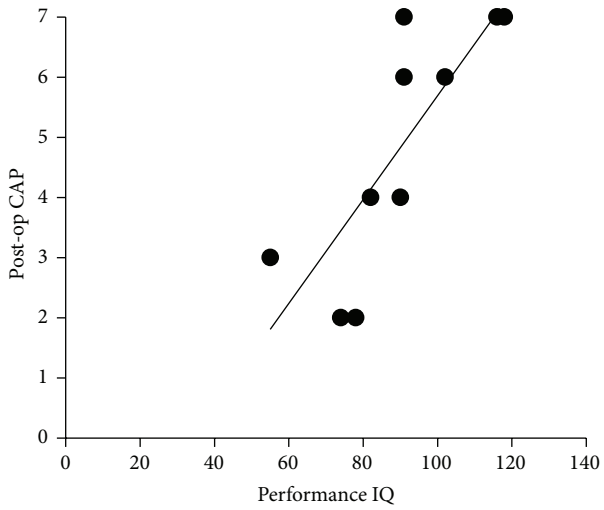

Figure 3: The correlation between the performance IQ and postoperative CAP score. There was correlation between the performance IQ and postoperative CAP score (Spearman's rho = 0.8977, $P = 0.0008$).

and performance IQs (Spearman's rho = 0.42, $P = 0.15$) (Figure 2(b)).

3.4. Correlation between Performance IQ and Postoperative CAP Score. Postoperative 1-2 year CAP scores were available for 10 of the 13 children. There was a strong correlation between the performance IQ and postoperative CAP scores (Spearman's rho = 0.8977, $P = 0.0008$) (Figure 3).

3.5. Correlation between Each Subset of the Performance IQ and Postoperative CAP Scores. We evaluated the correlation between each subset of the performance IQ and the postoperative CAP scores. The "picture arrangement" subset had the highest correlation with the postoperative CAP scores, followed by "picture completion." As mentioned above, "picture completion" and "picture arrangement" reflect social cognition. Therefore, we inferred that social cognition correlates well with the postoperative CAP scores (Figure 4).

4. Discussion

To our knowledge, this is the first study to assess the verbal and performance IQs of Korean-speaking CI users using the KEDI-WISC test. The mean performance IQ of our subjects fell in the category "average," which is in agreement with previous reports [20–22].

There were discrepancies between the verbal and performance IQs in our CI subjects. Profiles between the verbal and performance IQs are often found in children with developmental disorders, such as autism (verbal IQ > performance IQ) [23–26], and in children with hearing loss (verbal IQ < performance IQ) [21]. In addition, our results showed that the postoperative CI outcome is linked to cognitive function, especially to performance IQ rather than verbal IQ. A recent study has indicated that better spoken language and verbal reasoning skills are correlated with the verbal IQ [27]. In this regard, our results may partially be attributed to the fact that the highest CAP score is not complex enough to assess auditory functions that are needed for development of the higher verbal reasoning skills that are tested in verbal IQ tests. Third, of the performance IQ subscales, "picture completion" and "picture arrangement," which reflect social cognition, were associated with the post-CI outcome. This implies that not only intelligence but also social adaptation contributes to auditory rehabilitation after CI.

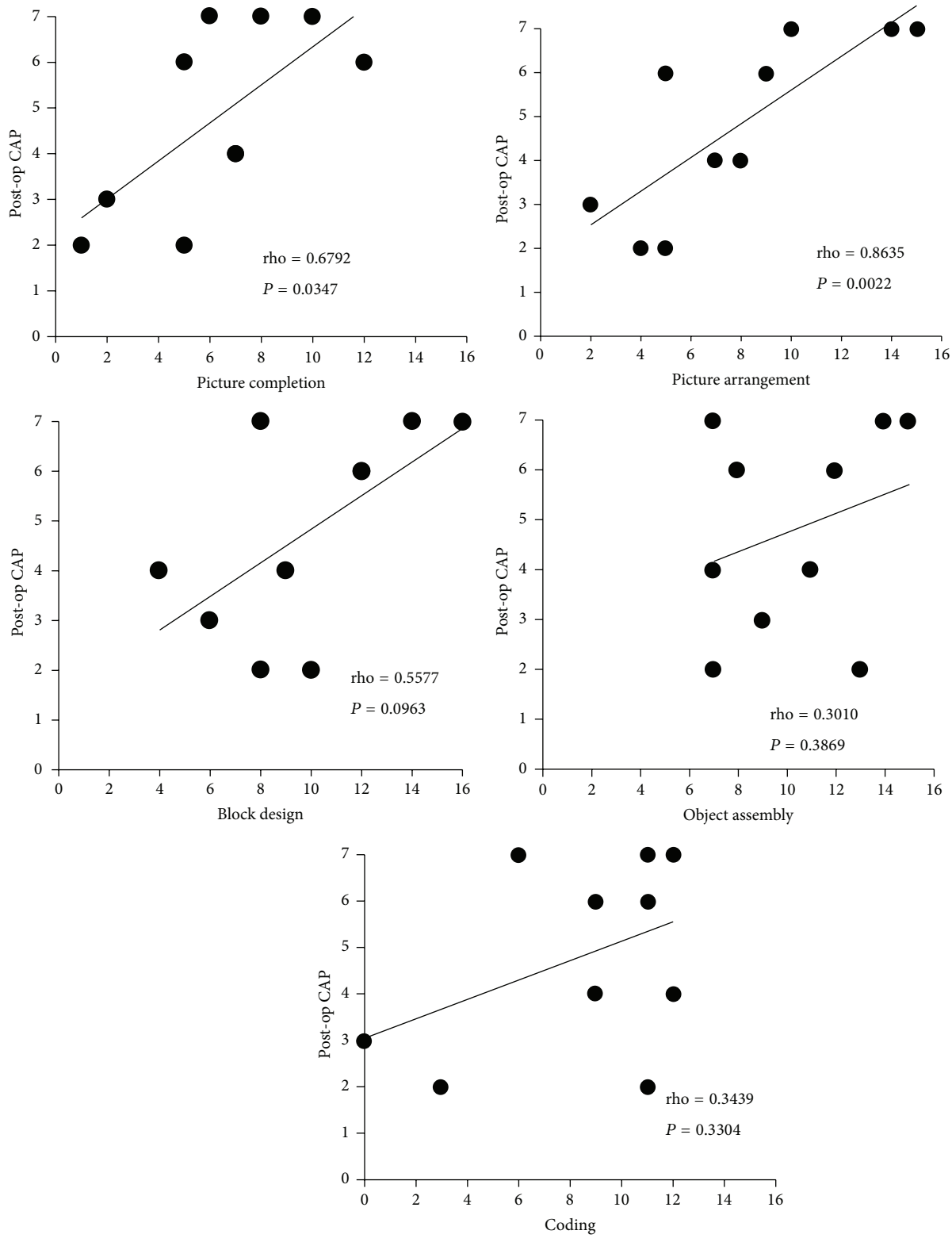

Figure 4: The correlation between each performance IQ subscale and the postoperative CAP score. "Picture arrangement" and "picture completion" had moderate to strong correlations with the postoperative CAP scores.

Verbal IQ reflects crystallized intelligence or knowledge coming from prior learning and past experiences [28]. Situations that require crystallized intelligence include reading comprehension and vocabulary examinations. This type of intelligence is based on facts and is rooted in experiences [28]. As we grow older and accumulate new knowledge and understanding, crystallized intelligence becomes stronger. Since deaf subjects do not go through these processes during the period of auditory deprivation before CI, their verbal IQ is lower. Conversely, performance IQ reflects fluid intelligence, which is the ability to perceive relationships independent of previous specific practices or instructions concerning those relationships. Therefore, the performance IQ of the CI subjects was comparable to that of their normal-hearing peers. This is in line with many previous reports [20–22].

Consistent with other research, we found that social cognition, as measured by "picture completion" and "picture arrangement," is relatively poor in CI users [29]. In addition, our finding of relatively good visual-motor coordination measured using "block design" or "object assembly" in CI subjects is consistent with one previous report [30]. This has been attributed to brain plasticity; that is, visual-motor integration ability is improved secondary to auditory deprivation. Notably, the mean score of "coding" was poor, although it reflects the visual motor coordination ability. This can be explained by the fact that "coding" has the greatest relevance to verbal intelligence among the performance IQ subscales [31, 32]. In addition, "coding" is the only performance IQ subscale that uses letters, numbers, and symbols [33].

Social cognition focuses on how people process, store, and apply information about other people and social situations [34]. It focuses on the role played by cognitive processes in our social interactions. Social competence is closely related to social cognition. In CI users, some studies have reported that language skills are not related to social competence [35], while others reported a strong positive correlation between language skills and social competence [36]. We support the latter, and this suggests that postoperative CI outcomes are associated with social rehabilitation.

In this study, the postoperative CI outcomes were assessed using the CAP score. Many studies have evaluated CI outcomes using open-set phonetically balanced word recognition tests or sentence tests [9]. These tests can evaluate the auditory performance quantitatively, but they can be applied only to children older than 5 years. Since the CAP score can be easily applied and followed longitudinally over time, the improvement in the speech perception of each subject can be evaluated. Moreover, it is applicable to all subjects regardless of their intelligence, age, and other characteristics.

Limitations of this study must be mentioned. First, because this study presents preliminary results obtained from a small sample, a future study of a larger group of CI subjects is mandatory to draw generalized conclusions. Second, as the developmental stages of the subjects differed, a longer follow-up and longitudinal evaluation are needed. Third, a more reliable result might be achieved if patients with the same total performance IQ were included to compare the performance IQ subscales. Finally, to explore the causal relationship between the performance IQ and CI speech outcome, a prospective study that includes a preoperative performance IQ evaluation should be conducted.

5. Conclusion

Performance intelligence, especially social cognition, is correlated with the postoperative speech outcome in CI users. Therefore, postoperative rehabilitation—including a social rehabilitation program—might help to maximize the postoperative CI outcome.

Conflict of Interests

The authors report no conflict of interests, financially or otherwise.

Acknowledgment

This research was supported by the National Research Foundation (NRF) funded by the Korean government (MSIP) (no. 2006-2005090).

References

[1] H. J. Lee, E. Kang, S.-H. Oh et al., "Preoperative differences of cerebral metabolism relate to the outcome of cochlear implants in congenitally deaf children," *Hearing Research*, vol. 203, no. 1-2, pp. 2–9, 2005.

[2] M. A. Svirsky, A. M. Robbins, K. I. Kirk, D. B. Pisoni, and R. T. Miyamoto, "Language development in profoundly deaf children with cochlear implants," *Psychological Science*, vol. 11, no. 2, pp. 153–158, 2000.

[3] D. S. Lazard, C. Vincent, F. Venail et al., "Pre-, per- and postoperative factors affecting performance of postlinguistically deaf adults using cochlear implants: a new conceptual model over time," *PLoS ONE*, vol. 7, no. 11, Article ID e48739, 2012.

[4] P. Blamey, P. Arndt, F. Bergeron et al., "Factors affecting auditory performance of postlinguistically deaf adults using cochlear implants," *Audiology and Neurotology*, vol. 1, no. 5, pp. 293–306, 1996.

[5] D. S. Lazard, H. J. Lee, M. Gaebler, C. A. Kell, E. Truy, and A. L. Giraud, "Phonological processing in post-lingual deafness and cochlear implant outcome," *NeuroImage*, vol. 49, no. 4, pp. 3443–3451, 2010.

[6] H.-J. Lee, A.-L. Giraud, E. Kang et al., "Cortical activity at rest predicts cochlear implantation outcome," *Cerebral Cortex*, vol. 17, no. 4, pp. 909–917, 2007.

[7] J. J. Song, G. Mertens, S. Deleye et al., "Neural substrates of conversion deafness in a cochlear implant patient: a molecular imaging study using H215O-PET," *Otology & Neurotology*, vol. 35, no. 10, pp. 1780–1784, 2014.

[8] J.-J. Song, A. K. Punte, D. de Ridder, S. Vanneste, and P. van de Heyning, "Neural substrates predicting improvement of tinnitus after cochlear implantation in patients with single-sided deafness," *Hearing Research*, vol. 299, pp. 1–9, 2013.

[9] C.-M. Wu, H.-L. Lee, J.-H. Hwang, Y.-S. Sun, and T.-C. Liu, "Intellectual ability of Mandarin-speaking children using cochlear implants," *Audiology and Neurotology*, vol. 13, no. 5, pp. 302–308, 2008.

[10] A. A. Zekveld, J. B. Deijen, S. T. Goverts, and S. E. Kramer, "The relationship between nonverbal cognitive functions and hearing loss," *Journal of Speech, Language, and Hearing Research*, vol. 50, no. 1, pp. 74–82, 2007.

[11] C. M. Conway, J. Karpicke, E. M. Anaya, S. C. Henning, W. G. Kronenberger, and D. B. Pisoni, "Nonverbal cognition in deaf children following cochlear implantation: motor sequencing disturbances mediate language delays," *Developmental Neuropsychology*, vol. 36, no. 2, pp. 237–254, 2011.

[12] K. Park, *KEDI-WISC Manual*, Korean Educational Institute, Seoul, Republic of Korea, 1991.

[13] M. H. Jeong, M.-S. Yum, T.-S. Ko, S. J. You, E. H. Lee, and H. K. Yoo, "Neuropsychological status of children with newly diagnosed idiopathic childhood epilepsy," *Brain & Development*, vol. 33, no. 8, pp. 666–671, 2011.

[14] P. K. Chae, H.-O. Jung, and K.-S. Noh, "Attention deficit hyperactivity disorder in Korean juvenile delinquents," *Adolescence*, vol. 36, no. 144, pp. 707–725, 2001.

[15] D. N. Allen and K. A. Barchard, "Identification of a social cognition construct for the WAIS-III," *Applied Neuropsychology*, vol. 16, no. 4, pp. 262–274, 2009.

[16] D. Wechsler, *Manual for the Wechsler Intelligence Scale for Children, Revised*, Psychological Corporation, 1974.

[17] C. L. Nicholson and C. L. Alcorn, "Interpretation of the WISC-III and its subtests," in *Proceedings of the Annual Meeting of the National Association of School Psychologists*, 1993.

[18] K. Park, J. Yoon, H. Park et al., *Korean Educational Developmental Institute-Wechsler Intelligence Scale for Children (KEDI-WISC)*, Korean Educational Development Institute, Seoul, Republic of Korea, 2002.

[19] H.-Y. Fang, H.-C. Ko, N.-M. Wang et al., "Auditory performance and speech intelligibility of Mandarin-speaking children implanted before age 5," *International Journal of Pediatric Otorhinolaryngology*, vol. 78, no. 5, pp. 799–803, 2014.

[20] P. M. Sullivan, "Administration modifications on the WISC-R performance scale with different categories of deaf children," *American Annals of the Deaf*, vol. 127, no. 6, pp. 780–788, 1982.

[21] M. Vernon, "Fifty years of research on the intelligence of deaf and hard-of-hearing children: a review of literature and discussion of implications," *Journal of Deaf Studies and Deaf Education*, vol. 10, no. 3, pp. 225–231, 2005.

[22] B. U. Watson, P. M. Sullivan, M. P. Moeller, and J. K. Jensen, "Nonverbal intelligence and English language ability in deaf children," *The Journal of Speech and Hearing Disorders*, vol. 47, no. 2, pp. 199–204, 1982.

[23] S. D. Mayes and S. L. Calhoun, "Ability profiles in children with autism: influence of age and IQ," *Autism*, vol. 7, no. 1, pp. 65–80, 2003.

[24] N. J. Minshew, C. A. Turner, and G. Goldstein, "The application of short forms of the wechsler intelligence scales in adults and children with high functioning autism," *Journal of Autism and Developmental Disorders*, vol. 35, no. 1, pp. 45–52, 2005.

[25] D. J. Siegel, N. J. Minshew, and G. Goldstein, "Wechsler IQ profiles in diagnosis of high-functioning autism," *Journal of Autism and Developmental Disorders*, vol. 26, no. 4, pp. 389–406, 1996.

[26] P. Szatmari, L. Tuff, M. A. J. Finlayson, and G. Bartolucci, "Asperger's syndrome and autism: neurocognitive aspects," *Journal of the American Academy of Child and Adolescent Psychiatry*, vol. 29, no. 1, pp. 130–136, 1990.

[27] L. D. Raeve, "Jacobs Earfoundation Nottingham video presentation," 2013.

[28] I. Bergman and O. Almkvist, "The effect of age on fluid intelligence is fully mediated by physical health," *Archives of Gerontology and Geriatrics*, vol. 57, no. 1, pp. 100–109, 2013.

[29] R. L. Schum, "Communication and social growth: a developmental model of social behavior in deaf children," *Ear & Hearing*, vol. 12, no. 5, pp. 320–327, 1991.

[30] H. E. Krouse, *The Structure of Intelligence of Deaf and Hard of Hearing Children: A Factor Analysis of the WISC-IV*, North Carolina State University, 2012.

[31] R. P. Rugel, "WISC subtest scores of disabled readers: a review with respect to Bannatyne's recategorization," *Journal of Learning Disabilities*, vol. 7, no. 1, pp. 48–55, 1974.

[32] A. E. Maxwell, "A factor analysis of the wechsler intelligence scale for children," *British Journal of Educational Psychology*, vol. 29, no. 3, pp. 237–241, 1959.

[33] N. R. Riggs, C. B. Blair, and M. T. Greenberg, "Concurrent and 2-year longitudinal relations between executive function and the behavior of 1st and 2nd grade children," *Child Neuropsychology*, vol. 9, no. 4, pp. 267–276, 2004.

[34] T. M. Ostrom, "The sovereignty of social cognition," in *Handbook of Social Cognition*, vol. 1, pp. 1–38, 1984.

[35] L. Ketelaar, C. Rieffe, C. H. Wiefferink, and J. H. M. Frijns, "Social competence and empathy in young children with cochlear implants and with normal hearing," *The Laryngoscope*, vol. 123, no. 2, pp. 518–523, 2013.

[36] C. H. Wiefferink, C. Rieffe, L. Ketelaar, and J. H. M. Frijns, "Predicting social functioning in children with a cochlear implant and in normal-hearing children: the role of emotion regulation," *International Journal of Pediatric Otorhinolaryngology*, vol. 76, no. 6, pp. 883–889, 2012.

Hindawi Publishing Corporation
BioMed Research International
Volume 2015, Article ID 282164, 8 pages
http://dx.doi.org/10.1155/2015/282164

Research Article

Written Language Ability in Mandarin-Speaking Children with Cochlear Implants

Che-Ming Wu, Hui-Chen Ko, Yen-An Chen, Yung-Ting Tsou, and Wei-Chieh Chao

Department of Otolaryngology-Head and Neck Surgery, Chang-Gung Memorial Hospital, College of Medicine, Chang-Gung University, Linkou Branch, Taoyuan 333, Taiwan

Correspondence should be addressed to Che-Ming Wu; bobwu506@hotmail.com

Received 28 November 2014; Accepted 3 April 2015

Academic Editor: Prepageran Narayanan

Objectives. To examine narrative writing in cochlear implant (CI) children and understand the factors associated with unfavorable outcomes. *Materials and Methods*. Forty-five CI children in grades 2–6 participated in this study. They received CIs at 4.1 ± 2.1 years of age and had used them for 6.5 ± 2.7 years. A story-writing test was conducted and scored on 4 subscales: Total Number of Words, Words per Sentence, Morphosyntax, and Semantics. Scores more than 1.5 SD lower than the mean of the normal-hearing normative sample were considered problematic. Language and speech skills were examined. *Results*. Significantly more implanted students were problematic on "Total Number of Words" ($p < 0.001$), "Words per Sentence" ($p = 0.049$), and "Semantics" ($p < 0.001$). Poorer receptive language and auditory performance were independently associated with problematic "Total Number of Words" ($R^2 = 0.489$) and "Semantics" ($R^2 = 0.213$), respectively. "Semantics" problem was more common in lower graders (grades 2–4) than in higher graders (grades 5-6; $p = 0.016$). *Conclusion*. Implanted children tend to write stories that are shorter, worse-organized, and without a plot, while formulating morphosyntactically correct sentences. Special attention is required on their auditory and language performances, which could lead to written language problems.

1. Introduction

Writing could be one of the most complex tasks for all students, whether being normal-hearing or hearing-impaired students. For Mandarin Chinese students, who use a logographic orthography, they must know the correct spatial arrangements of strokes of a character, the conventions of punctuation, and the use of proper vocabulary and syntactical structures in order to write at a basic level. At a higher level, they have to choose topics and plan and organize their ideas [1].

It was indicated that early writing patterns during elementary school years are related to spoken language trends [2]. Deaf children were thus often found to use simple and short sentences with limited vocabulary and recurring phrases [3–7]. Their compositions were also reported to have fewer adjectives and adverbs [8] and more errors in the use of function words (e.g., omission or wrong usage of prepositions and pronouns) [9] due to the difficulty acquiring knowledge of syntactical and morphological structures [10, 11]. As a result, Antia et al. [12] reported that the mean written quotient of their deaf children was in the below-average range as compared to that of the hearing peers. Although the hearing-impaired students did improve their writing skills with age [1, 5], they made slower progress than the hearing children [5, 6, 13, 14], which could have an impact on their academic performance throughout the school years [15].

With the restoration of hearing via a cochlear implant (CI), it is expected that the improvements in spoken language may also lead to the improvements in other language skills such as writing. Spencer et al. [2] found that the children with CIs performed within 1 standard deviation (SD) of the normal-hearing age mates on the measure of writing accuracy. One study also indicated that the spelling skills of the implanted children aged between 6 to 12 years were comparable to those with normal-hearing who were matched for reading ability [16]. However, when compared to the age-matched children, a significant difference was found between the two groups of children. The CI children's performance on formulating sentences was found to fall behind the hearing

peers as well, and they were reported to produce fewer words on the expository writing although no significant difference was noted in terms of total words per clause [2].

The problem with written language was not necessarily eased with age. It was found that high-school students with CIs also spelled significantly poorer than the hearing peers, and less than 50% of them scored within 1 SD of the hearing group on the expository writing task [17]. The age at implantation may also affect writing performance. Those who were implanted after the age of 4 years were reported to have difficulty with lower-level writing, that is, expression formation and productiveness, while those who received CIs before that age had problem with higher-level writing, that is, assisting key tone [18].

Nevertheless, to date, most of the studies on the written language skills in the implanted population use only subjects with an alphabetic language background, such as English. There is hardly any study investigating the patient group that uses Mandarin Chinese, a logographical language. While the basic unit for writing in alphabetic languages is segments [19, 20], it is the characters in Chinese (e.g., "馬"), each representing a syllable in sound (/ma3/) and a morpheme in meaning ("horse"). This means that the phoneme-grapheme correspondence in Chinese characters is not transparent. However, when children in Taiwan enter elementary school, they are compulsorily taught a system of alphabetic symbols called Zhu-Yin (including 37 symbols) to learn the pronunciation of Chinese characters [21]. These features of Chinese characters could result in different writing performance in Mandarin-speaking patient group from that of the alphabetic language users reported by previous studies.

Therefore, this study aimed (1) to examine the narrative writing performance in Mandarin-speaking elementary-school students with cochlear implants and (2) to understand the family/child-related, implant-related, and language-related factors associated with less favorable writing performance.

2. Patients and Methods

2.1. Participants. Forty-five prelingually deafened patients (20 boys, 25 girls) who received CIs in our center participated in this study. They all met the inclusion criteria: (1) the subjects were in grades 2–6 of elementary school; (2) the subjects did not have any developmental problems or additional handicaps (e.g., intellectual disability, attention deficit, language disorders, learning disability, and autism); (3) the subjects used oral communication and Mandarin Chinese as their major language; (4) the subjects went to mainstream schools and were not placed in the resource class; (5) the subjects' performance intelligence quotient [22, 23] was higher than 85. They were 8.0–13.3 years of age (mean = 10.6 ± 1.6) when taking the tests. They received the implantation at a mean age of 4.1 ± 2.1 years during years 2000–2010 and had used the implant for a mean duration of 6.5 ± 2.7 years.

The socioeconomic status (SES) of the family was determined based on the Hollingshead two-factor index of social status [24], which used a five-level item to rate the level of parents' educational background (1 = illiterate; 5 = with a graduate degree or above) and occupational status (1 = unskilled workers; 5 = higher executives/major professionals). The parents of the subjects were required to fill out a form to report the information.

All informed consents signed by participants and guardians were obtained before the test procedures. The study protocol was approved by the Institutional Review Board, Chang-Gung Memorial Hospital, Taoyuan, Taiwan.

2.2. Test Materials and Procedures

2.2.1. Written Language Ability Measure

(1) Written Language Ability Diagnostic Test for Children. The test, designed based on the Myklebust Picture Story Language Test [25], is used to assess the written language skills of Mandarin-speaking students in elementary school [26]. The subjects were asked to write a story as long as possible by themselves about a given picture (see Figure 2). They were encouraged to write the entire article with Chinese characters, but Zhu-Yin symbols was also allowed in cases that they did not know how to write some of the characters. There was no time limit, and the picture was available throughout the test session. Their product was graded according to four subscales: (1) the subscale of Total Number of Words of the written story ("Total N Words"); (2) the subscale of number of words per sentence ("Words per Sentence"); (3) the "Morphosyntax" subscale that yielded a quotient computed from the number of incorrect language usages (including miswritten words, improper punctuations, and wrong dictions), which could be further classified as errors due to addition, omission, substitution, and transposition; (4) the "Semantics" subscale that rated the story by five levels according to its concreteness/abstractness (1 = nonsense; 2 = concrete description; 3 = concrete imagination; 4 = abstract description; 5 = abstract imagination). Higher scores indicated better skills. The raw scores were converted to standard T scores derived from a normative sample of 1800 normal-hearing students (mean = 50 ± 10) provided by the test developer [26]. The performance of our CI subjects was also compared to the normative sample and was classified as excellent (more than 2 SD higher than the normative mean), good (0.5 to 2 SD higher), normal (±0.5 SD of the normative mean), marginal (0.5 to 1.5 SD lower than the normative mean), or clinical (more than 1.5 SD lower). Marginal or clinical performances were considered unfavorable in this study, and thus those subjects that fell within these two ranges were defined as within the "problematic range" for further analysis. The validity and reliability of the test have been confirmed [26].

2.2.2. Auditory Performance and Speech Intelligibility Measures

(1) Categorical Auditory Perception (CAP) and Speech Intelligibility Rating (SIR) Scales. The CAP and SIR scales are designed to assess deaf patients' auditory performance and speech

production intelligibility, respectively (see Table 6). The CAP is a nonlinear hierarchical rating scale with 8 points (0 = unaware of environmental sounds; 7 = able to converse on the telephone with a familiar person). The SIR is a nonlinear scale that classifies children's speech production intelligibility into 5 levels (1 = unintelligible; 5 = easily understood by all listeners). The reliability of both scales has been confirmed [27–29].

2.2.3. Language Skill and Speech Perception Measures

(1) Test of Reading Comprehension. This test evaluates the paragraph reading ability in elementary-school students [30] (Table 5). It includes 12 articles, each with 6–9 corresponding multiple-choice questions. The articles and the questions are shown only with Chinese characters, not accompanied by alphabetic Zhu-Yin symbols. The text remained available while answering, and there was no time limit. The number of correctly answered questions was turned into percentages to obtain overall scores. The reliability and validity of this test have been confirmed [30].

(2) Graded Chinese Character Recognition Test. This is a standardized test for assessing monosyllabic word identification in children in grades 1–9 [31]. The subjects need to identify 200 characters on the word list by writing down the Zhu-Yin symbols of each character. The raw scores were transformed to T scores according to the data of a grade-matched normative sample provided by the test developer [31].

(3) Revised Primary School Language Assessment. This test is designed to assess the language abilities in 6- to 12-year-old children from 4 aspects: receptive language, expressive language, voice and fluency, and articulation/tone error pattern (see the appendices of Wu et al. [32] for details about the test) [30]. Only receptive and expressive language subtests were included in this study, which were given orally to the subjects. Both tests deal with the semantic and pragmatic aspects of language use (i.e., understanding/expressing the meaning of a phrase or a sentence in a certain context). The raw scores were converted into T scores based on an age-matched normal-hearing normative sample (mean = 50 ± 10) [30].

(4) Peabody Picture Vocabulary Test: Revised. This test evaluates receptive vocabulary knowledge in children aged 3–12 years [33]. The students were presented with sets of four pictures and asked to point out one picture that best described the word spoken by the examiner, following basal and ceiling rules to administer the test. T scores (mean = 100 ± 15) were derived from the normal-hearing normative sample provided by the test developer [33].

(5) Phonetically Balanced Word Perception Test. This test uses 25 phonetically balanced monosyllabic words to test word perception ability [34]. The examiner spoke each word with mouth covered, and the subjects needed to verbally repeat the words they heard. They were scored based on the number of words they correctly repeated, which was converted into percentages for further analysis.

Table 1: Results of Written Language Ability Diagnostic Test in the children with cochlear implants.

Test results	Range	Mean ± SD
Total Number of Words	22.0–314.0	127.0 ± 69.3
Total Number of Words (T score)	32.0–56.0	40.9 ± 6.5
Total number of sentences	3.0–32.0	13.2 ± 6.8
Words per Sentence	6.6–13.0	9.5 ± 1.7
Words per Sentence (T score)	35.0–59.0	44.7 ± 5.3
Morphosyntax (T score)	10.0–63.0	51.6 ± 12.2
Semantics (T score)	28.0–77.0	42.5 ± 11.3

2.3. Statistical Analysis. The SPSS software (version 17.0; SPSS, Inc., Chicago, IL, USA) was employed to do the statistical analysis. The analysis of the written language ability was performed based on the ranges (normal range = 0; problematic range = 1) rather than on the T scores to make sure that we targeted on the patients who had problems with expressive writing. A chi-square goodness-of-fit test was used to compare the distribution of writing outcomes between our CI users and the normative sample. A Mann-Whitney U test was employed to make between-group comparison of test results. A binary logistic regression analysis was utilized to investigate the significance of child/family characteristics and language/speech skills in association with narrative writing problems. These variables of interest were split into two groups according to the medians for regression analysis. The chronological age and grade were not entered into the analysis because in this study T scores, which were derived from grade-matched normative sample, were used for evaluation. A p value of less than 0.05 was considered statistically significant.

3. Results

3.1. Narrative Writing Performance in Cochlear Implanted Children. The implanted subjects averagely produced 127.0 ± 69.3 words in their stories, each sentence with 9.5 ± 1.7 words (Table 1). The mean rate of making morphosyntactical mistakes in their production was 5.6% in total (Table 2), meaning that, in every 100 words, only 5.6 elements (characters or punctuations) were used incorrectly. Regarding "Semantics," 20 subjects (44.4%) were at level 2 (concrete description), 14 (31.1%) at level 3 (concrete imagination), 5 at level 4 (abstract description), and 6 at level 5 (abstract imagination). None were regarded as producing nonsensical stories (i.e., at level 1; see Table 3).

The CI subjects had T score of 40.9 ± 6.5, 44.7 ± 5.3, 51.6±12.2, and 42.5±11.3 on the subscales of "Total N Words," "Words per Sentence," "Morphosyntax," and "Semantics," respectively (see Table 1). The results suggest that their average T scores were within 1 SD of the mean of the normal-hearing normative sample (i.e., 50 ± 10, as provided by the test developer). 46.7%, 82.2%, 84.4%, and 57.8% of the subjects

Table 2: Error rates of each of assessment items on the "Morphosyntax" subscale.

	Addition	Omission	Substitution	Transposition	Total
Diction (%)	1.06	0.97	0.55	0.09	2.68
Miswritten words (%)	0.06	0.07	0.63	0.00	0.77
Punctuation (%)	0.09	1.35	0.74	n/a	2.18
Total (%)	1.21	2.40	1.92	0.09	5.62

Table 3: Description of each level on the "Semantics" subscale and number (%) of cochlear implanted patients at each level.

Semantic level	Raw score		Number of children (%)
(1) Nonsense	0	Daubing; nonsensical phrases; unrelated subject to the given picture.	0 (0)
(2) Concrete description	1	Using a series of nouns.	3 (6.7)
	2	Using verb-noun structure to signal actions; using only one verb.	6 (13.3)
	3	Using nouns, verbs (more than one), and adjectives; able to make categorization.	11 (24.4)
(3) Concrete imagination	4	With a main point and a structure; description of actions and feelings of people in the picture.	7 (15.6)
	5	With a consistent main point throughout the story and a better organized structure; description of actions, feelings, and relations of people in the picture.	7 (15.6)
(4) Abstract description	6	With some plot; describing people in the picture as a group.	4 (8.9)
	7	With a setting; the entire story being set in one single context (e.g., family, school, playground, and park); structuring the story based on what the storyteller feels and perceives.	1 (2.2)
(5) Abstract imagination	8	With a plot, which is developed based on the picture; description of how people in the story feel and their motivations of taking certain actions.	3 (6.7)
	9	Longer story with more details and a more complicated plot; able to show causal relationship; description of events that are imaginary or may happen in the future.	1 (2.2)
	10	Description of abstract concepts that are beyond the picture contents; writing a prose/essay, exposition or fable rather than a story; expressing concerns about moral issues or welfare of human beings.	2 (4.4)

fell within the range of 1 SD from the normative mean of "Total N Words," "Words per Sentence," "Morphosyntax," and "Semantics," respectively (Figures 1(a)–1(d)).

However, there were significantly more CI students in the problematic range (i.e., more than 1.5 SD lower than the normative mean) on the subscales of "Total N Words" ($p < 0.001$), "Words per Sentence" ($p = 0.049$), and "Semantics" ($p < 0.001$; see Table 4). Actually, more than three-fourths of the CI subjects were in the problematic range on "Total N Words" subscale.

3.2. Clinical Factors Associated with Problematic Written Language. The factors related to child/family characteristics and language/speech skills were entered into a binary logistic regression analysis. The child/family characteristics included age at implantation, duration of implant use, SES, CAP, and SIR scores. The language-related parameters included paragraph reading, Chinese character recognition, receptive vocabulary, receptive language, expressive language, and word perception. Results showed that lower scores of receptive language (i.e., lower than the median score = 48.5) were independently associated with problematic performance on the "Total N Words" subscale ($p = 0.026$; odds ratio = 26.8; 95% confidence interval = 1.5–489.4; $R^2 = 0.489$). Lower scores of CAP (i.e., lower than the median score = 7) were independently associated with problematic "Semantics" ($p = 0.035$; odds ratio = 10.7; 95% confidence interval = 1.2–96.4; $R^2 = 0.213$).

3.3. Development of Written Language Skills during Elementary-School Years. Although chronological age and grade were not taken into concern in the regression analysis, we still would like to know how written language ability was developed during elementary-school years in the implanted children. Therefore, the subjects were split into two groups according to their grades (median = 4): the lower graders (those who are in grades 2–4; $n = 24$); and the higher graders (in grades 5-6; $n = 21$). The results showed that significantly more lower graders had problematic "Total N Words," "Words per Sentence," and "Semantics" compared to the grade-matched normative sample (see Table 4). Also, significantly more higher graders fell within the problematic range regarding their performances on "Total N Words" and "Semantics." When compared the lower graders with those in the higher grades, significantly more lower graders were regarded as having problematic "Semantics" ($p = 0.016$), while no significant differences were noted between the two groups regarding the other three subscales ($p > 0.05$).

4. Discussion

Written language ability is essential for academic performance. Yet, it has never been carefully examined in prelingually deaf CI children with a Mandarin Chinese language background. Our preliminary results show that, compared to normal-hearing grade-matched children, significantly more implanted children have problematic performance on "Total

Table 4: Percentage of patients in the normal range and the problematic range on the four subscales of the Written Language Ability Diagnostic Test and a comparison between the distribution of cochlear implanted subjects and that of the normal-hearing grade-matched normative sample using chi-square goodness-of-fit test.

Subjects for comparison	Range	Total *N* Words (%)	Words per Sentence (%)	Morphosyntax (%)	Semantics (%)
All subjects	Normal	24.4	55.6	77.8	62.2
	Problematic	75.6	44.4	22.2	37.8
	p value[a]	<0.001	0.049	0.208	<0.001
Lower graders	Normal	33.3	45.8	70.8	50.0
	Problematic	66.7	54.2	29.2	50.0
	p value[a]	<0.001	0.01	0.85	<0.001
Higher graders	Normal	14.3	66.7	85.7	76.2
	Problematic	85.7	33.3	14.3	23.8
	p value[a]	<0.001	0.809	0.099	0.002

[a]The performances of the CI subjects (all, lower graders, and higher graders) on "Total N Words," "Words per Sentence," "Morphosyntax," and "Semantics" were compared to a normal-hearing grade-matched normative sample, where 30.9%, 30.9%, 30.9%, and 6.7% of the students were in the problematic range on each subscale, respectively.

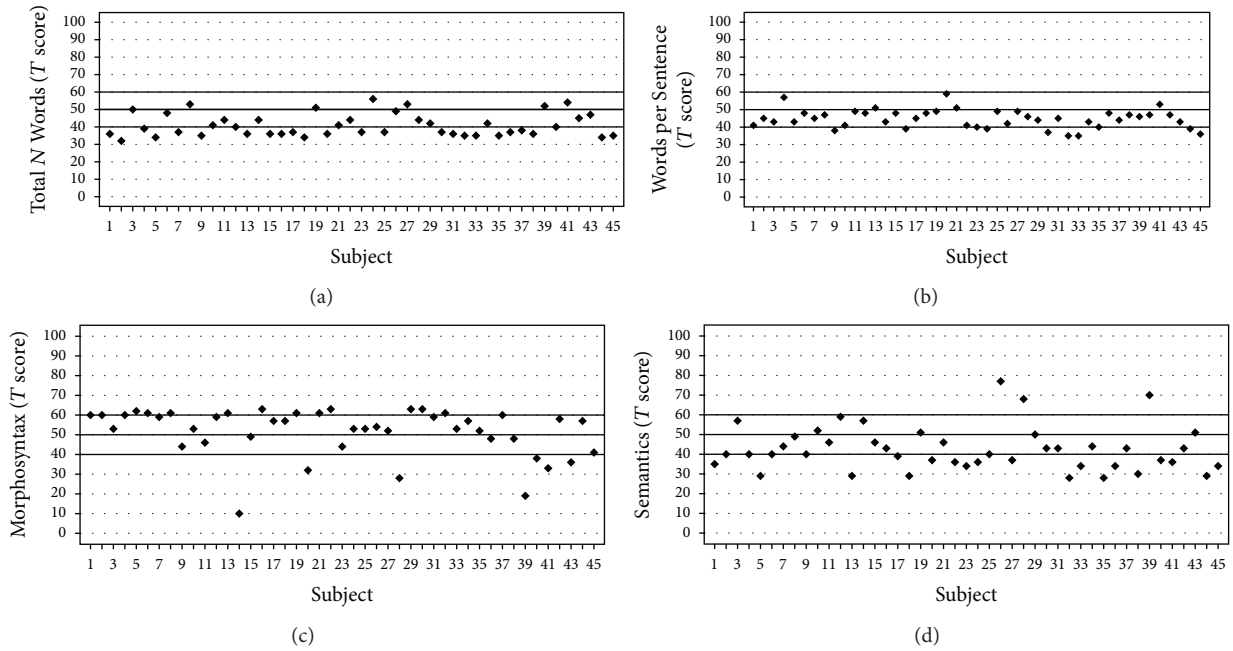

Figure 1: Individual standard scores for the four subscales of the Written Language Ability Diagnostic Test plotted for 45 children, with subscales including (a) "Total Number of Words," (b) "Words per Sentence," (c) "Morphosyntax," and (d) Semantics. Horizontal lines indicate standard scores within 1 SD of the normal-hearing normative sample.

N Words" and "Semantics" during narrative writing. Their receptive language skills and auditory performance have a close association with these problems, respectively.

CI children's narrative writing ability is examined from four perspectives, among which "Total N Words" seems to be the most problematic for the implanted students. Their production is significantly shorter than that of the normal-hearing children. This finding is in line with most of the previous studies on deaf and cochlear implanted children [2–6, 35]. It suggests that the productiveness is one of the most serious problems with deaf children's writing. This weakness, as our regression results show, is associated with the subjects' receptive language skills. That is, writing not only is about formulation of sentences but also is related to the ability to understand what is communicated orally. It is very likely because early writing patterns in deaf children follow spoken language trends during elementary-school years [2]. Spencer et al. [2] further indicate that the sentences composed by 9- to 15-year-old deaf children evolve in structure, from conjoined to embedded sentence structure. It shows that, with the development of spoken language, deaf children gradually learn to increase the complexity of form in writing. Therefore, specialists should not just focus on syntactical problems but also pay attention to the development of receptive language ability because it could be an underlying cause of their unproductiveness in writing.

Table 5: Demographical data of the cochlear implanted subjects and the outcomes of language skill and speech perception measures.

Parameters	Mean ± SD	Median
Child/family-related		
Age at implantation (years)	4.1 ± 2.1	3.3
Duration of CI use (years)	6.5 ± 2.7	6.9
Grade	4.2 ± 1.6	4.0
SES[a]	2.3 ± 0.6	2.0
CAP	6.2 ± 0.5	6.0
SIR	4.7 ± 0.6	5.0
Language/speech-related		
Paragraph reading (%)	59.9 ± 19.6	60.0
Word recognition (*T* score)	51.4 ± 12.7	52.0
Receptive language (*T* score)	49.0 ± 12.6	48.5
Expressive language (*T* score)	52.4 ± 11.8	52.0
Receptive vocabulary	90.0 ± 13.5	90.0
Word perception (%)	85.7 ± 13.0	92.0

CI: cochlear implant; SES: socioeconomic status; CAP: Categorical Auditory Performance; SIR: Speech Intelligibility Rating.
[a]SES of the family (1 = low SES; 5 = high SES) was determined based on the Hollingshead two-factor index of social status that referenced to the parents' occupational status (1 = unskilled workers; 5 = higher executives/major professionals) and educational level (1 = illiterate; 5 = with a graduate degree or above).

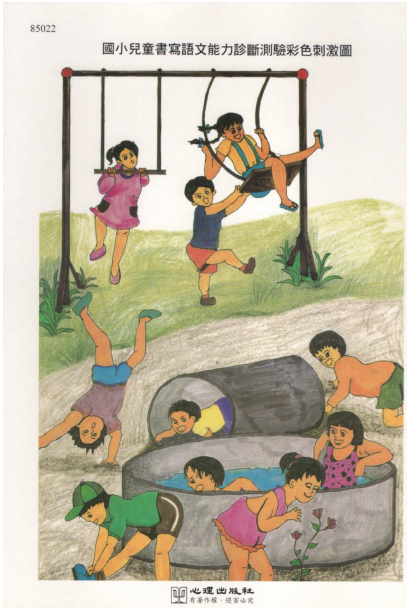

Figure 2: Stimulus picture for the Written Language Ability Diagnostic Test for children.

However, although the implanted children are less productive, it seems that they have no difficulty forming morphosyntactically correct sentences. Actually, almost 80% of our subjects show normal or better-than-normal performance on the "Morphosyntax" subscale. Only a mean error rate of 5.6% was found in all subjects (Table 2), and their scores on this subscale are not significantly different from those of the normal-hearing. Unlike many past studies that indicate more errors with language use made by deaf or hard-of-hearing children than by normal-hearing ones [6, 9, 15], the present study shows that our Mandarin-speaking children with CIs have normal use of grammar at character and sentence levels.

This discrepancy occurs not only because our subjects have used the CIs for a long duration of 6.5 years averagely, but also very likely as a result of the logographic orthography used in Mandarin Chinese and the type of test applied in the current study. The written language test administered in this study focuses more on the morphology than the syntax on the "Morphosyntax" subscale. That is, it examines, firstly, whether the subjects make mistakes in words and punctuations and secondly, whether the error with words/punctuations is made because of addition, omission, substitution, or transposition. It remains unknown how well or erroneously these CI children manipulate different lexical categories, such as nouns, verbs, and adverbs, and different structures, such as interrogative and coordinate sentences.

Moreover, when these Mandarin-speaking students write in Chinese, they engage with logographemes rather than phonemes, so their auditory performance may not impede "spelling," resulting in a mean miswritten word rate of only 0.8% (see Table 2). Although CI students are not necessarily bad "spellers" as Geers and Hayes [17] claim them to be (the study used English-speaking high-school students with CIs), it is indeed a limitation that we did not include a Zhu-Yin spelling test to analyze their phonological ability, which was due to lack of a standardized test for this purpose. Therefore, a test that more comprehensively examines different aspects of written language is certainly needed for Mandarin-speaking patients. It requires further investigations to develop such a test in the future.

Another problem with the stories written by our CI students is that they tend to engage only with concrete description. That is, more than two-fifths (44%) of the subjects write a story that does not have a main point and is not well organized or consistent (Table 3). Also, these children merely describe the objects they see in the given picture without mentioning the actions or feelings of the people in the picture. Only 13% of the children write a story that has a plot (Level 5). This weakness in writing is also found in English-speaking students with deafness who are indicated to have lower ratings of various aspects of semantics [13] and elaborate their ideas less fully [6] than the normal-hearing students. Geers and Hayes [17] also found that their CI students in high school obtained the lowest score on "organization" in expository writing. Fortunately, it is possible that the implanted children improve their semantic performance with age as our result shows that less higher graders (in grades 5-6) are deemed as having problematic "Semantics" compared to the lower graders (in grades 2–4) in spite of the fact that the performance of the higher graders is still worse than their normal-hearing grade mates.

The lack of capability of developing a story and expressing themselves fully may be associated with their less satisfactory auditory performance, considering that the CAP score is an independently associated factor of "Semantics" subscale in this study. It suggests that the ability to express oneself

Table 6: Criteria of Categorical Auditory Performance and Speech Intelligibility Rating scales.

Rating	Criteria of Categorical Auditory Performance	Criteria of Speech Intelligibility Rating
7	Use of telephone with known listener	n/a
6	Understanding of conversation without lip-reading	n/a
5	Understanding of common phrases without lip-reading	Connected speech is intelligible to all listeners. Child is understood easily in everyday contexts
4	Discrimination of some speech sounds without lip-reading	Connected speech is intelligible to a listener who has a little experience of a deaf person's speech
3	Identification of environmental sounds	Connected speech is intelligible to a listener who concentrates and lip-reads
2	Response to speech sounds	Connected speech is unintelligible. Intelligible speech is developing in single words when context and lip-reading cues are available
1	Awareness of environmental sounds	Connected speech is unintelligible. Prerecognizable words in spoken language, primary mode of communication may be manual
0	No awareness of environmental sounds	n/a

n/a = not applicable.

and organize a story in writing may develop with the increase in auditory experiences. Special trainings may be needed to improve their narrative writing ability because children with CIs seem to develop such ability at a slower rate than the normal-hearing ones, resulting in their lower scores on this subscale throughout the elementary-school years.

It has to be noted, however, that the structure organization of the story was not taken into concern in the current study. We focus on the semantic and morphosyntactical levels to understand the basic writing ability in students with CIs. Yet, narrative production does have a close association with the ability of linguistic structure organization, that is, the ability to concatenate different parts into a story (e.g., a beginning, a conflict and a corresponding resolution, and an ending), and the productiveness of written narratives is related to the production of oral narratives, as our result shows. It is therefore of particular interest to learn the correlation between oral and written narratives on a discursive level of language in future studies.

5. Conclusions

Our preliminary results show that children with CIs tend to write shorter stories which are not well organized and without a plot. These weaknesses in narrative writing are associated with their poorer receptive language skills and auditory performance. However, their ability to formulate morphosyntactically correct sentences is as good as the normal-hearing grade mates. Specialists thus are suggested not to focus only on syntactical problems but also on the development of auditory perception and receptive language for they could be the underlying causes of the writing problems. Also, a test that more thoroughly examines different aspects of written language needs to be developed in the future in order to better evaluate the written language problems in Mandarin-speaking patients with CIs.

Conflict of Interests

The authors have no conflict of interests relevant to this paper to disclose. The authors have no financial relationships relevant to this paper to disclose.

Acknowledgments

This study was supported by the Chang-Gung Memorial Hospital Research Program (CMRPG391121, CMRPG3B1143, and CMRPG3C1402). The authors would like to thank all the children and their parents who participated in the study.

References

[1] A. R. Powers and S. Wilgus, "Linguistic complexity in the written language of hearing-impaired children," *The Volta Review*, vol. 85, pp. 201–210, 1985.

[2] L. J. Spencer, B. A. Barker, and J. B. Tomblin, "Exploring the language and literacy outcomes of pediatric cochlear implant users," *Ear and Hearing*, vol. 24, no. 3, pp. 236–247, 2003.

[3] H. P. Karasu and U. Girgin, "Assessment of writing skills of hearing impaired students who attend mainstream classes," *Anadolu University Journal of Social Sciences*, vol. 7, no. 1, pp. 467–488, 2007.

[4] L. M. van Beijsterveldt and J. G. van Hell, "Evaluative expression in deaf children's written narratives," *International Journal of Language and Communication Disorders*, vol. 44, no. 5, pp. 675–692, 2009.

[5] D. L. Heefner and P. C. Shaw, "Assessing the written narratives of deaf students usina the six-trait analytical scale," *The Volta Review*, vol. 98, no. 1, pp. 147–165, 1996.

[6] C. Yoshinaga-Itano, L. S. Snyder, and R. Mayberry, "How deaf and normally hearing students convey meaning within and between written sentences," *The Volta Review*, vol. 98, no. 1, pp. 9–38, 1996.

[7] H. Tur-Kaspa and E. Dromi, "Grammatical deviations in the spoken and written language of Hebrew-speaking children with

hearing impairments," *Language, Speech, and Hearing Services in Schools*, vol. 32, no. 2, pp. 79–89, 2001.

[8] M. Marschark, V. Mouradian, and M. Halas, "Discourse rules in the language productions of deaf and hearing children," *Journal of Experimental Child Psychology*, vol. 57, no. 1, pp. 89–107, 1994.

[9] E. H. Lichtenstein, "The relationships between reading processes and English skills of deaf college students," *Journal of Deaf Studies and Deaf Education*, vol. 2, pp. 80–134, 1998.

[10] D. F. Moores, *Educating the Deaf: Psychology, Principles, and Practices*, Houghton Mifflin, Boston, Mass, USA, 1996.

[11] P. Paul, *Literacy and Deafness: The Development of Reading, Writing, and Literate Thought*, Allyn & Bacon, Boston, Mass, USA, 1998.

[12] S. D. Antia, S. Reed, and K. H. Kreimeyer, "Written language of deaf and hard-of-hearing students in public schools," *Journal of Deaf Studies and Deaf Education*, vol. 10, no. 3, pp. 244–255, 2005.

[13] K. A. Gormley and A. B. Sarachan-Deily, "Evaluating hearing-impaired students' writing: a practical approach," *The Volta Review*, vol. 89, no. 3, pp. 157–176, 1987.

[14] C. Yoshinaga-Itano and L. S. Snyder, "Form and meaning in the written language of hearing-impaired children," *The Volta Review*, vol. 87, pp. 63–96, 1985.

[15] C. Musselman and G. Szanto, "The written language of deaf adolescents: patterns of performance," *Journal of Deaf Studies and Deaf Education*, vol. 3, no. 3, pp. 245–257, 1998.

[16] H. Hayes, B. Kessler, and R. Treiman, "Spelling of deaf children who use cochlear implants," *Scientific Studies of Reading*, vol. 15, no. 6, pp. 522–540, 2011.

[17] A. E. Geers and H. Hayes, "Reading, writing, and phonological processing skills of adolescents with 10 or more years of cochlear implant experience," *Ear and Hearing*, vol. 32, pp. 49S–59S, 2011.

[18] A. Yasamsal, E. E. Yucel, and G. Sennaroglu, "Relationship between age of cochlear implantation with written language skills in children," *Journal of International Advanced Otology*, vol. 9, no. 1, pp. 38–45, 2013.

[19] N. O. Schiller, "Masked syllable priming of English nouns," *Brain and Language*, vol. 68, no. 1-2, pp. 300–305, 1999.

[20] N. O. Schiller, "The masked onset priming effect in picture naming," *Cognition*, vol. 106, no. 2, pp. 952–962, 2008.

[21] M. J. Chen and J. C. Yuen, "Effects of pinyin and script type on verbal processing: comparisons of China, Taiwan, and Hong Kong experience," *International Journal of Behavioral Development*, vol. 14, no. 4, pp. 429–448, 1991.

[22] D. Wechsler, *Wechsler Intelligence Scale for Children*, Psychological Corporation, San Antonio, Tex, USA, 3rd edition, 1991.

[23] R. H. Chen, *Wechsler Intelligence Scale for Children*, Mandarin Version, Chinese Behavioral Science Corporations, Taipei, Taiwan, 3rd edition, 1997.

[24] A. B. Hollingshead, *Two-Factor Index of Social Position*, Department of Sociology, Yale University, New Haven, Conn, USA, 1957.

[25] H. R. Myklebust, *Development and Disorders of Written Language (Vol. I): Picture Story Language Test*, Grune and Stratton, New York, NY, USA, 1965.

[26] K. T. Yang, S. Y. Li, S. H. Chang, and C. C. Wu, *Written Language Ability Diagnostic Test for Children*, Psychological Publishing Company, Taipei, Taiwan, 2003, (Chinese).

[27] S. Archbold, M. E. Lutman, and T. Nikolopoulos, "Categories of auditory performance: inter-user reliability," *British Journal of Audiology*, vol. 32, no. 1, pp. 7–12, 1998.

[28] M. C. Allen, T. P. Nikolopoulos, and G. M. O'Donoghue, "Speech intelligibility in children after cochlear implantation," *American Journal of Otology*, vol. 19, no. 6, pp. 742–746, 1998.

[29] C. Allen, T. P. Nikolopoulos, D. Dyar, and G. M. O'Donoghue, "Reliability of a rating scale for measuring speech intelligibility after pediatric cochlear implantation," *Otology and Neurotology*, vol. 22, no. 5, pp. 631–633, 2001.

[30] B. G. Lin and P. H. Chi, *The Assessment of School Language Disorders*, National Taiwan Normal University Press, Taipei, Taiwan, 2007.

[31] S. S. Huang, *Graded Chinese Character Recognition Test: Instruction Manual*, Psychological Publishing Company, Taipei, Taiwan, 2001.

[32] C. M. Wu, Y. A. Chen, K. C. Chan et al., "Long-term language levels and reading skills in mandarin-speaking prelingually deaf children with cochlear implants," *Audiology and Neurotology*, vol. 16, no. 6, pp. 359–380, 2011.

[33] L. Lu and H. Liu, *Peabody Picture Vocabulary Test—Mandarin Version*, Psychological Publishing Company, Taipei, Taiwan, 1988.

[34] L. T. Wang and F. M. Su, "Development of standardized phonetically balanced word lists (Zhong kuo yu yin jun hen zi huei biao zhi bian zhi yian jiou)," *The Journal of Taiwan Otolaryngology-Head and Neck Surgery*, vol. 14, 1979.

[35] R. Heider and G. A. Heider, "A comparison of sentence structure of deaf and hearing children," *Psychological Monographs*, vol. 52, no. 1, pp. 42–103, 1940.

Hindawi Publishing Corporation
BioMed Research International
Volume 2015, Article ID 696281, 19 pages
http://dx.doi.org/10.1155/2015/696281

Research Article

Cochlear Implant Outcomes and Genetic Mutations in Children with Ear and Brain Anomalies

Micol Busi,[1] Monica Rosignoli,[2] Alessandro Castiglione,[3] Federica Minazzi,[2] Patrizia Trevisi,[3] Claudia Aimoni,[2] Ferdinando Calzolari,[4] Enrico Granieri,[5] and Alessandro Martini[3]

[1]*Department of Medical & Surgical Disciplines of Communication and Behavior, University Hospital of Ferrara, Via Fossato di Mortara 64/A, 44121 Ferrara, Italy*
[2]*ENT & Audiology Department, University Hospital of Ferrara, Via Aldo Moro 8, 44124 Ferrara, Italy*
[3]*Department of Neurosciences, Complex Operative Unit of Otorhinolaryngology and Otosurgery, University Hospital of Padua, Via Giustiniani 2, 35128 Padua, Italy*
[4]*Neuroradiology Service, University Hospital of Udine, Piazzale Santa Maria della Misericordia 15, 33100 Udine, Italy*
[5]*Neurological Clinic, University Hospital of Ferrara, Via Aldo Moro 8, 44124 Ferrara, Italy*

Correspondence should be addressed to Micol Busi; bsumcl@unife.it

Received 14 November 2014; Accepted 6 January 2015

Academic Editor: Prepageran Narayanan

Background. Specific clinical conditions could compromise cochlear implantation outcomes and drastically reduce the chance of an acceptable development of perceptual and linguistic capabilities. These conditions should certainly include the presence of inner ear malformations or brain abnormalities. The aims of this work were to study the diagnostic value of high resolution computed tomography (HRCT) and magnetic resonance imaging (MRI) in children with sensorineural hearing loss who were candidates for cochlear implants and to analyse the anatomic abnormalities of the ear and brain in patients who underwent cochlear implantation. We also analysed the effects of ear malformations and brain anomalies on the CI outcomes, speculating on their potential role in the management of language developmental disorders. *Methods*. The present study is a retrospective observational review of cochlear implant outcomes among hearing-impaired children who presented ear and/or brain anomalies at neuroimaging investigations with MRI and HRCT. Furthermore, genetic results from molecular genetic investigations (*GJB2/GJB6* and, additionally, in selected cases, *SLC26A4* or mitochondrial-DNA mutations) on this study group were herein described. Longitudinal and cross-sectional analysis was conducted using statistical tests. *Results*. Between January 1, 1996 and April 1, 2012, at the ENT-Audiology Department of the University Hospital of Ferrara, 620 cochlear implantations were performed. There were 426 implanted children at the time of the present study (who were <18 years). Among these, 143 patients (64 females and 79 males) presented ear and/or brain anomalies/lesions/malformations at neuroimaging investigations with MRI and HRCT. The age of the main study group (143 implanted children) ranged from 9 months and 16 years (average = 4.4; median = 3.0). *Conclusions*. Good outcomes with cochlear implants are possible in patients who present with inner ear or brain abnormalities, even if central nervous system anomalies represent a negative prognostic factor that is made worse by the concomitant presence of cochlear malformations. Common cavity and stenosis of the internal auditory canal (less than 2 mm) are negative prognostic factors even if brain lesions are absent.

1. Background

Cochlear implantation (CI) is a significant surgical innovation of the 20th century and is the first artificial sensory organ used in clinical practice. Currently, CI is an effective medical procedure. Nonetheless, there remain certain controversial issues from economic, clinical, and ethical point of view, especially in specific clinical conditions that could compromise the CI outcome and drastically reduce the chance of an acceptable development of perceptual and linguistic capabilities [1]. The CI has been devised to allow full access to verbal communication through the perception

of phonetic hallmarks. The success of this method is then given in general by the achievement of verbal communication performance by improving the skills of verbal perception to become comparable to people with normal hearing [2]. In the paediatric population, in children with profound hearing loss, which is unsuitable for obtaining significant results with traditional hearing aids, CI (if performed early) allows the optimal development of auditory and linguistic abilities, which drives toward adequate communication and intellectual development [2, 3]. Children with congenital profound hearing loss accumulate disadvantages over time in language skills and certain learning areas, which can lead to permanent limitations of personal skills at a later age. Because of the auditory habilitation/rehabilitation training with a cochlear implant, most of these patients can reach a complete disability "compensation" [2, 4]. Several studies have reported the results of the development of auditory perceptual and expressive verbal abilities in children with pre-, peri-, and postlingual deafness [3, 4]. Clinical experiences across the world have also shown that, among children with preverbal onset hearing loss, there is a critical period for the development of language skills, presumably due to the underlying neuronal plasticity, and learning would be strictly dependent on the presence of an adequate auditory input, which explains the need for early intervention to prevent the occurrence of a delay in language development and perceptive or expressive skills [5, 6].

The performance of the patients who received CIs varies significantly as a consequence of a substantial number of audiological and extra-audiological factors (age of hearing loss onset, duration of auditory deprivation, auditory function residuals, presence of associated disability and comorbidity, language skills at the time of the CI, duration of CI use, the presence of certain malformations of the inner ear, socioeconomic status, and familial environment) [7–9]. Even if a unique prediction of the results after CI is not yet available, mostly because of the extreme heterogeneity in the aetiology among profound hearing-impaired patients, there are many prognostic factors that can contribute to the audiological assessment [4, 10–12]. Among these, we emphasise the importance of inner malformations and brain anomalies.

Because cochlear implantation is an invasive and expensive surgical procedure, the identification of predictive factors is one of the most important goals; knowledge of the predictive factors can help to guide rehabilitation programs that are tailored to meet the expectations of clinicians, teachers, and parents [9]. The perception of verbal sounds is an important starting point to activate the processes of linguistic acquisition. The development of language depends on auditory skills and maturation of cortical functions (memory, attention, and intellectual abilities) [13, 14]. The linguistic processes typically follow the perceptive processes with a variable latency, which appears to be related to the age of the patients at the time of surgery [15, 16]. Specifically, children implanted in a very early age (8–12 months) experience linguistic evolution with a speed that is higher than that of normal hearing children of the same age, probably because of using lines of development in various linguistic domains that are different from the usual capabilities of normal hearing children [14, 15]. In other words, congenitally deaf patients develop many abilities to reach an adequate communication condition (lip-reading, visual reinforcement) that, when auditory function has recovered, work in synergy with auditory inputs, enhancing perceptual and visual skills; an analogous process is similar in visually impaired patients who develop, more than normal, auditory and olfactory skills [2]. On the other hand, it cannot be excluded that the normal auditory input is more detailed and complex and, thus, that it takes more time to develop and integrate superior central functions. In contrast, cochlear implant stimuli are simpler; thus, they do not need complex integration in the corpus callosum or cortical areas [17].

With the advances in molecular genetics over the past 20 years, our understanding of the pathogenesis of sensorineural hearing loss has greatly increased [18–21]. The most common mutations that are responsible for hearing loss involve the *GJB2* gene; *SLC26A4* mutations are the second cause of genetic hearing loss and the first among syndromic deafness. The *SLC26A4* (PDS) gene mutations result in abnormalities of the endolymphatic system, which lead to the dilation of the vestibular aqueduct as seen in Pendred syndrome. Several studies have shown that patients who have mutations of *GJB2* (or Cx26) (OMIM ∗ 121011) usually have excellent perception of speech and an optimal language development after the cochlear implant [22–24]. Additionally, it has been reported that *GJB2* mutations are not usually accompanied by macroscopic inner ear malformations [19]. Nevertheless, there is no evidence that genetic mutations or the interaction of a genetic diagnosis with other prognostic factors (such as abnormalities of the ear and brain) can predict CI outcomes.

Preoperative neuroimaging is mandatory in cochlear implant candidates for diagnostic and surgical purposes. This step usually includes an MRI as well as a high-resolution computed tomography (HRCT) of the temporal bone. MRI should be performed with contrast (gadolinium), unless otherwise noted or unless the test is in children who are not believed to have lesions that require contrast to be diagnosed. HRCT of the temporal bone does not require iodine contrast. Note that magnetic resonance imaging (MRI) is relatively contraindicated after cochlear implantation or it is arguably possible. Various experimental studies have shown that MRI scans can safely be performed with the CI in place [25]. This arrangement does not imply that it is generally safe to perform MRI in CI patients, because the type of implant, fixation method, and MRI units and sequences could vary. Even if it can be performed safely, the distortion that is caused by the implanted magnet will cause suboptimal interpretations. For the aforementioned reasons, cochlear implantation can be contraindicated in patients who need periodic follow-up with MRI [25].

At our clinic, preoperative radiological imaging of cochlear implant candidates includes both HRCT and MRI of the temporal bone during the same session, during anaesthesia, if required, which usually occurs in children. In addition to the MRI of the inner ear, we also perform brain and brainstem MRI scans. These scans enable us to exclude any incidental brain abnormalities that can contraindicate CI surgery. MRI is the best diagnostic tool for detecting malformations such as cochlear nerve hypoplasia or aplasia, and it is the

best screening tool for early cochlear ossification following bacterial meningitis [26, 27]. HRCT provides better images and definition of the facial nerve canal, middle ear, and otic capsule [28]. Central nervous system findings have been reported in 20–40% of the patients [29–32]. Some of these findings could result in neurodevelopmental delay and could negatively impact the outcome of cochlear implantation [30]. Nonetheless, increased experience in cochlear implantation has led to more children with abnormal cochleovestibular anatomy being considered as candidates [4, 11]. According to the literature, approximately 20% of the children who have sensorineural hearing loss have associated radiological anomalies of the temporal bone [33–36]. These temporal bone anomalies are accompanied by a wide range of hearing acuity, varying degrees of progression of hearing loss, and the presence or absence of related nonotological anomalies [33].

In general, "cochlear implantation is a relatively safe procedure with a low complication rate that ranges from 6% to 20%. Major complications are those that are life threatening or require surgery, whereas minor complications are those that can be medically treated. The inner ear malformations can increase the risk of meningitis, cerebrospinal fluid leakage, and facial nerve palsy" [37–41]. We should note that the rate of postoperative complications was higher in patients with anomalous inner ears than in patients with normal inner ears; most of them were minor and could be managed conservatively [41]. Nevertheless, the functional results reached by these children (perceptual and linguistic performance) are still poorly described and have not been predictable. Case studies have limited conclusions because of the high interindividual variability. For these reasons, it is not yet possible to draw clear guidance from the literature on which to base the selection of candidates [12, 13, 41]. The malformations in fact allow the correct insertion of a number of electrodes that are usually sufficient, and the patterns of neural responses are adequate to accomplish the recognition of an open set words. However, specific conditions that prevent a correct coupling between the electrode array and the cochlear nerve, even if the latter is present, such as a common cavity, are usually characterised by a poor outcome, unless very specific surgical strategies are enacted.

Approximately 80% of the children who have a congenital hearing loss have no macroscopic abnormalities of the ear, and their hearing loss is assumed to be the result of dysfunctions at a cellular level in the membranous inner ear. The remaining 20% can present inner ear dysplasia, which can be demonstrated on high-quality neuroimaging (HRCT without contrast and MRI, with contrast in adults or in specific cases). The inner ear abnormalities, whether dysplastic or nondysplastic, can be isolated or can be part of a multiorgan syndrome [19]. Developmental malformations that affect the otic capsule result in anomalies of both the membranous and bony labyrinth. The specific timing of the insult during otic capsule development determines the resulting type of malformation along a spectrum of congenital inner ear malformations that can occur when the normal process of development is impacted, even if it is not necessarily understood why this result occurs. The best review of these developmental anomalies is given by Cullen et al. [24] and Heller et al. [25], which is an update on the valuable original work by Jackler et al. [34], and the present study is essentially based on their classification (Figure 1) [42–46]. In clinical practice, CNS lesions are usually represented by neoplasms/neoformations, malformations, vascular/ischemic and gliotic lesions, white-matter disorders, demyelinating disorders, and viral/bacterial infections (meningitis and cytomegalovirus infections) (Figures 2, 3, 4, and 5).

The aims of this work were to study the diagnostic value of HRCT and MRI in children who have sensorineural hearing loss and who were candidates for cochlear implants; we also aim to analyse anatomic abnormalities of the ear and brain in patients who underwent CI. We analysed the effects of ear malformations and brain anomalies on the language development and CI outcomes. Finally, we described the genetic mutations that we found in the study group. A control study group of implanted patients without ear and brain anomalies was obtained (virtually) from clinical data and literature data for statistical purposes [47–50].

2. Methods

This study is a retrospective observational review of cochlear implant outcomes among hearing-impaired children who presented ear and/or brain anomalies at neuroimaging investigations with MRI and HRCT. Furthermore, genetic results from molecular genetic investigations (*GJB2*/*GJB6* and, additionally, in selected cases, *SLC26A4* or *mitochondrial-DNA* mutations) on this study group were herein described. Longitudinal and cross-sectional analyses were conducted using statistical tests. To create more homogenic groups and more study-specific findings (e.g., EVA) and to obtain more significant analysis, the main study group was divided into different subgroups, which were named with alphabetic letters.

A control study group was created starting from literature data and randomised selected cases (from our casuistry) of implanted children without neuroradiological findings [50]. A long-term follow-up was performed, which reported that the Geers and Moore score was achieved at 3, 6, 12, 24, and 36 months. Each of the subgroups was compared with the control study group. Furthermore, the subgroups were compared with each other only if the same patients were not present in either. Specific findings were reported as singular cases. A nonparametric test was used for statistical analysis: the Mann-Whitney U test. Furthermore, we used the ANOVA test (analysis of variance) for the comparison between patients with monolateral CI and patients with bilateral CI.

2.1. Audiological Assessment. Before implantation, all of the children had documented severe to profound or profound sensorineural HL (hearing loss) and failed an appropriate hearing-aid trial. Each patient has been investigated from an audiological point of view using objective tests, such as OAEs (otoacoustic emissions), ABR (auditory brainstem response), and ASSR (auditory steady state response), to estimate the pure-tone threshold and, in selected cases, to perform ECochG (electrocochleography). When possible,

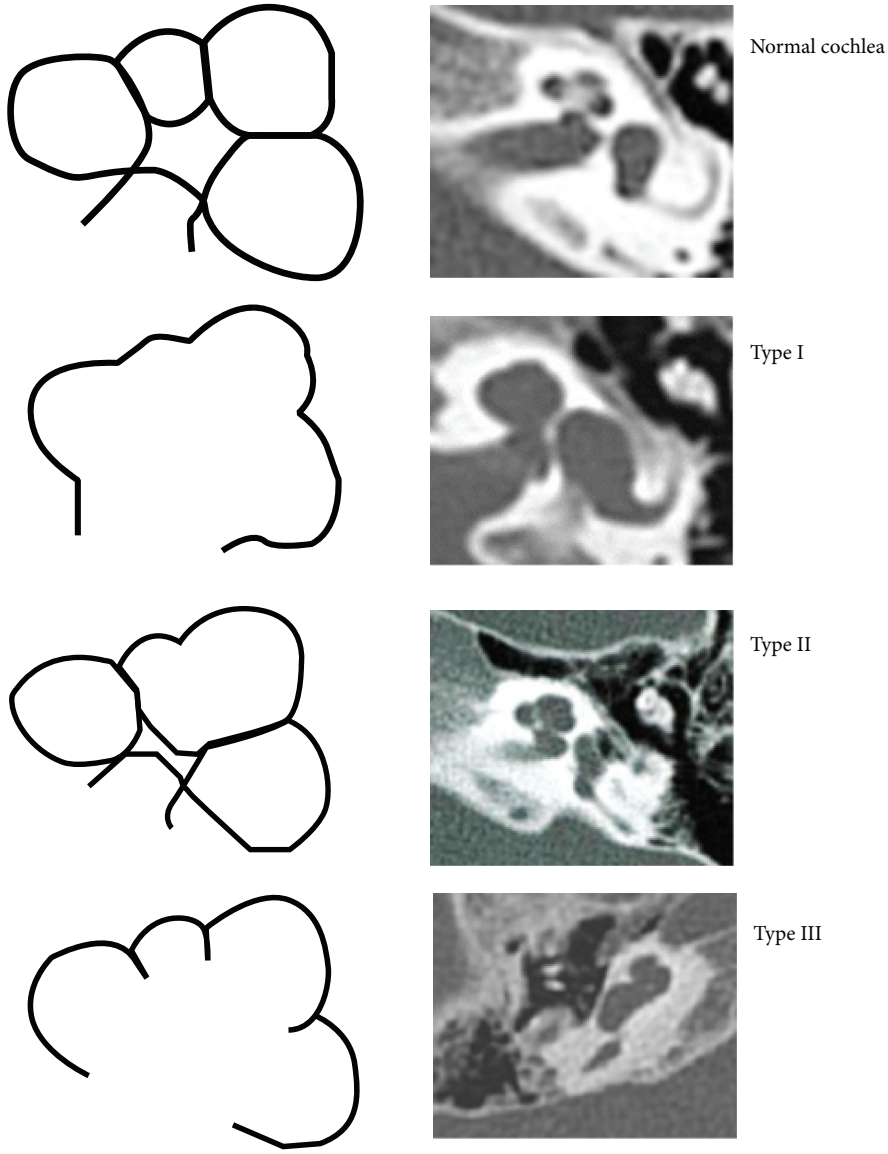

Figure 1: Incomplete partition types [45].

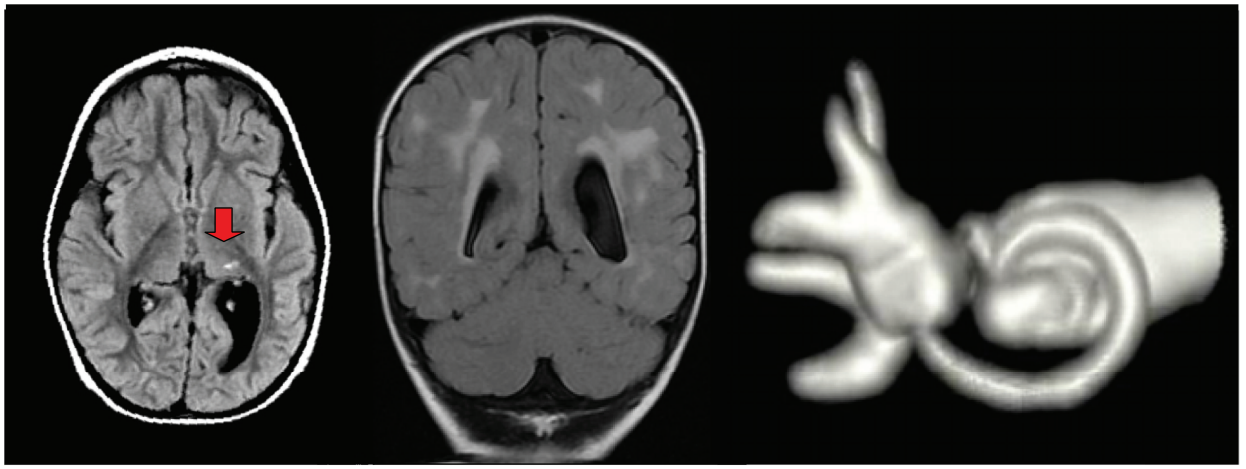

Figure 2: MRI scans, after effects of CMV meningoencephalitis, with patchy lesions of the white matter (red arrow) and dilation of the left lateral ventricle. 3D MR image of a case of semicircular canal occlusion, complication of CMV meningoencephalitis.

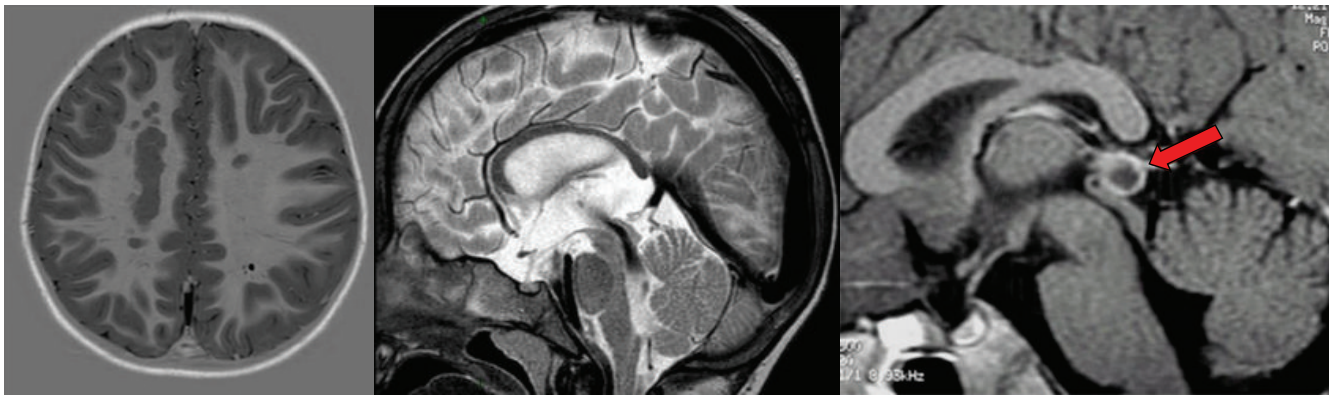

Figure 3: MRI scans: gray matter heterotopia, hypoplasia of the corpus callosum. Red arrow: pineal cyst.

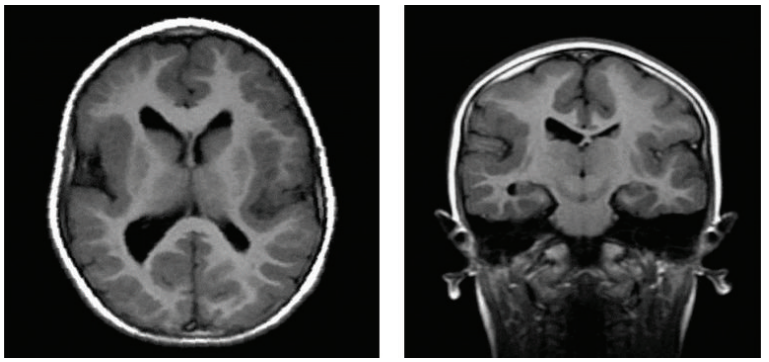

Figure 4: MRI scans. Cortical dysplasia.

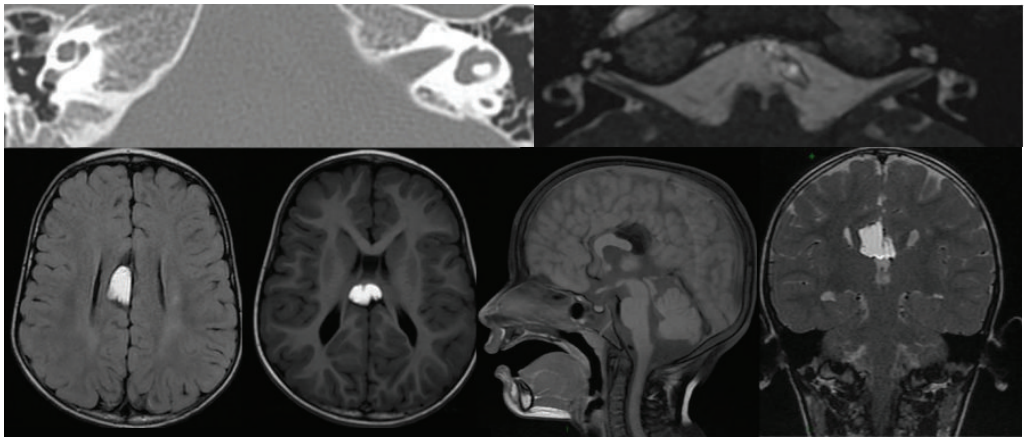

Figure 5: CT and MRI scans. Hypoplastic lateral semicircular canal; lipoma of the corpus callosum; agenesis of the posterior part and splenium of the corpus callosum; pellucid septum cyst; dilated cisterna magna (or cerebellomedullary cistern).

the audiological assessment was completed using behavioural and tonal audiometry with and without previously described hearing aids.

Children of 6–36 months of age underwent conditioned orientation reflex (COR) and visual reinforcement audiometry (VRA) tests to investigate the tonal threshold at low frequencies and to assess the effectiveness of the hearing aids. From the age of three to four years, the pure-tone hearing thresholds can be obtained by motivational games that range from peep shows to finger-raising techniques, and at an age of six years, most children can perform formal audiometry the same as that used in adults. The testing is dependent only on the degree of cooperation of the child and the experience of the tester. Microotoscopy, tympanometry, and recording of stapedius reflex thresholds were part of the test procedure. The interpretation and diagnostic validity of

stapedius-reflex-threshold testing in children are similar to the testing of adults, but the test might be difficult to perform in very young children.

2.2. Imaging Data. High resolution HRCT (high resolution computed tomography) and MRI (magnetic resonance imaging) were conducted in all patients to obtain a radiological examination of the temporal bone and brain. If necessary, children underwent neuroradiological scans during general anaesthesia. HRCT scanning with contiguous 0.3–1 mm thick images through the petrous temporal bone in the axial and direct coronal planes was performed. Ear, brainstem, and encephalon MRI scanning was acquired at 1.5 T and included high resolution axial and coronal T2-weighted imaging axial and coronal T1-weighted imaging, using CISS (constructive interference in steady state) and FIESTA (fast imaging employing steady state acquisition). If contrast was required, then postcontrast T1-weighted images were acquired in all three planes. CISS and FIESTA are a gradient-echo MRI sequence that are used to investigate a wide range of pathologies when routine MRI sequences do not provide the desired anatomic information. MRI brain scanning was also acquired at 1.5 T and included axial T2-weighted imaging, axial fast fluid-inversion recovery sequence (FLAIR) imaging, axial T1-weighted inversion recovery imaging, and, if contrast was required, axial T1-weighted imaging.

The neuroimaging findings of the temporal bone were categorised as

(1) cochlear malformations,

(2) vestibular and semicircular canal malformations,

(3) IAC (internal auditory canal) anomalies,

(4) EVA (enlarged vestibular aqueduct).

The vestibular aqueduct is defined as enlarged if its diameter is greater than 1.5 mm at the midpoint. Vestibular and labyrinthine abnormalities included partial SCC aplasia and total SCC aplasia. Cochlear malformations were subsequently divided as follows:

(1) cochlear malformations:

   (a) common cavity deformity,
   (b) cochlear hypoplasia,
   (c) incomplete partition type I (IP-I),
   (d) incomplete partition type II (IP-II) (Mondini deformity),
   (e) incomplete partition type III (IP-III),
   (f) basal turn dysplasia.

Mondini malformation is a cochlear anomaly that is characterised by a fusion of the apical and middle turn (only one and a half turns are present out of the normal two and a half turns).

The brain MRI scans of all of the patients were reviewed, and all of the abnormal findings were identified and classified as follows:

(1) malformations:

   (a) aplasia, dysplasia, or hypoplasia,
   (b) dilatations,
   (c) Arnold-Chiari malformations;

(2) neoformations:

   (a) neoplasms (benign or malignant),
   (b) cystic lesions;

(3) white matter disorders:

   (a) leukomalacia,
   (b) *leukodystrophy*,
   (c) demyelination;

(4) gliotic lesions (including cytomegalovirus infections and ischemic lesions);

(5) other abnormalities.

2.3. Genetic and Molecular Analysis. Informed consent was obtained from patients and parents according to current national rules and laws. Molecular genetic studies of the *GJB2*, *GJB6*, and *SLC26A4* genes and mitochondrial DNA (mit-DNA) were performed in 77 patients. Genomic DNA was extracted by standard protocols from peripheral blood leukocytes of patients. Direct DNA sequencing of the *GJB2* gene (including analysis of the entire coding region) was performed. PCR amplification of the coding 21 exons, the flanking, and promoter regions of the *SLC26A4* gene was performed using specific primers. Amplification reactions were performed in a final volume of 25 mL containing 100 ng of genomic DNA, 200 mmol/L dNTPs, 10 mmol/L each primer 1.5 mmol/L $MgCl_2$, and 1 U of Taq polymerase. After 5 min of denaturation at 94°C, 35 PCR cycles were carried out, each cycle comprising 45 s of denaturation at 94°C, 45 s of annealing at 60°C, and 80 s of extension at 72°C. Direct sequencing of the PCR products on both strands was performed on an ABI PRISM 3130xl sequencer, using the ABI BigDye Terminator v3.1 Cycle Sequencing Kit (Applied Biosystems by Life Technologies).

2.4. Speech Perception (Preoperative Assessment and Postoperative Outcomes). Behavioural measures of speech perception scores [50–54] are routinely completed in all children in our study at follow-up visits and a database of these outcomes is maintained. The database also includes patient demographics (age at implant, gender, and duration of implant use), audiological characteristics (congenital versus progressive loss), and relevant medical history (other medical conditions, such as craniofacial syndromes).

Perceptive abilities are usually classified into 4 types of increasing complexity performances [52, 53]:

(1) detection: ability to respond to the presence or absence of a signal;

(2) discrimination: ability to distinguish differences or similarities between two stimuli;

(3) identification: ability to choose an item from a known set;

(4) recognition: ability to repeat or imitate spoken stimuli.

The achieved performance enabled us to include each patient in a specific perceptual category. Geers and Moog proposed perceptive classification with six categories, which are based on performances that have been analysed with sets of specific tests [14].

Geers and Moog perception was used for the present study. A comparison of specific speech perception tests was conducted between hearing impaired children with normal anatomy (called "well babies") and those who were affected by cochleovestibular and brain abnormalities. An excellent tool for monitoring progress in young children is the Clinical Red Flag Procedure [50], which is a matrix of auditory benchmarks that has been established for identifying children who are progressing at a slower-than-expected rate. These benchmarks are based on research and clinical findings that document the listening skills that are achieved by the average CI child during the first year of device use. Three different groups of CI children reflect different preimplant characteristics and show different patterns of skill achievement [50].

It appears evident that in the "well babies," the perceptual expected results after 3 months of use of the CI essentially comprise the detection of voice and first discrimination abilities until the recognition of words and phrases without the help of lip reading at 1 year of CI use. In summary, the expected perceptual results were the achievement of perceptual category 2 at 3 months from the CI activation, perceptual category 4 at 6 months, and perceptual category 6 at 12 months. The follow-up initially should be very tightly controlled and should be performed in the first year after surgery, at 3, 6, 9, and 12 months and then yearly. The evaluation of perceptual skills and communication has been made by the administration of different tests according to the stage of language development of the child (preverbal stage, transitional stage, and functional stage).

3. Results

Between January 1, 1996, and April 1, 2012, at the ENT-Audiology Department of the University Hospital of Ferrara, 620 cochlear implantations were performed. There were 426 implanted children at the time of the present study (who were <18 years).

Reviewing the neuroradiological findings of the 426 implanted children revealed no abnormalities in 283 cases and ear and/or brain anomalies in 143 cases (33.6% of 426). Among these 143 patients (64 females and 79 males), 123 children had unilateral cochlear implantation (68 in the right ear; 55 in the left ear), and 20 underwent bilateral cochlear implantations (3 simultaneously, 17 sequentially). The age of the main study group (143 implanted children) ranged from 9 months and 16 years (mean = 4.4; median = 3.0). These patients showed an average period of cochlear implant use of 74 months.

The CT and MRI scans of 143 children included in the present study were reevaluated, and the following abnormalities were detected: in 69 cases (48.2% of 143), ear malformations were present, of which 55 had bilateral ear involvement; therefore, the implanted ear was necessarily the malformed ear; in 11 children, the malformed ear was the right ear (of which only in one case the malformed side was the implanted side), and in 3 cases, the malformation was detected in the left side (also in this series only one child underwent cochlear implantation in the malformed ear); 74 cases (51.7% of 143) presented only brain anomalies. A total of 45 patients (31.5% of 143) presented either ear or brain abnormalities. Table 1 shows different aetiologies of hearing loss that we found in our series. Demographic groups and audiological features are resumed in Table 2.

Details of the identified cochleovestibular (inner ear) malformations are presented in Tables 3 and 4.

Finally, Table 5 reports in detail the brain anomalies that were found, with the total number of cases for each type. For statistical purposes, the main group was divided into subgroups, as follows (Table 6).

3.1. Postoperative Speech Perception Outcomes. After 3 months of using the cochlear implant, more than half of the patients in the main study group did not achieve the 3th category of perception at the Geers and Moog scale; in the same group, the 50% of the children did not reach the 4th category at the 6-month follow-up; nevertheless, they achieved the 5th category 6 months after (1-year follow-up). Only 2 years after cochlear implant activation, the majority of the patients attain a 6th perceptual category at the Geers and Moog scale (Table 7).

Statistical results are reported in full as the following graphs (Figure 6). These graphs show the comparison between the control group and each of the subgroups; nonetheless, different subgroups were compared.

Graphs are structured as follows: on the abscissa axis are reported the number of cases, and they are distributed over the time of the 3-, 6-, 12-, 24-, and 36-month follow-ups, using a colour code for identification (red for the 3-month control, green for the 6-month control, blue for the 12-month control, violet for the 24-month control, and azure for the 36-month control).

There was a statistically significant difference ($P \leq 0.01$) between the control group and the subgroup B (patients with internal auditory canal stenosis) at the 6-month follow-up. Similar results were obtained comparing control group and subgroup Q (patients affected by leukomalacia).

At the 1-year and long-term (2-3 years) follow-ups, statistically significant differences ($P \leq 0.05$) were also found comparing control group and subgroups A, B, D, and E, respectively.

Table 1: Suspected main aetiology of hearing loss among 143 children who underwent cochlear implantation and presented ear or brain anomalies.

Aetiology	Number of patients	%
Unknown	27	18.9
Cytomegalovirus infection	26	18.2
GJB2 mutations	24	16.8
Acquired conditions (prematurity, perinatal suffering/icterus)	16	11.2
Enlarged vestibular aqueduct (EVA)	14 (4 Pendred syndromes)	9.8
Cochleovestibular malformations	14	9.8
Meningitis/encephalitis	12/1	9.1
CHARGE association	3	2.1
Hydrocephalus	2	1.4
Waardenburg syndrome (with dilated vestibule and bilateral cochlear dysplasia)	1	0.7
Möbius syndrome (with microtia and facial nerve aplasia)	1	0.7
Williams syndrome (with EVA and semicircular canal dysplasia)	1	0.7
Other conditions (neurosurgery)	1	0.7
Total	**143**	**100**

Table 2: Demographic, clinical and audiological data and aetiologies of hearing loss.

	External ear malformations (total N° = 3 cases)	Middle ear malformations (total N° = 18 cases)	Inner ear malformations (total N° = 30 cases)	Brain anomalies (total N° = 119 cases)	Without brain anomalies (total N° = 24 cases)
Sex (female : male)	1 : 2	9 : 9	11 : 19	55 : 64	9 : 15
Mean age (in years) at the time of surgery	3.0	3.0	4.4	4.0	7.0
Mean period (in months) of using cochlear implant	78	73	74	75	71
Implanted ear ($^{\circ}$)	2L, 1R	8L, 7R, 3B	11L, 15R, 4B	42L, 61R, 16B	13L, 7R, 4B
% of progressive hearing loss	—	22.2%	30.0%	45.3%	54.1%
Cytomegalovirus infections	—	3	2	26	—
Meningitis	—	—	1	11	1
Genetic mutations	—	2	5	21	3
Syndromes	3	3	5	6	4
Unknown aetiology	—	3	—	26	1
Other conditions (*)	—	2	2	19	1

$^{\circ}$(R = right; L = left; B = bilateral); *(infant cerebral palsy, prematurity, perinatal suffering, hydrocephalus, ischemia, and neonatal icterus).

Table 3: Anatomic distribution of inner ear malformations.

	Cochlear malformations (total N° = 21 cases)	Vestibular and semicircular canal malformations (§) (total N° = 24 cases)	Abnormal internal auditory canal ($^{\bullet}$) (total N° = 15 cases)	EVA (N° = 21 cases)
Sex (female : male)	6 : 15	10 : 14	10 : 5	10 : 11
Mean age (in years) at the time of surgery	4	4	5	7
Mean period (in months) of using cochlear implant	75	77	84	54
Implanted ear ($^{\circ}$)	8L, 11R, 2B	6L, 13R, 5B	7L, 8R	12L, 7R, 2B
Malformed side ($^{\circ}$)	1L, 2R, 18B	1L, 2R, 21B	1R, 14B	1L, 3R, 17B
% of progressive hearing loss	28.6%	41.6%	26.6%	71.4%

$^{\circ}$(R = right; L = left; B = bilateral); §(6 hypoplasias; 7 dilatations; 3 aplasias); $^{\bullet}$(7 stenosis; 8 dilatations).

Table 4: Types of cochlear malformations.

	Common cavity	Cochlear hypoplasia (total N° = 6 cases)	Incomplete partition type 1 (total N° = 2 cases)	Incomplete partition type 2 (total N° = 7 cases)	Incomplete partition type 3 (total N° = 2 cases)	Cochlear basal turn dysplasia (total N° = 4 cases)
Sex (female : male)	—	2 : 4	0 : 2	3 : 4	1 : 1	0 : 4
Mean age (in years) at the time of surgery	—	5	3	5	7	2
Mean period (in months) of using cochlear implant	—	59	82	85	77	73
Implanted ear ($^{\circ}$)	—	2L, 4R	1L, 1R	2L, 4R, 1B	1L, 1R	2L, 1R, 2B
Malformed side ($^{\circ}$)	—	1L, 1R, 4B	2B	1R, 6B	2B	4B
% of progressive hearing loss	—	40%	—	28.6%	50%	25%

$^{\circ}$(R = right; L = left; B = bilateral).

Table 5: Brain anomalies that were found among 143 implanted children.

Type of lesion/malformation	Total number of cases among 143 implanted children
Gliosis	32
Dysmyelination/demyelination	25
Leukomalacia	24
Pineal cyst	9
Arnold-Chiari malformation (type 1)	7
Cerebellar hypoplasia	6
Cortical dysplasia	5
Calcifications	3
Arachnoid cyst	3
(External) Hydrocephalus	3
Dilated lateral ventricles	2
Corpus callosum hypoplasia	2
Dilated fourth ventricle	2
Trigonocephaly	2
Facial nerve aplasia	1
Pinealoma	1
Hamartoma	1
Hydrocephalus	1
Bulbar atrophy	1
Cisternal dilatation	1
Malignant neoplasm of encephalon (after surgery)	1
Pellucid septum cyst	1
Dilated subarachnoid space	1
Focal ischemic lesions	1
Microcephaly	1
Lipoma	1
(Occipital) Myelomeningocele	1
Leukodystrophy	1
Pachygyria	1
Temporal lobe hypoplasia	1

Comparing subgroups C and P we found that the first one achieved the "identification of verbal sounds" 6 months after device activation and the "vowel recognition" in closed set tests 6 months later, while the subgroup P more slowly reached the same perceptual skills. Nevertheless, at the long-term follow-up (2 years later) the results achieved by the two groups are optimal and similar (Table 8).

3.2. Outcomes in Patients with Genetic Mutations. Figure 7 shows the statistical results obtained from patients with or without genetic mutations.

As reported in Table 9, the most common mutation was the 35delG in the *GJB2* gene. All patients with *SLC26A4* mutations presented bilateral EVA. Note that they had mutations on both alleles. Among these mutations, to our knowledge, 2 have never been described before (Q235R e G557D) and 1 was recently reported in one of our scientific publications entitled "Novel Mutations in the *SLC26A4* Gene" [55].

After 3 months of using the cochlear implant, more than half of the patients belonging to the subgroup M (patients who presented EVA) did not achieve the 3th category of perception at the Geers and Moog scale; in the same group, the 50% of the children did not reach the 4th category at the 6-month follow-up; nevertheless, they achieved the 5th category 6 months after (1-year follow-up). Only 2 years after cochlear implant activation, the majority of these patients attained a 6th perceptual category at the Geers and Moog scale (Table 10). There was a statistically significant difference ($P \leq 0.05$) between the control group and the subgroup M (patients who presented EVA) at the 1-year follow-up (Figure 6).

3.3. Outcomes Based on Age at the Time of Surgery. Given the great importance of timing of surgery for the CI outcomes we compared the results obtained from patients with only malformations of the inner ear (subgroup C) and patients with inner ear and concomitant brain abnormalities (subgroup E); then we divided these patients in those who underwent CI within 3 years of age and those who underwent CI after 3 years of age (Figures 8 and 9). Similarly, we compared the

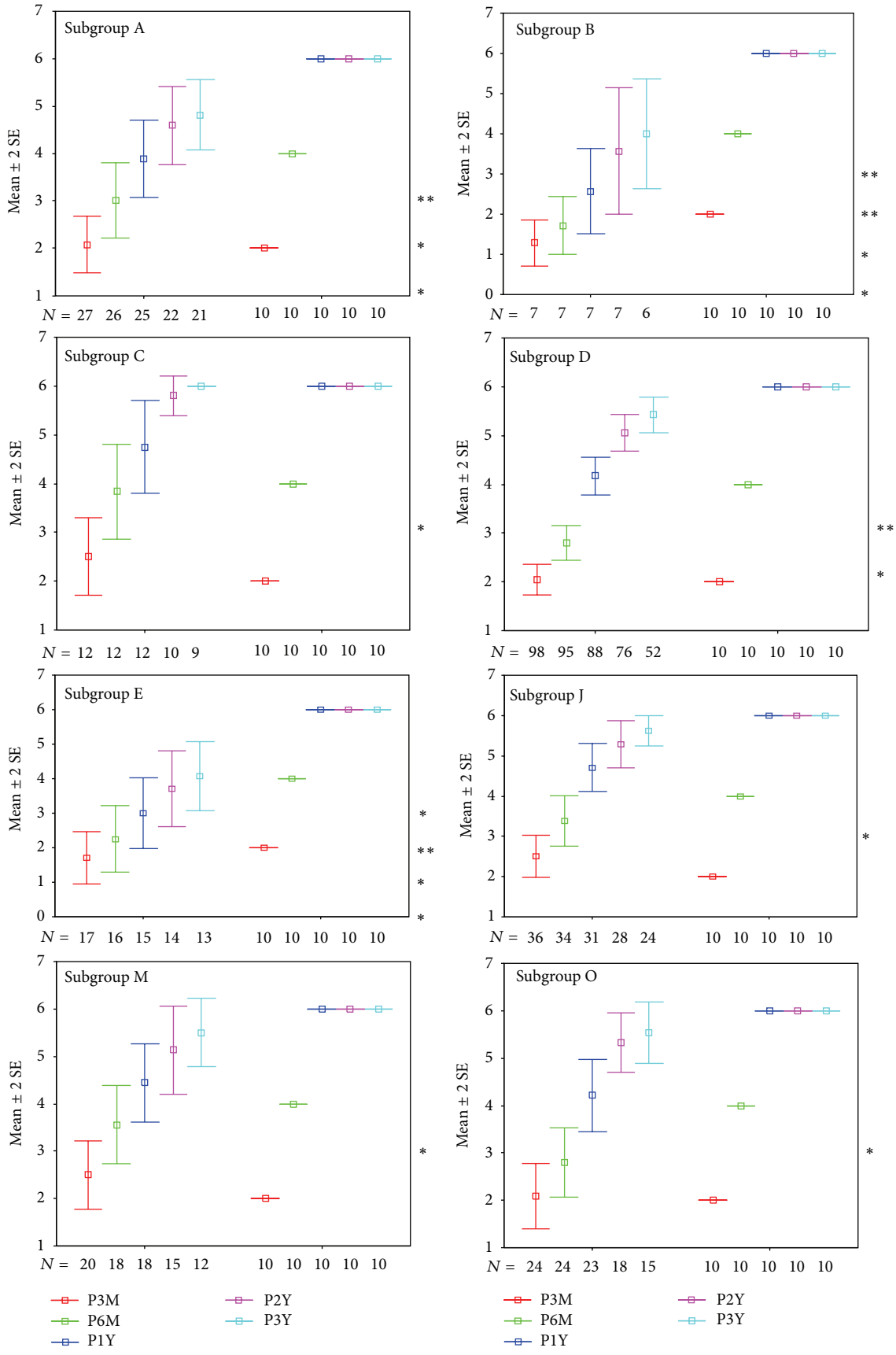

(a)

Figure 6: Continued.

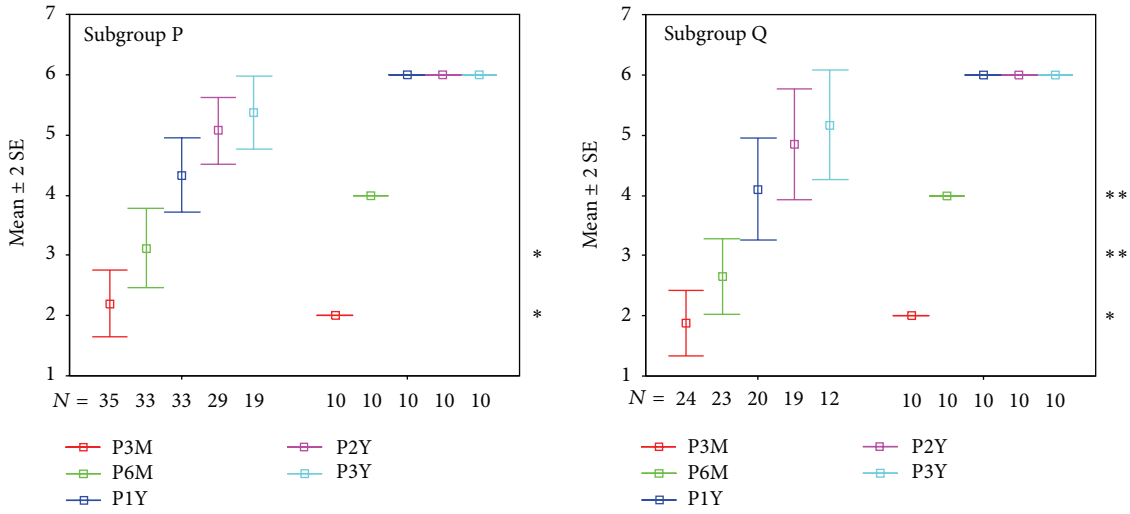

(b)

Figure 6: In the figure are reported all of the statistical graphs that were obtained from the comparison between the subgroups A, B, C, D, E, J, M, O, P, and Q and the control group. Colour code for identification (red for the 3-month control, green for the 6-month control, blue for the 12-month control, violet for the 24-month control, and azure for the 36-month control). $^{*}P \leq 0.05$; $^{**}P \leq 0.01$.

Table 6: Different subgroups were defined to implement the statistical analysis.

Groups	Inclusion criteria	Number of cases
Main study group	Cochlear implant recipients who were less than 18 years of age at the time of surgery and who presented neuroradiological findings at preoperative neuroimaging investigations	**143**
Subgroup A	Patients with inner ear malformations (with or without brain anomalies)	**23**
Subgroup B	Patients with internal auditory canal stenosis	**7**
Subgroup C	Patients with only inner ear malformations (without brain anomalies)	**13**
Subgroup D	Patients with only brain anomalies (without inner ear malformations)	**102**
Subgroup E	Patients with inner ear malformations and brain lesions or abnormalities (with brain anomalies)	**17**
Subgroup F	Monolateral CI	**123**
Subgroup G	Bilateral CI	**20**
Subgroup H	<3 years of age at the time of surgery	**61**
Subgroup I	>3 years of age at the time of surgery	**82**
Subgroup J	Patients with genetic mutations	**35**
Subgroup K	Cytomegalovirus	**26**
Subgroup L	Meningitis (as the cause of the hearing loss)	**13**
Subgroup M	Patients who presented EVA	**21**
Subgroup N	CHARGE association	**3**
Subgroup O	Demyelination	**25**
Subgroup P	Gliosis	**36**
Subgroup Q	Leukomalacia	**25**
Subgroup R	Patient with only cochlear malformations	**9**

patients with only brain abnormalities (subgroup D) and patients with inner ear malformations and concomitant brain abnormalities (Figures 10 and 11).

In our study, it should be noted that the performance after bilateral CI (Table 11) can be influenced down by the fact that results were collected starting from the first CI (dragging effect of the second device over the first one) and in case of a delay in the second CI (sequential surgery), the perceptual skills, at the 1-year follow-up, can still be related to the "effect" of the first CI and likely due to differences in time of using the second device. Comparing unilateral CI and bilateral CI (sequential in almost all cases), it was noted that, at the 1-year follow-up, 1 device allowed vowel recognition in closed set tests in 50% of patients (4th perceptual category), while 2 devices enabled 50% of patients to achieve speech recognition in open set tests (6th perceptual category).

Table 7: Perceptual outcomes of the main study group with a cochlear implant at the six-year follow-up.

Controls	*N*	Mean	SD	Percentiles		
				(25°	50°	75°)
3 m	133	2,113	1,579	1,00	2,00	3,00
6 m	127	2,945	1,844	1,00	3,00	4,00
1 y	117	4,120	1,890	2,00	5,00	6,00
2 y	100	4,940	1,693	4,00	6,00	6,00
3 y	70	5,243	1,408	4,75	6,00	6,00
4 y	44	5,432	1,301	6,00	6,00	6,00
5 y	29	5,896	0,409	6,00	6,00	6,00
6 y	24	6,000	0,000	6,00	6,00	6,00

Table 8: Comparison of the perceptual outcomes at the 3-month follow-up on congenital hearing loss without progression (C) and progressive hearing loss (P).

Controls		*N*	Mean	SD	Percentiles		
					(25°	50°	75°)
3 m	P	63	2,19	1,68	1	1	3
	C	74	2,05	1,47	1	2	2
6 m	P	60	3,13	1,96	1	3	5
	C	72	2,77	1,68	1	2	4
12 m	P	58	4,32	1,98	2	5,5	6
	C	67	3,98	1,79	3	4	6
2 y	P	53	4,96	1,70	4	6	6
	C	56	5,018	1,64	4	6	6
3 y	P	37	5,21	1,51	5	6	6
	C	44	5,40	1,26	6	6	6

Table 9: Mutations that were found among 143 implanted children.

Gene	Mutation	*N*°
GJB2	35delG/35delG	15
GJB2	35delG/R184P	4
GJB2	35delG/167delT	1
GJB2	35delG/R143V	1
GJB2	V27I/E114G	1
GJB2	VS1+1G>A/delE120	1
SLC26A4	G209V/Q235R	1
SLC26A4	L445W/G557D	1
SLC26A4	R409H/IVS2+1delG	1
SLC26A4	R409H/Q235R	1
MT-RNR1 (MIT DNA)	C722X (homoplasmy)	1

Table 10: Perceptual outcomes of subgroup M (EVA) at the 3-year follow-up.

Controls	*N*	Mean	SD	Percentiles		
				(25°	50°	75°)
3 m	20	2,50	1,60	1	2	3
6 m	18	3,55	1,75	2	3	5,25
12 m	18	4,44	1,75	3	5	6
2 y	15	5,13	1,80	6	6	6
3 y	12	5,50	1,24	6	6	6

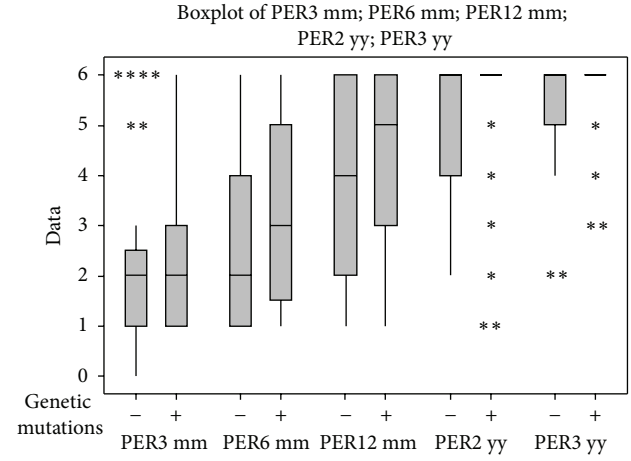

Figure 7: Perceptual outcomes at the 3-month follow-up on the children who underwent genetic investigation; differences between children with genetic mutations (+ = with pathogenic mutations) and children without mutations (− = without pathogenic mutations) are shown in the graphs.

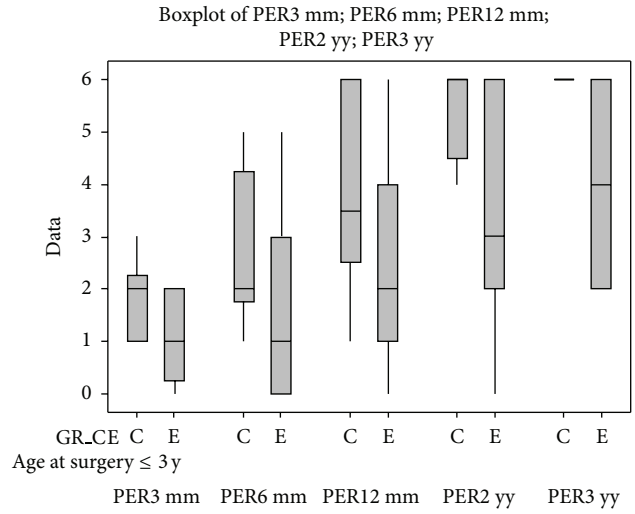

Figure 8: Comparison between the perceptual outcomes at the 3-year follow-up of children who were younger than 3 years old at the time of surgery and who belong to subgroups C and E.

More evident was the difference comparing 1 and 2 CI among patients belonging to the subgroup L in terms of rapidity in achieving the higher perceptual categories; in fact all bilateral cases had reached the "open set recognition" at the 1-year follow-up. In the subgroup L, there were 3 patients with postverbal, simultaneous, and bilateral CI (Table 11).

4. Discussion

In the present era, when cochlear implantation is a widely accepted therapy for sensorineural hearing loss, the selection of the patients is still a complex issue demanding close collaboration of experts in all different fields. There is no doubt that thorough radiological evaluation is of enormous

Table 11: Comparison between perceptual outcomes at 1-, 3-, and 5-year follow-ups of children who have 1 or 2 cochlear implants among the main group and subgroups K and L.

	Percentile	One-year follow-up			Three-year follow-up			Five-year follow-up		
		25°	50°	75°	25°	50°	75°	25°	50°	75°
Unilateral CI	Main group (*n*° 123)	2	4.5	6	4.5	6	6	6	6	6
	meningitis (*n*° 10)	1	2	4	2.5	5	6	6	6	6
	Cytomegalovirus (*n*° 21)	3	6	6	6	6	6	6	6	6
Bilateral CI	Main group (*n*° 20)	3	6	6	6	6	6	6	6	6
	meningitis (*n*° 3)	6	6	6	6	6	6	6	6	6
	Cytomegalovirus (*n*° 5)	3	5	6	6	6	6	6	6	6

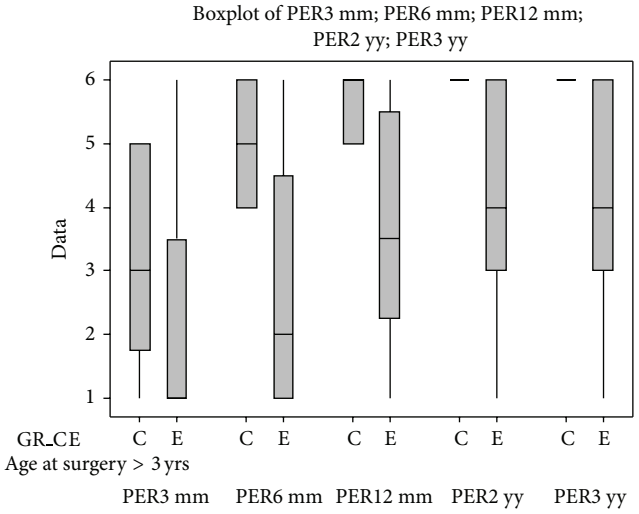

Figure 9: Comparison between perceptual outcomes at the 3-year follow-up of children who were older than 3 years at the time of surgery and who belong to the subgroups C and E.

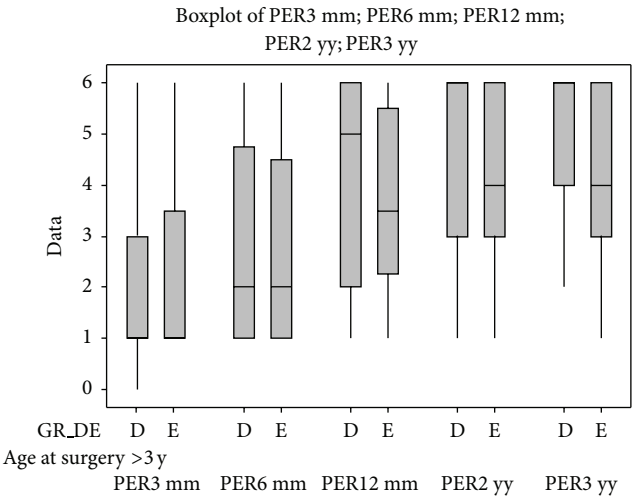

Figure 11: Comparison between perceptual outcomes at the 3-year follow-up of children who are older than 3 years of age at the time of surgery and who belong to the subgroups D and E.

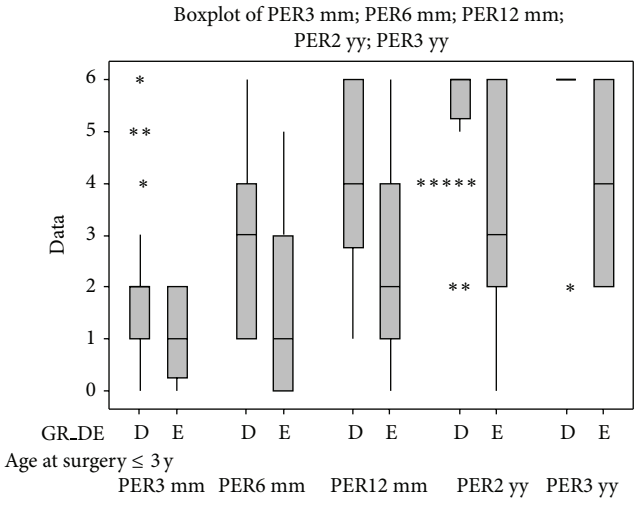

Figure 10: Comparison between perceptual outcomes at the 3-year follow-up of children who are younger than 3 years of age at the time of surgery and who belong to the subgroups D and E.

importance in malformed inner ears. An exact description and, if possible, classification of the abnormality builds the firm base of further evaluation. The results obtained allow us to affirm that abnormalities of the ear and brain are frequent findings among the cochlear implant candidates; for this reason, the neuroimaging has a fundamental diagnostic role. HRCT scans of the temporal bone help to define the surgical anatomy and provide information about cochlear abnormalities that can aid the surgeon in surgical planning and patient counselling. An absolute contraindication to cochlear implantation detectable by HRCT is the absence of the cochlea in Michel's aplasia. Although HRCT is the gold standard for evaluating most aspects of temporal bone anatomy, MRI is ideal in imaging soft tissue structures such as the membranous labyrinth and nerves. One disadvantage to using MRI in children, though, is the need for sedation [56].

Patients with severe inner ear malformations are expected to perform more poorly than patients with normal cochlea because of the likelihood of fewer spiral ganglion cells and the more complex surgery in malformed ears. Nevertheless, different types of electrode arrays have been introduced to

improve the placement of device and to develop speech performance. Because the electrodes may not be confined by scalar anatomy, electrode migration may occur, and individuals with cochlear malformations may require frequent reprogramming of the electrodes. Electrodes that are not intracochlear or that elicit facial nerve stimulation can be eliminated from the "map" as can electrodes that elicit facial nerve stimulation in implanted normal cochleae.

In previously published papers, several authors have shown that the benefits of implants in malformed inner ears are comparable to those gained by deaf children with morphological normal ears [36–38, 57, 58]. Indeed, assert that cochlear implantation can be successfully performed in children with inner ear malformations. The various types of inner ear malformations may have quite different prognoses for good auditory performance. In cases of cochlear ossification, the functional effects remain especially controversial. Predictors of good performance include the constellation of incomplete partition of cochlea: enlarged vestibular aqueduct (EVA), dilated vestibule (i.e., Mondini's malformation), isolated EVA, and partial semicircular canal aplasia. These patients achieve a different level of open set recognition in over the 80% of cases. Children with other cochlear dysmorphologies such as the common cavity or with associated pathologies like the CHARGE association and psychomotor retardation-developmental delay can have poor performance after implantation. Obtaining knowledge of cochlear malformation is especially important in counselling parents before implantation.

Kim et al. [9] observed that cochlear nerve hypoplasia was responsible for poor CI outcome that reduced the chance of an acceptable development of perceptual and linguistic capabilities. Other malformations can be responsible for delay in reaching the higher categories at the Geers and Moog scale. Nevertheless, they found no significant differences between the study group (with inner ear malformations) and control group (without inner ear malformations) at the 2-year follow-up. Loundon et al. [38] reported similar results that are summarized as follows: (1) at the 12-month follow-up, 83% of children achieved 75% of speech recognition in closed-set tests (corresponding to the 5th category at the Geers and Moog scale), (2) only 16% of those patients had obtained the same results during preoperative tests, (3) at the 2-year follow-up, they improved the perceptual abilities, and (4) 64% of children achieved 50% of speech recognition in open-set tests (corresponding to the 6th category at the Geers and Moog scale).

Eisenman and colleagues [57] found that all the subjects of their study showed improved performance on all measures of speech perception over time. Overall, the two groups showed no statistically significant differences in performance at 6 and 24 months. However, subjects with malformed cochleae evidenced slower rates of improvement than did their matched control subjects. Subjects with more severe malformations demonstrated poorer performance, but this may have been attributable to preoperative factors rather than to implant performance [57].

Incesulu and colleagues say that except cochlear or cochleovestibular nerve agenesis, inner ear malformations cannot be accepted as a contraindication for cochlear implantation. Although there can be difficulties during the surgery or in the postoperative period, patients with inner ear malformations can also benefit from cochlear implantation. It is essential that all possible complications and postoperative performance should be discussed with the parents [58].

Although there is controversial data in the literature on the prognostic value of specific factors, such as cochlear malformations and brain abnormalities, we can conclude that these factors do not necessarily affect the outcome of the cochlear implant; in fact, most of the factors that are typically encountered achieve satisfactory results. With the exception of a few special cases, such as stenosis of the internal auditory canal (<2 mm) and the common cavity, or instead the lack of the modiolus, which prevents an optimal pairing between electrodes and cochlear nerve fibres, the results, especially over a long-term period, are comparable to patients without neuroimaging findings, in terms of the achievement of perceptual abilities.

However, we must stress that, especially in the short term period (12 months), the presence of cochlear malformations could slow the attainment of more complete perceptual abilities; even more evident is the effect in the presence of disorders of the central nervous system. Note that the simultaneous presence of the inner ear malformations and anomalies of the brain determines a negative synergistic effect, with the achievement of lower perceptual categories (according to the Geers and Moog score) for the same period of use of the cochlear implant.

In the present study, 28% of implanted children were affected by brain anomalies identified by preoperative neuroimaging. Our results compare well with similar studies. Trimble et al. found central MRI abnormalities in 40% of the patients in their group compared to 20% in the study performed by Lapointe et al. [30]. Lapointe emphasized the importance of neuronal migrational delays resulting in the neurodevelopmental delay and potentially poor outcome from cochlear implantation. In addition to the brain MRI findings mentioned helping to predict speech perception and language outcome, Trimble et al. also commented on the importance of some findings to the anaesthetist (ventriculomegaly, hydrocephalus, Chiari malformation, and intracerebral haemorrhage) [29]. Of the abnormalities detected, 49% were related to known preexisting conditions. By far the most common abnormality detected in 84 patients was white matter changes (70%) and this was found in 13% of all patients investigated. Frequently the white matter changes were related to previous conditions/insults and included infection, ischaemia, hypoxia, and prematurity.

Apart from diagnosing incidental findings, MRI brain can aid in the diagnosis of hearing loss and has been shown to be important in predicting language and speech perception outcomes in patients with kernicterus and cytomegalovirus (CMV) infection as aetiological factors [31, 32, 59]. White matter changes have been shown to be an important determination of abnormal neurodevelopmental outcome and might

help predict future problems (seizures and intellectual impairment) in certain patients [60]. The full role of white matter changes in predicting hearing outcome in cochlear implant patients is still unclear.

A further potential advantage of preoperative brain MRI is that it might identify pathology that can be followed up with CT imaging, which is easily accessible postcochlear implantation. This was the case in three of the patients in this series with a lipoma, a hamartoma, and a pinealoma diagnosed on brain MRI whom required further imaging after cochlear implant. In addition, brain MRI will also provide a baseline for comparison with future MRI scans.

The group of patients with bilateral implantation was very heterogeneous by virtue of the great variability in the time of execution of the second cochlear implant; thus, it was not possible to determine the effect in the subgroups. We have focused the investigation on those patients with meningitis and cytomegalovirus infection because the number of cases available for comparison was higher and more homogeneous. Either subgroups (K and L) show a significant improvement after 1 year after the activation of the second cochlear implant.

In children, the most likely cause of cochlear ossification is meningitis. Twenty per cent of children acquire profound bilateral sensorineural hearing loss prior to the age of 3 years; 90 per cent of these cases are meningitic in origin [61]. Labyrinthitis ossificans results from severe inflammation of the inner ear and can be associated with a variety of pathology (advanced otosclerosis, viral or bacterial labyrinthitis, and autoimmune inner ear disease). Labyrinthitis ossification presents one of the greatest challenges to effective, safe cochlear implantation. Green and colleagues demonstrated that ossification due to meningogenic labyrinthitis extended further into the cochlea than ossification due to other causes. The extra bone growth makes the insertion of the electrode a difficult process [62]. In addition, the stimulation of surviving neural elements may be compromised by the bony obliteration, and histopathological reports have shown an association between the degree of bony occlusion and a decreased number of surviving spiral ganglion cells, particularly in cases of bacterial meningitis [63]. For these reasons, patients with labyrinthitis ossificans were often thought to perform at lower levels than those without ossification. In previously published papers [64, 65], several authors have shown that children with postmeningitic hearing loss and cochlear ossification could attain significant benefit from their implant, although children without ossification were likely to perform better. A key factor for success may be the timing of implantation. Ossification may appear as early as 2 months following meningitis, leaving a small time period during which electrode insertion is optimal. As mentioned previously, however, central nervous system sequelae of meningitis are likely to hold sway in determining outcome [66].

Hearing loss is the most common manifestation of congenital CMV infection making CMV a leading cause of nonhereditary congenital hearing loss [67]. The manifestations of CMV infection cover a broad spectrum ranging from asymptomatic to severe systemic disease resulting in significant morbidity and mortality. 90% of infants with congenital CMV are asymptomatic at birth. Despite being asymptomatic at birth, up to 7% of these children will develop sensorineural hearing loss that can be unilateral or bilateral, fluctuating or progressive, and range from mild to profound [68]. Approximately 10% of infants with congenital CMV are symptomatic at birth, and 40% of these patients will develop sensorineural hearing loss [69]. Given the relatively large number of children potentially affected by CMV-related hearing loss and the wide range of manifestations of congenital CMV infection, it is difficult to predict how a child with symptomatic CMV will perform with a cochlear implant. Congenital CMV infection accounted for a significant proportion of patients with SNHL, with an incidence rate comparable with that of *GJB2*-related SNHL.

Previous studies have shown that brain imaging may be a good predictor of adverse neurodevelopmental outcomes. In a study of children with a diagnosis of SNHL, 80% of the CMV positive children had abnormal brain MRI scans compared with only 33% of CMV negative children [70]. Our study demonstrated that certain imaging findings may correlate with worse outcomes after CI. Interestingly, the location of the abnormalities also seemed to correlate with worse perceptive outcomes. The majority of the abnormalities were found in the temporal lobe and parietal lobe. The parietal lobe processes sensory information and houses our language abilities, and the temporal lobe regulates emotion, hearing, language, and learning, which could explain why language outcomes are poorer in children with abnormalities in these regions.

Children with symptomatic congenital CMV appear to derive benefit from CI albeit at a slower rate. In a study of 13 children with symptomatic congenital CMV, 73% of implanted children achieved closed-set word recognition, and 63% achieved open-set word recognition [31, 32]. Ramirez Inscoe and Nikolopoulos demonstrated mixed results for speech perception and intelligibility with 50% of children with congenital CMV performing more poorly than controls, 31% performing similarly, and 19% performing better than controls. These children did, however, derive auditory benefit from cochlear implant [71].

Although our study has limitations including its retrospective nature and small sample size, it provides data that may further efforts to identify factors which may help predict which children with congenital symptomatic CMV will benefit from CI, albeit at a slower rate than other children. The location of central nervous system abnormalities, including gliosis and calcifications, may play a role in audiometric and perceptive outcomes after CI. Early measurements such as brain imaging findings and internal ear imaging findings may allow for more accurate counselling of families regarding anticipated postimplantation performance in children with symptomatic congenital CMV.

Cochlear implants can have impressive effects on a child's language abilities, yet outcomes remain variable across the paediatric population. Numerous studies have thus attempted to identify predictors determining postimplantation communication. So far, relevant factors are age at onset of deafness, age at implantation, length of implant use, amount of

residual hearing, duration of deafness, educational mode and resources, and psychosocial elements [2, 4–10].

A clear factor seems to be the age at implantation: children appear to perform better when implanted at earlier stages [72]. On IT-MAIS testing, Robbins and colleagues found that children implanted under the age of 19 months demonstrated faster progress and higher scores than those implanted between the ages of 2 and 3. As Geers found, though, this age advantage disappears after 2 years, implying a critical period of development within the first 2 years of life. At older ages, then, other factors begin to affect implant performance [50].

Although it is known from the literature that the precocity of diagnosis and treatment is an important prognostic factor in the auditory/habilitation, in our study the difference between the patients that, at the time of surgery, were younger than 3 years of age and those who were older than 3 years was not significant or at least fell short of expectations. More specifically, children who received implants within 3 years of age showed the worst results in the early controls (3 months); we cannot exclude a bias of the study due to the fact that children implanted at an early age, at three months after the implant activation, are not able to express perceptual skills that were included in the classification that was used. Nevertheless, at the 6-month follow-up, they started to show the "overtaking" effect in their perceptual performances. The outcome is not significantly different between the two groups, starting from the 1-year follow-up.

Paediatric audiological services should offer children with sensorineural hearing loss testing for mutations in Connexin proteins because mutations in at least two Connexins have been implicated in nonsyndromic hearing (*GBJ2* and *GBJ6*). As mentioned above, the most frequent mutation is found in Connexin 26 encoded by the *GBJ2* gene (35delG), resulting in DFNB1 [73]. Mutations in Connexin 26 result in sporadic and familial severe/profound prelingual hearing loss [24] and account for about 50% of recessive and 10% to 25% of sporadic nonsyndromic hearing loss in Southern European children. An evaluation from United States has shown that nearly 30% have Connexin 26-related hearing loss with all degrees of hearing loss [73] and thus it can be stated that mutations in Connexin 26 may result in all degrees of hearing loss. Thus, it is recommended that all children under 18 years of age with bilateral, permanent, nonsyndromic sensorineural, or mixed hearing loss, irrespective of the level of impairment, for which there is no other explanation, should be offered testing. The initial testing should check for 35delG and/or the other most frequent mutations in the background population. Unless the first screening identifies mutations on both alleles, testing should go on to screening of the entire coding region and splice sites for mutations. In addition, the presence of *GBJ6*/Cx30 deletions should be sought.

The perception at 3, 6, 12, 24, and 36 months shows no significant differences between subjects with genetic mutations (35delG in almost all cases) and patients without mutations. However, the obtained results show how the concomitant presence of malformations of the inner ear in the group of patients with mutation moves away from the expected outcome in patients with the same mutation but without abnormalities of the inner ear. The percentage of patients with mutations in our study group does not differ from the rates observed among patients without neuroimaging findings. This finding means that we are still far from establishing the true contribution of DNA mutations on the anatomy and development of the ear and brain. Therefore, it can be concluded that the detection of an abnormality of the ear or brain should not prevent the execution of genetic testing for mutations that are known to be those that are not associated with malformations (e.g., mutations in the gene *GJB2*).

As part of the protocol for diagnostic evaluation imaging techniques should be used in order to detect aplasia/hypoplasia and/or malformations such as enlarged vestibular aqueduct (EVA). EVA is often found in subjects with Pendred syndrome that is a recessive genetic hearing disorder. Sensorineural hearing loss may be fluctuant or progressive, ranging from mild to profound. The diagnosis of Pendred syndrome (or DFNB4) in such cases depends on analysis of mutations in the *PDS* gene, where the most frequent mutation is the *SLC26A4* [55]. An enlarged vestibular aqueduct remains the most common malformation of the inner ear, but it does not appear to influence the outcome of the cochlear implantation.

There were no significant differences between the group of children who had congenital profound hearing loss and children with progressive hearing loss, in either the short- or the long-term period. Comparing the perceptive outcomes of subgroups C (with inner ear malformations) and E (inner ear malformations with brain abnormalities) shows a significant difference starting from the 6-month follow-up ($P < 0.05$), which becomes more and more evident over time (at a 2- and 3-year follow-up, $P < 0.01$), in favour of those subjects who have only malformations of the inner ear and who have better performances.

We also compared the outcomes of the subgroups D (brain anomalies) and E (inner ear malformations with brain abnormalities) and, in this case, the differences begin to emerge at 12 months from the cochlear implantation ($P < 0.05$); they become more significant over time (at a 2- and 3-year follow-up, $P < 0.01$), in favour of those that have only brain anomalies that have better performances.

Brain anomalies affect the long-term outcome after cochlear implantation the most, especially among children who were older than 3 years at the time of surgery; comparing those children who belong to subgroups C and E showed an increasingly significant difference starting from 6 months ($P < 0.05$) after the cochlear implant activation. Furthermore, children who were older than 3 years and who belonged to subgroups D and E did not show any significant difference, from the underlying "dominant effect" of the brain abnormalities. This "dominant" effect appears to be less evident among the children who are younger than 3 years at the time of surgery, probably due to the greater neuronal plasticity.

5. Conclusions

A cochlear implant is a relatively safe and effective treatment for patients who have inner ear malformations and abnormalities of the brain. The aetiology remains unknown in most cases (18.9%). The cytomegalovirus infections are the main form of acquired deficit. The genetic mutation that is the most common among patients in this study remains the 35delG *GJB2* gene. The EVA is still the most common malformation of the inner ear, but it appears to have no specific effect on the outcome of the cochlear implant.

Gliotic injuries and disorders of the white matter brain abnormalities were more frequent, which in general showed a dominant effect on the outcome that was negative. In particular, difficult is fitting the result and the outcome of patients with stenosis of the internal auditory canal or in the presence of malformations with the cochlear absence of the modiolus.

Neuroimaging has been vital for a correct diagnosis and proper preoperative evaluation of cochlear implant candidates. Furthermore, the obtained data could be useful in defining the most appropriate timing of the follow-up, in specific cases and, if necessary, to develop better rehabilitation strategies in the event that the outcomes differ from the expected outcomes.

The CI outcome depends on many variables that range from the age at the time of the surgery to the communication mode. Nonetheless, before demanding a multidisciplinary approach, the otologist (or audiologist) has the responsibility to verify the correct functioning of the device, requiring, if necessary, a manufacturer's report to rule out technical failure. Afterwards, a clinical team should manage such unsatisfactory performances, after CI, starting from a self-review process of the applied paths (in terms of auditory rehabilitation or speech training), in order to detect errors in their settings. If there are persisting doubts concerning with the CI results after a technical and methodological review for challenging cases, the first functional and aetiological diagnosis should be reconsidered and reevaluated by a multidisciplinary team. Cooperation between parents, school administrators, teachers, and speech specialists is also vital to the success of the child.

Although further studies are necessary for the identification of predictive factors, especially in challenging cases, the results of the present study have confirmed the need to carry out diagnostic, therapeutic, and rehabilitation processes in specialised centres with extensive and proven experience.

Conflict of Interests

The authors declare that there is no conflict of interests regarding the publication of this paper.

References

[1] S. Funasaka, "The first artificial sensory organ applied in clinical medicine: cochlear implant," *Journal of the Japan Society of Mechanical Engineers*, vol. 100, no. 944, pp. 736–740, 1997.

[2] J. Busa, J. Harrison, J. Chappell et al., "Year 2007 position statement: principles and guidelines for early hearing detection and intervention programs," *Pediatrics*, vol. 120, no. 4, pp. 898–921, 2007.

[3] A. Martini, R. Bovo, P. Trevisi, F. Forli, and S. Berrettini, "Cochlear implant in children: rational, indications and cost/efficacy," *Minerva Pediatrica*, vol. 65, no. 3, pp. 325–339, 2013.

[4] B. C. Papsin and K. A. Gordon, "Cochlear implants for children with severe-to-profound hearing loss," *The New England Journal of Medicine*, vol. 357, no. 23, pp. 2380–2328, 2007.

[5] A. K. Cheng, G. D. Grant, and J. K. Niparko, "Meta-analysis of pediatric cochlear implant literature," *The Annals of Otology, Rhinology & Laryngology. Supplement*, vol. 177, pp. 124–128, 1999.

[6] F. Forli, E. Arslan, S. Bellelli et al., "Systematic review of the literature on the clinical effectiveness of the cochlear implant procedure in paediatric patients," *Acta Otorhinolaryngologica Italica*, vol. 31, no. 5, pp. 281–298, 2011.

[7] D. M. Hammes, M. A. Novak, L. A. Rotz, M. Willis, D. M. Edmondson, and J. F. Thomas, "Early identification and cochlear implantation: critical factors for spoken language development," *The Annals of Otology, Rhinology & Laryngology. Supplement*, vol. 189, pp. 74–78, 2002.

[8] C. Arnoldner, W. D. Baumgartner, W. Gstoettner et al., "Audiological performance after cochlear implantation in children with inner ear malformations," *International Journal of Pediatric Otorhinolaryngology*, vol. 68, no. 4, pp. 457–467, 2004.

[9] L. S. Kim, S. W. Jeong, M. J. Huh, and Y. D. Park, "Cochlear implantation in children with inner ear malformations," *Annals of Otology, Rhinology & Laryngology*, vol. 115, no. 3, pp. 205–214, 2006.

[10] M. Palmieri, S. Berrettini, F. Forli et al., "Evaluating benefits of cochlear implantation in deaf children with additional disabilities," *Ear and Hearing*, vol. 33, no. 6, pp. 721–730, 2012.

[11] B. C. Papsin, "Cochlear implantation in children with anomalous cochleovestibular anatomy," *Laryngoscope*, vol. 115, supplement 106, pp. 1–26, 2005.

[12] M. N. Pakdaman, B. S. Herrmann, H. D. Curtin, J. Van Beek-King, and D. J. Lee, "Cochlear implantation in children with anomalous cochleovestibular anatomy: a systematic review," *Otolaryngology—Head and Neck Surgery*, vol. 146, no. 2, pp. 180–190, 2012.

[13] A. Geers, C. Brenner, and L. Davidson, "Factors associated with development of speech perception skills in children implanted by age five," *Ear and Hearing*, vol. 24, no. 1, supplement, pp. 24S–35S, 2003.

[14] A. E. Geers and J. S. Moog, *Early Speech Perception Test for Profoundly Hearing-Impaired Children: Booklet*, Central Institute for the Deaf, St. Louis, Mo, USA, 1990.

[15] C. Yoshinaga-Itano, "Principles and guidelines for early intervention after confirmation that a child is deaf or hard of hearing," *Journal of Deaf Studies and Deaf Education*, vol. 19, no. 2, pp. 143–175, 2014.

[16] M. A. Svirsky, A. Silveira, H. Suarez, H. Neuburger, T. T. Lai, and P. M. Simmons, "Auditory learning and adaptation after cochlear implantation: a preliminary study of discrimination and labeling of vowel sounds by cochlear implant users," *Acta Oto-Laryngologica*, vol. 121, no. 2, pp. 262–265, 2001.

[17] J. T. Rubinstein, W. S. Parkinson, R. S. Tyler, and B. J. Gantz, "Residual speech recognition and cochlear implant performance: effects of implantation criteria," *American Journal of Otology*, vol. 20, no. 4, pp. 445–452, 1999.

[18] A. Martini, M. Milani, M. Rosignoli, M. Mazzoli, and S. Prosser, "Audiometric patterns of genetic non-syndromal sensorineural hearing loss," *Audiology*, vol. 36, no. 4, pp. 228–236, 1997.

[19] A. Martini, F. Calzolari, and A. Sensi, "Genetic syndromes involving hearing," *International Journal of Pediatric Otorhinolaryngology*, vol. 73, supplement 1, pp. S2–S12, 2009.

[20] V. Guaran, L. Astolfi, A. Castiglione et al., "Association between idiopathic hearing loss and mitochondrial DNA mutations: a study on 169 hearing-impaired subjects," *International Journal of Molecular Medicine*, vol. 32, no. 4, pp. 785–794, 2013.

[21] A. Castiglione, M. Busi, and A. Martini, "Syndromic hearing loss: an update," *Hearing, Balance and Communication*, vol. 11, no. 3, pp. 146–159, 2013.

[22] F. Gualandi, A. Ravani, A. Berto et al., "Exploring the clinical and epidemiological complexity of GJB2-linked deafness," *The American Journal of Medical Genetics*, vol. 112, no. 1, pp. 38–45, 2002.

[23] A. R. Sinnathuray, J. G. Toner, A. Geddis, J. Clarke-Lyttle, C. C. Patterson, and A. E. Hughes, "Auditory perception and speech discrimination after cochlear implantation in patients with connexin 26 (GJB2) gene-related deafness," *Otology and Neurotology*, vol. 25, no. 6, pp. 930–934, 2004.

[24] R. D. Cullen, C. A. Buchman, C. J. Brown et al., "Cochlear implantation for children with GJB2-related deafness," *Laryngoscope*, vol. 114, no. 8, pp. 1415–1419, 2004.

[25] J. W. Heller, D. E. Brackmann, D. L. Tucci, J. A. Nyenhuis, and C.-K. Chou, "Evaluation of MRI compatibility of the modified nucleus multichannel auditory brainstem and cochlear implants," *American Journal of Otology*, vol. 17, no. 5, pp. 724–729, 1996.

[26] L. Sennaroglu, I. Saatci, A. Aralasmak, B. Gursel, and E. Turan, "Magnetic resonance imaging versus computed tomography in pre-operative evaluation of cochlear implant candidates with congenital hearing loss," *Journal of Laryngology and Otology*, vol. 116, no. 10, pp. 804–810, 2002.

[27] L. Sennaroglu and I. Saatci, "A new classification for cochleovestibular malformations," *Laryngoscope*, vol. 112, no. 12, pp. 2230–2241, 2002.

[28] B. Isaacson, T. Booth, J. W. Kutz Jr., K. H. Lee, and P. S. Roland, "Labyrinthitis ossificans: how accurate is MRI in predicting cochlear obstruction?" *Otolaryngology—Head and Neck Surgery*, vol. 140, no. 5, pp. 692–696, 2009.

[29] K. Trimble, S. Blaser, A. L. James, and B. C. Papsin, "Computed tomography and/or magnetic resonance imaging before pediatric cochlear implantation? Developing an investigative strategy," *Otology and Neurotology*, vol. 28, no. 3, pp. 317–324, 2007.

[30] A. Lapointe, C. Viamonte, M. C. Morriss, and S. Manolidis, "Central nervous system findings by magnetic resonance in children with profound sensorineural hearing loss," *International Journal of Pediatric Otorhinolaryngology*, vol. 70, no. 5, pp. 863–868, 2006.

[31] D. J. Lee, L. Lustig, M. Sampson, J. Chinnici, and J. K. Niparko, "Effects of cytomegalovirus (CMV) related deafness on pediatric cochlear implant outcomes," *Otolaryngology—Head and Neck Surgery*, vol. 133, no. 6, pp. 900–905, 2005.

[32] A. Ciorba, R. Bovo, P. Trevisi, C. Bianchini, R. Arboretti, and A. Martini, "Rehabilitation and outcome of severe profound deafness in a group of 16 infants affected by congenital cytomegalovirus infection," *European Archives of Oto-Rhino-Laryngology*, vol. 266, no. 10, pp. 1539–1546, 2009.

[33] A. H. Park, B. Kou, A. Hotaling, B. Azar-Kia, J. Leonetti, and B. Papsin, "Clinical course of pediatric congenital inner ear malformations," *Laryngoscope*, vol. 110, no. 10, pp. 1715–1719, 2000.

[34] R. K. Jackler, W. M. Luxford, and W. F. House, "Congenital malformations of the inner ear: a classification based on embryogenesis," *Laryngoscope*, vol. 97, no. 3, pp. 2–14, 1987.

[35] P. D. Phelps, "Cochlear implants for congenital deformities," *Journal of Laryngology and Otology*, vol. 106, no. 11, pp. 967–970, 1992.

[36] F. Calzolari, G. Garani, A. Sensi, and A. Martini, "Clinical and radiological evaluation in children with microtia," *British Journal of Audiology*, vol. 33, no. 5, pp. 303–312, 1999.

[37] A. Ciorba, R. Bovo, P. Trevisi et al., "Postoperative complications in cochlear implants: a retrospective analysis of 438 consecutive cases," *European Archives of Oto-Rhino-Laryngology*, vol. 269, no. 6, pp. 1599–1603, 2012.

[38] N. Loundon, I. Rouillon, N. Munier, S. Marlin, G. Roger, and E. N. Garabedian, "Cochlear implantation in children with internal ear malformations," *Otology and Neurotology*, vol. 26, no. 4, pp. 668–673, 2005.

[39] L. Sennaroglu, S. Sarac, and T. Ergin, "Surgical results of cochlear implantation in malformed cochlea," *Otology and Neurotology*, vol. 27, no. 5, pp. 615–623, 2006.

[40] J. H. Ahn, J. W. Chung, and K.-S. Lee, "Complications following cochlear implantation in patients with anomalous inner ears: experiences in Asan Medical Center," *Acta Oto-Laryngologica*, vol. 128, no. 1, pp. 38–42, 2008.

[41] A. Benatti, A. Castiglione, P. Trevisi et al., "Endocochlear inflammation in cochlear implant users: case report and literature review," *International Journal of Pediatric Otorhinolaryngology*, vol. 77, no. 6, pp. 885–893, 2013.

[42] A. Aschendorff, R. Laszig, W. Maier et al., "Cochlear implant for malformations of the inner ear," *HNO*, vol. 57, no. 6, pp. 533–541, 2009.

[43] M. C. Dahm, H. L. Seldon, B. C. Pyman, R. Laszig, E. Lehnhardt, and G. M. Clark, "Three-dimensional reconstruction of the cochlea and temporal bone," *Advances in Oto-Rhino-Laryngology*, vol. 48, pp. 17–22, 1993.

[44] D. D. Purcell, N. J. Fischbein, A. Patel, J. Johnson, and A. K. Lalwani, "Two temporal bone computed tomography measurements increase recognition of malformations and predict sensorineural hearing loss," *The Laryngoscope*, vol. 116, no. 8, pp. 1439–1446, 2006.

[45] L. Sennaroglu, "Cochlear implantation in inner ear Malformations—a review article," *Cochlear Implants International*, vol. 11, no. 1, pp. 4–41, 2010.

[46] Y. Zheng, P. A. Schachern, H. R. Djalilian, and M. M. Paparella, "Temporal bone histopathology related to cochlear implantation in congenital malformation of the bony cochlea," *Otology and Neurotology*, vol. 23, no. 2, pp. 181–186, 2002.

[47] J. W. Casselman, F. E. Offeciers, P. J. Govaerts et al., "Aplasia and hypoplasia of the vestibulocochlear nerve: diagnosis with MR imaging," *Radiology*, vol. 202, no. 3, pp. 773–781, 1997.

[48] H. Rask-Andersen, W. Liu, E. Erixon et al., "Human cochlea: anatomical characteristics and their relevance for cochlear implantation," *Anatomical Record (Hoboken)*, vol. 295, no. 11, pp. 1791–1811, 2012.

[49] A. Sensi, S. Ceruti, P. Trevisi et al., "LAMM syndrome with middle ear dysplasia associated with compound heterozygosity for FGF3 mutations," *American Journal of Medical Genetics, Part A*, vol. 155, no. 5, pp. 1096–1101, 2011.

[50] A. M. Robbins, D. B. Koch, M. J. Osberger, S. Zimmerman-Phillips, and L. Kishon-Rabin, "Effect of age at cochlear implantation on auditory skill development in infants and toddlers," *Archives of Otolaryngology—Head and Neck Surgery*, vol. 130, no. 5, pp. 570–574, 2004.

[51] S. Archbold, "Monitoring progress in children at the pre-verbal stage," in *Cochlear Implants for Young Children*, B. McCormick, Ed., pp. 197–213, Whurr, London, UK, 1994.

[52] N. Erber, *Auditory Training*, Alexander Graham Bell Association, Washington, DC, USA, 1982.

[53] L. L. Elliott and D. R. Katz, *Northwestern University Children's Perception of Speech (NU-CHIPS)*, Auditec, St. Luis, Mo, USA, 1980.

[54] M. Ross and J. Lerman, *Word Intelligibility by Picture Identification (WIPI)*, Auditec, St. Louis, Mo, USA, 1980.

[55] M. Busi, A. Castiglione, M. Taddei Masieri et al., "Novel mutations in the SLC26A4 gene," *International Journal of Pediatric Otorhinolaryngology*, vol. 76, no. 9, pp. 1249–1254, 2012.

[56] J. K. Niparko, J. Leun, D. L. Tucci, M. J. Burton, and E. A. Mann, *Cochlear Implants in Children: A Review of Reported Complications, Patterns of Device Failure, and Assessment of Current Approaches to Surveillance*, Safe Medical Devices for Children, 2005.

[57] D. J. Eisenman, C. Ashbaugh, T. A. Zwolan, H. A. Arts, and S. A. Telian, "Implantation of the malformed cochlea," *Otology and Neurotology*, vol. 22, no. 6, pp. 834–841, 2001.

[58] A. Incesulu, M. Vural, U. Erkam, and S. Kocaturk, "Cochlear implantation in children with inner ear malformations: report of two cases," *International Journal of Pediatric Otorhinolaryngology*, vol. 65, no. 2, pp. 171–179, 2002.

[59] H. Yoshida, Y. Kanda, H. Takahashi, I. Miyamoto, T. Yamamoto, and H. Kumagami, "Cochlear implantation in children with congenital cytomegalovirus infection," *Otology & Neurotology*, vol. 30, no. 6, pp. 725–730, 2009.

[60] J. M. Perlman, "White matter injury in the preterm infant: an important determination of abnormal neurodevelopment outcome," *Early Human Development*, vol. 53, no. 2, pp. 99–120, 1998.

[61] S. A. Telian, S. Zimmerman-Phillips, and P. R. Kileny, "Successful revision of failed cochlear implants in severe labyrinthitis ossificans," *American Journal of Otology*, vol. 17, no. 1, pp. 53–60, 1996.

[62] J. D. Green Jr., M. S. Marion, and R. Hinojosa, "Labyrinthitis ossificans: histopathologic consideration for cochlear implantation," *Otolaryngology—Head and Neck Surgery*, vol. 104, no. 3, pp. 320–326, 1991.

[63] J. B. Nadol, "Patterns of neural degeneration in the human cochlea and auditory nerve: implications for cochlear implantation," *Otolaryngology—Head and Neck Surgery*, vol. 117, no. 3, pp. 220–228, 1997.

[64] R. L. Steenerson and L. B. Gary, "Multichannel cochlear implantation in children with cochlear ossification," *The American Journal of Otology*, vol. 20, no. 4, pp. 442–444, 1999.

[65] H. K. El-Kashlan, C. Ashbaugh, T. Zwolan, and S. A. Telian, "Cochlear implantation in prelingually deaf children with ossified cochleae," *Otology and Neurotology*, vol. 24, no. 4, pp. 596–600, 2003.

[66] H. W. Francis, M. B. Pulsifer, J. Chinnici et al., "Effects of central nervous system residua on cochlear implant results in children deafened by meningitis," *Archives of Otolaryngology—Head and Neck Surgery*, vol. 130, no. 5, pp. 604–611, 2004.

[67] R. F. Pass, "Congenital cytomegalovirus infection and hearing loss," *Herpes*, vol. 12, no. 2, pp. 50–55, 2005.

[68] A. J. Dahle, K. B. Fowler, J. D. Wright, S. B. Boppana, W. J. Britt, and R. F. Pass, "Longitudinal investigation of hearing disorders in children with congenital cytomegalovirus," *Journal of the American Academy of Audiology*, vol. 11, no. 5, pp. 283–290, 2000.

[69] A. Kenneson and M. J. Cannon, "Review and meta-analysis of the epidemiology of congenital cytomegalovirus (CMV) infection," *Reviews in Medical Virology*, vol. 17, no. 4, pp. 253–276, 2007, Review.

[70] J. W. Kimani, C. A. Buchman, J. K. Booker et al., "Sensorineural hearing loss in a pediatric population: association of congenital cytomegalovirus infection with intracranial abnormalities," *Archives of Otolaryngology—Head and Neck Surgery*, vol. 136, no. 10, pp. 999–1004, 2010.

[71] J. M. Ramirez Inscoe and T. P. Nikolopoulos, "Cochlear implantation in children deafened by cytomegalovirus: speech perception and speech intelligibility outcomes," *Otology and Neurotology*, vol. 25, no. 4, pp. 479–482, 2004.

[72] A. E. Geers, "Speech, language, and reading skills after early cochlear implantation," *Archives of Otolaryngology—Head and Neck Surgery*, vol. 130, no. 5, pp. 634–638, 2004.

[73] P. W. Bauer, A. E. Geers, C. Brenner, J. S. Moog, and R. J. H. Smith, "The effect of GJB2 allele variants on performance after cochlear implantation," *Laryngoscope*, vol. 113, no. 12, pp. 2135–2140, 2003.

Hindawi Publishing Corporation
BioMed Research International
Volume 2015, Article ID 359537, 12 pages
http://dx.doi.org/10.1155/2015/359537

Research Article

Hypoxia Induces a Metabolic Shift and Enhances the Stemness and Expansion of Cochlear Spiral Ganglion Stem/Progenitor Cells

Hsin-Chien Chen,[1] Jen-Tin Lee,[2] Cheng-Ping Shih,[1,3] Ting-Ting Chao,[4] Huey-Kang Sytwu,[3,5] Shiue-Li Li,[1] Mei-Cho Fang,[6] Hang-Kang Chen,[3] Yi-Chun Lin,[3] Chao-Yin Kuo,[1] and Chih-Hung Wang[1,3,5]

[1]*Department of Otolaryngology-Head and Neck Surgery, Tri-Service General Hospital, National Defense Medical Center, No. 325, Section 2, Cheng-Kung Road, Taipei 114, Taiwan*
[2]*Department of Otolaryngology, Auditory Medical Center, Cheng Hsin General Hospital, No. 45, Cheng Hsin Street, Taipei 112, Taiwan*
[3]*Graduate Institute of Medical Sciences, National Defense Medical Center, No. 161, Section 6, Minquan East Road, Taipei 114, Taiwan*
[4]*Medical Research Center, Cardinal Tien Hospital, No. 362, Zhongzheng Road, Xindian District, New Taipei City 23148, Taiwan*
[5]*Graduate Institute of Microbiology and Immunology, National Defense Medical Center, No. 161, Section 6, Minquan East Road, Taipei 114, Taiwan*
[6]*Laboratory Animal Center, National Defense Medical Center, No. 161, Section 6, Minquan East Road, Taipei 114, Taiwan*

Correspondence should be addressed to Chih-Hung Wang; chw@ms3.hinet.net

Received 28 August 2014; Accepted 3 October 2014

Academic Editor: Chung-Feng Hwang

Previously, we demonstrated that hypoxia (1% O_2) enhances stemness markers and expands the cell numbers of cochlear stem/progenitor cells (SPCs). In this study, we further investigated the long-term effect of hypoxia on stemness and the bioenergetic status of cochlear spiral ganglion SPCs cultured at low oxygen tensions. Spiral ganglion SPCs were obtained from postnatal day 1 CBA/CaJ mouse pups. The measurement of oxygen consumption rate, extracellular acidification rate (ECAR), and intracellular adenosine triphosphate levels corresponding to 20% and 5% oxygen concentrations was determined using a Seahorse XF extracellular flux analyzer. After low oxygen tension cultivation for 21 days, the mean size of the hypoxia-expanded neurospheres was significantly increased at 5% O_2; this correlated with high-level expression of hypoxia-inducible factor-1 alpha (Hif-1α), proliferating cell nuclear antigen (PCNA), cyclin D1, Abcg2, nestin, and Nanog proteins but downregulated expression of p27 compared to that in a normoxic condition. Low oxygen tension cultivation tended to increase the side population fraction, with a significant difference found at 5% O_2 compared to that at 20% O_2. In addition, hypoxia induced a metabolic energy shift of SPCs toward higher basal ECARs and higher maximum mitochondrial respiratory capacity but lower proton leak than under normoxia, where the SPC metabolism was switched toward glycolysis in long-term hypoxic cultivation.

1. Introduction

Unlike cochlear hair cells in the peripheral pathway, spiral ganglion neurons play a central role by sending sound information from the cochlea to the brain for hearing transduction [1]. However, similar to various nerve cells in the body, the spiral ganglion may undergo degeneration or damage through aging, noise exposure, chemical toxins, disease, and genetic disorders and usually cannot be replaced after being destroyed. Such neurodegeneration not only affects the integrity of the auditory system, but also may limit the functional benefit of cochlear implants [2, 3]. The recent emergence of stem cell-based medicine has the potential to revolutionize the study of neurodegenerative diseases. It has therefore motivated intense investigation on developing stem cell therapy as a new therapeutic strategy, for example,

through the transplantation of stem cells into the inner ear for hearing restoration [4].

Postnatal adult stem cells currently have attracted intense interest in stem cell research due to the lower possibility of teratoma formation, accessible donor cells, and tissue-specific cell fate determination. Since a very limited number of isolated adult stem cells may exist in some specific organs, such as the eye and cochlea [5, 6], it is very important to develop strategies to expand sufficient populations of adult stem cells for present investigation and future application.

Previously, we reported that short-term hypoxic cultivation would benefit from expanding cochlear stem/progenitor cells and maintaining their stemness markers through activation of hypoxia-inducible factor-1 alpha (Hif-1α) [7]. Similar benefits of mild hypoxia had also been observed in cultivated human neural stem cells by enhancing their expansion and multipotency [8]. Since the metabolic state is likely to influence the maintenance of the stem cell population and determine the cell fate of stem cells [9–11], it would be interesting to elucidate whether the metabolic signature is correlated with hypoxia-related stemness status and differentiation potential.

We hypothesized that the metabolism of cochlear spiral ganglion stem/progenitor cells (SPCs) in hypoxia differs from that in a normoxic condition. To test this, we cultivated cochlear spiral ganglion SPCs at different oxygen tensions to delineate their metabolic status and stemness properties; this represents the first such report in the literature.

2. Materials and Methods

2.1. Isolation and Culture of Cochlear Spiral Ganglion SPCs. The cochlear spiral ganglion SPCs were isolated using the method described in our previous report [7]. Briefly, the cochlear modiolus housing spiral ganglion cells and neuronal fibers were harvested from the cochleae of postnatal day 1 (P1) CBA/CaJ mouse pups. Using enzymatic and mechanical methods, these newly dissociated spiral ganglion-derived cells were plated in a noncoated T25 flask (Nunc) at 37°C in a 5% CO_2 atmosphere serum-free DMEM/F12 supplemented with penicillin-G, 20 ng/mL of epidermal growth factor (EGF, R&D), 10 ng/mL of basic fibroblast growth factor (b-FGF, R&D), 50 ng/mL of insulin growth factor (IGF, R&D), and N2 and B27 (GIBCO) supplements on the first day *in vitro* (DIV). The medium was changed every 3 days. After 7 DIV, primary spheres were observed. For secondary spheres, primary spheres were collected followed by mechanical dissociation with a Pasteur pipette and 0.05% trypsin. The dissociated primary spheres were maintained in a T25 flask for secondary sphere formation. To allow for continuous expansion, half of this medium was replaced every day and cultures were passaged every seventh day.

2.2. Immunocytochemistry. For immunocytochemistry staining, secondary spheres were either transferred to 24-well plates with coverslips and cultured in DMEM/F12 medium supplemented with 10% fetal bovine serum (FBS) overnight or prepared using a cytospin at 1,200 rpm for 5 min. The attached spheres were fixed in phosphate-buffered saline- (PBS-) buffered 4% paraformaldehyde and 2% sucrose, washed three times with PBS, permeabilized with 3% bovine serum albumin in PBS containing 0.3% Triton X-100, and blocked with 5% normal goat serum. Coverslips were incubated with mouse monoclonal anti-nestin antibody (1 : 500; Abcam) and rabbit polyclonal anti-Nanog antibody (1 : 200; Abcam) at 4°C overnight. After three washes with PBS, coverslips were incubated with fluorescein isothiocyanate- (FITC-) or tetramethyl rhodamine isocyanate- (TRITC-) conjugated secondary antibody (1 : 200; Thermo Fisher Scientific) to reveal the cell markers and stained with 4′,6-diamidino-2-phenylindole, dihydrochloride (DAPI; 0.66 mg/mL in PBS; Molecular Probes) for visualization of nuclei. Coverslips were mounted onto slides and examined under an epifluorescence microscope.

2.3. Cell Differentiation. Secondary spheres were cultured under adherent conditions in 24-well plates filled with DMEM and 10% FBS. The medium was changed every second day. After 96 h, differentiated cells were analyzed by immunocytochemistry. We used mouse monoclonal antibody to β-III tubulin (1 : 500; Thermo) and rabbit polyclonal antibody to glial fibrillary acidic protein (GFAP; 1 : 500; Abcam).

2.4. Bromodeoxyuridine (BrdU) Incorporation. Detection of BrdU incorporation in DNA-synthesizing cells was performed by adding 10 mM of BrdU (Sigma) to the secondary sphere. After a 72-h incubation period, spheres were plated onto coverslips in a 24-well plate containing DMEM/F12 and 10% FBS. After 24 h of cell seeding, coverslips were fixed and incubated in 2N HCl for 30 min at 37°C. Immunodetection of BrdU was performed using a monoclonal antibody against BrdU (1 : 500; Sigma). Fluorescence TRITC-tagged secondary antibody (1 : 200) was employed for visualization.

2.5. Hypoxia Incubation. Hypoxic culture conditions were continuously applied to newly isolated spiral ganglion cells or dissociated primary spheres in a N_2/CO_2 multigas incubator (APM-50D, Astec, Japan) by setting two different low oxygen tension (1% and 5% O_2) conditions and in a 5% CO_2 atmosphere at 37°C for the indicated time interval. The control group was exposed to a normoxic incubator at 37°C with 95% air and 5% CO_2. The medium was changed every 3 to 4 days.

2.6. Cell Proliferation Assay. Dissociated primary spheres were seeded in a 96-well plate (5×10^3 cells/well) and exposed to 1%, 5%, and 20% O_2 conditions in a 5% CO_2/37°C incubator for the indicated time interval. The medium was changed every 4 days. To determine cell proliferation, 10% WST-1 (Roche) agent was added to cell suspension in each well and incubated for 4 h. The reaction was catalyzed by a mitochondrial reductase in active cells, and the amount of formazan dye could be quantified by measuring the absorbance at 450 nm using Bio-Rad enzyme-linked immunosorbent assay (ELISA) reader to calculate the optical density (OD) values (A450 nm–A655 nm). Statistical analysis was determined using the Student's t-test, with $P < 0.05$ considered significant.

2.7. Western Blot Analysis. Primary spheres were seeded in six-well plates and cultured for 96 h at different oxygen concentrations (1%, 5%, and 20% O_2), respectively. Total cell lysates were prepared by lysing the spheres in a sample buffer (66 mM Tris-HCl, pH 7.4, 2% sodium dodecyl sulfate [SDS]) at 90°C. Lysates containing equal amounts of protein were loaded and separated on 8% SDS polyacrylamide gels. After electrophoresis, the gels were transferred to polyvinylidene difluoride (PVDF) membranes (Millipore), blocked with 5% skimmed milk in TBST (0.2 M Tris-base, 1.37 M NaCl, and 0.1% Tween 20), and probed with the indicated primary antibody at 4°C overnight. After washing three times with TBST, the membranes were then incubated with a peroxidase-conjugated secondary antibody for 1 h at room temperature and washed with TBST. The immunoreactive bands were stained using a light emitting nonradioactive method (ECL; Millipore). The specific primary antibody includes mouse anti-Hif-1α monoclonal antibody (1 : 500; Santa Cruz), mouse anti-proliferating cell nuclear antigen (PCNA) monoclonal antibody (1 : 1,000; BD Bioscience), mouse anti-cyclin D1 monoclonal antibody (1 : 1,000; Santa Crus), mouse anti-Abcg2 monoclonal antibody (1 : 1,000; Millipore), mouse anti-nestin monoclonal antibody (1 : 1,000; Abcam), rabbit anti-Nanog polyclonal antibody (1 : 1,000; Abcam), mouse anti-p27 monoclonal antibody (1 : 1,000; Neo-Markers), and rabbit anti-actin polyclonal antibody (1 : 2,000; Chemicon).

2.8. Side Population (SP) Cell Analysis Using Hoechst 33342 Staining and Flow Cytometry. SP cell analysis was carried out using the method previously described [12]. Briefly, following different oxygen tension exposures for 96 h, newly isolated spiral ganglion cells (5×10^5 cells/well) were dissociated and suspended in prewarmed medium at 37°C for 30 min. In the absence or presence of 1 μM fumitremorgin C (FTC; Alexis Biochemicals), cells were incubated with 5 μg/mL Hoechst 33342 (Sigma) at 37°C for 60 min, followed by washing with PBS. Samples were centrifuged and resuspended in cold PBS supplemented with 3% FBS (Biological Industries). Propidium iodide (PI; Sigma-Aldrich) was added at a final concentration of 2 μg/mL to exclude dead cells. FACS was performed using the BD FACSAria flow cytometer (BD Biosciences). The Hoechst dye was excited with an ultraviolet (UV) laser at 355 nm. A live gate was defined on the FACS using Hoechst red and blue axes to exclude dead cells and debris. Flow cytometry using Hoechst 33342 dye exclusion as a guiding parameter can determine the boundary between SP and non-SP cells. After 10^5 events were collected within the live gates, SP and non-SP cells were sorted and defined as Hoechst-low and Hoechst-bright cells, respectively.

2.9. Oxygen Consumption and the Extracellular Acidification Rate (ECAR). The mitochondrial oxygen consumption rate (OCR) and ECAR were measured using a Seahorse Bioscience XF24 extracellular flux analyzer (Seahorse Bioscience). Before the day of the assay, the cartridge sensor was hydrated overnight with 1 mL Seahorse Bioscience XF24 Calibration Buffer at 37°C without CO_2. On the day of the assay, SPCs were seeded in an XF24 Islet Capture Microplate and the growth medium was replaced with serum-free DMEM/F12 lacking sodium bicarbonate. Cells were then incubated at 37°C in a non-CO_2 incubator for 1 h. OCR and ECAR values were monitored under basal condition and measured after the injection of oligomycin (1 μM), FCCP (carbonyl cyanide p-trifluoromethoxyphenylhydrazone, 1 μM), and antimycin A (1 μM) to the well in succession. OCR and ECAR results were analyzed using the Seahorse XF-24 software. Every point represents an average of five different wells.

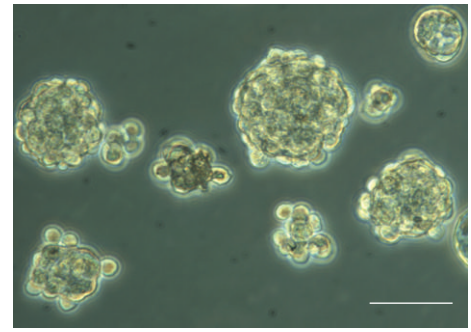

Figure 1: Newly isolated spiral ganglion SPCs derived from mice cochleae of P1 neonates formed spheres at day 7 in the ultralow plate containing serum-free medium. Scale bar = 75 μm.

2.10. Determination of Intracellular ATP. For comparison of relative ATP levels between hypoxic and normoxic conditions, the ATP assay was conducted using the ATP Bioluminescence Assay Kit CLS II (Roche). Cells (2×10^5) were lysed and centrifuged at 10,000 g for 60 s. The supernatant was reacted with luciferase reagent as instructed in the manufacturer's protocol.

2.11. Statistical Analysis. Statistical analysis was performed using a two-tailed Student's t-test. Results are expressed as means ± standard error of the mean (SEM). Differences were considered significant at $P < 0.05$.

3. Results and Discussion

3.1. Identification and Characterization of Cochlear Spiral Ganglion SPCs. Primary spheres derived from the cochlear spiral ganglion with a solid morphological population were produced after 7 DIV (Figure 1). These spheres were further dissociated and cultured in ultralow-attachment 6-well plates for another 7 days to generate secondary spheres. We used the secondary spheres to identify the stem cell markers and investigate their proliferative ability. Immunostaining confirmed the expression of stem cell markers nestin (Figure 2(a)) and Nanog (Figure 2(b)) in these spheres with BrdU incorporation (Figure 2(c)), implying that the spheres possess stem-like and self-renewal properties.

To investigate the potency of spiral ganglion SPCs, secondary spheres were cultured in adherent condition with 10% FBS containing DMEM/F12 for 96 h to allow for differentiation. Figure 3 demonstrates that the differentiated cells from spiral ganglion SPCs were able to express glial cell protein GFAP or neural marker βIII-tubulin. In addition, a small population of cells expressed both neural and glial

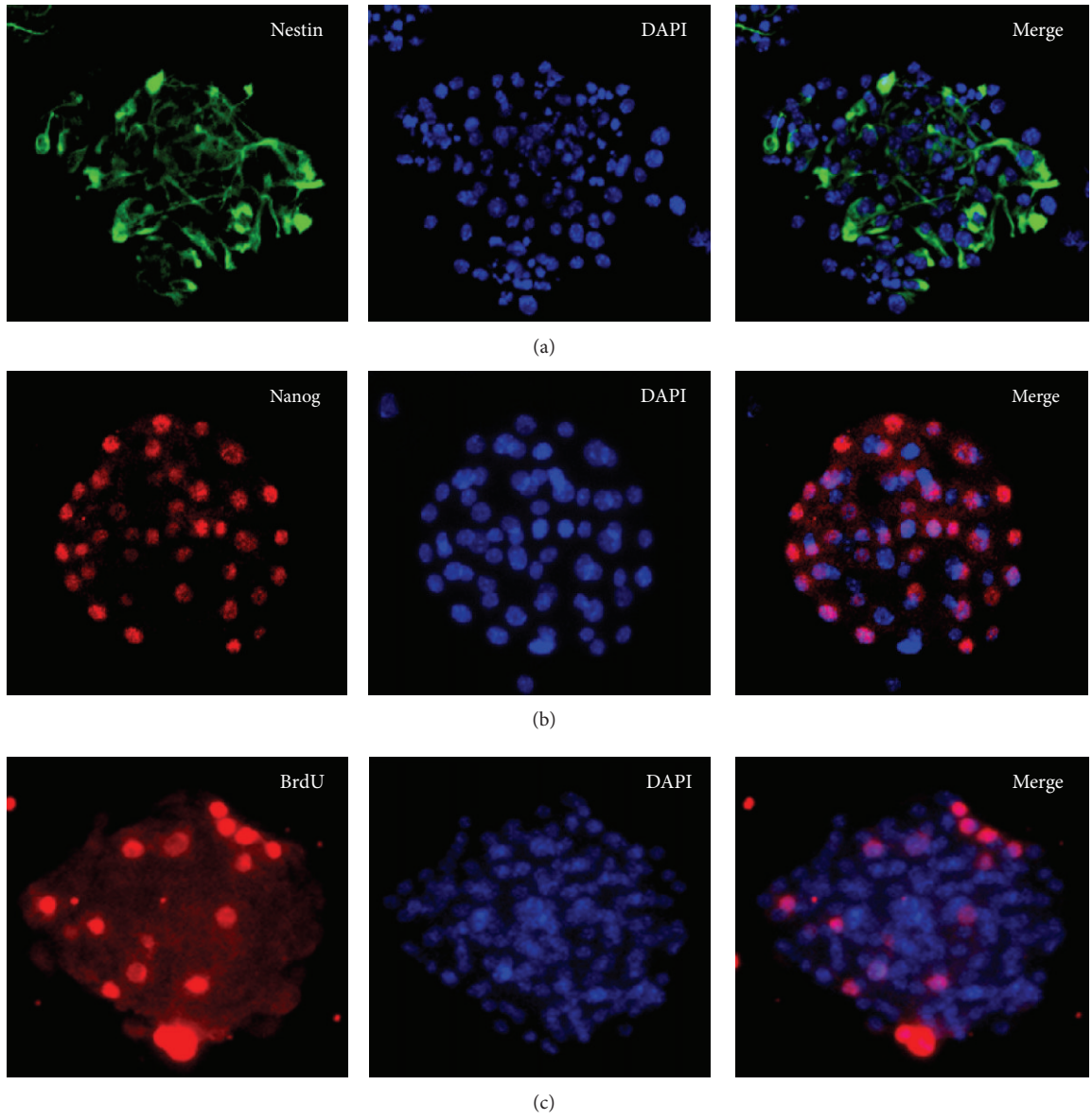

Figure 2: SPC markers and BrdU incorporation were revealed by immunocytochemistry. (a) Secondary spheres derived from spiral ganglion SPCs express nestin, an intermediate filament protein predominantly expressed by neural stem cells. (b) Nanog expression was observed in the nuclei of the majority of sphere-forming cells. (c) BrdU incorporation was detected in the nuclei of spheres. The blue-fluorescent DAPI nucleic acid stain for visualization of nuclei. Original magnification ×200.

cell proteins simultaneously. These results suggest that SPCs derived from the P1 mouse spiral ganglion are capable of proliferating and possess multipotency to differentiate into neuron and glial cells; this finding is supported in other reports [13] and is consistent with our previous research, which showed that cochlear SPCs from a postnatal cochlea retain characteristic stem-like and pluripotent differentiation potential [7].

The successful induction of cochlear spiral ganglion SPCs into neuron and glial cells may have several effects. First, it implies that spiral ganglion-derived SPCs are ready to adopt a spiral ganglion cell fate without the need for further genomic manipulation of donor cells. Second, in our study, spiral ganglion SPCs were proved to differentiate easily into neuronal lineages. Finally, replacement of damaged spiral ganglion neurons is feasible either via direct transplantation of SPCs into the inner ear alone or via being combined with cochlear implant surgery. Recently, Zhang et al. [3] identified mouse inner ear statoacoustic ganglion-derived neural progenitors that could be successfully induced into spiral ganglion-like cells by nerve growth factor after implantation into the adult mammalian inner ear. By transplantation of otic neural progenitor cells that were derived from human embryonic stem cells (hESCs) and able to differentiate *in vitro* into hair-cell-like cells and auditory neurons, Chen et al. [4] demonstrated a restoration of auditory evoked responses

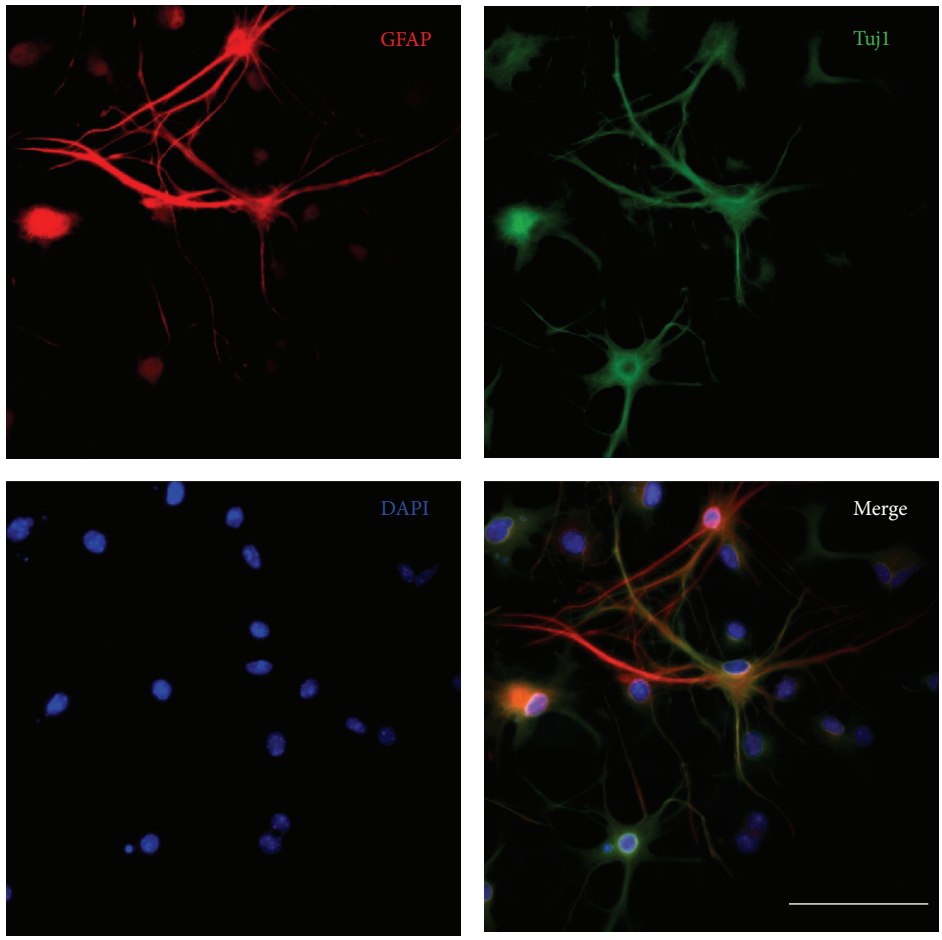

Figure 3: Induction of differentiation in spiral ganglion spheres. Secondary spheres were cultured in adherent conditions with the presence of 10% FBS in DMEM/F12 medium for 96 h. Immunocytochemistry reveals that some of them were found to differentiate into glial-like cells by expressing GFAP (red). Concurrently some sphere-forming cells differentiated into neural cells by expressing neuron-specific βIII tubulin (Tuj1, green). A small population of cells was immunostained by both GFAP and Tuj1 (merge). Scale bar = 100 μm.

from an auditory neuropathy model. These studies have provided a new promising approach to restoring lost hearing by neural progenitor cell replacement therapy.

3.2. Hypoxia Enhances the Sphere Formation and Proliferation of Cochlear Spiral Ganglion SPCs. To evaluate the hypoxia effect on cell proliferation, newly dissociated SPCs following different oxygen tension exposures for 48, 72, and 96 h were compared by WST-1 assay. The results indicated that low oxygen tensions significantly enhanced the proliferation of SPCs compared with normoxic conditions at each indicated time point (Figure 4(a)). In addition, newly dissociated single primary spiral ganglion cells underwent culturing at 1%, 5%, or 20% O_2; sphere formation could be observed in each oxygen tension group after 7 DIV, and the spheres were found to increase in size following long-turn culturing. On 21 DIV, a significant sphere size difference was observed between the hypoxia and the normoxia groups (Figures 4(b) and 4(c)). Furthermore, in hypoxic conditions, the sphere size at 5% O_2 was even significantly larger than that at 1% O_2 (330.67 $\pm$ 132.76 μm versus 190.00 $\pm$ 68.25 μm, $P < 0.05$; Figure 4(c)). These results indicate that low oxygen tensions benefit expanding cochlear spiral ganglion SPCs *in vitro*, which is in agreement with previous studies demonstrating that the culture of human stem cells over a physiological range of low oxygen tensions improves cell growth and expends their lifespan [14, 15]. Moreover, exposure of mammalian cells to 20% O_2 was shown to result in DNA damage [16, 17], whereas low oxygen tension improved the genetic stability of cultured human mesenchymal stem cells [14].

3.3. Hypoxia Upregulated the Expressions of Proliferation and Stemness Markers of Cochlear Spiral Ganglion SPCs. Previously, we demonstrated that cochlear SPCs cultured at 1% O_2 for 24 h enhanced their growth through Hif-1α [7]. However, the effect of different low oxygen tensions on the protein expression profile of proliferation and stemness of cochlear spiral ganglion SPCs has not yet been demonstrated. Given that Hif-1α is regulated mainly by oxygen tension through the oxygen-dependent degradation of its α subunit, we expected that low oxygen tension would be involved in controlling the cell cycle, cellular proliferation, or apoptosis by initiating a gene expression program through the Hif-1α. As shown in the results, the protein level of Hif-1α was

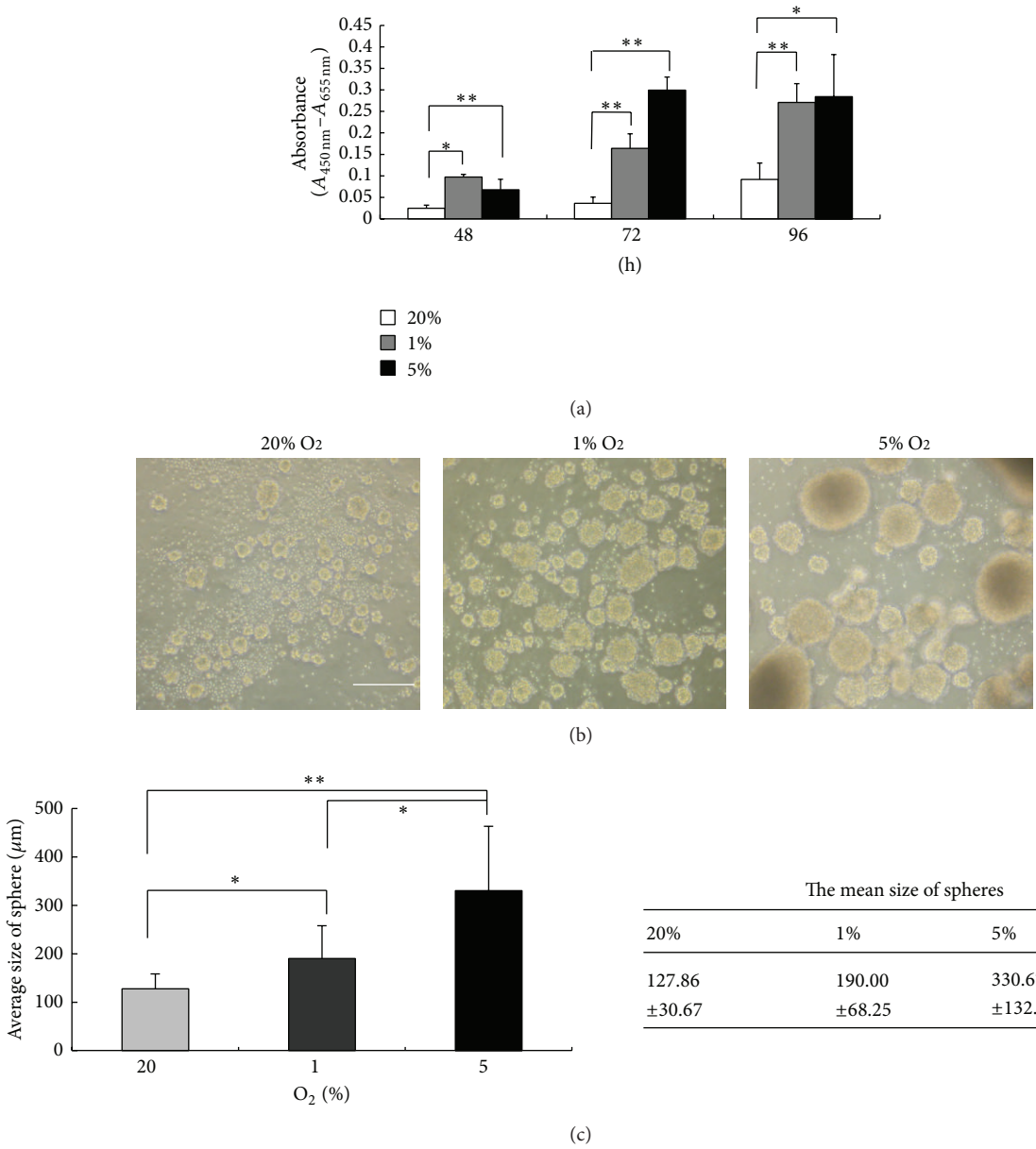

The mean size of spheres

20%	1%	5%	O_2
127.86 ±30.67	190.00 ±68.25	330.67 ±132.76	(μm)

FIGURE 4: (a) The effects of different oxygen tensions on the proliferation of cochlear spiral SPCs were examined using the WST-1 test. The proliferative capacities in the hypoxic groups significantly increased compared with the normoxic group at each time point. (b) Morphological changes of the spheres in each oxygen tension group were observed on 21 DIV. (c) Quantitative analysis of sphere sizes generated from single-cell cultures of SPCs undergoing different oxygen tension culturing was carried out on 21 DIV. Results are expressed as mean ± SEM with $n = 5$ for each bar. Scale bar = 300 μm; $*$ indicates $P < 0.05$; $**$ indicates $P < 0.01$.

increased at 1% and 5% O_2 compared to that at 20% O_2 (Figure 5(a)). Meanwhile, cyclin D1 and PCNA protein levels were also increased in low oxygen tensions, concomitant with a decreased protein level of $p27^{Kip1}$ (p27) (Figure 5(a)).

G1/S-specific cyclin D1 functions as a regulatory subunit of cyclin-dependent kinases (CDKs), whose activity is required for cell cycle G1/S transition. Overexpression of cdk4/cyclin D1 was found to increase the generation of basal progenitors and shorten the G1 of neural stem cells; thus, it can be used to increase progenitor expansion [18]. Regarding the significance of PCNA protein expression, Walters and Zuo showed that mouse cochleae at P1 and P2 were able to exhibit PCNA in hair cells and supporting cells, whereas by P5, PCNA was no longer detected in these cells [19]. This implies that persistence of PCNA in postnatal cochlear hair cells and supporting cells may retain some of the factors necessary for cell cycle entry. Therefore, PCNA can be used to mark cell proliferation and to identify a population of progenitor cells [20]. The role of the cell cycle inhibitor p27 in maintaining the stemness of hESCs has been demonstrated by showing the low expression level of p27 in hESCs, but this will lead to a G1 phase arrest, cell

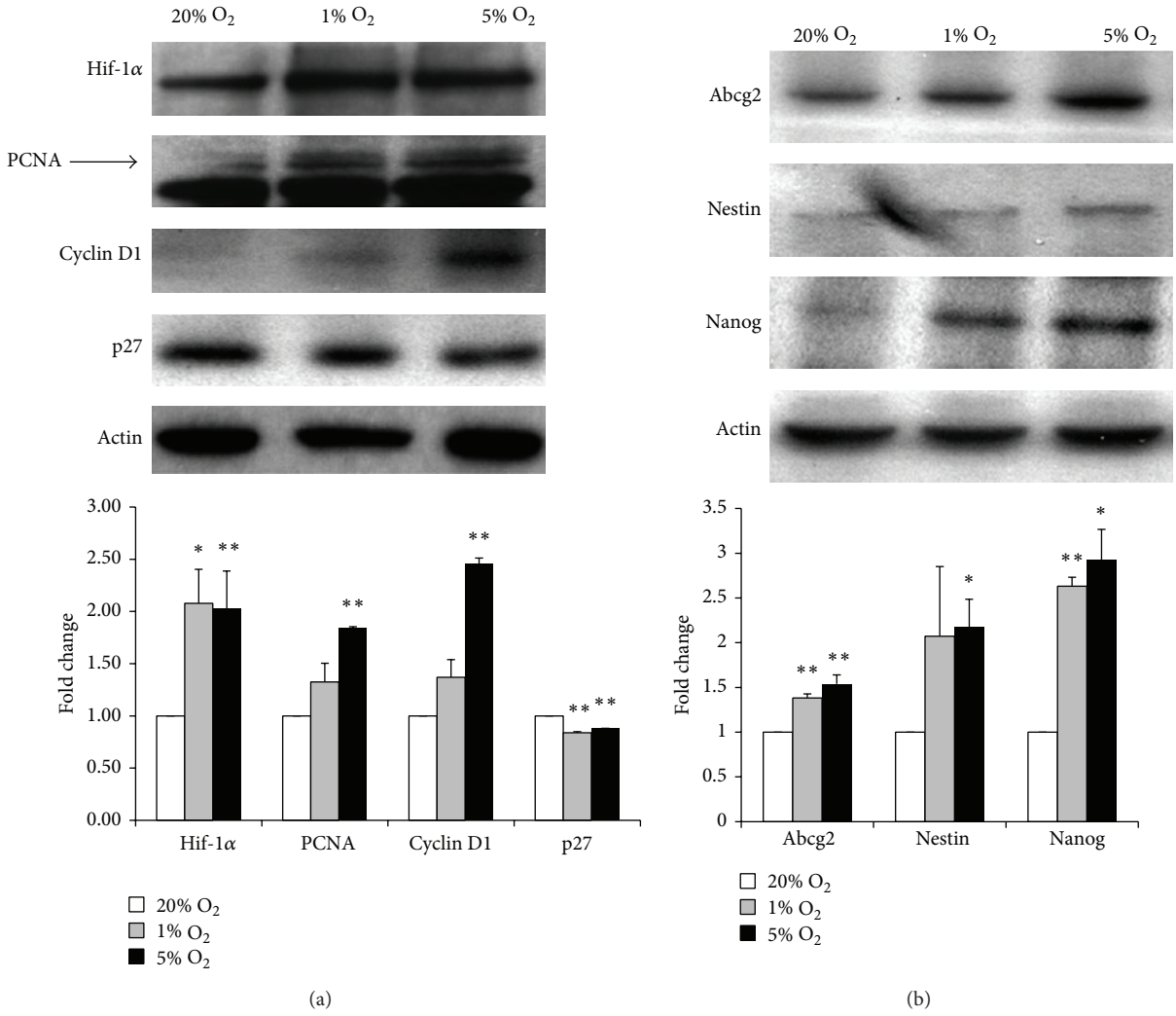

Figure 5: Western blot-based comparison of proliferation (a) and stemness (b) related proteins on cochlear spiral ganglion SPCs when exposed to different oxygen tensions for 4 days. Densitometric analysis of the western blot is reported in the histogram and shown in the lower panels. For the comparison, the expression levels of each protein (mean ± SEM, $n = 3$) were normalized to control actin protein levels and expressed as a fold change of the cells cultured at 20% O_2. ∗ indicates $P < 0.05$; ∗∗ indicates $P < 0.01$.

differentiation, and consequent loss of self-renewal ability when p27 is overexpressed [21]. Taken together, in this study, we found that hypoxia activates and amplifies cochlear spiral ganglion SPCs, reflected by the elevated expression of cyclin D1 and PCNA and decreased expression of p27. Concurrently, stemness-related protein expression, including Abcg2, nestin, and Nanog, was markedly induced at low oxygen tension compared to that at standard 20% O_2, with the most abundant protein level found at 5% O_2 (Figure 5(b)).

Hif-1α is believed to play a role of pivotal link between oxygen availability in the cell and several important processes such as energy metabolism, angiogenesis, and cell proliferation and viability [14, 22]. The impact of hypoxia involving Hif-1α signaling on SPC self-renewal, differentiation, maturation, and homing in various *in vitro* and *in vivo* settings was shown in our previous study [7] and other published literatures [23–25]. We demonstrated again in this study that Hif-1α is activated and associated with enhanced proliferation and stemness-related gene expression in cochlear spiral ganglion SPCs when exposed to low oxygen tensions.

3.4. Hypoxia Enhanced the SP Distribution. Isolation of SP cells has been recognized as a useful technique for the identification of cochlear SPCs [12, 26]. As shown in Figure 6, SPCs cultured at 5% O_2 prompted a prominent increase in the percentage of SP cells to 3.2%, whereas at 20% O_2, SPCs contained only 1.3% SP cells. That the obtained SP fraction markedly diminished through the addition of FTC helped to verify the specificity of the SP subpopulation obtained from the spiral ganglion SPCs. These results support low oxygen tension culture as a strategy for efficiently expanding cochlear SPCs or spiral ganglion SPCs without losing stem cell properties such as proliferation and self-renewal.

Although most organisms require O_2 for survival, as this is the primary substrate for energy production in the cell,

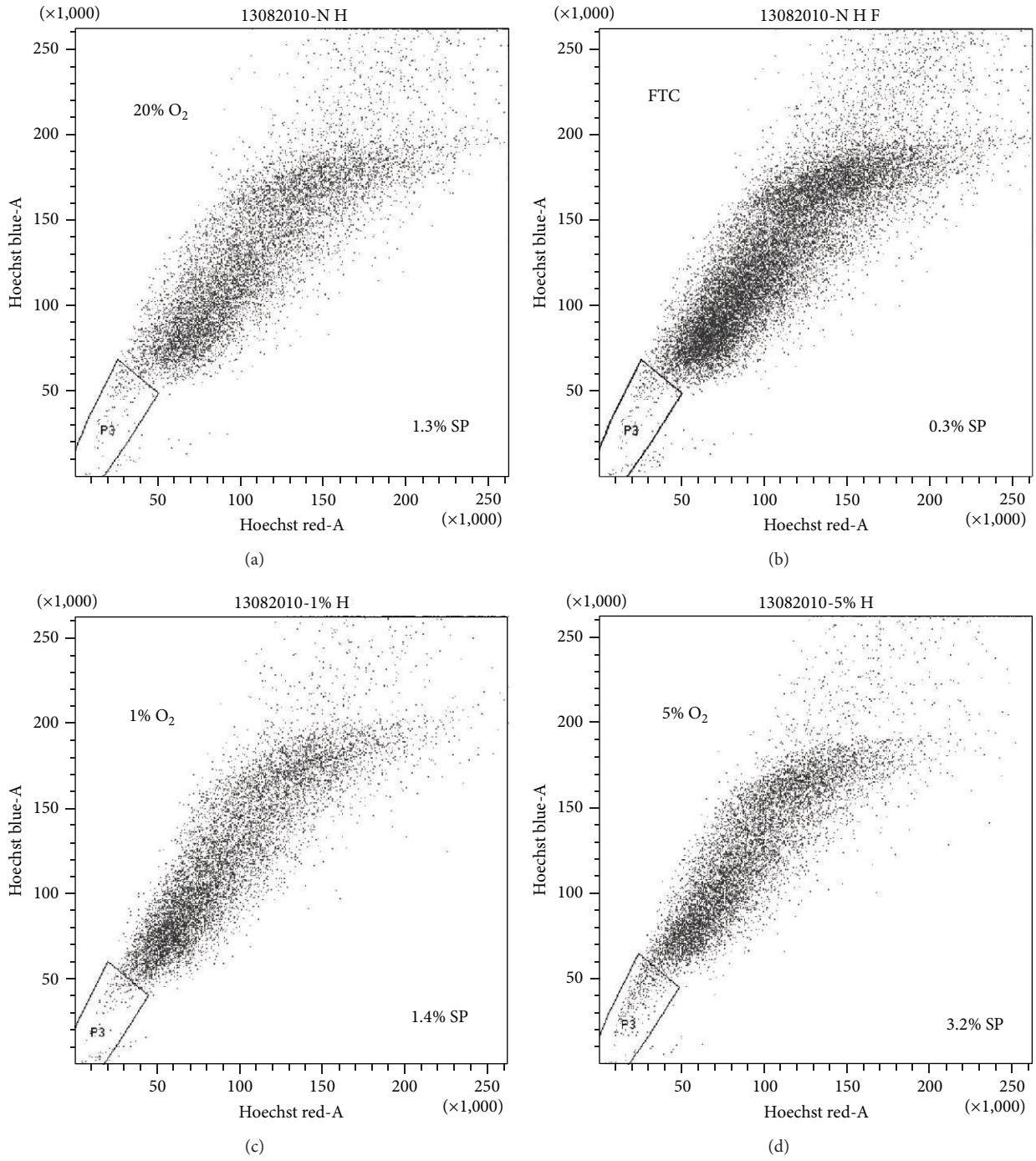

Figure 6: Isolation of an SP cell population was conducted on SPCs following different oxygen tension exposures for 4 days. Cells were stained with Hoechst 33342 dye either alone or in the presence of FTC and analyzed by flow cytometry. SP cells were gated and are shown as the percentage of total SPCs when cultured at 1%, 5%, or 20% O_2. Hoechst dye efflux was markedly diminished in FTC-treated SPCs.

physiological O_2 concentrations in developing embryos are generally lower (2–9% O_2) than in ambient air (21% O_2) [27]. In this study, we observed that low oxygen tensions drastically increased the number and size of sphere formation, as well as the SP fraction in cochlear spiral ganglion SPCs, indicating that *ex vivo* expansion of spiral ganglion SPCs under hypoxia may be practically applied for the large-scale production and maintenance of SPCs for stem cell-based replacement therapy. Given that low oxygen tensions maintain undifferentiated states of embryonic, hematopoietic, mesenchymal, and neural stem cell phenotypes and modulate proliferation and cell-fate commitment [28], it is reasonable to assume that a much lower oxygen tension than that of ambient air in some specific environments of the cochlea may be more suitable

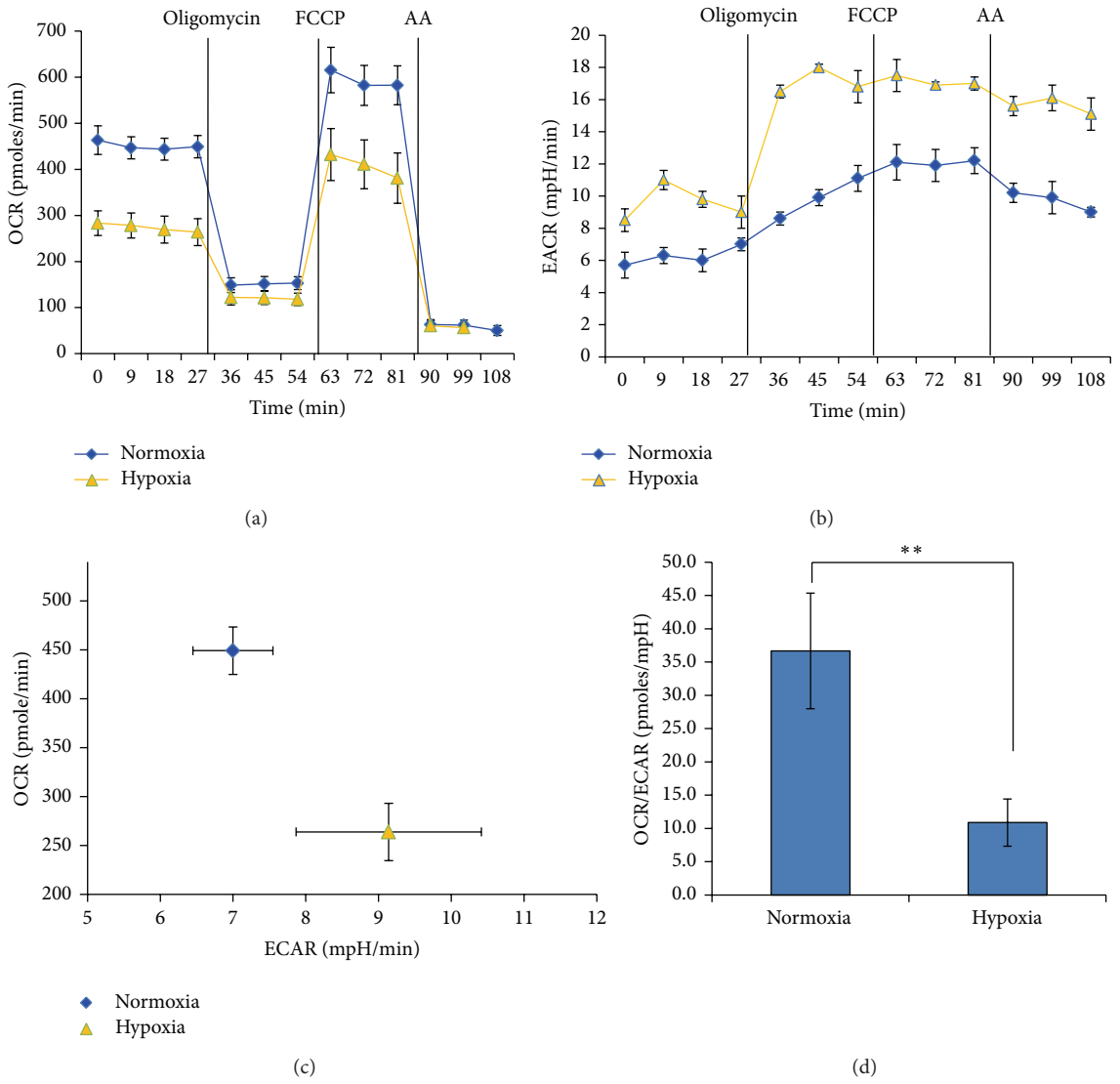

Figure 7: Cochlear spiral ganglion SPCs cultured in hypoxia conditions undergo a metabolic switch from oxidative phosphorylation to glycolysis. Real-time measurements (mean ± SEM, $n = 5$) of (a) the mitochondrial OCR (pMols/min) and (b) ECAR (mpH/min) of SPCs cultured in normoxia or hypoxia conditions were measured under basal condition and in response to the indicated mitochondrial inhibitors. The OCR was lower in hypoxia condition. (c) The basal OCR and ECAR values of normoxia- and hypoxia-cultured SPCs were plotted to illustrate the difference in cellular bioenergetics (mean ± SEM, $n = 5$). (d) OCR to ECAR ratios measured by the XF24 extracellular flux analyzer (mean ± SEM, $n = 5$) show a significant decrease in SPCs exposed to hypoxia, indicating a metabolic transition from mitochondrial oxidative phosphorylation to glycolysis. ∗∗ indicates $P < 0.01$; FCCP: carbonyl cyanide p-trifluoromethoxyphenylhydrazone; AA: antimycin A.

for stem or progenitor cell populations to reside. Meanwhile, a real stem cell niche in the adult cochlea needs to be explored further.

3.5. Hypoxia Shifts the Metabolic Pathway of Spiral Ganglion SPCs Predominantly toward Glycolysis. The relationship between mitochondrial metabolism and cell proliferation and stemness in spiral ganglion SPCs remains poorly understood. We further characterized the bioenergetics status change of SPCs at different oxygen tensions using Seahorse noninvasive technology [29]. We determined the mitochondrial OCR and ECAR, which represent the measurement of oxidative phosphorylation (OXPHOS) and glycolysis, respectively, from cells grown at either 20% or 5% O_2 for 2 months. We showed that the basal OCR of SPCs was markedly low at 5% O_2 compared with 20% O_2 (Figure 7(a)). The addition of oligomycin, a natural antibiotic that inhibits F0/F1 ATPase (complex V), differentiates the ATP-linked respiration from the proton leak. Following oligomycin addition, the maximal respiratory rate was determined by subsequent addition of FCCP, an uncoupler that raises OCR to an extremely high level. Finally, injection of antimycin A inhibited the flux of electrons through complex III and thus determined the remaining OCR resulting from nonmitochondrial respiration, as no further oxygen was consumed at the cytochrome c oxidase.

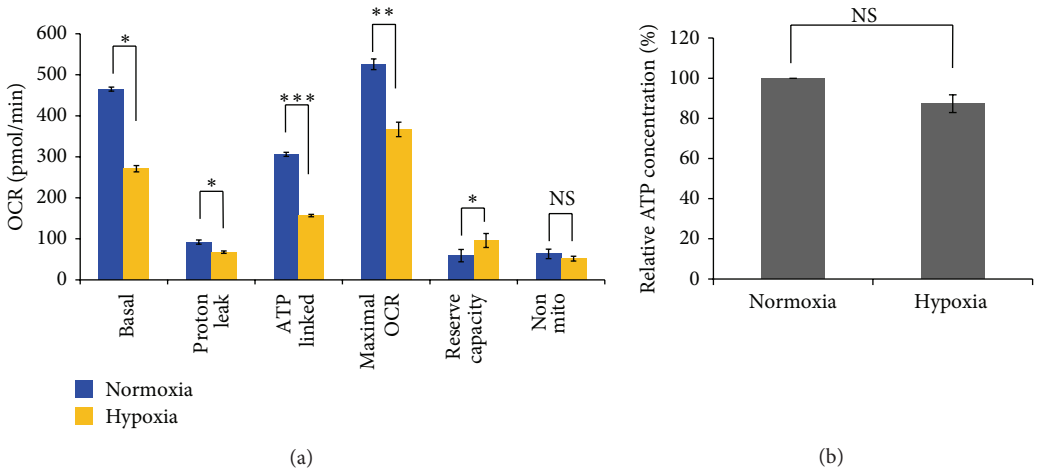

Figure 8: Measurement of mitochondrial function in cochlear spiral ganglion SPCs cultured in normoxic and hypoxic conditions. Results are expressed as mean ± SEM with $n = 5$ for each bar. NS indicates a non-significant difference; ∗ indicates $P < 0.05$; ∗∗ indicates $P < 0.01$; ∗ ∗ ∗ indicates $P < 0.005$.

As shown in Figure 7(b), the response of ECAR at each oxygen tension to mitochondrial toxicants reflected a concurrent glycolytic rate after mitochondrial perturbation. Following oligomycin treatment, the greater response of ECAR in hypoxia-cultured cells suggested that SPCs cultured under hypoxia are more sensitive to mitochondria perturbation than under normoxia. Another plausible explanation is that glycolysis is less efficient than OXPHOS in gathering energy from glucose; hypoxic SPCs therefore need to increase the rate of glucose uptake and glycolysis to meet its energy demands [30].

When SPC cells were cultured under hypoxia, OXPHOS levels decreased by at least 40%, while basal ECAR activity increased by 30% in relation to normoxia, indicating a metabolic pathway change from OXPHOS to glycolysis (Figure 7(c)). This was also reflected in the greatly reduced OCR to ECAR ratio when SPCs were cultured under hypoxia (Figure 7(d)). Such metabolic switch is likely attributable to the activation of Hif-1α signaling, because cells exposed to low oxygen levels that fall below a certain threshold would increase the amount of glycolytic enzymes and glucose transporters through the Hif-1α pathway [31, 32], while downregulating the enzymes driving mitochondrial metabolism [33]. Overexpression of Hif-1α in ESCs has also been shown to switch their energy production pathways from bivalent toward higher glycolytic activity [34].

3.6. Cochlear Spiral Ganglion SPCs Display Higher Maximal Mitochondrial Respiratory Capacity in Hypoxic Conditions. Although cochlear spiral ganglion SPCs consumed O_2 at a lower rate in hypoxia than in normoxia, as demonstrated in Figure 7(a), it was unclear what proportion of their maximal electron transport capacity was being utilized. The difference in mitochondrial function of SPCs cultured in normoxic and hypoxic conditions was defined by sequentially adding specific mitochondrial inhibitors, which allowed each component of the respiratory chain to be delineated. FCCP is a mitochondrial uncoupler (protonophore) that dissipates the mitochondrial membrane potential to stimulate maximal electron transport and O_2 consumption [35]. As shown in Figure 8(a), the reserve capacity of cells grown in hypoxia was significantly greater than for normoxia, implying that hypoxia-cultured SPCs may have greater substantial capacity than those in normoxia in response to stress or pathologically relevant injury, increasing energy demands for the maintenance of organ function, cellular repair, or detoxification of reactive species [36]. In contrast, proton leak significantly decreased at a lower oxygen tension, suggesting that SPCs grown under hypoxia might have less mitochondrial membrane damage compared to normoxic culture. The decreased proton leak shown in hypoxia SPCs may imply reduced oxidative stress encountered in such a microenvironment. Together, these results support the view that a general description of stem cell metabolism usually involves increased glycolysis, limited oxidative metabolism, and resistance to oxidative damage [37].

To examine whether there is difference of ATP production between hypoxia and normoxia, the data showed that SPCs maintain equivalent levels of ATP when cultured in normoxia and hypoxia (Figure 8(b)). This suggests that SPCs cultured in hypoxia were able to upregulate glycolysis and maintain sufficient ATP levels following the inhibition of OCR by mitochondrial inhibitors.

4. Conclusions

In this study, we demonstrated that cochlear spiral ganglion SPCs from P1 neonates could be amplified by hypoxia, with subsequent differentiation into neurons and glia. The effect of low oxygen tension on spiral ganglion SPCs not only resulted in enhancing proliferation in the cell amount and diameter of neurospheres, but also increased the protein expression of cyclin D1 and PCNA, while at the same time suppressing the p27 level. Coupled with this is the upregulation of stemness-related marker proteins Abcg2, nestin, and Nanog.

Within a new field of cellular bioenergetics investigation, we showed that SPCs grown at low oxygen tension have a significantly higher mitochondrial reserve capacity compared to that under normoxia. Hypoxia also significantly decreased their proton leak when SPCs were cultured in hypoxia. These data suggest a diminished oxidative stress encountered in a hypoxic microenvironment of spiral ganglion SPCs, along with a greater substantial capacity than normoxia in response to mitochondrial perturbation due to a higher maximum respiratory capacity. Unlike cells grown in normoxia, hypoxia-cultured SPCs shift their metabolic pathway predominantly to glycolysis but still maintain sufficient ATP levels as they would grow under normoxia. The upregulated Hif-1α shown in hypoxia-cultured SPCs indicated that the dominant glycolytic metabolism and cellular proliferation may be mediated through Hif-1α activation. These findings suggest a role of Hif-1α for spiral ganglion SPCs in response to hypoxia *in vitro* and suggest a possible mechanism for their enhanced proliferation under hypoxic conditions.

Conflict of Interests

The authors declare that there is no conflict of interests regarding the publication of this paper.

Acknowledgments

This work was supported in part by Grants from the National Science Council, Taiwan, (NSC101-2314-B-016-012-MY3 to C.-H. Wang), Tri-Service General Hospital (TSGH-C103-043 to H.-C. Chen and TSGH-C103-044 to C.-H. Wang), National Defense Medical Research Grants (103-M005 to C.-H. Wang and 103-M006 to H.-K. Sytwu), and a Cheng Hsin Research Grant (103-20 to J.-T. Lee).

References

[1] B. A. Nayagam, M. A. Muniak, and D. K. Ryugo, "The spiral ganglion: connecting the peripheral and central auditory systems," *Hearing Research*, vol. 278, no. 1-2, pp. 2–20, 2011.

[2] S. B. Shibata, S. R. Cortez, L. A. Beyer et al., "Transgenic BDNF induces nerve fiber regrowth into the auditory epithelium in deaf cochleae," *Experimental Neurology*, vol. 223, no. 2, pp. 464–472, 2010.

[3] L. Zhang, H. Jiang, and Z. Hu, "Concentration-dependent effect of nerve growth factor on cell fate determination of neural progenitors," *Stem Cells and Development*, vol. 20, no. 10, pp. 1723–1731, 2011.

[4] W. Chen, N. Jongkamonwiwat, L. Abbas et al., "Restoration of auditory evoked responses by human ES-cell-derived otic progenitors," *Nature*, vol. 490, no. 7419, pp. 278–282, 2012.

[5] C. Zhong, Y. Han, J. Qiu et al., "A comparison of the proliferative capacity and ultrastructure of proliferative cells from the cochleae of newborn rats of different ages," *International Journal of Pediatric Otorhinolaryngology*, vol. 74, no. 2, pp. 192–197, 2010.

[6] X.-X. Lou, T. Nakagawa, H. Ohnishi, K. Nishimura, and J. Ito, "Otospheres derived from neonatal mouse cochleae retain the progenitor cell phenotype after ex vivo expansions," *Neuroscience Letters*, vol. 534, no. 1, pp. 18–23, 2013.

[7] H.-C. Chen, H.-K. Sytwu, J.-L. Chang et al., "Hypoxia enhances the stemness markers of cochlear stem/progenitor cells and expands sphere formation through activation of hypoxia-inducible factor-1alpha," *Hearing Research*, vol. 275, no. 1-2, pp. 43–52, 2011.

[8] G. Santilli, G. Lamorte, L. Carlessi et al., "Mild hypoxia enhances proliferation and multipotency of human neural stem cells," *PLoS ONE*, vol. 5, no. 1, Article ID e8575, 2010.

[9] V. A. Rafalski, E. Mancini, and A. Brunet, "Energy metabolism and energy-sensing pathways in mammalian embryonic and adult stem cell fate," *Journal of Cell Science*, vol. 125, no. 23, pp. 5597–5608, 2012.

[10] C. T. Chen, S. H. Hsu, and Y. H. Wei, "Mitochondrial bioenergetic function and metabolic plasticity in stem cell differentiation and cellular reprogramming," *Biochimica et Biophysica Acta*, vol. 1820, no. 5, pp. 571–576, 2012.

[11] C. D. L. Folmes, P. P. Dzeja, T. J. Nelson, and A. Terzic, "Metabolic plasticity in stem cell homeostasis and differentiation," *Cell Stem Cell*, vol. 11, no. 5, pp. 596–606, 2012.

[12] T.-T. Chao, C.-H. Wang, H.-C. Chen et al., "Adherent culture conditions enrich the side population obtained from the cochlear modiolus-derived stem/progenitor cells," *International Journal of Pediatric Otorhinolaryngology*, vol. 77, no. 5, pp. 779–784, 2013.

[13] M. Diensthuber, V. Zecha, J. Wagenblast, S. Arnhold, A. S. Edge, and T. Stover, "Spiral ganglion stem cells can be propagated and differentiated into neurons and glia," *Bioresearch Open Access*, vol. 3, no. 3, pp. 88–97, 2014.

[14] J. C. Estrada, C. Albo, A. Benguría et al., "Culture of human mesenchymal stem cells at low oxygen tension improves growth and genetic stability by activating glycolysis," *Cell Death and Differentiation*, vol. 19, no. 5, pp. 743–755, 2012.

[15] C. Fehrer, R. Brunauer, G. Laschober et al., "Reduced oxygen tension attenuates differentiation capacity of human mesenchymal stem cells and prolongs their lifespan," *Aging Cell*, vol. 6, no. 6, pp. 745–757, 2007.

[16] S. Parrinello, E. Samper, A. Krtolica, J. Goldstein, S. Melov, and J. Campisi, "Oxygen sensitivity severely limits the replicative lifespan of murine fibroblasts," *Nature Cell Biology*, vol. 5, no. 8, pp. 741–747, 2003.

[17] Q. Chen, A. Fischer, J. D. Reagan, L.-J. Yan, and B. N. Ames, "Oxidative DNA damage and senescence of human diploid fibroblast cells," *Proceedings of the National Academy of Sciences of the United States of America*, vol. 92, no. 10, pp. 4337–4341, 1995.

[18] C. Lange, W. B. Huttner, and F. Calegari, "Cdk4/cyclinD1 overexpression in neural stem cells shortens G1, delays neurogenesis, and promotes the generation and expansion of basal progenitors," *Cell Stem Cell*, vol. 5, no. 3, pp. 320–331, 2009.

[19] B. J. Walters and J. Zuo, "Postnatal development, maturation and aging in the mouse cochlea and their effects on hair cell regeneration," *Hearing Research*, vol. 297, pp. 68–83, 2013.

[20] A. Y. Leung, J. C. Leung, L. Y. Chan et al., "Proliferating cell nuclear antigen (PCNA) as a proliferative marker during embryonic and adult zebrafish hematopoiesis," *Histochemistry and Cell Biology*, vol. 124, no. 2, pp. 105–111, 2005.

[21] C. Menchón, M. J. Edel, and J. C. I. Belmonte, "The cell cycle inhibitor p27 Kip1 controls self-renewal and pluripotency of human embryonic stem cells by regulating the cell cycle, Brachyury and Twist," *Cell Cycle*, vol. 10, no. 9, pp. 1435–1447, 2011.

[22] C. J. Schofield and P. J. Ratcliffe, "Oxygen sensing by HIF hydroxylases," *Nature Reviews Molecular Cell Biology*, vol. 5, no. 5, pp. 343–354, 2004.

[23] L. Zhou and C. A. Miller, "Mitogen-activated protein kinase signaling, oxygen sensors and hypoxic induction of neurogenesis," *Neurodegenerative Diseases*, vol. 3, no. 1-2, pp. 50–55, 2006.

[24] X. Chen, Y. Tian, L. Yao, J. Zhang, and Y. Liu, "Hypoxia stimulates proliferation of rat neural stem cells with influence on the expression of cyclin D1 and c-Jun N-terminal protein kinase signaling pathway *in vitro*," *Neuroscience*, vol. 165, no. 3, pp. 705–714, 2010.

[25] L. de Filippis and D. Delia, "Hypoxia in the regulation of neural stem cells," *Cellular and Molecular Life Sciences*, vol. 68, no. 17, pp. 2831–2844, 2011.

[26] E. Savary, J. P. Hugnot, Y. Chassigneux et al., "Distinct population of hair cell progenitors can be isolated from the postnatal mouse cochlea using side population analysis," *Stem Cells*, vol. 25, no. 2, pp. 332–339, 2007.

[27] M. C. Simon and B. Keith, "The role of oxygen availability in embryonic development and stem cell function," *Nature Reviews Molecular Cell Biology*, vol. 9, no. 4, pp. 285–296, 2008.

[28] A. Mohyeldin, T. Garzón-Muvdi, and A. Quiñones-Hinojosa, "Oxygen in stem cell biology: a critical component of the stem cell niche," *Cell Stem Cell*, vol. 7, no. 2, pp. 150–161, 2010.

[29] D. A. Ferrick, A. Neilson, and C. Beeson, "Advances in measuring cellular bioenergetics using extracellular flux," *Drug Discovery Today*, vol. 13, no. 5-6, pp. 268–274, 2008.

[30] J. C. Maher, M. Wangpaichitr, N. Savaraj, M. Kurtoglu, and T. J. Lampidis, "Hypoxia-inducible factor-1 confers resistance to the glycolytic inhibitor 2-deoxy-D-glucose," *Molecular Cancer Therapeutics*, vol. 6, no. 2, pp. 732–741, 2007.

[31] I. Papandreou, R. A. Cairns, L. Fontana, A. L. Lim, and N. C. Denko, "HIF-1 mediates adaptation to hypoxia by actively downregulating mitochondrial oxygen consumption," *Cell Metabolism*, vol. 3, no. 3, pp. 187–197, 2006.

[32] J.-W. Kim, I. Tchernyshyov, G. L. Semenza, and C. V. Dang, "HIF-1-mediated expression of pyruvate dehydrogenase kinase: a metabolic switch required for cellular adaptation to hypoxia," *Cell Metabolism*, vol. 3, no. 3, pp. 177–185, 2006.

[33] G. L. Semenza, "Regulation of metabolism by hypoxia-inducible factor 1," *Cold Spring Harbor Symposia on Quantitative Biology*, vol. 76, pp. 347–353, 2011.

[34] W. Zhou, M. Choi, D. Margineantu et al., "HIF1α induced switch from bivalent to exclusively glycolytic metabolism during ESC-to-EpiSC/hESC transition," *The EMBO Journal*, vol. 31, no. 9, pp. 2103–2116, 2012.

[35] P. G. Heytler, "Uncouplers of oxidative phosphorylation," *Methods in Enzymology*, vol. 55, no. C, pp. 462–472, 1979.

[36] B. G. Hill, B. P. Dranka, L. Zou, J. C. Chatham, and V. M. Darley-Usmar, "Importance of the bioenergetic reserve capacity in response to cardiomyocyte stress induced by 4-hydroxynonenal," *Biochemical Journal*, vol. 424, no. 1, pp. 99–107, 2009.

[37] N. M. Vacanti and C. M. Metallo, "Exploring metabolic pathways that contribute to the stem cell phenotype," *Biochimica et Biophysica Acta*, vol. 1830, no. 2, pp. 2361–2369, 2013.

Hindawi Publishing Corporation
BioMed Research International
Volume 2015, Article ID 109702, 10 pages
http://dx.doi.org/10.1155/2015/109702

Research Article

Highly Flexible Silicone Coated Neural Array for Intracochlear Electrical Stimulation

P. Bhatti,[1,2] J. Van Beek-King,[3] A. Sharpe,[1] J. Crawford,[4] S. Tridandapani,[1,5] B. McKinnon,[6,7] and D. Blake[4]

[1]*School of Electrical and Computer Engineering, Georgia Institute of Technology, Atlanta, GA 30332, USA*
[2]*Department of Rehabilitative Medicine, Emory University School of Medicine, Atlanta, GA 30322, USA*
[3]*Department of Otolaryngology-Head & Neck Surgery, Georgia Regents University, Augusta, GA 30912, USA*
[4]*Department of Neurology, Brain and Behavior Discovery Institute, Georgia Regents University, Augusta, GA 30912, USA*
[5]*Department of Radiology and Imaging Sciences, Emory University School of Medicine, Atlanta, GA 30322, USA*
[6]*The Shea Ear Clinic, Memphis, TN 38119, USA*
[7]*Department of Otolaryngology-Head and Neck Surgery, University of Tennessee Health Sciences Center, Memphis, TN 38163, USA*

Correspondence should be addressed to P. Bhatti; pamela.bhatti@ece.gatech.edu

Received 20 August 2014; Accepted 22 January 2015

Academic Editor: Chung-Feng Hwang

We present an effective method for tailoring the flexibility of a commercial thin-film polymer electrode array for intracochlear electrical stimulation. Using a pneumatically driven dispensing system, an average 232 ± 64 μm (mean ± SD) thickness layer of silicone adhesive coating was applied to stiffen the underside of polyimide multisite arrays. Additional silicone was applied to the tip to protect neural tissue during insertion and along the array to improve surgical handling. Each array supported 20 platinum sites (180 μm dia., 250 μm pitch), spanning nearly 28 mm in length and 400 μm in width. We report an average intracochlear stimulating current threshold of 170 ± 93 μA to evoke an auditory brainstem response in 7 acutely deafened felines. A total of 10 arrays were each inserted through a round window approach into the cochlea's basal turn of eight felines with one delamination occurring upon insertion (preliminary results of the *in vivo* data presented at the 48th Annual Meeting American Neurotology Society, Orlando, FL, April 2013, and reported in Van Beek-King 2014). Using microcomputed tomography imaging (50 μm resolution), distances ranging from 100 to 565 μm from the cochlea's central modiolus were measured. Our method combines the utility of readily available commercial devices with a straightforward postprocessing step on the order of 24 hours.

1. Introduction

Since their introduction in the mid 1970s [1] planar thin-film arrays (TFAs) have become an invaluable scientific tool for systems neurophysiology. Through the utilization of integrated circuit fabrication methods, TFAs have been developed on a variety of substrates including sapphire, metal, glass, silicon, and polymers [1–5]. By layering and patterning dielectrics and conductors upon such substrates, multisite stimulating and recording electrode arrays have been realized with submicron precision. Serving as an essential interface between the nervous system and microelectronics, TFAs have enabled a greater understanding of electrical and chemical signaling in the brain [6–9], as well as a therapeutic option for overcoming sensory loss in the auditory [10–13] and visual [14, 15] systems. The ongoing validation, as well as the need, of multisite TFAs has ultimately led to the commercial availability of lithographically defined, batch-processed arrays (Neural Nexus Technologies, Ann Arbor, MI). Primarily based on silicon or polyimide substrates, these arrays can be custom-designed or selected from a design library, for neurophysiological studies.

While the availability of commercial TFAs alleviates the time-consuming burden of fabrication, many *in vivo* applications require some amount of postprocessing to enable a TFA to physically approach anatomic structures. One such example is the cochlea: the average human cochlea rotates through two and one half turns from base to apex and is

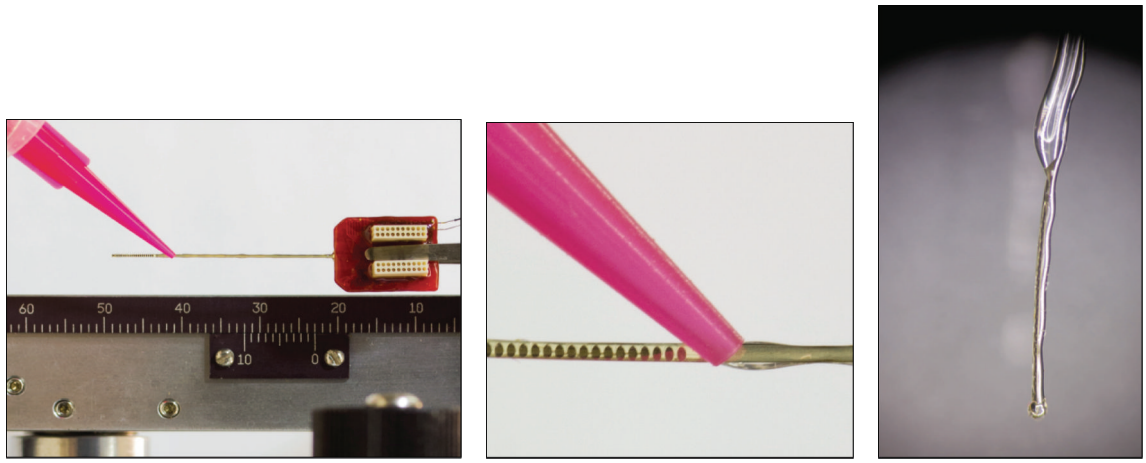

(a) (b) (c)

Figure 1: TFA and coating procedure. (a) TFA measured 27.8 mm × 0.4 mm × 20 μm ($L \times W \times H$) with 20 functional platinum sites (180 μm diameter, 250 μm pitch). Two 16-channel Omnetics connectors bonded to the backend of each array enable signal transfer. (b) Topside application of silicone adhesive. (c) Final silicone coated TFA (cTFA). Note silicone ball at distal tip to reduce the potential for insertion trauma.

comprised of three chambers, or scala. The efficacy of a silicon-based TFA for intracochlear stimulation has been reported in animal models [11, 16]. However, such arrays have proven difficult to insert and accurately place in the lower chamber (scala tympani) during acute *in vivo* studies. Given the stiffness of the silicon-based TFAs, a *flexible* TFA alternative is essential. Pursuing such an alternative we investigated flexible, biocompatible polyimide based TFAs for intracochlear stimulation. Our first postprocessing approach involved mechanically adhering a TFA to an insertion platform (IP) that is similar to commercial intracochlear arrays [17, 18]. Results were mixed in human cadaver insertion studies with TFA-IP devices ($n = 10$). Two delaminations, where the array separated from the IP, occurred. Moreover, microcomputed tomography imaging (50 μm resolution) revealed undesirable placement of two devices [19]. One TFA-IP was placed in the semicircular canal and one in the vestibule, indicating that significant improvement of the TFA-IP integration strategy was essential.

In this paper, we extend the applicability of TFAs for intracochlear stimulation through a simple and effective method. The robustness of a commercial thin-film polyimide intracochlear electrode array can be improved by layering silicon adhesive to the underside of the TFA. Furthermore, additional silicone handling points along the TFA may be provided for the surgeon since insertion requires force to advance the array along the cochlea [20–24]. We also discuss the method for constructing such arrays and report results of intracochlear stimulation using these arrays in acute feline studies.

2. Methods

2.1. Electrode Array Modification. Polyimide thin-film arrays were custom-designed for insertion into the basal turn of the cochlea and microfabricated by a commercial foundry (NeuroNexus Technologies). Composed of gold conducting traces sandwiched between layers of polyimide (Figure 1), each TFA measured 27.8 mm × 0.4 mm × 20 μm ($L \times W \times H$) and supported 21 platinum sites (180 μm dia., 250 μm pitch). For signal transfer, the array manufacturer provided two 16-channel connectors (Omnetics Connector Corp., Minneapolis, MN) bonded to the backend of each array.

Layers of MED-2000 Silicone RTV Adhesive (NuSil Silicone Technology LLC, Carpinteria, CA) were applied to the top and bottom surfaces of each flexible TFA (Young's modulus, 3 GPa) to provide the needed rigidity for insertion (Figure 1(a)). Each array was affixed to a micromanipulator and suspended vertically. A digitally controlled pneumatic dispenser system (Madell Technology Corp., Ontario, CA), with a 25-gauge plastic tip at a pressure of 25 PSI, was then used to dispense a layer of silicone adhesive along the entire underside length of the TFA. This was done carefully, in six-second intervals, ensuring that the adhesive was only applied to the bottom of the TFA. To compensate for the force generated by the needle applicator, a solid supporting edge was placed on the opposing side of the suspended array. The adhesive set quickly, mitigating any effects of gravity drawing the glue down. The TFA remained suspended in the micromanipulator for one hour to dry further. The TFA was then placed on a clean glass slide with the existing adhesive layer facing down to position the TFA for application of the second layer on the topside of the TFA (Figure 1(b)). Using a bench-top low-power microscope, additional adhesive was applied from the connector base down the length of the array within 1 mm of the active sites to further support the TFA. For this application, the dispenser tip was replaced with a 22-gauge tip and the pressure adjusted to 20 PSI. Applying a wider strip of adhesive enabled the adhesive to flow around the width of the array and bond to the rear layer, thus fully securing the array in silicone. Finally, a small amount of adhesive was added to the array tip that covered site 1 (most

distal site). The goal was to help distribute insertion forces and reduce insertion trauma. The completed coated TFA (cTFA) array was left to cure for 24 hours (Figure 1(c)).

Sites were inspected visually and validated functionally by measuring impedances in phosphorous-buffered saline solution (PBS). A custom connector box with cables was made to access the two 16-channel connectors on the back end of the cTFA. To test site impedance, a ±100 nA 1 kHz sinusoidal signal was applied independently to each site with a PlexStim 2.0 (Plexon Inc., Dallas, TX) 16-channel stimulator. The peak voltage for each site was measured using a Hameg HM507 oscilloscope and used to compute site impedance.

2.2. Surgical Procedure. The study was a prospective cochlear array insertion analysis with electrically evoked auditory brainstem response testing in a feline model, using previously published feline implantation techniques [25–27]. Approval was obtained from the Georgia Regents University and the Georgia Institute of Technology Institutional Animal Care and Use Committees (2011-0362, A12086). One resident veterinarian and one veterinarian technician were present for surgical preparation and throughout the experiment to monitor the subject. The surgical team included a board-certified otolaryngologist with 12 years of experience and a third-year otolaryngology resident. Eight healthy, adult wild-type felines weighing ≥ 3 kg (4 females and 4 males) were used as the subjects for all *in vivo* implantation and electrical stimulation tests. All proper quarantine protocols were strictly followed. Subjects were randomly assigned to undergo implantation of the right or left ear with a cTFA. The contralateral unimplanted ear of each feline served as the control for that feline. Intravenous access was obtained in a vein from one of the front legs. The subjects were anesthetized with intravenous ketamine : medetomidine (5 : 0.05 mg/kg) for induction, followed by endotracheal intubation for ventilation and isoflurane (1–3%). Later experiments used an intravenous acepromazine : butorphanol (0.1 : 0.3 mg/kg) induction, followed by propofol (8–10 mg/kg), followed by endotracheal intubation for ventilation, and isoflurane (1–3%). For the duration of the surgery, heart rate, respiratory rate, oxygen saturation, and end-tidal carbon dioxide were continually monitored and body temperature was maintained at 38°C using a controlled heating pad. Subjects received continuous infusion of intravenous Ringer's Lactate solution with 2.5 percent dextrose at a rate of 10 mL : kg : hr.

Preoperative auditory brainstem response (ABR) was obtained to ensure bilateral hearing after induction of general anesthesia, but prior to any surgical intervention. To verify the baseline, recordings were obtained using silver wires as electrodes inserted into the vertex of the scalp using a 22-gauge needle. Signals were measured differentially between ipsilateral bulla and vertex with the contralateral bulla as the ground for the control ear of each subject. The differential signal was AC coupled, amplified by 10 k, and bandpass-filtered over a 200 Hz to 10 kHz frequency range. The resulting analog signal was then converted to a digital signal using a 16-bit analog-to-digital converter at a 10 kHz sampling rate. A total of 1000 repetitions were averaged. A National Instruments (National Instruments Inc., Austin, TX) card with limits ±5 V served as the instrument control interface. Condensation acoustic clicks, 0.01 msec, were applied with a distance of 12 inches from the subject at a sound level of less than or equal to 80 dB SPL in one ear with the contralateral ear plugged. Waveforms were recorded for analysis using custom software written in LabView (National Instruments, Inc.). Click-evoked ABRs down to 60 dB SPL were confirmed in every case. A foam earplug was placed in the contralateral ear to avoid any interference of eliciting a response from the normal hearing ear during electrical stimulation.

The surgical approach to the cochlea was similar to that in humans, with feline specifications [25–27]. One of two surgeons performed each insertion. After palpating surgical landmarks including the temporal line and the posterior aspect of the external auditory canal, a C-shaped incision was made behind the randomly chosen ear. The outer ear canal was exposed and dissection continued to the osseous skull. An approximately 5 × 5 mm bullectomy was drilled to gain access to the cochlea under magnification. Perilymph was removed via wicking through the cochleostomy and replaced with 10 percent neomycin sulfate solution to induce acute hearing loss. After two minutes, fluid was once again wicked from the basal turn of the cochlea and replaced with 10 percent neomycin to acutely deafen the feline. This procedure was repeated until the lack of ABRs at 60 dB SPL was confirmed after neomycin treatments.

A cTFA was manually inserted into the scala tympani through the round window. Insertion was performed with microscopy and the array was advanced until some resistance was perceived by the surgeon. The cTFA was secured in place with a hemostat to avoid movement during electrical testing.

2.3. Electrical Testing Protocol. After insertion of the array, at least five site impedances along the length of the array were sampled. This was to detect if any transverse breaks along the cTFA occurred during insertion. Similar to the *in vitro* impedance testing mentioned above, a ±100 nA 1 kHz sinusoidal signal was applied with the PlexStim 2.0 Stimulator between each site and a 22-gauge needle ground electrode inserted into the local subcutaneous tissue behind the ipsilateral ear.

Monopolar electrical stimulation was applied between an intracochlear cTFA electrode and the ground return electrode. Sites spanning the entire array length were tested in a random order. Triggered by a TTL output pulse from the ABR recording instrument control, all stimuli were charge-balanced biphasic pulses, negative first, and balanced with a positive phase, (200 μsec per phase). An interphase gap of 10 μsec was applied during which the electrodes were grounded to prevent charge build-up. Applied stimulation current ranged from 100 to 500 μA in magnitude. Stimulus artifact was subtracted out by averaging with stimulation at an inverted phase. Stimulation occurred at 5–10 Hz and up to 1000 trials. The resulting electrically evoked auditory brainstem response (eABR) signal was processed following the same procedure as the ABR signal. For each site, threshold was determined as the level of applied current just below an appreciable eABR. Assessed visually by the attending

electrophysiologist, this occurred when the eABR response failed to evoke a triple peaked auditory brainstem response analogous to the acoustically evoked auditory brainstem response. EABR stimuli were repeated until a definitive assessment was made by the electrophysiologist. The specific details of the testing protocol are as follows. For the first site tested on each array, a stimulus midway between 100 μA and 500 μA was applied (300 μA). If an eABR was observed at the starting point of 300 μA, as confirmed by 2-3 trials, a stimulus level midway between 300 μA and 100 μA was applied (200 μA). Upon eABR confirmation, a lower stimulus level midway between 200 μA and 100 μA was applied to the site (150 μA). For the lowest bound, sub-100 μA stimuli were not applied since a threshold of 100 μA or less was considered to represent the normal-low range. Once an eABR was lost, as confirmed by the loss of peaks P3 and P4 (Figure 2), the current was increased until the best peak 4-5 msec into the plot was observed over multiple runs. This current level was assigned as the threshold value for the site under test. In the opposite direction, a similar procedure was followed with 500 μA as the upper bound. For subsequent sites on a given array, testing began with the threshold value of the previous site as a starting point. The stimulus level was increased and decreased in a similar fashion described above by bisecting the interval between the immediate value and the upper or lower bound. Given the variability in ABRs in general, the precision in threshold values is estimated as 50 μA. When eABR stimuli failed to evoke a triple peaked (Waves P2–P4; see Figure 2) auditory brainstem response over the entire applied current range for at least two trials, the eABR was recorded as indeterminate for the site under testing.

To validate electrode site functionality and examine impedance changes due to stimulation, poststimulation impedance values were determined similar to prestimulation impedance testing.

2.4. Computed Tomography Imaging. Two cTFAs were independently imaged in a microcomputed tomography (CT) system, and one cTFA was imaged in a harvested feline cochlea after the electrical testing was completed. Imaging studies were conducted at the Emory School of Medicine's Center for Systems Imaging, Atlanta, GA, using a Siemens Inveon MicroPET:CT Preclinical Scanner (Siemens Medical Solutions USA, Inc.; Hoffman Estates, IL). The MicroCT images were made with a pixel size of 20 × 20 μm, slice thickness 21.5 μm, and resolution of 46.499 pixels per mm. Total slice size was 1152 × 1152 pixels (24.77 × 24.77 mm). The volume data was reoriented so that the distal end of the array was in the image plane. Measurements were made using OsiriX MD (Pixmeo SARL; Geneva, Switzerland) digital imaging software by a board-certified radiologist.

3. Results

3.1. Electrode Array Impedance Measurements. A total of 19 TFAs were coated. For each TFA, all site impedance values at 1 kHz were provided by the manufacturer to demonstrate site viability (one site each on four TFAs sites was nonfunctional as indicated by the manufacturer). The average of all site impedances was 90.4 ± 36.3 kΩ (mean ± SD). Postsilicone adhesive application site impedances (for the first 10 cTFAs tested, only the first 16 sites and the 21st site were electrically accessible due to routing error in the custom connector box. For the next 9 cTFAs all sites were accessible) measured in PBS demonstrated an average value of 119.9±92.4 kΩ. The tip site (site 0) was not considered in the calculation given that it was coated with silicone to reduce insertion trauma. For each cTFA, sites that presented an *in vitro* impedance greater than 500 kΩ were considered nonfunctional resulting in 7 percent of sites deemed as nonfunctional (24 out of 346 sites).

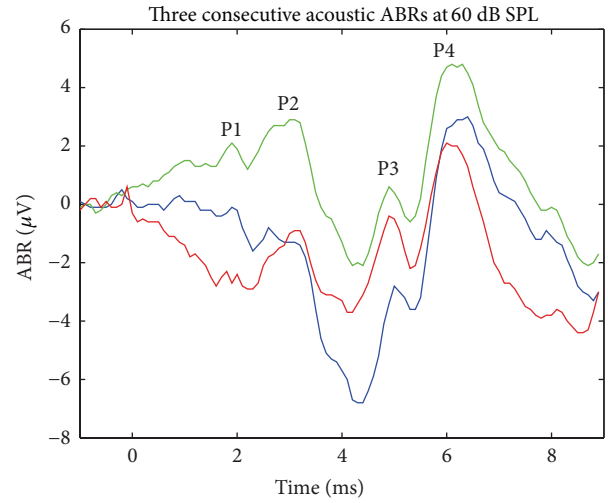

Figure 2: Click-evoked auditory brainstem response at 60 dB SPL. The responses were averaged over 1000 repetitions. A 1 msec delay occurs due to placement of the speaker 12 inches from the ear. Three consecutive responses are plotted (order: blue, green, and red).

3.2. Intracochlear Electrical Stimulation. All eight felines had baseline hearing documented by ABR. Figure 2 illustrates three consecutive ABRs at 60 dB SPL labeled with the appropriate positive response peaks [28]. A 1 msec delay occurs due to the placement of the speaker at 12 inches from the ear. The noise is small with a substantial artifact on some runs, and these occur in different positions. However, consistency is observed in multiple plots. Thus the data appears to be statistically well behaved.

Feline demographics are listed in Table 1. Unilateral deafening was achieved following four to eight applications of 10 percent neomycin. Following this, normal hearing was documented in unimplanted ears. All felines had subjectively easy, full insertion of the cTFA, with full insertion established at point of first resistance.

Ten of the 19 cTFAs were used *in vivo* for electrical stimulation. No sites were lost during the stimulation process. One delamination, where the silicone coating separated from the TFA, was observed upon cTFA removal. In this particular animal (feline 3) facial nerve activation was observed and is discussed below.

Table 1: Summary of feline demographics and average eABR threshold.

Feline	1	2	3	4	5	6	7	8
Sex	Female	Female	Female	Male	Male	Male	Male	Female
Weight (kg)	3.80	4.64	4.29	6.67	5.31	4.47	4.68	3.42
Side	Left	Left	Left	Right	Right	Right	Right	Right
eABR threshold mean ± SD (μA)	273 ± 133	206 ± 59	N:A *Facial nerve stimulation*	119 ± 21	145 ± 37	100 ± 25	141 ± 46	228 ± 93

The average *in vivo* site impedances were 184.5 ± 147.9 kΩ before stimulation and 67.1 ± 43.3 kΩ after stimulation. To further examine site impedance trends the cTFA was divided into three physical segments with reference to the insertion point: proximal, central, and distal (Table 2). Note that each cTFA was inserted into the basal turn only. Thus the segments represent more basal, central, and more apical sites, in the basal turn itself. For each segment, poststimulation site impedances were measured for one to three sites and averaged per cTFA as well as across all inserted cTFAs per segment (Table 2).

Five consecutive eABRs are shown in Figure 3. Using the eABR as a guide, the average intracochlear stimulating current threshold was 170 ± 93 μA. The per-array thresholds and per-segment thresholds, which are summarized in Figures 4(a)-4(b), further illustrate the per-segment thresholds as well as per-site thresholds across all arrays tested. For comparison, Figure 5 illustrates a composite of acoustic (60 dB SPL) and electrically (170 μA) evoked auditory brainstem responses. The acoustic ABR is shifted by 1 msec due to the placement of the speaker 12 inches from the ear.

In one animal, facial nerve twitching was observed with 400 μA biphasic stimulation at site six. The stimulator was disconnected immediately from the animal. To investigate if the nerve twitching was segment specific, sites in each segment were stimulated. Two outcomes were observed, twitching at approximately 200 μA, or no eABR at approximately 100 μA. The cTFA was explanted and delamination was observed. A second array was then inserted into the same animal and tested but eABRs were not observed.

3.3. Computed Tomography Imaging. Two cTFAs were imaged independently to measure silicone coating thickness. Topside coating thickness was measured at 1–1.5 mm intervals averaging 357 ± 81 μm. Bottom-side coating, under the sites, was measured at 500 μm intervals and averaged 232 ± 64 μm in thickness. One of the cTFAs was imaged after insertion revealing no structural changes.

The cTFA in feline 4 was imaged to observe placement (Figure 6), illustrating insertion through the round window and into the base. A maximum distance of 565 μm from the modiolus and a minimum distance of 100 μm at approximately site 8 were measured. Since the angle of insertion into the cochlea cannot be accurately measured, the true depth of insertion cannot be calculated accurately. There was trauma to the osseous spiral lamina with the tip of the electrode in the scala vestibuli.

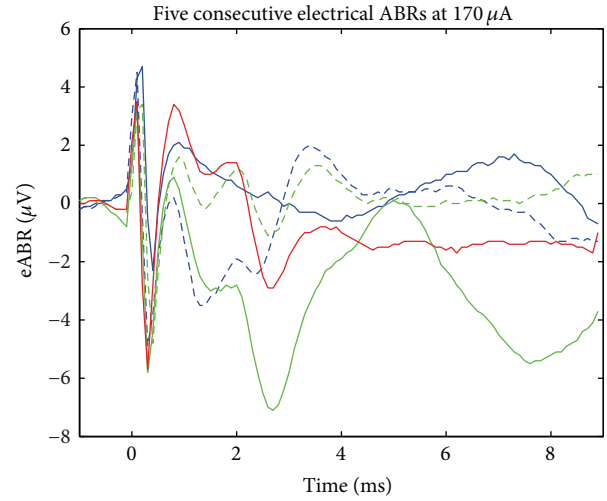

Figure 3: Electrically evoked auditory brainstem responses. The first 0–0.5 msec is artifact. The following 0.8–5 msec is electrical ABR. Based on 500 repetitions, the threshold as indicated by the eABR is 170 μA of monopolar current. Five consecutive responses are plotted (order: blue, blue dash, green, green dash, and red) illustrating the range of observations.

4. Discussion and Conclusion

This paper demonstrates a simple, cost-effective method to adjust the flexibility of fabricated polymeric thin-film arrays. The addition of a medical grade silicone coating enabled (1) insertion of a research array via the round window approach into the basal turn of the cochlea and (2) the associated electrical activation of the central auditory system. From a mechanical standpoint the cTFAs were not compromised during insertion or stimulation. This was validated by prestimulation and postsite impedance; that is, no open circuits were found. Considering the site impedance values, the observed *in vivo* impedances were appreciably high when compared with contemporary electrode arrays (typically 10–20 kΩ). This may be in part attributed to dramatically reduced site area. The high-density arrays present a site area of 0.025 mm^2, nearly one order of magnitude smaller than contemporary arrays. With respect to the silicone coating, only one delamination occurred. In situ imaging of one TFA gave no indication of delamination or localized separation of the coating from the TFA.

During the process of electrical stimulation, poststimulation site impedance varied across the arrays with the smallest

Table 2: (a) Site impedance, segment means, and overall cTFA mean ± standard deviation [based on image below]. (b) eABR threshold, segment means, and overall cTFA mean ± standard deviation.

(a)

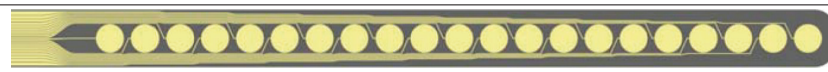

	Proximal segment			Central segment			Distal segment			
Feline 1										
Site number	21		16	12		10	6		2	
Impedance (kΩ)	44.6		NT	40.0		36.4	35.6		36.6	
Mean (kΩ)		43.6			38.2			36.1		38.4 ± 3.4
Feline 2										
Site number	21		16	12		10	6		2	
Impedance (kΩ)	44.0		38.0	42.0		NT	44.0		36.0	
Mean (kΩ)		41.0			42.0			40.0		40.8 ± 3.6
Feline 3										
Site number	21		16	12		10	6		2	
Impedance (kΩ)	52.0		196.0	NT		34.0	128.0		56.0	
Mean (kΩ)		124.0			34.0			92.0		93.2 ± 67.8
Feline 4										
Site number	21		16	12		10	6		2	
Impedance (kΩ)	76.0		48.0	NT		50.0	52.0		48.0	
Mean (kΩ)		62.0			50.0			50.0		54.8 ± 11.9
Feline 5										
Site number	21		16	12		10	6		2	
Impedance (kΩ)	64.0		68.0	NT		156.0	156.0		180.0	
Mean (kΩ)		66.0			156.0			168.0		124.8 ± 54.6
Feline 6										
Site number	21		16	12	10	8	6	4	2	
Impedance (kΩ)	40.0		44.0	48.0	48.0	48.0	52.0	52.0	48.0	
Mean (kΩ)		52.0			48.0			50.7		47.5 ± 3.9
Feline 7										
Site number	20		14	12		10	6		2	
Impedance (kΩ)	65.0		145.0	NT		90.0	50.0		60.0	
Mean (kΩ)		105.0			90.0			55.0		82.0 ± 38.2
Per segment mean (kΩ)	71.0 ± 46.9			59.2 ± 37.4			68.9 ± 45.9			

(b)

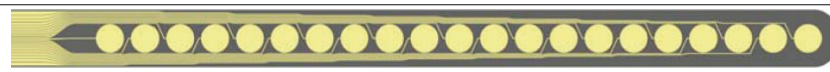

Ref.	21	20	19	18	17	16	15	14	13	12	11	10	9	8	7	6	5	4	3	2	1	
Segment	Proximal						Central							Distal								
	Proximal segment						Central segment							Distal segment								
Feline 1																						
Site number	21					16	12					10		6						2		
Threshold (μA)	*ind					NT	450					300		170						170		
Mean (μA)		*ind						375							170							273 ± 133
Feline 2																						
Site number	21					16	12					10		6						2		
Threshold (μA)	300					220	190					NT		150						170		
Mean (μA)		260						190							160							206 ± 59
Feline 3																						
Site number	21					16	12					10		6						2		
Threshold (μA)	125					150	NT					100		100		120						
Mean (μA)		137.5						100											110			119 ± 21
Feline 4																						
Site number	21					16	12					10		6						2		
Threshold (μA)	100					150	NT					100		150						1125		
Mean (μA)		125						100								137.5						145 ± 37
Feline 5																						
Site number	21					16	12					10		6						2		
Threshold (μA)	125					125	NT					100		75						75		
Mean (μA)		125						100								75						100 ± 25
Feline 6																						
Site number	21					16	12		10		8			6		4				2		
Threshold (μA)	*ind					*ind	180		200		*ind			125		100				100		
Mean (μA)		*ind							190							108.3						141 ± 46
Feline 7																						
Site number	20					14	12					10		6						2		
Threshold (μA)	320					NT	100					200		320						200		
Mean (μA)		320						150								260						228 ± 93
Per segment mean (μA)	179 ± 81						202 ± 107							143 ± 61								

Based on image above, NT = not tested and *ind = indeterminate response to eABR stimuli.

average and standard deviation occurring in the central array segment. When compared with commercial arrays, the cTFAs were not tapered to follow the widening of the base or the narrowing toward the apex. Possibly, the central sites that are the closest to the modiolus (Figure 6) demonstrated the largest impedance values. Additionally, similar to human implantations, it is likely that there was some variability in insertion depth.

Electrically evoked auditory brainstem response waveforms were consistent with those reported for the feline model previously [29, 30]. Threshold data exhibited considerable variability with no obvious correlation to a segment or site. Nonetheless, in some of the animals tested, a pronounced distal versus proximal threshold effect was observed.

A potential challenge is the insertion. Intracochlear insertion trauma is an important concern as the minimization of trauma is essential for hearing preservation techniques. In previous work using cadaveric human temporal bones, the percentage trauma was 26 percent overall for all TFA electrode insertions (30 percent for the cochleostomy and 22 percent for the round window approaches), though interestingly, intracochlear trauma due to embalming and cold storage was noted in 29 percent of controls not implanted [17]. Evaluation of trauma using the Cochlear (New South Wales, Australia) devices showed that intracochlear trauma was found in 16 percent of cochlea implanted with the banded electrode arrays and 13 percent of cochlea implanted with the contour [20], on average. The Advanced Bionics (Valencia,

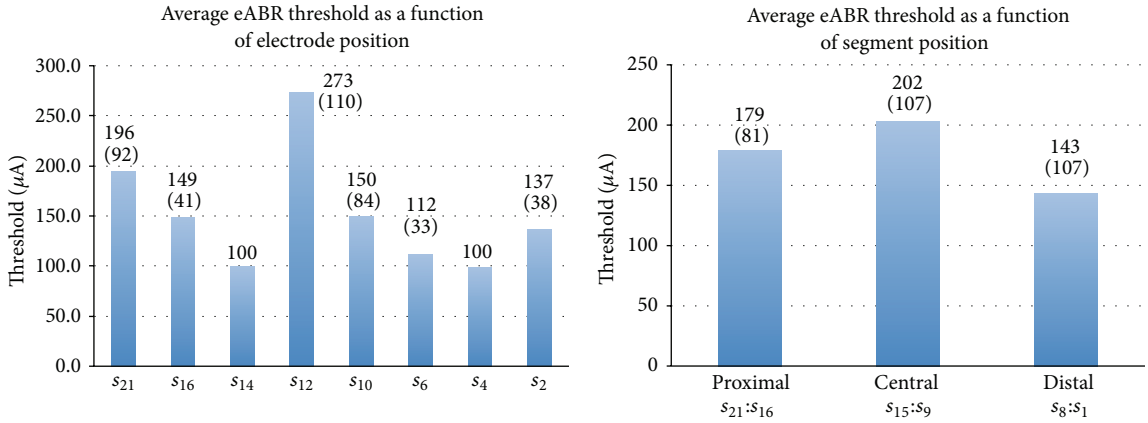

(a) Average eABR threshold as a function of electrode position

(b) Average eABR threshold as a function of segment position

FIGURE 4: (a) Average of eABR as a function of site position for all arrays tested ($n = 7$). (b) Average of eABR as a function of segment for all arrays tested ($n = 7$). Standard deviation in parentheses.

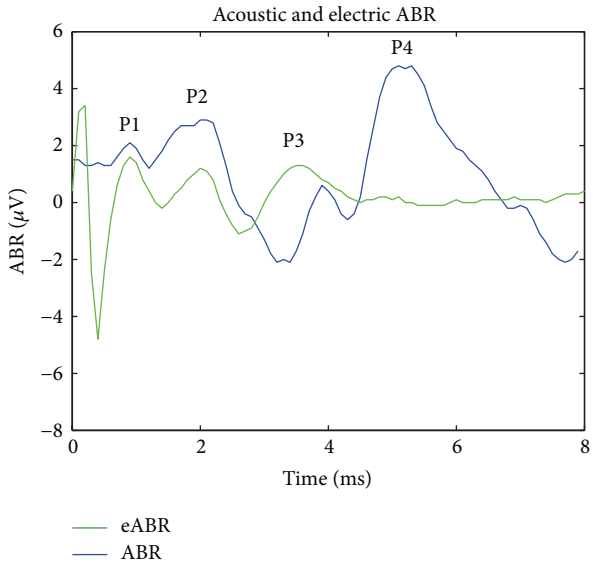

FIGURE 5: Composite of acoustically and electrically evoked auditory brainstem responses at 60 dB SPL and 170 μA, respectively. Acoustic ABR shifted by 1 msec to account for delay from speaker 12 inches from ear.

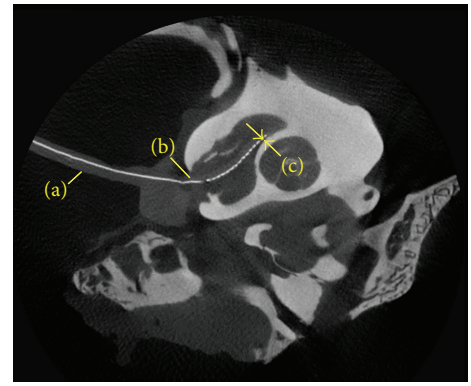

FIGURE 6: cTFA insertion into the basal turn. (a) Electrode array, (b) round window, (c) at approximately site 8; a distance of 100 microns from the modiolus was measured.

CA) Spiral, a precurved, perimodiolar design, appeared to cause intracochlear trauma in 9.5 percent of cochlea undergoing short insertion (<400°) and intracochlear trauma in 31 percent undergoing insertion the entire electrode length. The incidence of intracochlear trauma with the HiFocus II was 8.3 percent during the short insertion and 44.5 percent trauma during full electrode insertion [21].

While possible scala vestibule placement was seen in the single feline cochlea imaged, based on past experience with this design, intracochlear insertion trauma is expected to be less than that seen with other electrode designs. Furthermore, while the placement is suboptimal, there were no detectable changes to the silicone coating or TFA. This suggests that the silicone coating can withstand surgical handling as the cTFA is advanced into the cochlea. Undoubtedly, contemporary electrode arrays as part of commercial cochlear implant systems demonstrate reliable insertion and placement. However, they are constructed by hand and consist of wire bundles encased in silicone and are therefore difficult to modify.

Looking toward the future, to explore advanced stimulation strategies with more electrode sites [31], these arrays cannot simply be scaled up. The resulting array size precludes insertion past the second turn of the scala tympani, which narrows to 200 μm in humans [32]. In contrast, the microfabrication process for TFAs enables electrode site densities to expand two to three times more than commercial devices while remaining within the minimum scalar dimension. Furthermore, when considering the development of combined acoustical and electrical stimulation for patients with residual hearing in the low frequencies, hearing preservation is paramount. Studies have indicated that thinner arrays are associated with lower postimplantation hearing thresholds in animal models [33], and thinner tips (250–350 μm) are

associated with lower insertion forces during implantation [34].

The method of coating thin-films with silicone reported in this work could be refined to a repeatable manufacturing method. For example, layers of silicone could be molded onto the TFAs in consistent thicknesses and exact locations. Furthermore, modulating the substrate flexibility could possibly enable the application of existing neural recording and stimulating arrays to more reliably probe spaces and expand our understanding of signaling and modulation in the cochlea and beyond.

Conflict of Interests

The authors declare that there is no conflict of interests regarding the publication of this paper.

Acknowledgments

This work was funded in part by the Georgia Regents University, the National Science Foundation awards 1055801 and 1133625, and the National Center for Advancing Translational Sciences of the National Institutes of Health under Award Number UL1TR000454, KL2TR000455. The authors thank the Georgia Regents University Veterinary Staff and Paul Spurlock, DVM. The authors would also like to acknowledge Dr. Debbie Colesa and James Weiler at the Kresge Hearing and Research Institute at the University of Michigan for their contributions to the *in vivo* studies, as well as James Steinberg and Hakan Toreyin at the Georgia Institute of Technology, School of Electrical and Computer Engineering for hardware support and *in vitro* testing. The authors would also like to thank Claude Jolly, Marek Polak, and Ilona Anderson from MED-EL Medical Electronics, GmbH, Innsbruck, Austria, for their guidance on eABR data with contemporary arrays and for an unrestricted educational graft funded by MED-EL.

References

[1] K. D. Wise and J. B. Angell, "A low capacitance multielectrode probe for use in extracellular neurophysiology," *IEEE Transactions on Biomedical Engineering*, vol. 22, no. 3, pp. 212–219, 1975.

[2] M. Sonn and W. M. Feist, "A prototype flexible microelectrode array for implant prosthesis applications," *Medical and Biological Engineering*, vol. 12, no. 6, pp. 778–791, 1974.

[3] R. L. White, "Stanford cochlear prosthesis system: ten years of evolution," in *Cochlear Implants*, R. A. Schinder and M. M. Merzenich, Eds., pp. 131–142, Raven Press, New York, NY, USA, 1985.

[4] G. M. Clark and R. J. Hallworth, "A multiple-electrode array for a cochlear implant," *The Journal of Laryngology & Otology*, vol. 90, no. 7, pp. 623–627, 1976.

[5] S. A. Shamma-Donoghue, G. A. May, N. E. Cotter, R. L. White, and F. B. Simmons, "Thin film multielectrode arrays for a cochlear prosthesis," *IEEE Transactions on Electron Devices*, vol. 29, no. 1, pp. 136–144, 1982.

[6] J. Csicsvari, B. Jamieson, K. D. Wise, and G. Buzsáki, "Mechanisms of gamma oscillations in the hippocampus of the behaving rat," *Neuron*, vol. 37, no. 2, pp. 311–322, 2003.

[7] R. L. Snyder, J. A. Bierer, and J. C. Middlebrooks, "Topographic spread of inferior colliculus activation in response to acoustic and intracochlear electric stimulation," *Journal of the Association for Research in Otolaryngology*, vol. 5, no. 3, pp. 305–322, 2004.

[8] M. D. Johnson, R. K. Franklin, M. D. Gibson, R. B. Brown, and D. R. Kipke, "Implantable microelectrode arrays for simultaneous electrophysiological and neurochemical recordings," *Journal of Neuroscience Methods*, vol. 174, no. 1, pp. 62–70, 2008.

[9] R. J. Vetter, J. C. Williams, J. F. Hetke, E. A. Nunamaker, and D. R. Kipke, "Chronic neural recording using silicon-substrate microelectrode arrays implanted in cerebral cortex," *IEEE Transactions on Biomedical Engineering*, vol. 51, no. 6, pp. 896–904, 2004.

[10] T. E. Bell, K. D. Wise, and D. J. Anderson, "A flexible micromachined electrode array for a cochlear prosthesis," *Sensors and Actuators, A: Physical*, vol. 66, no. 1–3, pp. 63–69, 1998.

[11] P. T. Bhatti and K. D. Wise, "A 32-site 4-channel high-density electrode array for a cochlear prosthesis," *IEEE Journal of Solid-State Circuits*, vol. 41, no. 12, pp. 2965–2973, 2006.

[12] J. Wang and K. D. Wise, "A thin-film array with integrated position sensing," *IEEE Journal of Micro Electro Mechical Systems*, vol. 18, no. 12, pp. 385–394, 2009.

[13] H. H. Lim and D. J. Anderson, "Spatially distinct functional output regions within the central nucleus of the inferior colliculus: implications for an auditory midbrain implant," *Journal of Neuroscience*, vol. 27, no. 32, pp. 8733–8743, 2007.

[14] S. K. Kelly, D. B. Shire, J. Chen et al., "A hermetic wireless subretinal neurostimulator for vision prostheses," *IEEE Transactions on Biomedical Engineering*, vol. 58, no. 11, pp. 3197–3205, 2011.

[15] M. S. Humayun, J. D. Dorn, L. Da Cruz et al., "Interim results from the international trial of second sight's visual prosthesis," *Ophthalmology*, vol. 119, no. 4, pp. 779–788, 2012.

[16] K. D. Wise, P. T. Bhatti, J. Wang, and C. R. Friedrich, "High-density cochlear implants with position sensing and control," *Hearing Research*, vol. 242, no. 1-2, pp. 22–30, 2008.

[17] K. C. Iverson, P. T. Bhatti, J. Falcone, R. Figueroa, and B. J. McKinnon, "Cochlear implantation using thin-film array electrodes," *Otolaryngology—Head and Neck Surgery*, vol. 144, no. 6, pp. 934–939, 2011.

[18] A. Sharpe, J. van Beek-King, A. Crane, B. McKinnon, and P. Bhatti, "Integration of a polymeric thin-film array with an insertion platform for a high-density cochlear electrode array," in *Proceedings of the 12th International Conference on Cochlear Implants and Other Implantable Auditory Technologies*, Baltimore, Md, USA, 2012.

[19] P. T. Bhatti, J. Van Beek-King, S. Tridandapani, K. Olsen, K. Iverson, and B. McKinnon, "An Integrated thin-film high-density intracochlearelectrode array and insertion platform: in-vitro validation and temporal bone insertion," in *Proceedings of the Abstract of 40th Neural Interfaces Conference*, Salt Lake City, Utah, USA, 2012.

[20] P. Wardrop, D. Whinney, S. J. Rebscher, J. T. Roland Jr., W. Luxford, and P. A. Leake, "A temporal bone study of insertion trauma and intracochlear position of cochlear implant electrodes. I: comparison of Nucleus banded and Nucleus Contour electrodes," *Hearing Research*, vol. 203, no. 1-2, pp. 54–67, 2005.

[21] P. Wardrop, D. Whinney, S. J. Rebscher, J. T. Roland Jr., W. Luxford, and P. A. Leake, "A temporal bone study of insertion trauma and intracochlear position of cochlear implant

electrodes. II: comparison of Spiral Clarion and HiFocus II electrodes," *Hearing Research*, vol. 203, no. 1-2, pp. 68–79, 2005.

[22] S. Biedron, A. Prescher, J. Ilgner, and M. Westhofen, "The internal dimensions of the cochlear scalae with special reference to cochlear electrode insertion trauma," *Otology & Neurotology*, vol. 31, no. 5, pp. 731–737, 2010.

[23] S. J. Rebscher, A. M. Hetherington, R. L. Snyder, P. A. Leake, and B. H. Bonham, "Design and fabrication of multichannel cochlear implants for animal research," *Journal of Neuroscience Methods*, vol. 166, no. 1, pp. 1–12, 2007.

[24] S. J. Rebscher, A. Hetherington, B. Bonham, P. Wardrop, D. Whinney, and P. A. Leake, "Considerations for design of future cochlear implant electrode arrays: electrode array stiffness, size, and depth of insertion," *Journal of Rehabilitation Research and Development*, vol. 45, no. 5, pp. 731–747, 2008.

[25] S. M. Rajguru, A. I. Matic, A. M. Robinson et al., "Optical cochlear implants: evaluation of surgical approach and laser parameters in cats," *Hearing Research*, vol. 269, no. 1-2, pp. 102–111, 2010.

[26] E. A. Kretzmer, N. E. Meltzer, C.-A. Haenggeli, and D. K. Ryugo, "An animal model for cochlear implants," *Archives of Otolaryngology—Head & Neck Surgery*, vol. 130, no. 5, pp. 499–508, 2004.

[27] A. E. Kirby and J. C. Middlebrooks, "Auditory temporal acuity probed with cochlear implant stimulation and cortical recording," *Journal of Neurophysiology*, vol. 103, no. 1, pp. 531–542, 2010.

[28] P. Ungan and S. Yagcioglu, "Origin of the binaural interaction component in wave P4 of the short-latency auditory evoked potentials in the cat: evaluation of serial depth recordings from the brainstem," *Hearing Research*, vol. 167, no. 1-2, pp. 81–101, 2002.

[29] R. E. Beitel, R. L. Snyder, C. E. Schreiner, M. W. Raggio, and P. A. Leake, "Electrical cochlear stimulation in the deaf cat: comparisons between psychophysical and central auditory neuronal thresholds," *Journal of Neurophysiology*, vol. 83, no. 4, pp. 2145–2162, 2000.

[30] Z. M. Smith and B. Delgutte, "Using evoked potentials to match interaural electrode pairs with bilateral cochlear implants," *Journal of the Association for Research in Otolaryngology*, vol. 8, no. 1, pp. 134–151, 2007.

[31] J. H. Goldwyn, S. M. Bierer, and J. A. Bierer, "Modeling the electrode-neuron interface of cochlear implants: effects of neural survival, electrode placement, and the partial tripolar configuration," *Hearing Research*, vol. 268, no. 1-2, pp. 93–104, 2010.

[32] E. Erixon, H. Högstorp, K. Wadin, and H. Rask-Andersen, "Variational anatomy of the human cochlea: implications for cochlear implantation," *Otology and Neurotology*, vol. 30, no. 1, pp. 14–22, 2009.

[33] Y. Nguyen, M. Miroir, G. Kazmitcheff et al., "Cochlear implant insertion forces in microdissected human cochlea to evaluate a prototype array," *Audiology and Neurotology*, vol. 17, no. 5, pp. 290–298, 2012.

[34] Y. Nguyen, I. Mosnier, S. Borel et al., "Evolution of electrode array diameter for hearing preservation in cochlear implantation," *Acta Oto-Laryngologica*, vol. 133, no. 2, pp. 116–122, 2013.

Hindawi Publishing Corporation
BioMed Research International
Volume 2015, Article ID 574209, 9 pages
http://dx.doi.org/10.1155/2015/574209

Research Article

Cochlear Dummy Electrodes for Insertion Training and Research Purposes: Fabrication, Mechanical Characterization, and Experimental Validation

Jan-Philipp Kobler,[1] Anandhan Dhanasingh,[2] Raphael Kiran,[2] Claude Jolly,[2] and Tobias Ortmaier[1]

[1] *Institute of Mechatronic Systems, Gottfried Wilhelm Leibniz Universität Hannover, Appelstraße 11a, 30167 Hanover, Germany*
[2] *MED-EL Medical Electronics, Fuerstenweg 77a, 6020 Innsbruck, Austria*

Correspondence should be addressed to Jan-Philipp Kobler; kobler@imes.uni-hannover.de

Received 21 November 2014; Accepted 9 March 2015

Academic Editor: Hung-Ching Lin

To develop skills sufficient for hearing preservation cochlear implant surgery, surgeons need to perform several electrode insertion trials in *ex vivo* temporal bones, thereby consuming relatively expensive electrode carriers. The objectives of this study were to evaluate the insertion characteristics of cochlear electrodes in a plastic scala tympani model and to fabricate radio opaque polymer filament dummy electrodes of equivalent mechanical properties. In addition, this study should aid the design and development of new cochlear electrodes. Automated insertion force measurement is a new technique to reproducibly analyze and evaluate the insertion dynamics and mechanical characteristics of an electrode. Mechanical properties of MED-EL's FLEX^{28}, FLEX^{24}, and FLEX^{20} electrodes were assessed with the help of an automated insertion tool. Statistical analysis of the overall mechanical behavior of the electrodes and factors influencing the insertion force are discussed. Radio opaque dummy electrodes of comparable characteristics were fabricated based on insertion force measurements. The platinum-iridium wires were replaced by polymer filament to provide sufficient stiffness to the electrodes and to eradicate the metallic artifacts in X-ray and computed tomography (CT) images. These low-cost dummy electrodes are cheap alternatives for surgical training and for *in vitro, ex vivo*, and *in vivo* research purposes.

1. Introduction

Cochlear implants (CI) are currently the only solution to restore hearing in patients with profound deafness. Electrodes, which are one of the important components of CI, have more than one stimulating channel placed inside the scala tympani to elicit action potentials in the auditory neural tissues tonotopically. Recently, the indication for CI has been extended to partial deafness [1, 2]. As a result, hearing preservation (HP), by soft surgical techniques to protect the intracochlear fine structures, is the latest trend especially for patients with good residual hearing in the mid- to low-frequency apical region. Hearing preservation may also be important for future therapies that may need these fine structures in place for the regeneration of the neural fibers [3]. Although the correlation between the intracochlear trauma due to insertion and the conservation of residual acoustic hearing has not been distinctly stated, it is assumed that atraumatic electrode insertion is essential to prevent neuronal cell death and trauma to the internal structures [4–7]. One of the main factors influencing the outcome of soft surgical procedures is how surgeons handle and push the electrode gently inside the scala tympani [8–10]. Performing this soft surgical technique requires a high level of surgical skill and a wealth of hands-on experience.

Cochlear implant electrodes are made of biocompatible conducting wires and electrode contacts housed within a flexible biocompatible elastomer. The electrode contacts (typically made of platinum/iridium or gold) are electrically connected to the wires for operationally contacting intracochlear

structures of the CI user to deliver the electrical signal. The soft elastomers generally preserve the basilar membrane and the organ of Corti during the insertion process. Electrode atraumaticity depends on the stiffness of the wires and the smoothness of the elastomer. The size, shape, stiffness, and length of the electrodes vary among manufacturers [11].

Surgeons need to perform several electrode insertion trials in *ex vivo* temporal bones to develop the skills necessary for successful HP surgery in a patient. The electrodes required for such training, however, are expensive due to the high cost of the raw materials and the manufacturing.

The metallic artifact that cochlear electrodes create with clinical and μCT imaging is also a problem [12–14]. For many *ex vivo* research purposes and medical studies, for example, studying the impact of electrode insertion on the intracochlear fine structures or cochlear duct length measurement, the metallic artifact is a great hindrance. Such temporal bone studies also help to evaluate the mechanical properties of newly developed electrode arrays. This includes evaluating the damage to the basilar membrane, lateral, and medial cochlear walls due to the insertion of an electrode array, the positioning of the electrode array within the scala, and so forth. In radiographs, however, metallic artifacts from the electrode array overshadow the fine tissue structures.

In order to address the abovementioned problems, we developed silicone dummy cochlear electrodes of various array lengths. If successful, cost-effective, easy-to-fabricate dummy electrodes could be used for *ex vivo* research purposes and for insertion training.

The objective of this study was to develop electrode arrays with comparable mechanical properties to those of the FLEX series (MED-EL GmbH, Innsbruck, Austria) by using radio opaque polymer filament to replace the metallic wires. The mechanical properties of these dummy electrodes were determined using an automated insertion tool with integrated force-sensing capability [15]. This tool was originally developed for minimally invasive cochlear implant surgery [16–18], but it also serves as an instrument for reproducible electrode characterization within a bench top setup since it minimizes variations in the insertion procedure due to human interaction [19]. The measured insertion force, combined with video documentation of the automated insertions, was considered to compare characteristics of the dummy electrodes to those of their commercially available wire-based counterparts.

2. Materials and Methods

2.1. Materials. To fabricate the dummy electrodes, we used two polymer filaments that varied in material and thickness, obtained from Goodfellow Cambridge Ltd., Huntingdon, United Kingdom. Monofilament made of polyethylene terephthalate (PET) had a thickness of 100 μm and the monofilament made of fluorinated ethylene propylene copolymer (FEP) had a thickness of 280 μm. Medical grade silicone elastomer from NuSil Technology LLC, Carpinteria, CA, USA, was used as electrode carrier and 10% iridium blended platinum wire (×1) with a thickness of 25 μm was used as the electrode tracker, which helps to locate the dummy implant in CT images.

Table 1: Characteristics of dummy electrodes fabricated in this study.

Reference	Dummy identifier	Characteristic	Number of prototypes
FLEX^{28}	F28 01	FEP filament	1
	F28 02	PET filament	3
	F28 03	PET filament with reduced length	1
FLEX^{24}	F24 01	PET filament	1
FLEX^{20}	F20 01	PET filament	1

2.2. Electrode Fabrication. We fabricated the dummy electrode array in 28 mm, 24 mm, and 20 mm lengths, equivalent to the FLEX^{28}, FLEX^{24}, and FLEX^{20} electrodes, commercially available brands from MED-EL GmbH. The inner surface of the mold was first painted with a thin layer of silicone followed by the polymer filament placement together with a platinum wire (10% iridium). The mold halves were closed, injected with silicone, and cured at 110°C for 4 hours. The mold halves were separated to remove the cured electrode. Table 1 gives an overview of the manufactured dummy electrodes for consideration in this study.

With the standard fabrication procedure, the wire and the polymer filament were inserted up to the position of the first stimulation contact. This contact is not functional in the dummy electrodes but helps to localize the tip of the implant in X-ray and CT images. To analyze the effects of a more flexible electrode tip, one prototype (F28 03) was manufactured using filament that went up to the original position of the second stimulation contact (see also Figure 1). Figure 2 shows one such dummy electrode (F24 01) which was fabricated according to the dimensions of the FLEX^{24} model.

In order to assess the manufacturing costs of the dummy electrodes, the polymer filament, wires, and silicone required for fabrication are considered. Based on the current pricing of these components, the manufacturing costs of the dummy electrodes are estimated to be approximately 2% of those required to fabricate the commercially available models.

2.3. Insertion Force Measurement. In cochlear implantation surgery that aims for HP, trauma associated with electrode insertion needs to be minimized to preserve both the delicate intracochlear membranes and the sensory hair cells. Arguably, insertion trauma and loss of residual hearing are due to intracochlear forces applied during electrode deployment. It is widely accepted that the magnitude of such insertion forces correlates with the amount of intracochlear trauma [20, 21]. Considering straight electrodes, insertion forces depend on the mechanical properties of the electrode carriers and other parameters which are not assessed but kept constant in this study [22, 23]. Here, the measured insertion

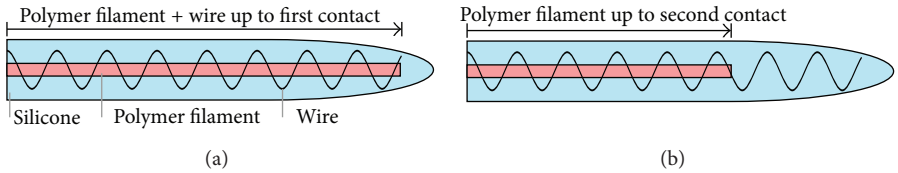

Figure 1: Cross-section of dummy electrodes: standard fabrication procedure (a) and fabrication using filament with reduced length (b).

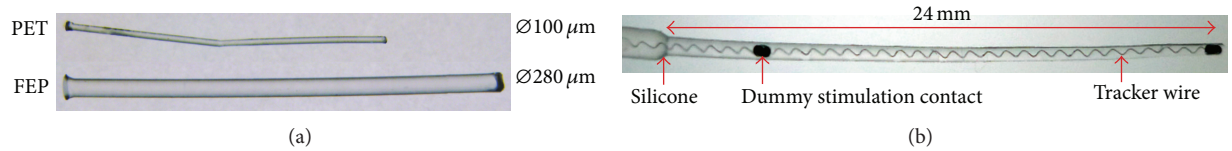

Figure 2: Samples of PET and FEP filament (a), fabricated dummy electrode F24 01 (b). The stimulation contacts (not connected) and the tracker wire are included to facilitate localization of the electrode in CT images. The opaque PET filament is not visible in this picture.

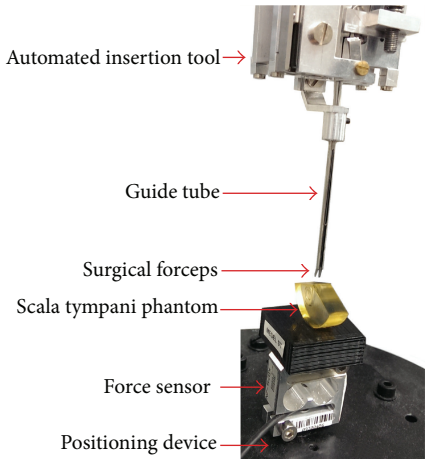

Figure 3: Overview of the experimental setup for automated insertion studies and components involved.

force is considered to compare the dummy electrodes to their commercial counterparts.

Insertion force measurements, for which an automated insertion tool was used, were performed according to the experimental setup proposed by Kobler et al. [15]. The components involved are given in Figure 3. The automated insertion tool was originally designed for both straight and preformed electrode carriers, which are preoperatively straightened by a platinum wire. The tool therefore incorporates two linear actuators to independently actuate the implant feed and the position of the straightening wire. Since only straight electrodes were considered in this study, one actuator remained passive during the trials. The actuators based on piezo technology provide a traveling range of 45 mm and a position accuracy of 1 μm (SL1560, SmarAct GmbH, Oldenburg, Germany). The electrode carrier to be inserted can be grasped by surgical forceps with flat jaws attached to the implant actuator. This grasping mechanism is covered by a u-shaped guide tube to provide guidance of the implant during the insertion process.

All insertions were performed into an acrylic scala tympani phantom developed by MED-EL GmbH and based on histological human temporal bone data. Further specifications of the phantom are given in Leon et al., 2014 [24]. To measure insertion force, we used a commercially available, s-shaped, single axis load cell with a measuring range of up to 2 N (KD24S-2 N), onto which the phantom was placed. This sensor was also mounted on a passive positioning device, which allowed the precise adjustment of the phantom's position and orientation with respect to the insertion tool and, therefore, the feed motion of the electrode carrier. The load cell was operated using a carrier frequency amplifier system (MGCplus and ML55B, Hottinger Baldwin Messtechnik, Darmstadt, Germany). The analogue output of the measurement amplifier was connected to a 16-bit DAQ-System (NI USB-6251 BNC, National Instruments, Austin, Texas, USA) and sampled at a rate of 1,000 Hz. The resulting resolution of the measuring system was well below 1 mN.

2.4. Insertion Protocol. To derive a gold standard for the evaluation of the dummy electrodes, the insertion force profiles of the commercially available FLEX^{28}, FLEX^{24}, and FLEX^{20} electrodes were recorded. For each electrode, the following procedure was followed: (1) the implant was loaded into the automated insertion tool, (2) the phantom was filled with a soap solution and the electrode was positioned just inside the opening of the lumen (see also Figure 4), and (3) the automated insertion was performed at a constant velocity of 0.5 mm/s while insertion forces were acquired simultaneously. Each tested electrode carrier was inserted five times while maintaining both the grasping and the initial position of the implant.

Considering the commercial models, three electrodes of each type were tested according to the procedure described above, resulting in 15 insertions per model. The insertion depth, that is, the linear displacement from the electrode's initial position, was considered as 27 mm for the FLEX^{28}, 23 mm for the FLEX^{24}, and 19.5 mm for the FLEX^{20}.

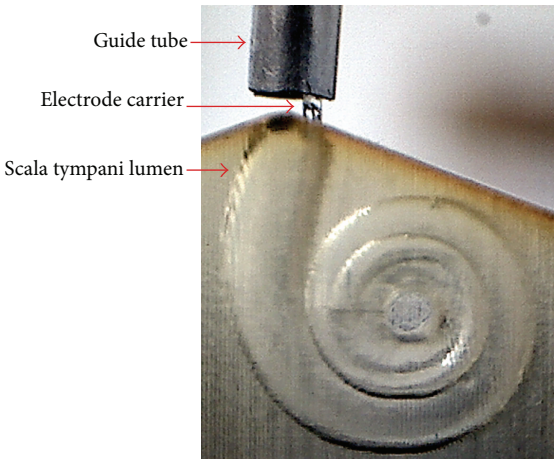

Figure 4: Initial position and orientation of the implant with respect to the phantom.

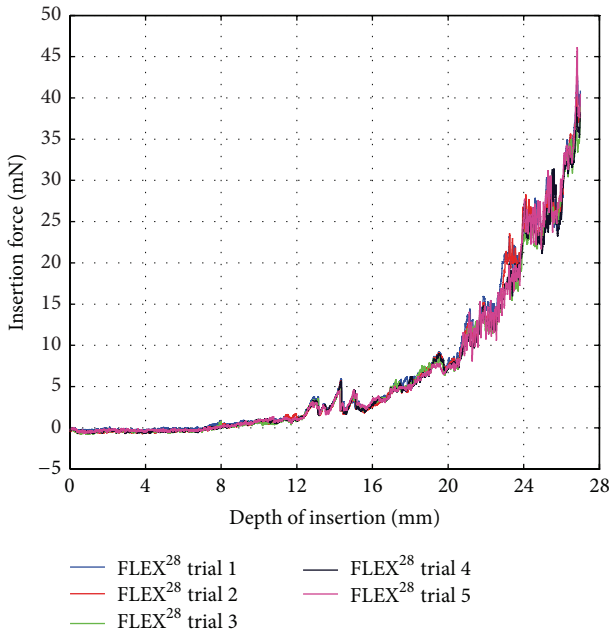

Figure 5: Insertion force curves measured during five consecutive insertions of the same FLEX^{28} electrode.

The same protocol was followed to evaluate the dummy electrodes and compare them with their commercially available counterparts. Each prototype, listed in Table 1, was inserted five times. The fourth insertion of each series was documented using a digital video microscope. It is important to note that, in order to minimize measurement errors due to human intervention, the relative alignment between the insertion tool and the phantom was maintained throughout the study.

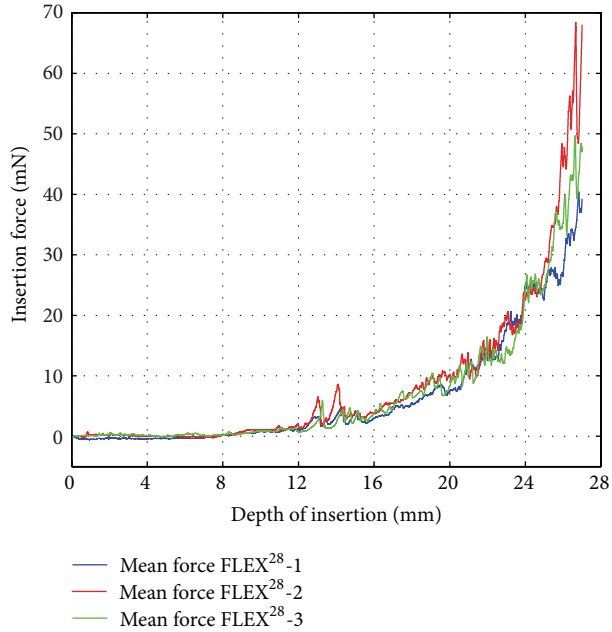

Figure 6: Mean insertion forces of three similar FLEX^{28} electrodes.

3. Results and Discussion

80 automated insertions (45 insertions of commercially available models and 35 insertions of dummy electrodes) were successfully performed.

To assess the repeatability and reproducibility of an insertion force curve using the proposed experimental setup, Figure 5 gives the force data obtained during five consecutive measurements of the same FLEX^{28} electrode. The results of the five trials were very similar and strongly correlated. Here, the smallest correlation coefficient resulting from a pairwise comparison between the five force curves equaled 0.86. When averaging the force curves over insertion depth, the maximum standard deviation, 4 mN at a depth of 25.88 mm, is low. This confirms that sufficient repeatability was achieved.

Due to the similarity of the results, the mean insertion force over the five trials was considered a suitable approximation for characterization of one electrode. Figure 6 gives the mean insertion force curves of three similar FLEX^{28} electrodes (denoted as FLEX28-1, FLEX28-2, and FLEX28-3). Again, the presumably identical electrodes exhibit similar characteristics up to a depth of approximately 25 mm and then diverge slightly during the final three millimeters of the insertion. Because each electrode is manufactured by hand, such marginal variations are to be expected.

To compare the commercially available electrodes to their corresponding dummy electrodes, the following vectors were computed based on the recorded data, that is, 15 insertion force curves per electrode: the arithmetic average and the minimum and maximum insertion force over insertion depth. Furthermore, the arithmetic average curve

Table 2: Curve fitting parameters of MED-EL electrode insertion forces.

Name	a	b	c	d	RMSE (in mN)	r^2
FLEX^{20}	0.063	0.303	$7.120 \cdot 10^{-8}$	1.009	0.6839	0.9942
FLEX^{24}	0.025	0.310	−0.531	−0.221	0.4906	0.9952
FLEX^{28}	$2.056 \cdot 10^{-8}$	0.754	0.157	0.202	0.8724	0.9934

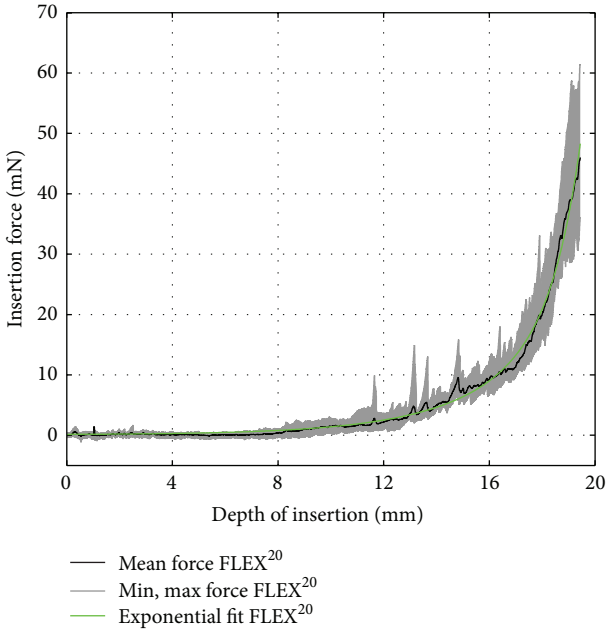

Figure 7: FLEX^{20} insertion force model.

was approximated by fitting an exponential function of the following formula:

$$f_i(d_i) = ae^{bd_i} + ce^{dd_i} \quad (1)$$

to obtain a compact representation of the relation between insertion force f_i and insertion depth d_i. The choice of an exponential function was motivated by the following physical assumptions: given a straight, flexible electrode carrier, the measured insertion force is believed to depend on the radius of curvature of the scala tympani's outer wall, which can be modeled by a logarithmic spiral whose radius is defined as an exponential function of the spiral angle, that is, the insertion angle in this case [25]. Furthermore, according to the Capstan equation [26], the frictional forces between the outer wall of the scala tympani and the silicone carrier, which make a significant contribution to the total insertion force [10], increase exponentially depending on the insertion angle. For the commercially available electrodes, the computed data are given in Figures 7–9. The results of the curve fitting procedure can be found in Table 2. The coefficients of determination (r^2) confirm that the measured insertion force curves of the commercially available electrodes were suitably approximated by an exponential function of the chosen form [27].

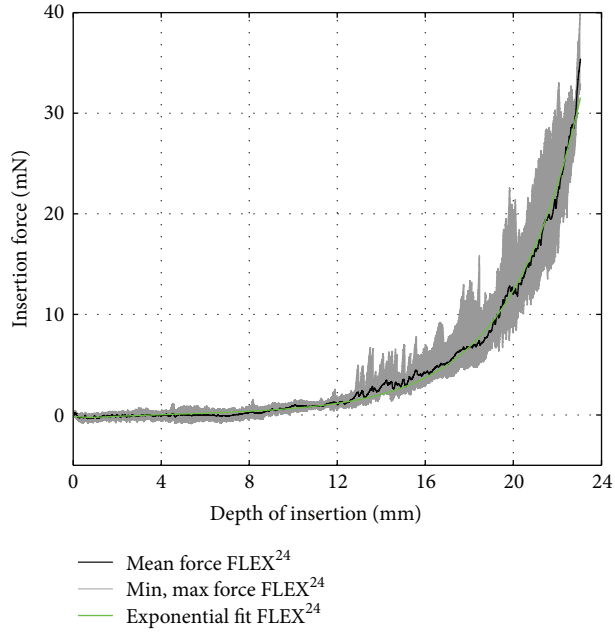

Figure 8: FLEX^{24} insertion force model.

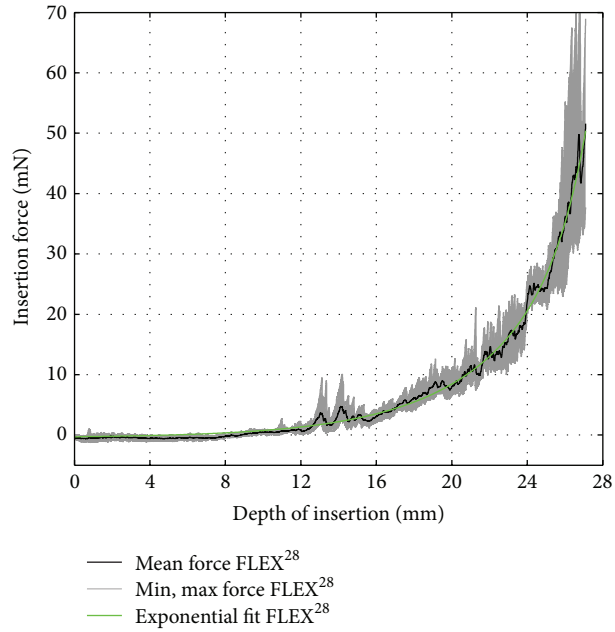

Figure 9: FLEX^{28} insertion force model.

A similar evaluation procedure was followed for the dummy electrodes. For each prototype, the mean insertion force over insertion depth was computed by averaging the recorded data of five consecutive trials. Figure 10 (F20 01) and Figure 11 (F24 01) compare the dummy electrodes to their commercially available counterparts. A similar comparison is given in Figure 12 for all electrodes made according to the FLEX^{28} specifications. Furthermore, the insertion procedures of FLEX^{28}, F28 01, F28 02 (B), and F28 03 at characteristic insertion depths (indicated in Figure 12) are given in

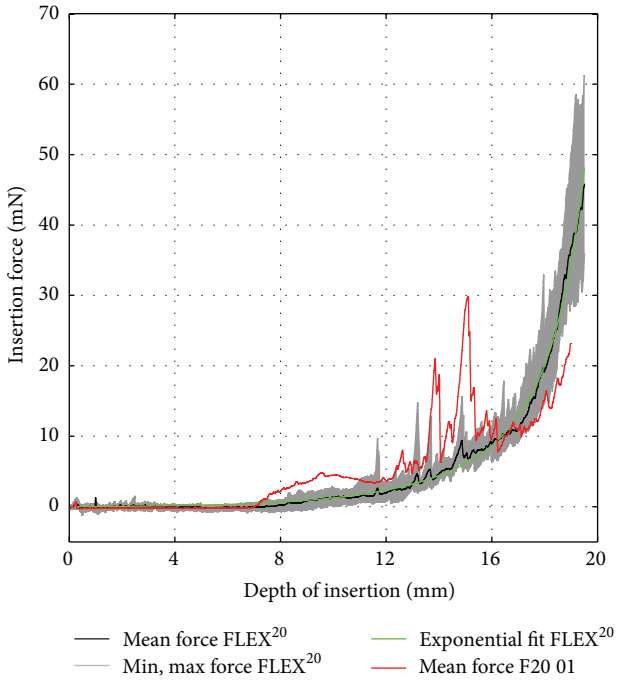

Figure 10: Insertion force comparison between commercially available FLEX[20] electrode (black curve) and PET filament dummy (red curve).

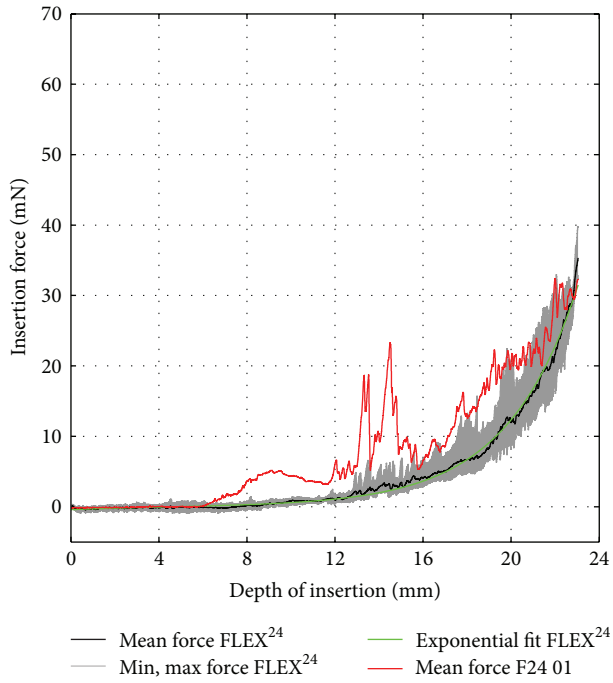

Figure 11: Insertion force comparison between commercially available FLEX[24] electrode (black curve) and PET filament dummy (red curve).

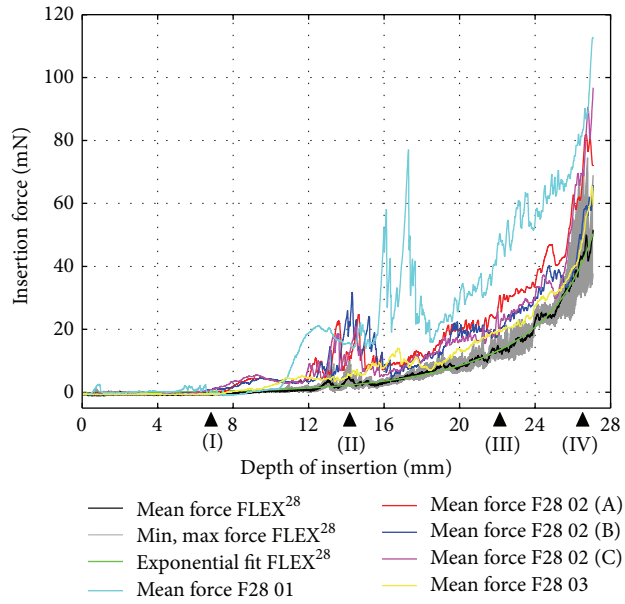

Figure 12: Insertion force comparison between commercially available FLEX[28] electrode (black curve) and dummy electrodes characterized by PET filament (red, blue, and magenta curves), FEP filament (cyan curve), and PET filament with reduced length (yellow curve).

Figure 13. Regardless of electrode length, the insertion force curves of the dummy electrodes exhibit similar characteristics. An increase in insertion force for the dummy electrodes at a depth of approximately 6.5–8 mm was observed (see also position (I) in Figure 13), which did not occur when measuring the commercially available electrodes. This was due to the initial contact of electrode tip on the outer wall of the scala tympani phantom. The polymer filament inside the silicone carrier gives a homogenous mechanical strength from the base to the apex of the electrode, although arrays with a flexible tip are generally preferable for atraumatic insertion. Because the tip of the dummy electrode is slightly stiffer and more rigid than is ideal, the insertion force measurement showed two characteristic peaks at 14 mm and 16 mm, as, at this insertion depth, the tip of the electrode had to make an almost complete turn (position (II) in Figure 13). The measured insertion force was mainly composed of (1) the force needed to bend the electrode and (2) Capstan friction due to the silicone carrier being in contact with the inner surface of the scala tympani phantom. With the polymer filament inside the dummy electrode, the mechanical property of the dummy electrode is similar from the base to the apex of the electrode, which is not the case with the regular wire-based electrode. This could be the reason for the peaks in the insertion forces at different insertion depths. The results also reveal that, due to the characteristics mentioned above, an exponential function cannot approximate the insertion force curves of the dummy electrodes in a suitable way.

To enable a quantitative comparison between the insertion force curves of the commercially available and the

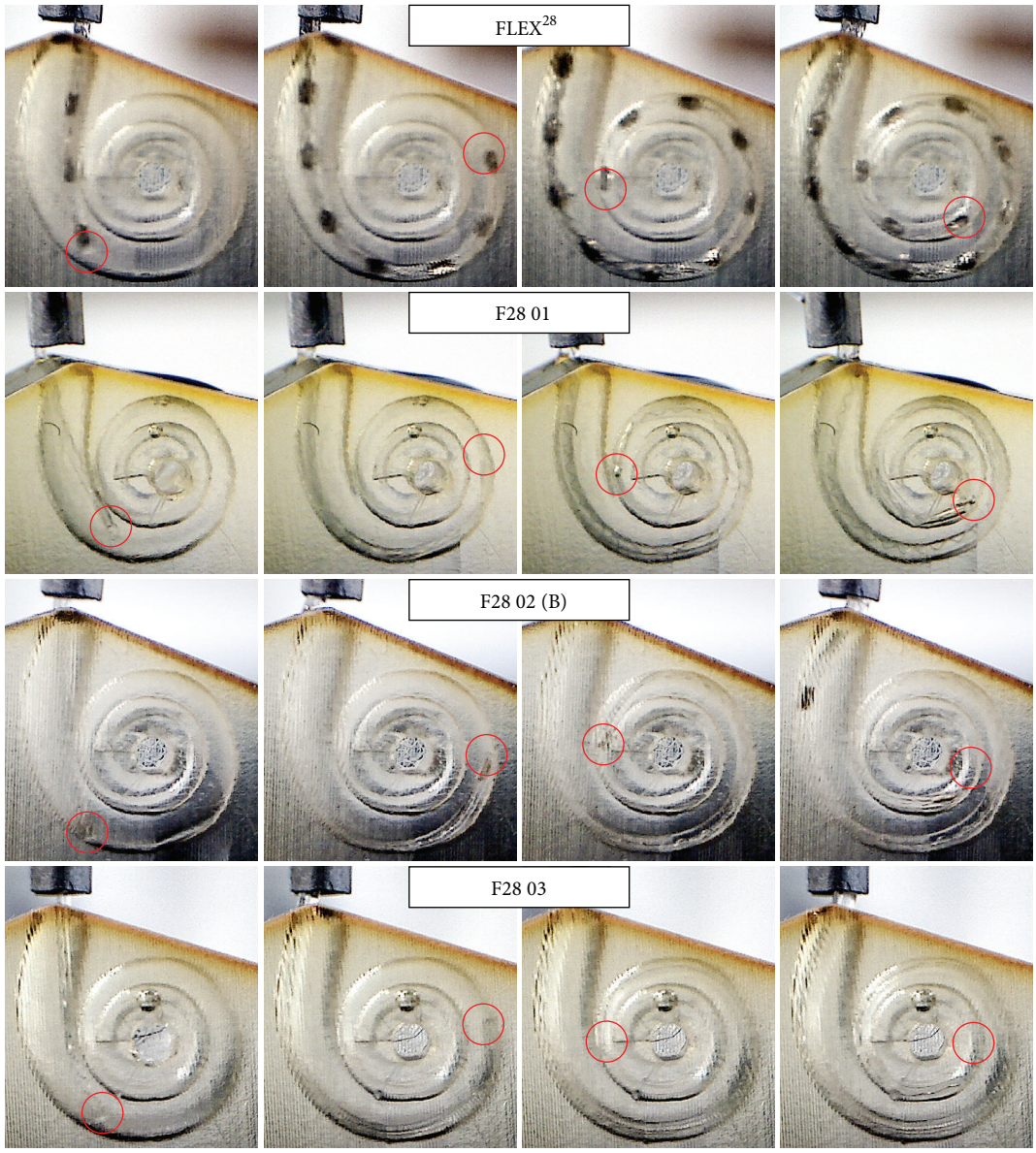

FIGURE 13: Documentation of the insertion procedure at characteristic insertion depths (see also Figure 12) for FLEX[28] and three different dummy electrode types. Due to the opaque material of the dummy electrodes, the position of the tip is indicated by a red circle.

dummy electrodes, the following metrics were considered and computed:

(i) **M1** was defined as the root-mean-square-error (RMSE) between the mean insertion force of the commercial electrode and the mean insertion force of the dummy electrode.

(ii) **M2** was defined as the RMSE between the exponential fit of the commercially available electrode and the mean of the dummy electrode. This metric was expected to be similar to **M1** in case the exponential function was a good approximation of the force curves.

(iii) The third metric was based on the assumption that the mean insertion forces of a dummy electrode should be higher than the minimum and lower than the maximum insertion forces of its commercially available counterpart. For each insertion depth the following conditions were checked:

(1) If the mean force of the dummy electrode was above the maximum of the commercially available electrode's mean force, an error value was defined as the absolute deviation from the maximum.

(2) If the mean force of the dummy electrode was below the minimum of the commercially available electrode's mean force, the error value was

Table 3: Considered metrics for the evaluation of dummy electrodes.

Dummy identifier	**M1** (in mN)	**M2** (in mN)	**M3** (in mN)
F20 01	4.5169	4.6307	3.1427
F24 01	5.2742	5.3238	3.5782
F28 01	21.9785	21.9664	19.1608
F28 02 (A)	10.1176	10.1219	7.1303
F28 02 (B)	6.9967	7.0418	5.2088
F28 02 (C)	8.8904	8.9263	5.5272
F28 03	4.0276	3.9461	2.3394

defined as the absolute deviation from the minimum.

(3) If the mean force of the dummy electrode was between the minimum and maximum insertion force of the commercially available electrode's mean force, the error value was equal to zero.

Finally, **M3** was defined as the RMS of the error values described above.

All of the considered metrics penalize deviations of the dummy electrodes' insertion forces from the references of their commercially available counterpart; therefore, the lower the metric is, the closer the dummy electrode is to its commercially available counterpart. Table 3 lists the values of these metrics for all considered dummy electrodes.

All considered metrics yielded a similar "ranking" of the dummy electrodes. According to the values, electrode F28 01, which was made using FEP filament, is the least suitable prototype in terms of insertion force. This rating is in good agreement with the results seen in Figure 12 and confirms that the measured force was considerably higher compared to FLEX^{28}. The prototypes made using PET filament (F20 01, F24 01, and F28 02) generally exhibited smaller deviations from the force curves of the commercially available electrodes. The best match, however, compared to the reference was achieved using the specifications of the shortest electrode carrier, that is, FLEX^{20}, while the divergences increased for FLEX^{24} and FLEX^{28}. Referring to the metrics in Table 3, the force curve of prototype electrode F28 03, which is characterized by PET filament with a reduced length, was the closest to that of the commercially available FLEX^{28} implant. According to our observations, the softer tip of the silicone carrier brings the mechanical properties of this dummy electrode closer to those of the regular, wire-based model. Consequently, when the first contact with the outer wall of the phantom takes place, the soft tip kinks and deflects (see also position (I) in Figure 13). As a result, the characteristic increase in insertion force, usually observed at an insertion depth of 6.5 to 8 mm, is delayed by approximately 3 mm, since the filament is pushed against the outer wall of the phantom. This increase was, however, less distinct than that of the rest of the measured dummy electrodes.

4. Conclusions

To evaluate the mechanical properties of MED-EL's FLEX series electrodes, we performed the insertion force measurement in a plastic scala tympani model with dummy electrodes of equivalent mechanical characteristics. The experimental setup, comprising of an automated insertion tool, was suitable for electrode characterization and comparison since it provided sufficient reproducibility of insertion force curves and low standard deviation among consecutive trials. Reproducibility was mainly achieved by keeping constant the relevant parameters that influence insertion force, for example, the alignment of insertion tool and phantom. Furthermore, automation of the insertion procedure minimizes the required amount of human intervention between consecutive trials, which, in turn, leads to reduced variations in the experimental results.

Statistical analysis and curve fitting showed that the measured insertion force of straight, commercially available electrodes increased exponentially with the insertion depth. Due to the curve fitting procedure, a compact, formal representation of this relation is given in this paper, taking into account three commercially available electrode models. The parameters of the exponential functions are considered a valuable contribution to further studies on insertion force since the curves given in this paper can easily be reproduced by other researchers.

Further studies are required to determine the factors affecting insertion force, which include manufacturing variability, thickness of metallic wire, contact spacing, tip diameter, lubricants, and insertion speed. Based on the deviation of the quantitative comparison of dummy and reference electrodes, the F28 03 was the dummy electrode closest to the reference in terms of insertion force. The use of PET filament with reduced length (as shown in Figure 1) was therefore the most suitable creation technique. It serves as a basis for further optimization, which aims at matching the force curves of commercially available electrodes even closer with those of the dummy electrodes.

Future studies are planned to evaluate (1) the mechanical properties by nanoindenter-based bending test and (2) temporal bone insertion followed by μCT imaging to assess the traumaticity and the radio opaque characteristics of the dummy electrodes. In this context, we also aim for a direct comparison between dummy electrodes and commercial models in the hands of surgeons to determine the handling characteristics and the suitability for training purposes. The insertion tool used in this study can also be used for benchmarking the traumaticity of electrodes and can serve in the design and development of new electrodes.

Conflict of Interests

The authors declare that there is no conflict of interests regarding the publication of this paper.

Acknowledgments

The authors would like to thank Mr. Philipp Schindler (MED-EL GmbH, Innsbruck) for the provision of the plastic scala tympani phantom and Michael Todd (MED-EL GmbH, Innsbruck), who edited a version of this paper. They acknowledge support by Deutsche Forschungsgemeinschaft and Open Access Publishing Fund of Leibniz Universität Hannover.

References

[1] A. L. L. Sampaio, M. F. S. Araújo, and C. A. C. P. Oliveira, "New criteria of indication and selection of patients to cochlear implant," *International Journal of Otolaryngology*, vol. 2011, Article ID 573968, 13 pages, 2011.

[2] P. C. Miranda, A. L. L. Sampaio, R. A. F. Lopes, A. Ramos Venosa, and C. A. C. P. de Oliveira, "Hearing preservation in cochlear implant surgery," *International Journal of Otolaryngology*, vol. 2014, Article ID 468515, 6 pages, 2014.

[3] E. W. Rubel, S. A. Furrer, and J. S. Stone, "A brief history of hair cell regeneration research and speculations on the future," *Hearing Research*, vol. 297, pp. 42–51, 2013.

[4] O. Adunka, J. Kiefer, M. H. Unkelbach, T. Lehnert, and W. Gstoettner, "Development and evaluation of an improved cochlear implant electrode design for electric acoustic stimulation," *The Laryngoscope*, vol. 114, no. 7, pp. 1237–1241, 2004.

[5] M. Miroir, Y. Nguyen, G. Kazmitcheff, E. Ferrary, O. Sterkers, and A. B. Grayeli, "Friction force measurement during cochlear implant insertion: application to a force-controlled insertion tool design," *Otology & Neurotology*, vol. 33, no. 6, pp. 1092–1100, 2012.

[6] W. Gstoettner, J. Kiefer, W.-D. Baumgartner, S. Pok, S. Peters, and O. Adunka, "Hearing preservation in cochlear implantation for electric acoustic stimulation," *Acta Oto-Laryngologica*, vol. 124, no. 4, pp. 348–352, 2004.

[7] T. J. Balkany, S. S. Connell, A. V. Hodges et al., "Conservation of residual acoustic hearing after cochlear implantation," *Otology & Neurotology*, vol. 27, no. 8, pp. 1083–1088, 2006.

[8] G. P. Rajan, G. Kontorinis, and J. Kuthubutheen, "The effects of insertion speed on inner ear function during cochlear implantation: a comparison study," *Audiology & Neurotology*, vol. 18, no. 1, pp. 17–22, 2013.

[9] O. Adunka and J. Kiefer, "Impact of electrode insertion depth on intracochlear trauma," *Otolaryngology—Head and Neck Surgery*, vol. 135, no. 3, pp. 374–382, 2006.

[10] C. A. Todd, F. Naghdy, and M. J. Svehla, "Force application during cochlear implant insertion: an analysis for improvement of surgeon technique," *IEEE Transactions on Biomedical Engineering*, vol. 54, no. 7, pp. 1247–1255, 2007.

[11] A. K. Lalwani and M. Pfister, Eds., *Recent Advances in Otolaryngology—Head and Neck Surgery*, vol. 3, Jp Medical, 2nd edition, 2013.

[12] M. W. Skinner, D. R. Ketten, M. W. Vannier, G. A. Gates, R. L. Yoffie, and W. A. Kalender, "Determination of the position of nucleus cochlear implant electrodes in the inner ear," *Otology & Neurotology*, vol. 15, no. 5, pp. 644–651, 1994.

[13] A. Aschendorff, R. Kubalek, A. Hochmuth et al., "Imaging procedures in cochlear implant patients—evaluation of different radiological techniques," *Acta Oto-Laryngologica*, vol. 124, no. 552, pp. 46–49, 2004.

[14] B. M. Verbist, J. H. M. Frijns, J. Geleijns, and M. A. van Buchem, "Multisection CT as a valuable tool in the postoperative assessment of cochlear implant patients," *American Journal of Neuroradiology*, vol. 26, no. 2, pp. 424–429, 2005.

[15] J.-P. Kobler, D. Beckmann, T. S. Rau, O. Majdani, and T. Ortmaier, "An automated insertion tool for cochlear implants with integrated force sensing capability," *International Journal of Computer Assisted Radiology and Surgery*, vol. 9, no. 3, pp. 481–494, 2014.

[16] J.-P. Kobler, J. Kotlarski, J. Öltjen, S. Baron, and T. Ortmaier, "Design and analysis of a head-mounted parallel kinematic device for skull surgery," *International Journal of Computer Assisted Radiology and Surgery*, vol. 7, no. 1, pp. 137–149, 2012.

[17] J.-P. Kobler, J. Kotlarski, G. J. Lexow, O. Majdani, and T. Ortmaier, "Design optimization of a bone-attached, redundant and reconfigurable parallel kinematic device for skull surgery," in *Proceedings of the IEEE International Conference on Robotics and Automation (ICRA '14)*, pp. 2364–2371, IEEE, Hong Kong, China, May 2014.

[18] J.-P. Kobler, M. Schoppe, G. J. Lexow et al., "Temporal bone borehole accuracy for cochlear implantation influenced by drilling strategy: an in vitro study," *International Journal of Computer Assisted Radiology and Surgery*, vol. 9, no. 6, pp. 1033–1043, 20149.

[19] O. Majdani, J.-P. Kobler, D. Beckmann, T. Ortmaier, T. Lenarz, and T. S. Rau, "Force measurement at the insertion process of cochlear implant electrodes," *Biomedical Engineering*, vol. 57, supplement 1, 2012.

[20] T. S. Rau, A. Hussong, M. Leinung, T. Lenarz, and O. Majdani, "Automated insertion of preformed cochlear implant electrodes: evaluation of curling behaviour and insertion forces on an artificial cochlear model," *International Journal of Computer Assisted Radiology and Surgery*, vol. 5, no. 2, pp. 173–181, 2010.

[21] S. A. Wade, J. B. Fallon, A. K. Wise, R. K. Shepherd, N. L. James, and P. R. Stoddart, "Measurement of forces at the tip of a cochlear implant during insertion," *IEEE Transactions on Biomedical Engineering*, vol. 61, no. 4, pp. 1177–1186, 2014.

[22] G. Kontorinis, T. Lenarz, T. Stöver, and G. Paasche, "Impact of the insertion speed of cochlear implant electrodes on the insertion forces," *Otology & Neurotology*, vol. 32, no. 4, pp. 565–570, 2011.

[23] G. Kontorinis, G. Paasche, T. Lenarz, and T. Stöver, "The effect of different lubricants on cochlear implant electrode insertion forces," *Otology and Neurotology*, vol. 32, no. 7, pp. 1050–1056, 2011.

[24] L. Leon, M. S. Cavilla, M. B. Doran, F. M. Warren, and J. J. Abbott, "Scala-Tympani phantom with cochleostomy and round-window openings for cochlear-implant insertion experiments," *Journal of Medical Devices*, vol. 8, no. 4, Article ID 041010, 10 pages, 2014.

[25] J. Xu, S.-A. Xu, L. T. Cohen, and G. M. Clark, "Cochlear view: postoperative radiography for cochlear implantation," *The American Journal of Otology*, vol. 21, no. 1, pp. 49–56, 2000.

[26] E. A. Avallone and T. Baumeister, *Marks' Standard Handbook for Mechanical Engineers*, McGraw-Hill Professional, 10th edition, 1996.

[27] N. R. Draper and H. Smith, *Applied Regression Analysis*, John Wiley & Sons, New York, NY, USA, 3rd edition, 1981.

Hindawi Publishing Corporation
BioMed Research International
Volume 2015, Article ID 853072, 6 pages
http://dx.doi.org/10.1155/2015/853072

Clinical Study

Stability Testing of a Wide Bone-Anchored Device after Surgery without Skin Thinning

Malou Hultcrantz

Department of Otorhinolaryngology, Karolinska University Hospital, 171 76 Stockholm, Sweden

Correspondence should be addressed to Malou Hultcrantz; malou.hultcrantz@karolinska.se

Received 15 July 2014; Revised 21 January 2015; Accepted 22 January 2015

Academic Editor: Chung-Feng Hwang

Objective. To longitudinally follow the osseointegration using Resonance Frequency Analysis (RFA) for different lengths of abutment on a new wide bone-anchored implant, introduced with the non-skin thinning surgical technique. *Study Design*. A single-center, prospective 1 year study following adults with bone-anchored hearing implants. *Materials and Methods*. Implantation was performed and followed for a minimum of 1 year. All patients were operated on according to the tissue preserving technique. A 4.5 mm wide fixture (Oticon Medical) with varying abutments (9 to 12 mm) was used and RFA was tested 1 week, 7 weeks, 6 months, and 12 months later. Implant Stability Quotient (ISQ), was measured from 1 to 100. Stability was compared to a group of patients ($N = 7$) implanted with another brand (Cochlear BI400) of 4.5 mm fixtures. *Results*. All 10 adults concluded the study. None of the participants lost their implant during the test period indicating a good anchoring of abutments to the wide fixture tested. Stability testing was shown to vary depending on abutment length and time after surgery and with higher values for shorter abutments and increasing values over the first period of time. One patient changed the abutment from 12 to 9 mm and another from a 9 to a 12 during the year. No severe skin problems, numbness around the implant, or cosmetic problems arose. *Conclusion*. After 1 year of follow-up, combination of a wide fixture implant and the non-skin thinning surgical technique indicates a safe procedure with good stability and no abutment losses.

1. Introduction

Osseointegration of titanium implants is affected by several factors such as bone quality and thickness, implant geometry, insertion torque, and the relation between burr diameter when drilling and implant diameter. Traditionally, the first Brånemark-Tjellström titanium implant for bone-anchored hearing systems had a diameter of 3.75 mm, gave good stability after a few weeks of osseointegration, and demonstrated good long-term clinical results [1–3]. A consensus from 2005 recommends that the implant can be safely loaded after 4–6 weeks, but lately, 3 weeks between surgery and loading, has been reported to be sufficient in adults with normal bone conditions [4–6]. It is known that while patients with soft bone have higher susceptibility to early implant loss, increased primary stability can potentially allow these patients to load early after the surgery [7]. In order to study the progression of implant stability after implantation, the Osstell system has been developed to incorporate Resonance Frequency Analysis (RFA) [8]. Values are influenced by firmness of the fixation, degree of osseointegration, hardness of the bone, and geometry of the implants (e.g., length and width). The RFA is transformed into Implant Stability Quotient (ISQ). The ISQ is a numerical value (1–100) where high ISQ values indicate good stability and low values a bad integration between the implant and the surrounding bone [8]. Potential benefits that arise from stability measurements include following the titanium-bone integration, deciding appropriate timing for processor loading, comparing different implant design, and foreseeing an eventual loss when stability measurements decrease.

Using the non-skin-thinning surgical technique for installation of bone-anchored hearing implants (BAHI) has shown many benefits and few negative effects. The procedure is quick, can be performed under local anesthesia, and can also be implemented in children [9–11]. It is performed as a one-step surgery which omits the skin thinning step of the classical BAHI implantation procedure, and the skin

surrounding the abutment is left in its natural thickness without any scar tissue.

The first implants produced in the 1980s were 3 or 4 mm in length with a diameter of 3.75 mm and were for many years to follow installed with the skin thinning technique. A 5.5 mm abutment was always used in the thinned cutis [12, 13]. The new surgical technique without skin thinning requires an individual variation of abutment lengths suitable for the variation in skin thickness. Due to the longer leverage, the forces on the fixture can potentially be higher with a longer abutment and implants that hold a wider diameter have been introduced to the market in order to increase stability and osseointegration [14–16]. To primarily optimize and later stabilize and reduce strain on the surrounding bone, the Wide Ponto with OptiGrip geometry was launched in 2012. The implant geometry provides a large initial bone contact surface (increased by 10% compared to the previous generation) in combination with a wider implant diameter (⌀ 4.5 mm) [15]. The screw head and abutment head are designed to fit the Resonance Frequency Analysis (FRA) testing equipment.

The present study evaluates the tissue preservation surgical technique when using the new wider implant. Longitudinal testing of the RFA allowed for a review of implant stability in abutments of variable length, not earlier described.

2. Materials and Methods

A single-center prospective study was completed with a follow-up time of 1 year in ten consecutively operated adults, all older than 18 years of age. All participants were operated on by the same surgeon with the same osseointegrating system (Oticon Medical, Askim, Sweden). Prior to surgery, patients were tested with audiometry and were given a bone-anchored device on a soft-band to sample for 3-4 weeks.

Patients were operated on according to the tissue-preserving surgical technique without skin thinning under local anesthesia by the same surgeon. Total thickness of the skin is measured with a syringe before the skin is opened (3 cm long incision), a 3 mm or 4 mm burr is used to drill in the skull bone behind the ear to test the actual bone thickness, the opening is widened, and the predrawn fixture width and individual length of the abutment are inserted. The wide Ponto implant (⌀ 4.5 mm) with a fixture length of 4 mm was used throughout the study and abutments used were 9 or 12 mm. Thereafter a hole was punched through the entire thickness of the skin, the abutment was externalized, and the skin was closed with intracutaneous soluble sutures [9].

The patients' medical records provided information concerning clinical signs and symptoms, gender, concomitant medication, and skin diseases. Peri-implant infections, numbness around the implant, change of abutment length, abutment loss, skin overgrowth, use of hearing devices, and stability were recorded after surgery. Peri-implant infections were scored according to Holgers' scale (1–4) [17].

The Osstell system (Osstell, Gothenburg, Sweden) was used, with the help of resonance frequencies, to measure implant stability as a function of stiffness of the bone-implant interface. When testing, a rod (SmartPeg) is attached to the implanted abutment top. The probe of the Osstell instrument measures, contact-free, over a range of frequencies, by exciting the SmartPeg which starts to vibrate in the directions where highest and lowest resonance frequency occur. If there is an instable osseointegration, the vibrations will be high and give a low ISQ value, and the reverse. According to the recommendations 2 tests were always recorded at every visit, perpendicular to the peg in 2 directions 90 degrees from each other in the same plane. Each test gives a high and a low value depending on the vibrations, further used for the study analysis.

For comparison of measured stability, 7 adults implanted with another system, the Cochlear BI400, with a fixture of 4.5 mm in diameter and 4 mm length, are reported. Surgery, surgeon, and implantation technique are the same as described above, 6 with a 10 mm abutment and 1 with a 12 mm.

Appointments and checkups were arranged 1 week, 7 weeks, 6 months, and 12 months after surgery. At each time point (5 times), the RFA method was used and the 2 ISQ values were noted.

The clinical study was conducted in accordance with the ethical regulations of the Declaration of Helsinki and in adherence to Swedish law and regulations with an ethical permission (nr 2012/452-31/3).

2.1. Statistical Analysis. Ten was considered to be an appropriate number of operated patients followed for 1 year. Statistical analyses were carried out with Student's t-tests, where a P value less than 0.05 was considered to be statistically significant.

3. Results

Mean age of the patients, including 7 females and 3 males, was 54 years. Table 1 reveals background information for all patients. Indications for surgery included mixed hearing loss (MHL) $n = 4$, single-sided deafness (SSD) $n = 3$, atresia $n = 2$, and sensorineural hearing loss (SNHL) $n = 1$. All patients were operated unilaterally, and the skin thickness varied from 6 to 12 mm. Seven patients used a 9 mm long abutment and the remaining patients received a 12 mm long abutment. In order not to have to select preoperatively for the patient which special processor they should use, the Oticon implant system is useful since this implant is compatible with both the Ponto processors and the Cochlear processors. Any brand of sound processor can therefore be utilized with the Oticon wide implants and abutments. Eight patients chose a Ponto processor (Oticon Medical, Askim, Sweden) while 2 chose a BP 100 (Cochlear, Gothenburg, Sweden). Selection of sound processors was this way based on patients' personal taste.

The most common concomitant diseases reported among the group were asthma, high blood pressure, and heart problems. Two individuals with syndromes were included

Table 1: Demographics from 10 patients implanted with a wide implant, during a 1-year period.

Age	Indication	Abutm. loss	Peri-impl. inf.	Holgers scale	Numbness	Side	Skin thickness mm	Abutm. length mm	Abutm. change	ISQ start	ISQ end
58	SSD	—	—		—	L	6	9		52,49	60,59
46	Atresia	—	—		—	L	10	12		43,43	53,51
87	EO, SNHL	—	—		—	L	6	9		58,57	58,57
65	SSD	—	—		—	R	8	9		57,55	60,60
39*	COM	—	—		—	R	12	12		53,51	57,57
45	SSD	—	Yes	2	—	R	6	9		51,49	57,57
61	COM	—	—		—	R	7	9		53,54	57,56
59	COM	—	—		—	L	7	9		49,46	51,30
35	COM	—	—		—	L	6	9	9 to 12	61,58	61,62**
46	Atresia	—	—		—	L	9	12	12 to 9	39,39	46,46**
Total										52,51	56,54***

*Patient with 12 mm thick skin where a minor skin thinning was performed.
**Patient started with 1 abutment length and ended with another.
***$n = 8$, 2 patients changed the abutment length during the study.

(Rubenstein Taybi and Treacher Collins), as was one who suffered from Parkinson's disease.

Mean surgical time was 12.4 min, except for one male who needed minimal tissue reduction due to a skin thickness of 12 mm where surgical time was 23 min. In all patients, surgical wounds healed within 10 days after implantation. None of the patients complained of numbness at the 1-year follow-up.

A partial overgrowth was found in the male patient who had a skin thickness of 12 mm. Since there are no longer abutments available, a small revision surgery with a minor skin reduction had to be performed after 3 months in an outpatient setting.

The ISQ stability test across all 10 patients varied over time from a starting median value of 52 and 51, high and low, respectively, to 56 and 54 after 1 year. The ISQ values decreased at 1 week after surgery compared to the value at installation, which was statistically significant ($P < 0.05$), and seem to have reached a plateau around 3 months later. In the group of only 9 mm abutments ($n = 7$), the initial values were 54 and 53 (range 43 to 61) and these values increased after 1 year to 58 and 54 (range 46 to 60). In the 12 mm abutment group ($n = 3$), the values measured were 45 and 44 (range 39–57) postsurgically and 51 and 49 (range 43 to 60) after 1 year (Figure 1).

When comparing the stability test from the 7 control patients the ISQ values were for the 10 mm abutment length initially 46.5 and after 1 year 52.5 and for the 12 mm (only $n = 1$) 45 and 48, respectively.

Change of abutment was performed, as an outpatient procedure in two patients. One female patient had a 9 mm abutment replaced by a 12 mm, and one male patient had a 12 mm abutment changed to a 9 mm so as to better fit the processor (Figure 2). The measured ISQ values changed minimally.

No implants were lost and no abutments were permanently removed.

One minor skin reaction was noted in one female patient 3 months after surgery, with a Holgers' scale scoring 2. This patient was treated with extra cleaning and lapisation (silvernitrate), and no further problems were experienced. None of the other patients had any skin reaction during the 1 year follow-up period.

4. Discussion

The current follow-up study is a 1-year prospective clinical trial designed to evaluate stability in a new wider fixture, fitted with variable length of abutments in combination with the tissue preservation surgical technique which has not been reported earlier. Patients have excellent results subjectively and objectively and almost all (nine out of ten) were wearing their processor daily after 1 year.

Prior to the current study, research suggested that the non-skin-thinning surgical technique is beneficial when implanting BAHIs in both children and adults and many of the earlier known complications disappeared or were reduced [9–11, 16]. The present study confirms and reinforces those results. The longer abutments required for this technique can increase the force transferred to the fixture with higher demand on osseointegration and stability. The manner in which stability varies between the different abutments and fixtures has not been fully reported clinically. The new wide Ponto implant showed improved stability in the laboratory, and the current study confirms that this improved stability leads to few implant losses [15].

There are now a greater number of studies reporting ISQ values in the literature, but still no consensus has been reached as to what exact level an implant is considered to be fully osseointegrated. Indications suggest that levels of ISQ around 60 demonstrate normal values for good stability, but most information gathered is reported with older, shorter abutments (5.5 or 6 mm). For comparison implantation with

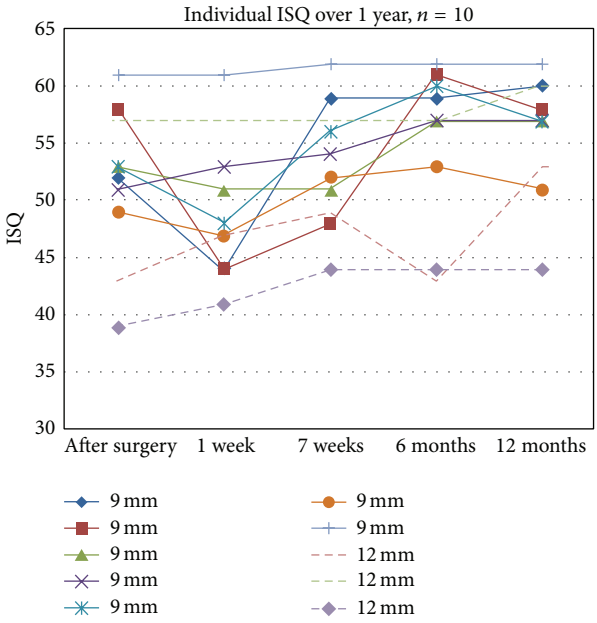

Figure 1: Stability test from time for surgery to the endpoint at 1 year, showing individual ISQ values for 10 patients. High ISQ values are shown.

Figure 2: Implant with a 9 mm abutment 3 months after surgery. The abutment was recently changed from 12 to 9 mm. ISQ high and low values increased minimally from 44 and 45 to 46 and 46.

a 4.5 mm wide BIA300 implant (Cochlear, Gothenburg, Sweden) showed with the linear incision technique (skin thinning) and 5.5 mm abutments a ISQ of 62 after 6 months which is in the range of ISQ reported presently, but here with longer abutments and a higher level of the skin around the abutment [18]. Comparing the present wide implant stability with older more narrow ones is impossible since the SmartPeg for testing ISQ does not fit the older abutments.

Caution must be taken when comparing specific ISQ values, as ISQ values in a soft bone, although well-integrated, give lower ISQ values than an insufficiently integrated implant in hard bone [19]. The highest survival rates in implants after osseointegration are reported from stability tests after placement in the temporal region as compared to other bones [20–22]. Research has also shown that poorer bone quality, younger children, and syndromic patients have a higher extrusion rate, indicating that behavioral and biological factors must be taken into account [23–25]; however, high success rates in implantations have been reported after irradiation and also in low mineralized bone [26–28].

Basic studies in the laboratory indicate ISQ values with the same implant but different abutment lengths increasing from 46 (12 mm abutment) to 54 (9 mm) and 62 (6 mm), respectively, giving an estimation of stability loss of 3 to 4 ISQ for each mm of longer abutment [15]. Higher values in a shorter abutment can also be confirmed in the present study and also when compared to the control group. In the 9 mm abutment group the difference of ISQs over the year increased totally with 4 (ISQ high) and with 6 in the 12 mm group (not statistically significant). Among the controls the 10 mm abutment group increased with 6 and the 12 mm group with 3 ISQ units during the one year tested. These values indicate small, but increasing values over time and also comparable results for long abutments. Increasing ISQ values during the first part of the illustrated year and a difference between abutment lengths are noted but are not remarkable and the number of patients in each group is low. Exact values cannot be compared to other studies, due to differences in abutment length, surgical technique, bone quality, and position of the fixture, but when compared with dental studies, using different abutment lengths, increasing values are confirmed over time [14]. Recent studies of early loading with a 5.5 mm abutment showed that all included patients had values over 60, 1 week after surgery, with increasing values over time, demonstrating almost immediate implant stability [6, 29].

When considering the fixtures and their different lengths, it has been shown in a group of pediatric implantations that there was no favor reported for a 4 mm fixture, 3.75 mm in diameter, over a 3 mm fixture with the same diameter in number of osseointegration failure rates [16]. When the fixtures were placed transcalvarian, the 3 mm fixtures were even more stable. Total osseointegration failure rates were 21% in children as compared to 0% among adults which are not surprising when considering the softness of the skull bone in developing children. However, good stability and indications for early loading are given to be ISQ > 60 in children [30]. New information of implanted children with longer abutments demonstrates that a low ISQ value of 30 could indicate a value where an implant loss can be considered [24].

Individual patient factors possibly play a larger role in the failures than the surgical implantation and fixture length. Presently, only adult patient was included and the wide fixture seems to be pertinent to hold both abutment lengths tested based on stability tests, due to the fact that no implant was lost. The implant design and the surgical technique may account for the high survival rates. New studies will be needed to confirm the statistical analysis, since the number of patients included is low and further follow-up of patients will be reported.

5. Conclusion

The present prospective, one year follow-up study performing a BAHI surgical technique without skin thinning in ten consecutively operated patients, reveals that the non-skin-thinning technique in combination with a wide implant

(4.5 mm in diameter) provides few complications. The absence of implant losses indicates a safe procedure for the patients. The ISQ values indicate small differences between the wide fixture with either 9 or 12 mm abutments all with good stability (ISQ 54 and 57, resp.) 1 year after implantation.

Conflict of Interests

The author declares that there is no conflict of interests regarding the publication of this paper.

References

[1] A. Tjellström, J. Lindström, O. Hallén, T. Albrektsson, and P. I. Brånemark, "Osseointegrated titanium implants in the temporal bone. A clinical study on bone-anchored hearing aids," *The American Journal of Otology*, vol. 2, no. 4, pp. 304–310, 1981.

[2] A. Tjellström, J. Lindström, O. Hallén, T. Albrektsson, and P. I. Brånemark, "Direct bone anchorage of external hearing aids," *Journal of Biomedical Engineering*, vol. 5, no. 1, pp. 59–63, 1983.

[3] A. Tjellström, G. Granström, and M. Odersjö, "Survival rate of self-tapping implants for bone-anchored hearing aids," *Journal of Laryngology and Otology*, vol. 121, no. 2, pp. 101–104, 2007.

[4] A. F. Snik, E. A. M. Mylanus, D. W. Proops et al., "Consensus statements on the BAHA system: where do we stand at present?" *The Annals of Otology, Rhinology & Laryngology. Supplement*, vol. 195, pp. 2–12, 2005.

[5] C. M. McLarnon, I. Johnson, T. Davison et al., "Evidence for early loading of osseointegrated implants for bone conduction at 4 weeks," *Otology and Neurotology*, vol. 33, no. 9, pp. 1578–1582, 2012.

[6] H. T. Faber, C. A. J. Dun, R. C. Nelissen, E. A. M. Mylanus, C. W. R. J. Cremers, and M. K. S. Hol, "Bone-anchored hearing implant loading at 3 weeks: stability and tolerability after 6 months," *Otology and Neurotology*, vol. 34, no. 1, pp. 104–110, 2013.

[7] J. J. Wazen, B. Wycherly, and J. Daugherty, "Complications of bone-anchored hearing devices," *Advances in Oto-Rhino-Laryngology*, vol. 71, pp. 63–72, 2011.

[8] http://www.oticonmedical.com/~asset/cache.ashx?id=12638&type=14&format=web.

[9] M. Hultcrantz, "Outcome of the bone-anchored hearing aid procedure without skin thinning: a prospective clinical trial," *Otology and Neurotology*, vol. 32, no. 7, pp. 1134–1139, 2011.

[10] A. Lanis and M. Hultcrantz, "Percutaneous osseointegrated implant surgery without skin thinning in children: a retrospective case review," *Otology and Neurotology*, vol. 34, no. 4, pp. 715–722, 2013.

[11] R. A. Goldman, A. Georgolios, and W. T. Shaia, "The punch method for bone-anchored hearing aid placement," *Otolaryngology: Head & Neck Surgery*, vol. 148, no. 5, pp. 878–880, 2013.

[12] A. Tjellström, B. Håkansson, J. Lindström et al., "Analysis of the mechanical impedance of bone-anchored hearing aids," *Acta Oto-Laryngologica*, vol. 89, no. 1-2, pp. 85–92, 1980.

[13] J. J. Wazen, D. L. Young, M. C. Farrugia et al., "Successes and complications of the baha system," *Otology and Neurotology*, vol. 29, no. 8, pp. 1115–1119, 2008.

[14] C. Aparicio and P. Orozco, "Use of 5-mm-diameter implants: Periotest values related to a clinical and radiographic evaluation," *Clinical Oral Implants Research*, vol. 9, no. 6, pp. 398–406, 1998.

[15] P. Westerkull and L. Jinton, "The new wide Ponto implant design-clinical and surgical aspects," Oticon Medical White Paper, 2012.

[16] P. Marsella, A. Scorpecci, R. D'Eredità, A. Della Volpe, and P. Malerba, "Stability of osseointegrated bone conduction systems in children: a pilot study," *Otology and Neurotology*, vol. 33, no. 5, pp. 797–803, 2012.

[17] K.-M. Holgers, A. Tjellstrom, L. M. Bjursten, and B.-E. Erlandsson, "Soft tissue reactions around percutaneous implants: a clinical study of soft tissue conditions around skin-penetrating titanium implants for bone-anchored hearing aids," *American Journal of Otology*, vol. 9, no. 1, pp. 56–59, 1988.

[18] R. D'Eredità, M. Caroncini, and R. Saetti, "The new baha implant: a prospective osseointegration study," *Otolaryngology—Head and Neck Surgery*, vol. 146, no. 6, pp. 979–983, 2012.

[19] C. P. C. Sim and N. P. Lang, "Factors influencing resonance frequency analysis assessed by Osstell *mentor* during implant tissue integration: I. Instrument positioning, bone structure, implant length," *Clinical Oral Implants Research*, vol. 21, no. 6, pp. 598–604, 2010.

[20] C. E. Lee, L. Christensen, G. T. Richter, and J. L. Dornhoffer, "Arkansas BAHA experience: transcalvarial fixture placement using osseointegration surgical hardware," *Otology and Neurotology*, vol. 32, no. 3, pp. 444–447, 2011.

[21] M. Eeg-Olofsson, S. Stenfelt, A. Tjellstrom, and G. Granstrom, "Transmission of bone-conducted sound in the human skull measured by cochlear vibrations," *International Journal of Audiology*, vol. 47, no. 12, pp. 761–769, 2008.

[22] B. Karayazgan-Saracoglu, H. Zulfikar, A. Atay, and Y. Gunay, "Treatment outcome of extraoral implants in the craniofacial region," *Journal of Craniofacial Surgery*, vol. 21, no. 3, pp. 751–758, 2010.

[23] S. Ali, L. Hadoura, A. Carmichael, and N. K. Geddes, "Bone-anchored hearing aid A single-stage procedure in children," *International Journal of Pediatric Otorhinolaryngology*, vol. 73, no. 8, pp. 1076–1079, 2009.

[24] M. Hultcrantz and A. Lanis, "Stability testing after osseointegrated implant surgery without skin thinning in children: case reports after abutment loss," *Otology and Neurotology*, vol. 35, no. 6, pp. 1102–1104, 2014.

[25] C. A. J. Dun, M. J. F. de Wolf, M. K. S. Hol et al., "Stability, survival, and tolerability of a novel BAHA implant system: six-month data from a multicenter clinical investigation," *Otology & Neurotology*, vol. 32, pp. 1001–1007, 2011.

[26] G. Soo, M. C. F. Tong, W. S. S. Tsang et al., "The BAHA hearing system for hearing-impaired postirradiated nasopharyngeal cancer patients: a new indication," *Otology and Neurotology*, vol. 30, no. 4, pp. 496–501, 2009.

[27] M. D. Wilkie, K. A. Lightbody, A. A. Salamat, K. M. Chakravarthy, D. A. Luff, and R. H. Temple, "Stability and survival of bone-anchored hearing aid implant systems in post-irradiated patients," *European Archives of Oto-Rhino-Laryngology*, 2014.

[28] U. Held, D. Rohner, and D. Rothamel, "Early loading of hydrophilic titanium implants inserted in low-mineralized (D3 and D4) bone: one year results of a prospective clinical trial," *Head and Face Medicine*, vol. 9, no. 1, article 37, 2013.

[29] M. Wróbel, W. Gawęcki, and W. Szyfter, "New insight into Baha implant stability measurements: observations on resonance frequency analysis results," *Otology and Neurotology*, vol. 34, no. 6, pp. 1018–1020, 2013.

[30] C. McLarnon, I. Johnson, T. Davison et al., "Resonance frequency analysis of osseo-integrated implants for bone conduction in a pediatric population—a novel approach for assessing stability for early loading," *International Journal of Pediatric Otorhinolaryngology*, vol. 78, no. 4, pp. 641–644, 2014.

Hindawi Publishing Corporation
BioMed Research International
Volume 2015, Article ID 236364, 9 pages
http://dx.doi.org/10.1155/2015/236364

Research Article

Evaluation of Intracochlear Trauma Caused by Insertion of Cochlear Implant Electrode Arrays through Different Quadrants of the Round Window

Graziela de Souza Queiroz Martins,[1,2] Rubens Vuono Brito Neto,[2] Robinson Koji Tsuji,[2] Eloisa Maria Mello Santiago Gebrim,[3] and Ricardo Ferreira Bento[2]

[1]*Department of Medicine, Faculdade de Medicina, University of Sao Paulo, Avenida Dr. Eneás de Carvalho Aguiar 255, Sala 6167, 05403-000 São Paulo, SP, Brazil*
[2]*Department of Otorhinolaryngology, Clinical Hospital, FMUSP, Avenida Dr. Eneás de Carvalho Aguiar 255, Sala 6167, 05403-000 São Paulo, SP, Brazil*
[3]*Department of Radiology, Clinical Hospital, FMUSP, Avenida Dr. Eneás de Carvalho Aguiar 255, Sala 6167, 05403-000 São Paulo, SP, Brazil*

Correspondence should be addressed to Graziela de Souza Queiroz Martins; gazumartins@uol.com.br

Received 13 November 2014; Revised 23 February 2015; Accepted 4 March 2015

Academic Editor: Hung-Ching Lin

Hypothesis. This study aimed to evaluate whether there is a difference in the degree of intracochlear trauma when the cochlear implant electrode arrays is inserted through different quadrants of the round window membrane. *Background*. The benefits of residual hearing preservation in cochlear implant recipients have promoted the development of atraumatic surgeries. Minimal trauma during electrode insertion is crucial for residual hearing preservation. *Methods*. In total, 25 fresh human temporal bones were subjected to mastoidectomy and posterior tympanotomy. The cochlear implant electrode array was inserted through the anterosuperior quadrant of the round window membrane in 50% of the bones and through the anteroinferior quadrant in the remaining 50%. The temporal bones were dehydrated, embedded in epoxy, serially polished, stained, viewed through a stereomicroscope, and photographed with the electrode arrays *in situ*. The resulting images were analyzed for signs of intracochlear trauma. *Results*. Histological examinations revealed varying degrees of damage to the intracochlear structures, although the incidence and severity of intracochlear trauma were not influenced by the quadrant of insertion. *Conclusions*. The incidence and severity of intracochlear trauma were similar in all samples, irrespective of electrode array insertion through the anterosuperior or anteroinferior quadrant of the round window membrane.

1. Introduction

Cochlear implants (CIs) represent a well-established treatment for severe and profound bilateral hearing loss. The development of CIs in the last 30 years is considered one of the milestones of modern medicine, and, to date, the outcomes of CIs have been remarkable and superior to those of any other type of neural prosthesis [1]. These results have encouraged the expansion of the selection criteria for CIs [2]. Therefore, the number of candidates with significant residual hearing who are eligible to receive CIs has increased, fostering several studies on the preservation of postoperative residual hearing in these patients. Intracochlear trauma during CI-related surgical interventions is one of the factors associated with residual hearing loss [3–5]. Previous studies have highlighted the possibility of electrode array insertion using atraumatic surgical techniques, which have been designated as soft surgeries [4, 6–9].

Among the steps involved in soft surgeries, electrode array insertion is the most frequently studied. CI arrays can be inserted via cochleostomy or through the round window (RW). According to Banfai [10], RW was the first choice of

route for CI electrode array insertion. However, with the development of longer, thicker, and less flexible electrodes, insertion through RW became difficult and necessitated cochleostomy. Over the last few years, the development of thinner and more flexible electrodes has again enabled insertion through RW [11]. The possibility of electrode array insertion via these two distinct routes stimulated further comparative studies [12–15]. Numerous studies on cochleostomy have been conducted to determine any variations in intracochlear trauma according to its location. However, to date, no studies have evaluated differences in the degree of intracochlear trauma caused by electrode array insertion through different quadrants of the RW membrane.

Therefore, this study was conducted to determine differences in intracochlear trauma caused by CI electrode array insertion through the anterosuperior and anteroinferior quadrants of the RW membrane.

2. Materials and Methods

The Research Ethics Committee of the Department of Medicine, Universidade de São Paulo, approved this study. Twenty-five human temporal bones were retrieved within 24 h after death and were frozen and stored. To avoid divergence in relation to the laterality of the ears, the samples were first divided into two groups corresponding to the right and left ears. Then, they were randomly assigned to group 1, wherein the electrode array was inserted through the anterosuperior quadrant of the RW membrane, or group 2, wherein the electrode array was inserted through the anteroinferior quadrant.

On the day of dissection, the temporal bones were thawed at room temperature, placed in the surgical position, and subjected to mastoidectomy and posterior tympanotomy under a microscopic view. Following the identification of the RW niche, false membranes or mucous folds, when present, were removed to expose the RW membrane. In addition, any bony projections that restricted the visualization of the RW membrane were drilled, keeping the RW membrane intact. The quadrants of the round window were divided visually. Two perpendicular lines were drawn. The first was drawn at larger longitudinal axis of the round window membrane and was called line a. The second was drawn in the middle of line a and was called line b. These lines define the anterosuperior (I) and the anteroinferior quadrant (II) (Figure 1).

The RW membrane was incised in the anterosuperior or anteroinferior quadrant (Figures 2 and 3). The point of insertion of the electrode array was always close to the annulus of the selected quadrant.

The electrode arrays were inserted using appropriate instruments through the openings in the respective quadrants by a single surgeon experienced in CI placement. The stapes footplate on all bones was removed to allow the flow of compounds used for histological examination throughout the cochlea. The electrode arrays were fixed with ethyl-cyanoacrylate glue in the region of the posterior tympanotomy.

The electrode array EVO (Oticon Medical, Gothenburg, Sweden; Oticon Medical/Neurelec, Vallauris, France),

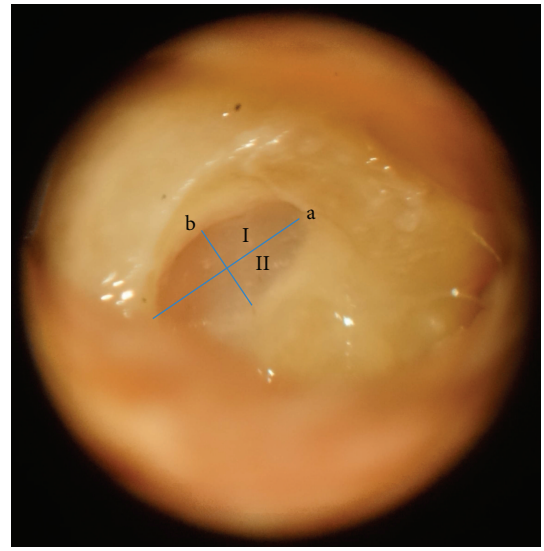

Figure 1: The round window membrane visualized through posterior tympanotomy after the removal of bony projections. Lines a and b dividing the quadrants of the round window membrane. I: anterosuperior quadrant. II: anteroinferior quadrant.

a straight array with a smooth surface and carrying 20 electrodes, was used. The total length was 24 mm, proximal diameter was 0.5 mm, and distal tip diameter was 0.4 mm [16].

After electrode array insertion, the bones were fixed in 10% formaldehyde and dehydrated using ethanol in increasing concentrations of 70%–100% and 100% acetone. The dehydrated bones were embedded in epoxy resin, placed in desiccators, and subjected to vacuum to promote resin penetration throughout the cochlea and to eliminate air bubbles. The histological examination procedure has been previously detailed by Plenk [17].

All the embedded bones were subjected to tomography to confirm the intracochlear position of the electrode array and to rule out kinking. Computed tomography was also performed to determine the position and orientation of the cochlea within the temporal bone block and to define the accurate plane for sectioning in each specimen.

Next, the epoxy blocks were transferred to a microgrinding machine, polished, and stained with toluidine blue. The stained surfaces were examined using a stereomicroscope under magnifications of 15x, 30x, 60x, 94x, and 120x and photographed. After image collection, the bone samples were polished once again to expose new surfaces; this procedure was repeated for every 500 μm until the entire cochlea could be visualized. The microgrinding technique has been previously detailed by Stöver et al. [18].

Blinded individuals who were experienced and comfortable with cochlear histopathology performed histological sectioning and analyses.

During histological analysis, each cochlea was divided into five segments to standardize the intracochlear regions (Figure 4).

The beginning of segment 1 corresponded to the RW membrane, while that of segments 2 and 4 indicated the

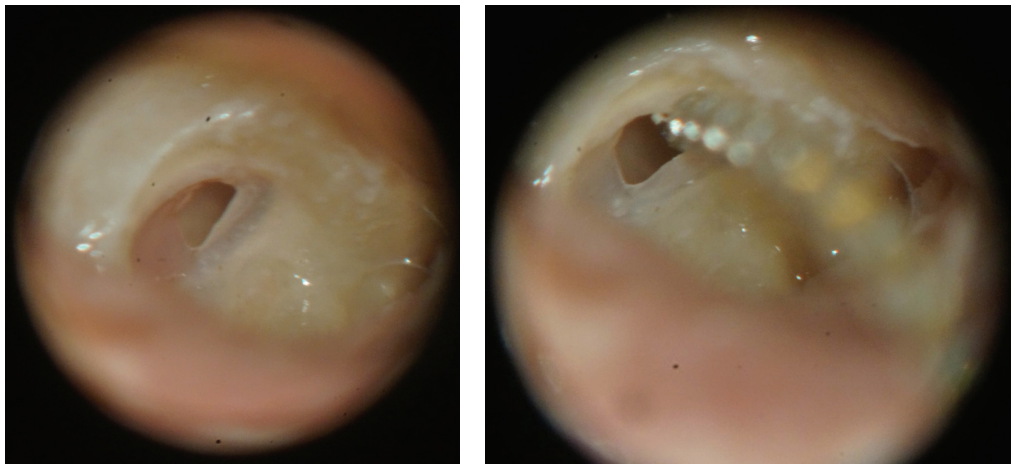

(a) (b)

Figure 2: Incision and electrode array insertion through the anterosuperior quadrant of the round window membrane. (a) Incision in the anterosuperior quadrant of the round window membrane. (b) Beginning of the insertion of the electrode array through the opening in the anterosuperior quadrant.

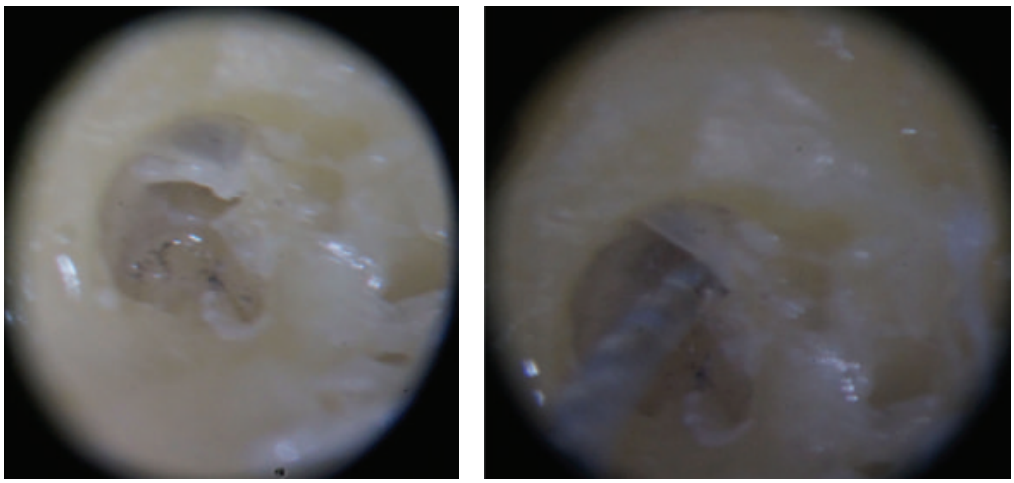

(a) (b)

Figure 3: Incision and electrode array insertion through the anteroinferior quadrant of the round window membrane. (a) Incision in the anteroinferior quadrant of the round window membrane. (b) Beginning of the insertion of the electrode array through the opening in the anteroinferior quadrant.

surface where the modiolus was no longer visualized. In the latter two segments, the electrode could be visualized in the transverse orientation.

Intracochlear trauma observed by histological analysis was graded according to the classification proposed by Eshraghi et al. [19]: grade 0, no trauma; grade 1, elevation of the basilar membrane; grade 2, rupture of the basilar membrane; grade 3, dislocation of the electrode array to the scala vestibuli; and grade 4, severe trauma such as fracture of the osseous spiral lamina, modiolus, or stria vascularis.

Two separate analyses of intracochlear trauma were performed for each segment in each group. In the first analysis, any trauma beyond grade 0 was considered positive trauma. In the second analysis, as reported in previous studies [12], only grade 2, 3, or 4 trauma was considered positive trauma. Grade 1 trauma was analyzed together with grade 0 trauma because it represented only elevation of the basilar membrane.

The numbers of temporal bones available for research were limited, so convenience sample, with 25 temporal bones, was adopted. The data obtained in the study were entered into a Microsoft Excel spreadsheet. In both groups, the number of exposed surfaces per sample, the presence of intracochlear trauma, and degree of trauma in each segment have been described with the use of absolute and relative frequencies. The existence of association between the presence of intracochlear trauma and the quadrant of insertion of the electrode array was verified by exact test of

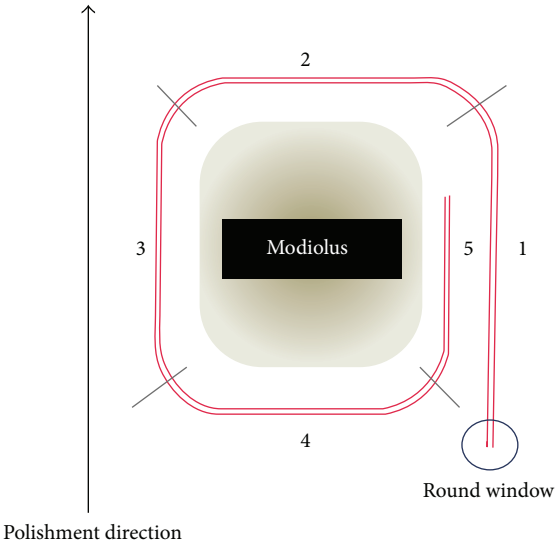

Figure 4: Diagrammatic representation of the intracochlear electrode array (red) and the division of the cochlea into five segments.

Fisher. The degrees of trauma in each segment were compared between groups with the Mann-Whitney test. In all tests, the descriptive level (P value) ≤ 0.05 was considered statistically significant.

3. Results

No temporal bone was excluded. The electrode array was inserted through the anterosuperior and anteroinferior quadrants of the RW membrane in 13 and 12 samples, respectively.

In all samples, drilling of bony projections in the RW niche was required because they restricted visibility of and accessibility to the RW membrane. Complete insertion of the electrode array was possible in 24 samples with minimal or no resistance. In the remaining sample, the electrode array receded a few millimeters after insertion. There were no technical limitations to electrode placement in the randomized quadrant in any of the temporal bone samples.

All samples were subjected to computed tomography. The electrode arrays could be visualized inside the cochlea in all temporal bones. No kinking was observed in any array (Figure 5).

All bone surfaces from the RW membrane to the end of the cochlea were analyzed.

Figure 6 shows the different intracochlear segments. Figures 6(c) and 6(d) represent the same temporal bone. Figure 6(c) shows the last surface where the modiolus could be visualized. In the next surface, shown in Figure 6(d), the modiolus could no longer be visualized, defining the beginning of segment 2.

Computed tomography helped in determining the orientation of the cochlea within the temporal bone block and in defining the accurate plane to initiate polishing in each specimen.

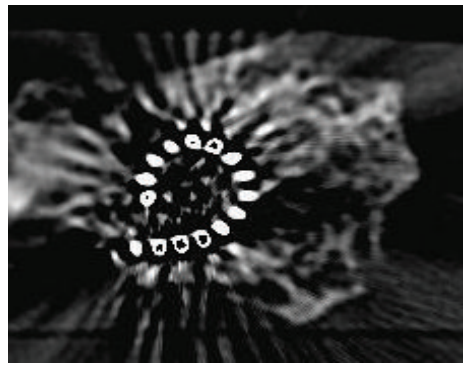

Figure 5: Computed tomography imaging with visualization of the electrode array within the cochlea.

A total of 372 bone surfaces were obtained for histological analysis. None of these surfaces exhibited artifacts that could prevent identification of the intracochlear structures.

Intracochlear trauma, when present, was clearly visible and could be graded according to the classification proposed by Eshraghi et al. [19].

Distinct damage to the intracochlear structures was identified. In all bones, the damage did not extend beyond the end of the CI electrode tip. When the same segment exhibited multiple grades of trauma, the trauma with the highest grade was considered. Figure 7 shows examples of histological surfaces, which illustrate the classification system for intracochlear trauma proposed by Eshraghi et al. [19].

The presence of intracochlear trauma in all segments according to both above-mentioned criteria (considering any trauma beyond grade 0 as positive trauma or considering grade 2, 3, or 4 trauma as positive trauma) showed no significant correlation with the quadrant of insertion ($P > 0.05$).

Furthermore, there were no significant differences in the grade of intracochlear trauma in each segment between the two groups ($P > 0.05$; Table 1).

4. Discussion

The present study demonstrated a similar degree of intracochlear trauma when CI electrode arrays were inserted through the anterosuperior and anteroinferior quadrants of the RW membrane.

The insertion of electrode arrays is considered an essential step of atraumatic surgery. Numerous authors have compared the advantages and disadvantages of CI insertion through cochleostomies performed in different positions. In this regard, cochleostomies performed at the inferior margin of RW are considered less traumatic and are associated with a lower frequency of erroneous electrode array placement in the scala media or scala vestibuli and a higher probability of residual hearing preservation compared with cochleostomies performed in the superior, anterior, and anteroinferior regions of the RW [20–24]. On the basis of these studies identifying differences in intracochlear trauma

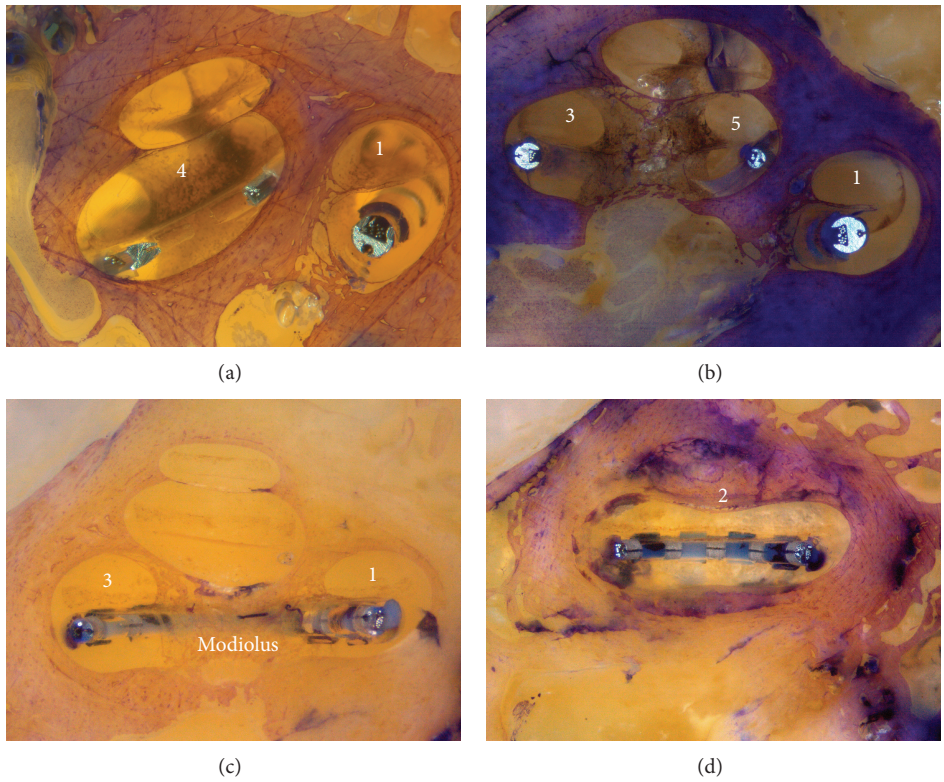

Figure 6: (a) Identification of segments 1 and 4. The modiolus is located deeper than the bone surface. (b) Identification of segments 1, 3, and 5. The modiolus is now visible on the surface of the bone. This defines the beginning of segments 3 and 5. (c) Visualization of segments 1 and 3 and the modiolus. (d) Visualization of the beginning of segment 2. The modiolus can no longer be visualized.

and audiological performance after CI electrode array insertion through different cochleostomy locations, our research group evaluated differences in intracochlear trauma caused by electrode array insertion through different quadrants of the RW membrane.

In the present study, the electrode arrays were inserted through the anterior segment of the RW membrane on the basis of the following findings in anatomical studies: difficulty in visualization of the posterior segment of the RW membrane because of its horizontal orientation, close proximity of the posterior segment to the inner ear structures, and the possibility of injuries to the osseous spiral lamina during drilling of the posterior bony projections for adequate visualization of the posterior margin of the RW membrane [3, 21, 23]. Therefore, we opted to compare the anterior quadrants of the RW membrane (anterosuperior and anteroinferior) and for no mandatory viewing of the posterior segment of the RW membrane.

Roland et al. [21] studied 15 temporal bones and estimated that the area covered by the vertical or anterior portion of the RW membrane varies from 0.8 to 1.75 mm^2, with a mean of 1.39 mm^2. We calculated a 0.19 mm^2 area occupied by the larger diameter of the electrode array using the following formula: $A = \pi \cdot r^2$. Mathematically, this facilitates insertion of the electrode array through any of the anterior quadrants of the RW membrane.

During the surgeries performed in the present study, bones overhangs of the RW niche that limited visualization of the membrane were observed in all samples, necessitating drilling of the anterior and anteroinferior bony projections. When necessary, the posterior projections were minimally drilled to improve exposure of the anterior margin and facilitate electrode array insertion. These results are in agreement with those of previous anatomical studies [5, 24], particularly the study by Roland et al. [21], who dissected 30 temporal bones and observed that anatomical projections restricted the visualization of the RW membrane in all samples. Furthermore, the need for drilling the promontory could not be ruled out in any of the samples, although the amount of drilling required would be minimal. According to Takahashi and Sando [25], electrode array insertion through the RW membrane required the removal of <1 mm of bone, which is lesser than that required for cochleostomy and decreases the possibility of trauma [14, 26].

The statistical analysis in the present study was two-tailed, considering that previous data did not indicate the direction in which the results were statistically significant. Indeed, the literature on this issue is conflicting. The hypothesis that intracochlear trauma is lesser with electrode array insertion through the anteroinferior quadrant of the RW membrane was raised because of the proximity of this quadrant to the inferior margin of RW, and, to date, cochleostomy at this margin has been considered less traumatic [20]. On the other hand, because of the downward direction of the scala tympani from RW, there is a higher probability of the electrode arrays being directed towards the superior

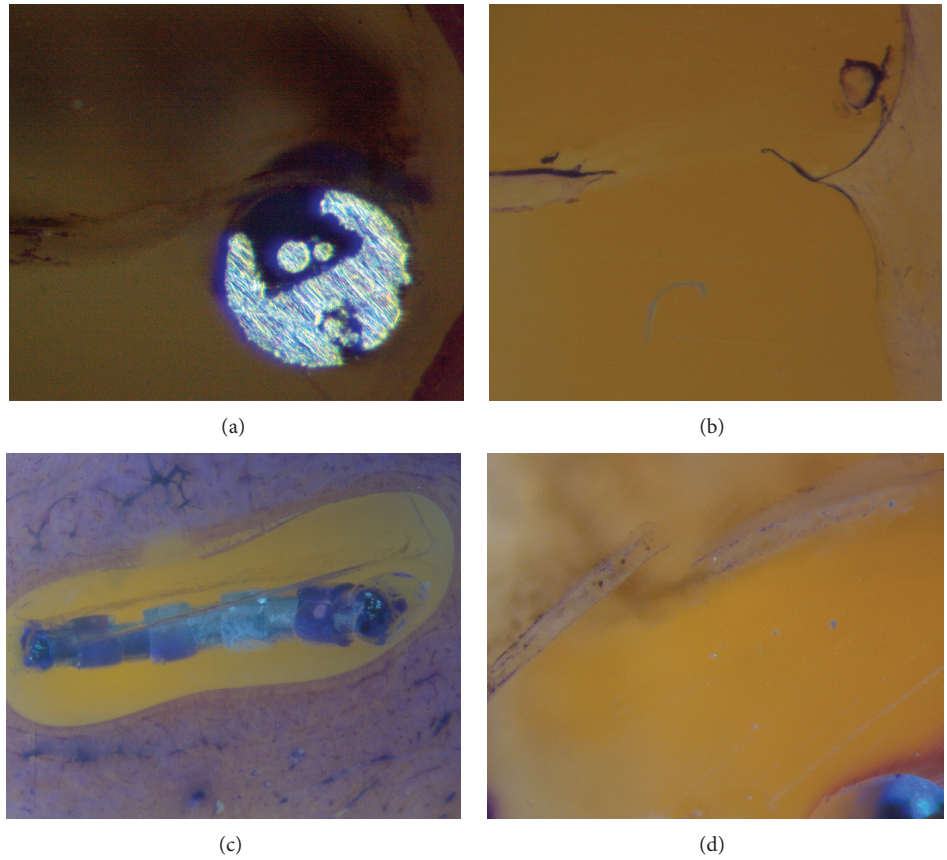

(a) (b) (c) (d)

Figure 7: (a) Electrode array in the scala tympani causing slight elevation of the basilar membrane (grade 1). (b) Identification of a ruptured basilar membrane (grade 2). (c) Dislocation of the electrode array from the scala tympani to the scala vestibuli (grade 3). (d) Identification of a fracture in the osseous spiral lamina (grade 4).

structures of the scala tympani during insertion through the anteroinferior quadrant [22, 27]. This suggests that the probability of intracochlear trauma is lower when the arrays are inserted through the anterosuperior quadrant of the RW membrane.

Briggs et al. [20] reported that cochleostomy at the inferior margin of RW requires complete skeletonization of the facial nerve and chorda tympani; therefore, many surgeons avoid cochleostomy at this location. In this study, we could visualize the anterior segment of the RW membrane in all bone samples. However, to expose the anteroinferior quadrant, enlargement of the posterior tympanotomy was necessary, with skeletonization of the mastoid segment of the facial nerve in some samples. Skeletonization would not be necessary to visualize only the anterosuperior quadrant; this observation is in agreement with that in previous studies. Although these studies did not involve electrode array insertion through RW, the surgical exposure required for cochleostomy at the inferior margin of RW is very similar to that required for insertion through the anteroinferior quadrant of the RW membrane. According to the results of the present study, surgeons who avoid more extensive dissection of the facial nerve for visualization of the anteroinferior quadrant of the RW membrane can implant electrode arrays through the anterosuperior quadrant, which requires less exposure.

Currently, the microgrinding technique is the most powerful technique for determining the localization of electrodes and insertion trauma to the cochlea [18]. The use of nondecalcified human temporal bones permits the *in situ* evaluation of intracochlear trauma caused by CI placement [28]. The primary advantages of this method are that the excellent image quality enables clear identification of the intracochlear structures, the electrode array, and the relationship between these two components. However, the microgrinding technique has some limitations. The cut sections are not preserved, and therefore evaluation of the temporal bone is limited to the time during which sectioning is performed and depends on the quality of photographic documentation. Another limitation is the time-consuming and cost-intensive method of electrode evaluation. Despite the disadvantages, this technique provides data of, so far, unknown clarity regarding the detection and localization of insertion trauma [18].

Assessment of the insertion depths of the electrode arrays was beyond the scope of this study; therefore, we decided to standardize the segmentation of the cochlea in a more visual manner, rather than segmentation in degrees, which could be achieved under computed tomography guidance.

Table 1: Grade of intracochlear trauma caused by electrode array insertion through the anterosuperior or anteroinferior quadrant of the round window membrane in each segment.

Variable	Insertion				Total		$P^{\S}$
	Group 1 ($N = 13$)		Group 2 ($N = 12$)		($N = 25$)		
	N	%	N	%	N	%	
Segment 1 (grade)							0.503
0	13	100	10	83.3	23	92.0	
1	0	0	0	0	0	0	
2	0	0	0	0	0	0	
3	0	0	0	0	0	0	
4	0	0	2	16.7	2	8.0	
Segment 2 (grade)							0.538
0	10	76.9	8	66.7	18	72.0	
1	1	7.7	0	0	1	4.0	
2	1	7.7	1	8.3	2	8.0	
3	1	7.7	1	8.3	2	8.0	
4	0	0	2	16.7	2	8.0	
Segment 3 (grade)							0.470
0	9	69.2	7	58.3	16	64.0	
1	2	15.4	0	0	2	8.0	
2	1	7.7	2	16.7	3	12.0	
3	0	0	0	0	0	0	
4	1	7.7	3	25.0	4	16.0	
Segment 4 (grade)							0.894
0	11	84.6	10	83.3	21	84.0	
1	1	7.7	0	0	1	4.0	
2	0	0	0	0	0	0	
3	1	7.7	1	8.3	2	8.0	
4	0	0	1	8.3	1	4.0	
Segment 5 (grade)							0.810
0	10	76.9	9	75.0	19	76.0	
1	1	7.7	0	0	1	4.0	
2	0	0	0	0	0	0	
3	1	7.7	0	0	1	4.0	
4	1	7.7	3	25.0	4	16.0	
Lowest grade							0.406
0	9	69.2	7	58.3	16	64.0	
1	1	7.7	0	0	1	4.0	
2	1	7.7	0	0	1	4.0	
3	1	7.7	0	0	1	4.0	
4	1	7.7	5	41.7	6	24.0	

Group 1: insertion through the anterosuperior quadrant of the round window membrane; group 2: insertion through the anteroinferior quadrant.
N = number of samples.
§Results of the Mann-Whitney U test.

To standardize the histological analysis was opted for classification system proposed by Eshraghi et al. [19] in 2003. This is the most widely used classification in histological studies of intracochlear trauma. However, it is considered a disadvantage of this classification that the negative functional consequences generated by an intracochlear trauma do not evolve according to the ascending numbering classification. As an example, consider a trauma grade 4, because of a fracture in the osseous spiral lamina. Although this trauma changes the cochlear function in the affected region, probably it does not interfere with gradients of ions and hemodynamics of intracochlear liquids. On the other hand, a level 2 trauma,

caused by rupture of the basilar membrane, presumably leads to more dispersed intracochlear damages. This occurs because this type of trauma causes the mixture of endolymph and perilymph, altering the normal gradient of the ions, which can lead to degeneration of hair cells and neural structures. Because of endocochlear flow all the cochlea may be compromised [29, 30].

This study has some limitations. First, dynamic monitoring of the electrode array during insertion was not implemented; therefore, we cannot describe if the trajectory differed with insertion through different quadrants of the RW membrane. Second, our study was a small study comparing two variables, and further larger studies to clarify our findings are required. Third, we used only straight electrodes; therefore, our results are not applicable to precurved electrodes.

5. Conclusions

In conclusion, there were no significant differences in the incidence and severity of intracochlear trauma caused by insertion of electrode arrays through the anterosuperior and anteroinferior quadrants of the RW membrane. Preservation of the fine intracochlear structures continues to be an important topic.

Conflict of Interests

The authors declare that there is no conflict of interests regarding the publication of this paper.

Acknowledgment

This paper received research support by FAPESP (São Paulo State Foundation for Research Support).

References

[1] B. S. Wilson and M. F. Dorman, "Interfacing sensors with the nervous system: lessons from the development and success of the cochlear implant," *IEEE Sensors Journal*, vol. 8, no. 1, pp. 131–147, 2008.

[2] B. S. Wilson and M. F. Dorman, "Cochlear implants: current designs and future possibilities," *Journal of Rehabilitation Research and Development*, vol. 45, no. 5, pp. 695–730, 2008.

[3] B. K. H. Franz, G. M. Clark, and D. M. Bloom, "Surgical anatomy of the round window with special reference to cochlear implantation," *Journal of Laryngology and Otology*, vol. 101, no. 2, pp. 97–102, 1987.

[4] T. J. Balkany, S. S. Connell, A. V. Hodges et al., "Conservation of residual acoustic hearing after cochlear implantation," *Otology & Neurotology*, vol. 27, no. 8, pp. 1083–1088, 2006.

[5] M. L. Carlson, C. L. W. Driscoll, R. H. Gifford et al., "Implications of minimizing trauma during conventional cochlear implantation," *Otology & Neurotology*, vol. 32, no. 6, pp. 962–968, 2011.

[6] M. V. S. Goffi-Gomez, M. C. Guedes, C. G. de Ornelas et al., "Hearing conservation after cochlear implant: pilot study," *Revista Brasileira de Otorrinolaringologia*, vol. 68, no. 5, pp. 698–702, 2002 (Portuguese).

[7] H. Skarzyński, A. Lorens, P. D'Haese et al., "Preservation of residual hearing in children and post-lingually deafened adults after cochlear implantation: an initial study," *ORL*, vol. 64, no. 4, pp. 247–253, 2002.

[8] C. James, K. Albegger, R. Battmer et al., "Preservation of residual hearing with cochlear implantation: how and why," *Acta Oto-Laryngologica*, vol. 125, no. 5, pp. 481–491, 2005.

[9] L. Garcia-Ibanez, A. R. MacIas, C. Morera et al., "An evaluation of the preservation of residual hearing with the Nucleus Contour Advance electrode," *Acta Oto-Laryngologica*, vol. 129, no. 6, pp. 651–664, 2009.

[10] P. Banfai, "A surgical approach for the cochlear implant," *HNO*, vol. 26, pp. 85–89, 1978 (German).

[11] T. Lenarz, T. Stöver, A. Buechner et al., "Temporal bone results and hearing preservation with a new straight electrode," *Audiology and Neurotology*, vol. 11, no. 1, pp. 34–41, 2006.

[12] O. Adunka, W. Gstoettner, M. Hambek, M. H. Unkelbach, A. Radeloff, and J. Kiefer, "Preservation of basal inner ear structures in cochlear implantation," *ORL*, vol. 66, no. 6, pp. 306–312, 2004.

[13] A. Paprocki, B. Biskup, K. Kozłowska, A. Kuniszyk, D. Bien, and K. Niemczyk, "The topographical anatomy of the round window and related structures for the purpose of cochlear implant surgery," *Folia Morphologica*, vol. 63, no. 3, pp. 309–312, 2004.

[14] O. Adunka, J. Kiefer, M. H. Unkelbach, T. Lehnert, and W. Gstoettner, "Development and evaluation of an improved cochlear implant electrode design for electric acoustic stimulation," *Laryngoscope*, vol. 114, no. 7, pp. 1237–1241, 2004.

[15] H. W. Pau, T. Just, M. Bornitz, N. Lasurashvilli, and T. Zahnert, "Noise exposure of the inner ear during drilling a cochleostomy for cochlear implantation," *Laryngoscope*, vol. 117, no. 3, pp. 535–540, 2007.

[16] Y. Nguyen, M. Miroir, G. Kazmitcheff et al., "Cochlear implant insertion forces in microdissected human cochlea to evaluate a prototype array," *Audiology and Neurotology*, vol. 17, no. 5, pp. 290–298, 2012.

[17] H. Plenk, "The microscopic evaluation of hard tissue implants," in *Techniques of Biocompability Testing*, D. F. Williams, Ed., pp. 35–81, CRC Press, Boca Raton, Fla, USA, 1986.

[18] T. Stöver, P. Issing, G. Graurock et al., "Evaluation of the advance off-Stylet insertion technique and the cochlear insertion tool in temporal bones," *Otology & Neurotology*, vol. 26, no. 6, pp. 1161–1170, 2005.

[19] A. A. Eshraghi, N. W. Yang, and T. J. Balkany, "Comparative study of cochlear damage with three perimodiolar electrode designs," *Laryngoscope*, vol. 113, no. 3, pp. 415–419, 2003.

[20] R. J. S. Briggs, M. Tykocinski, J. Xu et al., "Comparison of round window and cochleostomy approaches with a prototype hearing preservation electrode," *Audiology and Neurotology*, vol. 11, no. 1, pp. 42–48, 2006.

[21] P. S. Roland, C. G. Wright, and B. Isaacson, "Cochlear implant electrode insertion: the round window revisited," *Laryngoscope*, vol. 117, no. 8, pp. 1397–1402, 2007.

[22] O. F. Adunka, A. Radeloff, W. K. Gstoettner, H. C. Pillsbury, and C. A. Buchman, "Scala tympani cochleostomy II: topography and histology," *The Laryngoscope*, vol. 117, no. 12, pp. 2195–2200, 2007.

[23] P. M. M. C. Li, H. Wang, C. Northrop, S. N. Merchant, and J. B. Nadol Jr., "Anatomy of the round window and hook region of the cochlea with implications for cochlear implantation and

other endocochlear surgical procedures," *Otology and Neurotology*, vol. 28, no. 5, pp. 641–648, 2007.

[24] S. Berrettini, F. Forli, and S. Passetti, "Preservation of residual hearing following cochlear implantation: comparison between three surgical techniques," *Journal of Laryngology and Otology*, vol. 122, no. 3, pp. 246–252, 2008.

[25] H. Takahashi and I. Sando, "Computer-aided 3-D temporal bone anatomy for cochlear implant surgery," *Laryngoscope*, vol. 100, no. 4, pp. 417–421, 1990.

[26] O. Adunka and J. Kiefer, "Impact of electrode insertion depth on intracochlear trauma," *Otolaryngology: Head and Neck Surgery*, vol. 135, no. 3, pp. 374–382, 2006.

[27] Y. Shapira, A. A. Eshraghi, and T. J. Balkany, "The perceived angle of the round window affects electrode insertion trauma in round window insertion—an anatomical study," *Acta Oto-Laryngologica*, vol. 131, no. 3, pp. 284–289, 2011.

[28] W. K. Gstoettner, O. Adunka, P. Franz et al., "Perimodiolar electrodes in cochlear implant surgery," *Acta Oto-Laryngologica*, vol. 121, no. 2, pp. 216–219, 2001.

[29] F. B. Simmons, "The double membrane break syndrome in sudden hearing loss," *Laryngoscope*, vol. 89, no. 1, pp. 59–66, 1979.

[30] H. P. Zenner, "K^+-induced motility and depolarization of cochlear hair cells. Direct evidence for a new pathophysiological mechanism in Ménière's disease," *Archives of Oto-Rhino-Laryngology*, vol. 243, no. 2, pp. 108–111, 1986.